



**TECHNISCHE UNIVERSITÄT MÜNCHEN**

Fakultät für Medizin

Lehrstuhl für Stoffwechselerkrankungen

**„Mechanisms of immune activation versus  
regulation in obesity“**

Verena Barbara Ott

Vollständiger Abdruck der von der Fakultät für Medizin der Technischen Universität München zur Erlangung des akademischen Grades eines Doktors der Naturwissenschaften genehmigten Dissertation.

Vorsitzender: Prof. Dr. Percy A. Knolle

Prüfer der Dissertation: 1. Prof. Dr. Matthias H. Tschöp  
2. apl. Prof. Dr. Michael W. Pfaffl

Die Dissertation wurde am 05.04.2019 bei der Technischen Universität München eingereicht und durch die Fakultät für Medizin am 05.11.2019 angenommen.





**TECHNISCHE UNIVERSITÄT MÜNCHEN**

Fakultät für Medizin

Lehrstuhl für Stoffwechselerkrankungen

**„Mechanismen der Immunaktivierung versus  
Regulation in Adipositas“**

Verena Barbara Ott

2019



---

## Table of contents

|   |              |
|---|--------------|
| <b>Table of contents</b> .....  | <b>v</b>     |
| <b>List of Abbreviations</b> .....  | <b>viii</b>  |
| <b>List of Figures</b> .....  | <b>xi</b>    |
| <b>List of Tables</b> .....   | <b>xiii</b>  |
| <b>Summary</b> .....  | <b>xiv</b>   |
| <b>Zusammenfassung</b> .....  | <b>xvi</b>   |
| <b>1. Introduction: Obesity- an immune-metabolic disease</b> .....                  | <b>- 1 -</b> |
| 1.1. Characteristics of obesity and the metabolic part of the disease .....         | - 1 -        |
| 1.1.1. The prevalence and incidence of obesity.....                                 | - 1 -        |
| 1.1.2. The pathophysiology of obesity and its characteristics .....                 | - 1 -        |
| 1.1.3. Animal models of obesity .....   | - 3 -        |
| 1.1.4. The body's adipose tissue compartments.....                                  | - 5 -        |
| 1.2. Relevant immunological players in obesity.....                                 | - 7 -        |
| 1.2.1. Adaptive immune cells- differentiation and function .....                    | - 7 -        |
| 1.2.2. Mediators of immune tolerance: Regulatory T cells .....                      | - 8 -        |
| 1.2.3. T follicular helper cells.....   | - 12 -       |
| 1.2.4. The role of miRNAs in immune activation.....                                 | - 16 -       |
| 1.3. Immune-metabolic interactions in obesity .....                                 | - 18 -       |
| 1.3.1. The immunometabolism of CD4 <sup>+</sup> T cells drives their function ..... | - 18 -       |
| 1.3.2. Mechanisms of inflammation in the VAT and its systemic effects .....         | - 21 -       |
| 1.3.3. Insulin (receptor) signaling and insulin resistance .....                    | - 25 -       |
| 1.4. Objectives.....  | - 28 -       |

---

|   |               |
|---|---------------|
| <b>2. Methods.....</b>  | <b>- 30 -</b> |
| 2.1. Blood and tissue samples from human subjects .....   | - 30 -        |
| 2.2. Isolation of human naïve CD4 <sup>+</sup> T cells and <i>ex vivo</i> precursor TFH cell staining ..... | - 30 -        |
| 2.3. Human <i>in vitro</i> Treg induction assay .....   | - 31 -        |
| 2.4. Human <i>in vitro</i> TFH cell induction assay .....   | - 31 -        |
| 2.5. Mice.....  | - 31 -        |
| 2.6. Genotyping .....   | - 32 -        |
| 2.7. Dietary challenge .....  | - 32 -        |
| 2.8. Glucose Tolerance Test.....  | - 32 -        |
| 2.9. Murine cell isolation .....  | - 32 -        |
| 2.10. Murine <i>in vitro</i> Treg induction assay.....  | - 33 -        |
| 2.11. (Intracellular) staining of <i>ex vivo</i> Tregs and (precursor) TFH cells.....                       | - 33 -        |
| 2.12. <i>In vitro</i> Treg re-stimulation Assay.....  | - 34 -        |
| 2.13. Glucose uptake Assay .....  | - 34 -        |
| 2.14. Gene expression analysis of mRNAs and miRNAs .....  | - 34 -        |
| 2.15. Foxp3 CNS2 methylation analysis .....   | - 35 -        |
| 2.16. RNA Sequencing .....  | - 35 -        |
| 2.17. Proteomics.....   | - 36 -        |
| 2.18. Immunofluorescence stainings on cytopins .....  | - 37 -        |
| 2.19. Statistics .....  | - 38 -        |
| <b>3. Results .....</b>   | <b>- 39 -</b> |
| 3.1. (Precursor) TFH cells in obesity.....  | - 39 -        |
| 3.1.1. MiRNA92a and obesity affect TFH cell differentiation.....  | - 39 -        |
| 3.1.2. Preliminary data: TFH cells in human obesity.....  | - 49 -        |

---

|           |  |               |
|-----------|--|---------------|
| 3.2.      | Insulin (receptor) signaling and its effects on <i>de novo</i> Treg induction .....                      | - 52 -        |
| 3.2.1.    | Insulin impairs <i>de novo</i> Foxp3 <sup>+</sup> Treg induction .....                                   | - 52 -        |
| 3.2.2.    | A T cell-specific loss of InsR expression enhances <i>de novo</i> Foxp3 <sup>+</sup> Treg induction..... | - 59 -        |
| <b>4.</b> | <b>Discussion .....</b>  | <b>- 69 -</b> |
| 4.1       | (Precursor) TFH cells in obesity.....  | - 69 -        |
| 4.2       | Insulin (receptor) signaling and its effects on <i>de novo</i> Treg induction .....                      | - 77 -        |
| 4.3       | Conclusions and outlook.....   | - 86 -        |
| <b>5.</b> | <b>References .....</b>  | <b>- 88 -</b> |
| <b>6.</b> | <b>Permissions .....</b>   | <b>I</b>      |
|           | Proceedings of the National Academy of Sciences (PNAS).....  | I             |
|           | Cell Metabolism.....   | I             |
| <b>7.</b> | <b>Attachment: Overview of the used Material .....</b>   | <b>II</b>     |
|           | <b>Danksagung</b>  |               |

---

## List of Abbreviations

|                |  |
|----------------|--|
| Acetyl-CoA     | Acetyl-Coenzym A                                       |
| ADP            | Adenosine diphosphate                                  |
| Adrm1          | Proteasomal ubiquitin receptor Adrm1                   |
| Ahr            | Aryl hydrocarbon receptor                              |
| Akt            | Protein kinase B                                       |
| AMP            | Adenosine monophosphate                                |
| AMPK           | Monophosphate Activated Protein Kinase                 |
| APC(s)         | Antigen-presenting cell(s)                             |
| Ascl2          | E-protein Achaete-scute complex homolog 2              |
| Atf4           | Activating transcription factor 4                      |
| AT(s)          | adipose tissue(s)                                      |
| ATP            | Adenosine triphosphate                                 |
| BAT            | brown adipose tissue                                   |
| Bcl6           | B cell lymphoma 6                                      |
| Blimp1         | PR domain zinc finger protein 1                        |
| BMI            | body mass index  |
| Bst2           | Bone marrow stromal antigen 2                          |
| BW(s)          | body weight(s)   |
| Cbl            | E3 ubiquitin ligase casitas-B-lineage lymphoma protein |
| CCR (6 or 7)   | C-C chemokine receptor type (6 or 7)                   |
| Chk1           | Checkpoint kinase 1                                    |
| CNS2           | conserved noncoding sequence 2                         |
| CXCR (3 or 5)  | C-X-C chemokine receptor type (3 or 5)                 |
| Cyc1           | Cytochrome c1  |
| DC(s)          | dendritic cell(s)                                      |
| DIO            | diet-induced obese/obesity                             |
| Dld            | Dihydrolipoyl dehydrogenase                            |
| ETC            | electron transport chain                               |
| Etfb           | Electron transfer flavoprotein subunit beta            |
| FACS           | fluorescence-activated cell sorting                    |
| FAD/FADH2      | oxidized/reduced flavin adenine dinucleotide           |
| FAO            | fatty acid $\beta$ -oxidation                          |
| Fdxr (or Adxr) | Adrenodoxin reductase                                  |
| FFA            | free fatty acids                                       |

---

|                        |   |
|------------------------|---|
| Foxo                   | Forkhead box protein O  |
| Foxp3                  | Forkhead box protein 3  |
| Foxp3-GFP              | B6.Cg-Foxp3 <sup>tm2Tch/J</sup> mice                                  |
| FSC                    | forward scatter   |
| Gadd45β                | Growth arrest and DNA damage inducible beta                           |
| GC                     | germinal center   |
| GCK                    | Glucokinase or Hexokinase IV  |
| Gk5                    | Glycerokinase 5   |
| GLUT                   | Glucose transporter   |
| GSEA                   | Gene Set Enrichment Analysis  |
| Gsk3b                  | Glycogen synthase kinase 3 beta                                       |
| GTT                    | glucose tolerance test  |
| HFHS                   | high-fat, high-sugar  |
| ICOS                   | Inducible T cell costimulator   |
| IFN $\gamma$           | Interferon gamma  |
| IGF-I/ IGF-II          | Insulin-like growth factor I/II                                       |
| Il                     | Interleukin   |
| ingLNs                 | inguinal lymph nodes  |
| InsR                   | Insulin receptor  |
| InsR TKO mice          | mice with a T cell specific insulin receptor deficiency               |
| IRS                    | Insulin receptor substrate  |
| ITCH                   | E3 ubiquitin-protein ligase Itchy homolog                             |
| Klf2                   | Krueppel-like factor 2  |
| LNs                    | lymph node(s)   |
| MACS                   | magnetic activated cell sorting                                       |
| MapK(s)                | Mitogen-activated protein kinase(s)                                   |
| mesLNs                 | mesenteric lymph nodes  |
| MHC                    | self-peptide-major histocompatibility complex                         |
| miRNA                  | microRNA  |
| mTOR                   | Mammalian target of rapamycin   |
| NAD <sup>+</sup> /NADH | oxidized/reduced nicotinamide adenine dinucleotide                    |
| Ndufa (2,6,8,10)       | NADH dehydrogenase [ubiquinone] 1 alpha subcomplex subunit (2,6,8,10) |
| Ndufv1                 | NADH dehydrogenase [ubiquinone] flavoprotein 1                        |
| NFAT(s)                | Transcription factors nuclear factors of activated T cell(s)          |
| ob/ob                  | obese/obese, B6.Cg-Lep <sup>ob</sup> /J mice                          |

|               |  |
|---------------|--|
| OXPHOS        | oxidative phosphorylation                          |
| PBMCs         | Peripheral blood mononuclear cells                 |
| PD1           | Programmed cell death protein 1                    |
| PI3K          | Phosphoinositid-3-kinase                           |
| popLNs        | popliteal LNs                                      |
| PPAR $\gamma$ | Peroxisome proliferator-activated receptor gamma   |
| (p)S6         | (phosphorylated) ribosomal protein S6 kinase       |
| Pten          | Phosphatase and tensin homologue                   |
| RNAseq        | RNA Sequencing                                     |
| RT            | room temperature                                   |
| RT-qPCR       | real-time quantitative PCR                         |
| SAT           | subcutaneous adipose tissue                        |
| SD            | standardized control diet                          |
| SSC           | sideward scatter                                   |
| Stat          | Signal Transducers and Activators of Transcription |
| SVF           | stromal vascular fraction                          |
| T1D           | type 1 diabetes                                    |
| T2D           | type 2 diabetes                                    |
| TCA cycle     | tricarboxylic acid                                 |
| Tconv.        | conventional T cells                               |
| TCR           | T cell receptor                                    |
| Tfam          | Mitochondrial transcription factor A               |
| TFH           | T follicular helper                                |
| TGF $\beta$   | Transforming growth factor- $\beta$                |
| Tiparp        | TCDD-inducible poly-ADP-ribose polymerase          |
| TNF $\alpha$  | tumor necrosis factor $\alpha$                     |
| Tregs         | regulatory T cells                                 |
| TSDR          | Tregs-specific demethylated region                 |
| VAT           | visceral white adipose tissue                      |
| vs.           | versus   |
| WT            | wildtype, B6.SJL-Ptprca <sup>Pepcb/BoyJ</sup> mice |

---

## List of Figures

|   |        |
|---|--------|
| <b>Figure 1:</b> MiRNA92a affects human precursor TFH cell induction <i>in vitro</i> . .....  | - 40 - |
| <b>Figure 2:</b> BW upon different durations of a HFHS diet. ....   | - 41 - |
| <b>Figure 3:</b> Representative FACS plots for the identification of murine live<br>CD4 <sup>+</sup> CXCR5 <sup>+</sup> (PD1 <sup>hi</sup> ) TFH cells.....                             | - 42 - |
| <b>Figure 4:</b> miRNA92a expression in murine precursor TFH vs. non-TFH cells from<br>mesLNs upon a long-term HFHS diet. ....  | - 43 - |
| <b>Figure 5:</b> mRNA expression of genes associated with TFH cell differentiation.....   | - 44 - |
| <b>Figure 6:</b> <i>Ex vivo</i> (precursor) TFH cell frequencies in ingLNs and mesLNs are<br>influenced by the progression of obesity. ....   | - 45 - |
| <b>Figure 7:</b> (Precursor) TFH cells in mesLNs of genetically obese ob/ob mice.....   | - 47 - |
| <b>Figure 8:</b> Frequencies of <i>ex vivo</i> Foxp3 <sup>+</sup> Tregs and precursor TFH cells in murine<br>ATs upon a HFHS diet.....  | - 48 - |
| <b>Figure 9:</b> BMI of lean and obese individuals. ) .....   | - 49 - |
| <b>Figure 10:</b> Preliminary data: Analysis of precursor TFH cells in peripheral blood during<br>human obesity. ....   | - 50 - |
| <b>Figure 11:</b> Initial results: mRNA expression of genes associated with TFH cell<br>differentiation in total human VAT. ....  | - 51 - |
| <b>Figure 12:</b> Insulin affects <i>in vitro</i> CD25 <sup>hi</sup> Foxp3 <sup>+</sup> Treg induction, T cell proliferation, Treg<br>stability and T cell specific glucose uptake..... | - 53 - |
| <b>Figure 13:</b> Insulin affects targets downstream of InsR signaling. ....  | - 54 - |
| <b>Figure 14:</b> The effect of insulin on human <i>in vitro</i> Treg induction is sex dependent. ....  | - 55 - |
| <b>Figure 15:</b> The effect of insulin on <i>in vitro</i> Treg induction is maintained in genetic<br>obesity. ....   | - 56 - |
| <b>Figure 16:</b> BW upon different durations of a HFHS diet. ....  | - 57 - |
| <b>Figure 17:</b> The effect of insulin on <i>in vitro</i> Treg induction is maintained in dietary<br>induced obesity.....  | - 57 - |

---

|  |        |
|--|--------|
| <b>Figure 18:</b> Naïve CD4 <sup>+</sup> T cells from VAT and popliteal LNs (popLNs) of obese mice remain insulin-sensitive upon DIO. ....   | - 58 - |
| <b>Figure 19:</b> Characterization of mice with a T cell specific loss of the InsR. ....   | - 59 - |
| <b>Figure 20:</b> A T cell specific loss of the InsR affects <i>in vitro</i> Treg induction and T cell proliferation.....  | - 60 - |
| <b>Figure 21:</b> A T cell specific loss of the InsR affects <i>in vitro</i> Tregs induction and T cell proliferation using naïve CD4 <sup>+</sup> T cells from VAT and popLNs. .... | - 61 - |
| <b>Figure 22:</b> InsR deficiency and its effects on downstream signaling pathways. ....   | - 62 - |
| <b>Figure 23:</b> The effect of the InsR TKO depends on the T cell environment, glucose uptake and PI3K activation. ....   | - 63 - |
| <b>Figure 24:</b> BW of InsR TKO vs. Flox ctrl. mice upon a long-term HFHS diet.....   | - 64 - |
| <b>Figure 25:</b> The effect of a T cell specific InsR knockout on Treg induction upon DIO.....  | - 65 - |
| <b>Figure 26:</b> Transcriptomic Analysis of CD4 <sup>+</sup> T cells from InsR TKO vs. Flox ctrl. mice.....   | - 66 - |
| <b>Figure 27:</b> Proteomic Analysis of CD4 <sup>+</sup> T cells from InsR TKO vs. Flox ctrl. mice.....  | - 68 - |

## List of Tables

|                                    |    |
|------------------------------------|----|
| <b>Table 1:</b> Used Material..... | II |
|------------------------------------|----|

## Summary

Interactions between immune and environmental-metabolic responses were recently shown to be critically involved in the development of obesity which is accompanied by chronic, low-grade inflammation and insulin resistance. An obesogenic environment might affect the abundance, functionality and cell specific metabolism of various immune cell populations both in the lymphoid tissues and in particular at the site of inflammation, the adipose tissue. Pro-inflammatory CD4<sup>+</sup>CXCR5<sup>+</sup>(PD1<sup>hi</sup>Bcl6<sup>hi</sup>) effector T follicular helper (TFH) cells and suppressive, anti-inflammatory regulatory Foxp3<sup>+</sup>T cells (Tregs) are critical mediators of immune activation versus immune regulation. The latter are especially important for immune tolerance in the adipose tissue by dampening tissue inflammation and maintaining tissue homeostasis in obesity. The hormone insulin is crucial for the body's metabolic control and insulin resistance in the peripheral insulin-responsive tissues is a major hallmark of obesity. However, the specific involvement of TFH cells and Tregs in obesity as well as the metabolic signaling cues that link the metabolic and the immune system such as insulin signaling are not yet fully understood.

This thesis provides first evidence, that CD4<sup>+</sup>CXCR5<sup>+</sup>PD1<sup>hi</sup> precursor TFH cells are enriched in both the lymphoid tissue and inflamed visceral white adipose tissue (VAT) of mice exposed to a long-term or a sustained high-fat, high-sugar (HFHS) diet. Higher (precursor) TFH cell frequencies were also observed in genetically obese ob/ob mice. Here, levels of mature CD4<sup>+</sup>CXCR5<sup>+</sup>PD1<sup>hi</sup>Bcl6<sup>hi</sup>TFH cells in mesenteric lymph nodes (mesLNs) were significantly increased. Significantly higher levels of *Ii21* and a trend towards higher expression of *ICOS* and *Bcl6* represent characteristics of fully differentiated TFH cells and were both present in CD4<sup>+</sup>CXCR5<sup>+</sup> precursor TFH cells isolated from mesLNs of lean and obese mice. MicroRNA92a that was previously shown to be positively correlated with TFH cell levels in the autoimmune setting could not be confirmed as similarly important for linking obesity-associated chronic, low-grade inflammation with increased (precursor) TFH cell levels. A limited number of human peripheral blood samples and VAT biopsies were available to obtain insights into a possible relevance of TFH cells for human obesity. The abundance of precursor Th1-like, Th2-like and Th17-like TFH cells in human peripheral blood was influenced by the presence of obesity and insulin resistance. Furthermore, early TFH cell markers *Ascl2* and *Ii21* showed a trend towards a higher abundance in total VAT of obese, insulin-resistant individuals potentially reflecting a favorable environment for precursor TFH cells.

The expression of the insulin receptor (InsR) on activated CD4<sup>+</sup>T cells and the importance of the PI3K-Akt-mTOR pathway for both insulin-mediated metabolic responses and stable, functional Foxp3<sup>+</sup>Treg induction offer means of integrating environmental-metabolic signaling cues with Treg induction and function. In this thesis, insulin was shown to impair *in vitro* Foxp3<sup>+</sup>Treg induction from naïve CD4<sup>+</sup>T cells isolated from lymph nodes (LNs) or VAT of both lean and diet-induced obese (DIO) mice. Similarly, insulin interfered with Treg induction using naïve CD4<sup>+</sup>T cells from mesLNs of genetically obese ob/ob mice. Therefore, these results demonstrate that both DIO and ob/ob mice remain insulin-sensitive on the T cell level despite their insulin resistance in metabolic tissues such as liver, adipose tissue and muscle. In line with the insulin-mediated impairment in Treg induction, T cell specific InsR deficiency significantly increased Treg induction capacity using naïve T cells from mesLNs and VAT. This effect was maintained in DIO. From a mechanistic point of view, the results shown here provide evidence that insulin increases cellular glucose uptake which might lead to an increased glycolytic activity that results in the observed higher T cell proliferation and consequently negative effects on Treg induction. In contrast, T cell specific InsR deficiency diminished cellular glucose uptake, thereby potentially limiting glycolytic activity and T cell proliferation whilst promoting Treg induction.

In summary, the results of this thesis will help to better understand links between the metabolic and the immune system in order to more specifically target TFH cells and Tregs in future therapeutic strategies for the treatment of metabolic diseases including obesity and diabetes.

## Zusammenfassung

Kürzlich wurde gezeigt, dass Wechselwirkungen zwischen immunologischen-, metabolischen- und Umweltfaktoren eine entscheidende Rolle bei der Entstehung von Adipositas spielen, welche von chronischen, schwachen Entzündungsprozessen und Insulinresistenz begleitet wird. Eine obesogene Umgebung kann die Anzahl, Funktionalität und den zellspezifischen Metabolismus verschiedener Immunzellpopulationen im lymphatischen Gewebe, sowie insbesondere im Fettgewebe, welches als Entzündungsherd der Adipositas zählt, beeinflussen. Pro-inflammatorische  $CD4^+CXCR5^+(PD1^{hi}Bcl6^{hi})$  folliculäre Effektor-T-Helferzellen (TFH-Zellen) und suppressive, entzündungshemmende regulatorische  $Foxp3^+$ T-Zellen (Tregs) sind entscheidende Mediatoren der Immunaktivierung versus Immunregulation. Letztere sind besonders wichtig für die Immuntoleranz im Fettgewebe, da sie bei Adipositas die Entzündung des Gewebes dämpfen und somit dessen Homöostase aufrechterhalten. Das Hormon Insulin ist von entscheidender Bedeutung für die Stoffwechselkontrolle des Körpers und Insulinresistenz in den peripheren, insulin-sensitiven Geweben ist ein Hauptmerkmal der Adipositas. Jedoch ist der spezifische Beitrag von TFH-Zellen und Tregs, sowie von metabolischen Signalwegen (z.B. Insulin-Signalweg), welche den Metabolismus und das Immunsystem verbinden, zur Adipositas noch nicht vollständig entschlüsselt.

Die vorliegende Arbeit liefert erste Indizien dafür, dass die Anzahl von  $CD4^+CXCR5^+PD1^{hi}$ TFH Vorläufer-Zellen sowohl in den Lymphknoten als auch im entzündeten viszeralen weißen Fettgewebe von diätinduzierten adipösen Mäusen, erhöht ist. Eine erhöhte Anzahl an Vorläufer-TFH-Zellen wurde auch in genetisch adipösen ob/ob-Mäusen beobachtet. Hier war die Frequenz von ausgereiften  $CD4^+CXCR5^+PD1^{hi}Bcl6^{hi}$ TFH-Zellen in den mesenterialen Lymphknoten signifikant erhöht. Eine signifikant erhöhte Genexpression von *Ii21* und ein Trend zur höheren Expression von *ICOS* und *Bcl6* repräsentieren Charakteristika vollständig differenzierter TFH-Zellen und waren in  $CD4^+CXCR5^+$ TFH-Zellen aus mesenterialen Lymphknoten von normalgewichtigen und diätinduzierten adipösen Mäusen vorzufinden. Frühere Forschungsergebnisse im Bereich der Autoimmunität zeigten eine positive Korrelation zwischen der Expression von microRNA92a und der Anzahl an TFH-Zellen. MicroRNA92a konnte nicht als wichtige Verknüpfung zwischen Adipositas und der Anzahl an (Vorläufer-)TFH-Zellen bestätigt werden. Eine begrenzte Anzahl an humanen, peripheren Blutproben und viszeralen Fettgewebsbiopsien war verfügbar, um eine mögliche Relevanz von (Vorläufer-)TFH-Zellen für die Adipositas beim Menschen zu erforschen. Es konnte gezeigt werden, dass Adipositas und Insulinresistenz einen Einfluss auf die Anzahl von Th1-, Th2- und Th17-ähnlichen

(Vorläufer-)TFH-Zellen im menschlichen peripheren Blut haben. Darüber hinaus waren die frühen TFH-Zellmarker *Asc12* und *Il21* im viszeralen Fettgewebe von adipösen, insulinresistenten Individuen erhöht. Dies spiegelt das adipöse, viszerale Fettgewebe als günstiges Umfeld für (Vorläufer-)TFH-Zellen wider.

Die Expression des Insulinrezeptors auf aktivierten CD4<sup>+</sup>T-Zellen und die Bedeutung des PI3K-Akt-mTOR-Signalwegs für sowohl Insulin-vermittelte metabolische Reaktionen als auch eine stabile, funktionelle Induktion von Foxp3<sup>+</sup>Tregs, ergeben eine gute Möglichkeit den Einfluss von metabolischen Faktoren auf die Induktion und Funktion von Tregs zu erforschen. In dieser Arbeit wurde gezeigt, dass Insulin die *in vitro* Induktion von Foxp3<sup>+</sup>Tregs aus naiven CD4<sup>+</sup>T-Zellen der Lymphknoten oder des viszeralen Fettgewebes von normalgewichtigen und diätinduzierten adipösen Mäusen beeinträchtigt. In ähnlicher Weise verringerte Insulin die Treg-Induktion unter Verwendung naiver CD4<sup>+</sup>T-Zellen aus den mesenterialen Lymphknoten von genetisch adipösen ob/ob-Mäusen. Diese Ergebnisse zeigen, dass diätinduzierte adipöse und ob/ob-Mäuse trotz ihrer Insulinresistenz in den metabolisch aktiven Geweben wie Leber, Fettgewebe und Muskel, ihre Insulinsensitivität auf T-Zell-Ebene beibehalten. Im Einklang mit der insulinvermittelten Beeinträchtigung der Treg-Induktion führte ein T-Zell-spezifischer Insulinrezeptor-Knockout zu einer erhöhten Induktion von Tregs unter Verwendung von naiven T-Zellen aus mesenterialen Lymphknoten und viszeralem Fettgewebe. Dieser Effekt wurde in der diätinduzierten Adipositas aufrechterhalten. Aus mechanistischer Sicht belegen die hier gezeigten Ergebnisse, dass Insulin die zelluläre Glukoseaufnahme in T-Zellen erhöht, was zu einer gesteigerten glykolytischen Aktivität führen kann, welche die Proliferation von T-Zellen bedingt und die Induktion von Tregs negativ beeinflusst. Im Gegensatz dazu verringerte ein T-Zell-spezifischer Insulinrezeptor-Knockout die zelluläre Glukoseaufnahme, wodurch möglicherweise die glykolytische Aktivität und die Proliferation von T-Zellen vermindert werden, während die Treg-Induktion gefördert wird.

Zusammenfassend können die Ergebnisse der vorliegenden Arbeit dazu beitragen, die Zusammenhänge zwischen dem Immunsystem und dem Stoffwechsel besser zu verstehen, um in therapeutischen Strategien zur Behandlung von Stoffwechselkrankheiten und insbesondere von Adipositas und Diabetes gezielt auf TFH-Zellen und Tregs einzugehen.

# 1. Introduction: Obesity- an immune-metabolic disease

## 1.1. Characteristics of obesity and the metabolic part of the disease

### 1.1.1. The prevalence and incidence of obesity

The prevalence of overweight and obesity is rising dramatically worldwide. In 2016, about 15 % of all women and 11 % of all men of the world's adult population were obese. This accounts for 13 % of the world's total population and reflects nearly a triplication of the disease in the last 40 years. (WHO, 2017) Although obesity is less prevalent among children (< 20 years of age; 5 % prevalence), there is a more prominent increase in childhood compared to adult obesity as recently published and analyzed over 25 years in the "Global Burden of Disease Study" with a cohort of 68.5 million individuals in 195 countries (Collaborators et al., 2017). Overweight and obesity are characterized by a high body mass index (BMI), calculated as weight in kilograms divided by the square of the body height in meters, and are associated with an elevated risk of developing type 2 diabetes (T2D) and cardiovascular diseases. Globally around four million people died due to an elevated BMI (BMI: 25 - < 30 kg/m<sup>2</sup> overweight; BMI: ≥ 30 kg/m<sup>2</sup> obesity) and obesity-associated comorbidities in the last 40 years. (Collaborators et al., 2017) According to the definition of the International Diabetes Federation (IDF), the occurrence of central obesity together with two of the following conditions: elevated serum triglycerides, reduced high-density lipoprotein levels, raised blood pressure and elevated fasting plasma glucose levels, is defined as metabolic syndrome (IDF, 2006).

### 1.1.2. The pathophysiology of obesity and its characteristics

Obesity is a result of our modern, sedentary life style with decreased levels of physical activity and associated low energy expenditure in combination with increased intake of an always available, calorically dense, highly processed, inexpensive palatable and cheap diet (Chin et al., 2016; van der Klaauw & Farooqi, 2015). Besides these **environmental factors**, **gene variants** were identified as causal for obesity (van der Klaauw & Farooqi, 2015). ~20 single gene disruptions cause an extremely severe, autosomal form of obesity mainly by affecting the leptin-melanocortin pathway in the central nervous system (CNS) which is a critical regulator of whole-body energy homeostasis. Monogenetic obesity is caused by polymorphisms in genes that encode *e.g.* leptin, leptin receptor, melanocortin-4 receptor (MC4R) or pro-opiomelanocortin (POMC), resulting in increased appetite and diminished satiety. (O'Rahilly, 2009) Additionally, genome wide association studies (GWAS) identified > 80 genetic loci with single-nucleotide polymorphisms (SNPs) associated with the

susceptibility to obesity, including the FTO (fat mass and obesity-associated) locus (Frayling et al., 2007).

Obesity is a complex metabolic disease that affects multiple organs including adipose tissue (AT), liver, muscle, brain and pancreas simultaneously. Molecular, physiological and behavioral pathways play a critical role in obesity development, progression and persistence. The complexity of obesity complicates understanding its pathophysiology and exacerbates adequate treatment of the disease and its secondary complications. In addition, there is growing evidence for a cross physiological communication of the metabolic system with the immune system in the disease development. **Inflammation of the visceral white adipose tissue (VAT)** was identified as a key event in the pathogenesis of obesity and pathological and inflammatory changes in VAT were shown to ultimately affect the whole-body providing the basis for obesity-associated comorbidities (**compare chapter 1.3.2**). (Kanneganti & Dixit, 2012; Redinger, 2007)

**Insulin resistance** in the peripheral metabolic active tissues (liver, AT, muscle) is one major characteristic of obesity and is discussed in detail in **chapter 1.3.3**. Besides insulin resistance obese individuals suffer from **hyperglycemia** resulting from decreased utilization of insulin-stimulated muscle glucose and associated increased compensating hepatic gluconeogenesis. Hyperglycemia was identified both as source and consequence of insulin resistance. (Hatting et al., 2018) The pancreatic  $\beta$ -cell mass expands in obesity to prevent hyperglycemia by providing sufficient amounts of insulin. Increased insulin production in combination with insulin resistance results in systemic **hyperinsulinemia**. However, the causal role of insulin hypersecretion in obesity development remains controversial. Hyperinsulinemia was shown to affect lipid-and glucose metabolism and might trigger the progression of chronic AT inflammation, thereby strengthening disease progression. (Templeman et al., 2017) Furthermore, **dyslipidemia** (increased fasting plasma triglycerides) (Klop et al., 2013), **lipotoxicity** (enhanced lipolysis and release of free fatty acids (FFA) creating oxidative stress) (Yazici & Sezer, 2017) and **hypertension** (Jiang et al., 2016) are attributes of obesity. Persistent obesity is associated with **systemic inflammation**, the manifestation of the metabolic syndrome and progression to cardiovascular diseases and T2D. Additionally, obesity increases the risk for cancer and premature death. (Redinger, 2007; Templeman et al., 2017)

### 1.1.3. Animal models of obesity

Clinical investigation of obesity is limited to the analysis of body composition, peripheral blood samples, tissue biopsies and other non-or minimal invasive metabolic assessments (Collet, 2000). Model organisms are thus indispensable to overcome these limitations and to get more detailed information about the disease pathology. Several mouse models are currently available and are beneficial for reproducible pre-clinical investigation of both the immune system and the metabolism in genetic or diet-induced obesity (DIO) and insulin resistance. (Kleinert et al., 2018)

The leptin-null *Lep<sup>ob</sup>* mouse, commonly referred as *ob/ob* mouse, was discovered by chance in a colony at the Jackson Laboratory by Snell and colleagues in 1949 and the mutated gene was designated by the symbol *ob* (obese) (Ingalls et al., 1996). In 1994, Zhang and colleagues (Zhang et al., 1994) identified the hormone leptin as a product of the obese (*ob*) gene by positional cloning of this gene. They showed that the *ob* gene, then called *Lep* (Leptin), encodes a 4.5-kilobase AT messenger RNA with a highly conserved 167-amino-acid open reading frame. The *Lep* gene is encoded on Chromosome 6 in mice and a spontaneous, autosomal recessive, non-sense C to T mutation in codon 105 of this gene inhibits expression of the 16 kDa leptin protein. This mutation prevents the secretion of bioactive leptin by white adipocytes and impairs its impact on central circuits controlling food intake and glucose metabolism. (Zhang et al., 1994) The *ob/ob* mouse is a well-established and for decades intensively studied pre-clinical monogenetic mouse model of metabolic diseases. It is especially valuable to investigate monogenetic forms of obesity. (Kleinert et al., 2018) Traditionally, *ob/ob* mice are maintained on C57BL/6J background (Loten et al., 1974). *Ob/ob* mice are characterized by an early-onset of obesity caused by hyperphagia and decreased energy expenditure due to reduced non-shivering thermogenesis of the brown adipose tissue (BAT). Thereby *ob/ob* mice can reach three times the normal weight of their wildtype (WT) controls. Additionally, *ob/ob* mice are characterized by mild hyperglycemia, hyperinsulinemia caused by compensatory hypertrophy and hyperplasia of the  $\beta$ -cells to control high glucose levels, insulin resistance, hypothyroidism and increased circulating corticosterone levels. (Coleman, 1978; Garris & Garris, 2004; Himms-Hagen & Desautels, 1978)

Besides monogenetic mouse models, mice with targeted cell type specific gene modifications are an additional way to study metabolic pathways with regard to obesity pathology. On the contrary to global knockouts, Cre-lox recombination applies gene deletions, insertions, inversions and translocations at defined sites in the DNA of cells to enable targeted activation, repression or exchange of specific genes. The Cre-lox recombination technology

was developed by Sauer and Henderson in 1988 (Sauer & Henderson, 1988). Since then this simple and powerful method is widely used, among others to delete metabolism relevant genes in T cells *in vivo*. The Cre-lox recombination technology enables *e.g.* the crossing of mice in which the Cre-recombinase is expressed under the control of CD4 enhancer/promotor/silencer (CD4-Cre) with mice having the insulin receptor (InsR) gene flanked by *loxP* sites (InsRLox), resulting in mice with a T cell specific loss of the InsR, named InsR TKO mice. In this specific case, the InsR is knocked out in both CD4<sup>+</sup> and CD8<sup>+</sup>T cells, since CD4-Cre conditionally deletes genes in the double positive stage (CD4<sup>+</sup>CD8<sup>+</sup>T cells) of T cell development and in mature, single positive CD4<sup>+</sup>T cells, as described by Lee *et al.* (Lee et al., 2001).

In addition to genetic modifications of mice, the pathogenesis of human obesity can be resembled by DIO. DIO largely reflects the pathogenesis of human obesity with respect to its slow progression in body weight (BW) gain and the development of insulin resistance. To study the effect of obesity progression on the whole-body metabolism and on the immune system, mice can be *ad libitum* exposed to a standardized calorie-dense diet which is highly enriched in fats and sucrose (HFHS diet). The development of obesity and diabetes is then monitored by *e.g.* BW assessments and glucose tolerance tests (GTTs). Inbred C57BL/6J mouse strains are highly susceptible to DIO compared to other mouse strains and prone to develop severe hyperphagia-induced obesity, impaired glucose tolerance and moderate insulin resistance when put into an obesogenic environment. Thus, they are favored for metabolic studies. (Kleinert et al., 2018; Surwit et al., 1988; West et al., 1992; Winzell & Ahren, 2004) To reach optimal obesity progression, dietary intervention should start when the mice are  $\geq 8$  weeks of age (Nishikawa et al., 2007). The duration of DIO progressively increases hyperinsulinemia, accompanied by a worsening of insulin resistance. Already one week of a high-fat, high sugar (HFHS) diet slightly increases insulin levels and decreases insulin sensitivity. After 16-20 weeks of HFHS diet obesity is normally manifested and characterized by peripheral insulin resistance, hyperinsulinemia, adipocyte hyperplasia, fat deposition in the mesentery, increased fat mass and hypertension. The degree of insulin resistance depends on genetic factors *e.g.* sex and strain and environmental factors *e.g.* housing. (Speakman et al., 2007; Winzell & Ahren, 2004) Male C57BL/6J mice show higher susceptibility to DIO characterized by early onset of obesity and both more pronounced insulin resistance and glucose intolerance compared to females (Hong et al., 2009; Medrikova et al., 2012; Yang et al., 2014). They develop more VAT and less subcutaneous (SAT) fat mass than females (Macotela et al., 2009). However, since the obesity pandemic affects both male and females, research should be conducted in both sexes to ameliorate the translational value (Kleinert et al., 2018).

#### 1.1.4. The body's adipose tissue compartments

Given the importance of VAT inflammation for the pathogenesis of obesity, it is of great interest to gain a closer look on the body's AT compartments, mainly consisting of adipocytes. These cells are classically divided into two subtypes that might originate from different mesenchymal stem cell lineages, but share a subsequent peroxisome proliferator-activated receptor gamma (PPAR $\gamma$ ) driven adipogenic differentiation program (Giralt & Villarroya, 2013). Unilocular white adipocytes store excess calories in form of triglycerides in order to provide energy during periods of starvation (Konige et al., 2014), representing their function as key regulators of nutritional homeostasis and energy balance (Rutkowski et al., 2015). On the contrary, multilocular brown adipocytes are densely packed with mitochondria and are involved in thermogenesis by dissipating stored chemical energy in form of heat through the activation of uncoupled respiration using uncoupling protein 1 (UCP1) (Giralt & Villarroya, 2013). Cold exposure, chronic  $\beta$ 3-adrenergic receptor activation or a short-term high calorie diet were shown to trigger the appearance of inducible, beige adipocytes at anatomical sites characteristic for white AT. Beige adipocytes show similar morphology, function and overlapping, but distinct gene expression patterns compared to brown adipocytes. (Rothwell & Stock, 1997; Wu et al., 2012)

The distribution of the different ATs is highly complex and depends on age, sex, genetics and physiological status. In men and mice, white AT is dominantly located in visceral (intra-abdominal) (VAT) and subcutaneous (beneath the skin) (SAT) localities. (Lidell et al., 2013; Mann et al., 2014) Murine BAT accumulates in the interscapular and perirenal regions (Mann et al., 2014), whilst human BAT can only be found deep in the supraclavicular and spinal regions of adults and interscapularly in infants (Lidell et al., 2013).

VAT represents a loose connective tissue, consisting of an adipocyte and a stromal vascular fraction (SVF). Adipocytes comprise about 90 % of the AT volume, whilst accounting for only 20-40 % of the AT's cellular mass. (Martyniak & Masternak, 2017; Rosen & Spiegelman, 2014) The cellular composition of VAT undergoes continuous dynamic remodeling in response to physiological changes such as reduced energy expenditure and excess calories that need to be stored. In obesity, this process assumes pathological dimensions associated with alterations in AT function (**compare chapter 1.3.2**). (Choe et al., 2016; Wang et al., 2013) Cells of the SVF surround adipocytes and include a variety of innate and adaptive immune cells, pre-adipocytes, endothelial cells and fibroblasts (Kanneganti & Dixit, 2012). More specifically, the immune cell population residing in the SVF comprises among others macrophages (Weisberg et al., 2003; Xu et al., 2003), CD4<sup>+</sup> and CD8<sup>+</sup>T cells (Nishimura et al., 2009; Zhao et al., 2018), B cells (Winer et al., 2011), neutrophils (Talukdar et al., 2012),

eosinophils (Wu et al., 2011), group 2 innate lymphoid cells (ILC2s) (Brestoff et al., 2015; Lee et al., 2015) and mast cells (Liu et al., 2009). Immune cells can be observed histologically as “crown-like structures” surrounding predominantly death adipocytes in obese VAT (Cinti et al., 2005; Coats et al., 2017; Feuerer et al., 2009), as milky spots (tiny white-colored areas of lymphoid tissue) (Rangel-Moreno et al., 2009) or are dispersed through the AT (Kolodin et al., 2015). Obesity is characterized by qualitative and quantitative changes in immune cells of the AT, affecting its function. This suggests that VAT serves as an important intersection linking immunity with metabolism. The specific characteristics and functions of AT-residing CD4<sup>+</sup>T cells and their Treg subpopulation are highlighted in **chapter 1.3.2.2** (Grant & Dixit, 2015).

## 1.2. Relevant immunological players in obesity

### 1.2.1. Adaptive immune cells- differentiation and function

The immune system effectively protects the body against diseases by innate and adaptive immune responses both contributing to immune homeostasis. Leukocytes are the cellular components of the immune system. They derive from pluripotent hematopoietic stem cells in the bone marrow and can differentiate into common lymphoid progenitors and subsequently into T and B cells. Antigen-specific T and B cells are key components of the adaptive immunity fulfilling different, distinct functions. B cells mature in the bone marrow and directly migrate to the peripheral lymphoid organs, whereas precursor T cells migrate to the thymus where Notch signaling instructs T cell lineage commitment (CD4 versus (vs.) CD8 decision) and where T cells undergo somatic T cell receptor (TCR) rearrangement. This results in an incredible diversity and specificity in their TCR repertoires and enables highly specific immune responses. (Moticka, 2016; Murphy & Weaver, 2016; Radtke et al., 2013; Zhu et al., 2010)

TCRs that are compatible with self-peptide-major histocompatibility complex (MHC) molecules are characteristic for self-reactive T cells. These cells are eliminated by the immune system by mechanisms of central and peripheral tolerance which are present throughout life. (Xing & Hogquist, 2012) Immune tolerance is indispensable for human health, since it avoids reactions against the body's own structures (autoimmunity), a phenomenon that was already described in the early 20<sup>th</sup> century as "horror autotoxicus" by Paul Ehrlich (Ehrlich, 1906). Central tolerance is induced during somatic TCR rearrangement in the thymus, resulting in the elimination of self-reactive T cells by a process called negative selection (Daley et al., 2017; Kappler et al., 1987; Kisielow et al., 1988). Autoreactive T cells that escape negative selection enter peripheral lymphoid and non-lymphoid tissues and are eliminated via peripheral, dominant tolerance which is mainly conducted by regulatory T cells (Tregs) (**compare chapter 1.2.2**) (Sakaguchi et al., 1995; Thornton & Shevach, 1998).

T cells that have TCRs with low affinity for self-peptide-MHC complexes are positively selected, enter the bloodstream, circulate through peripheral lymphoid tissues, return via the lymphatics to the bloodstream and recirculate between blood and peripheral lymphoid tissues (Murphy & Weaver, 2016; Xing & Hogquist, 2012). Here, antigen-specific, yet naïve T cells of the CD4 lineage (CD4<sup>+</sup>T cells) get rapidly activated upon interaction of their TCR with cognate peptide-MHCII ligands presented by antigen-presenting cells (APCs). T cell activation is followed by clonal expansion and differentiation into various different types of effector T lymphocytes. (Smith-Garvin et al., 2009)

The distinct cytokine milieu determines the T cell fate, resulting in T helper (Th) 1, Th2, Th17 and T follicular helper (TFH) cells and several other T helper cell subsets with distinct effector functions and alternatively into suppressive Tregs (Murphy & Weaver, 2016; Zhu et al., 2010). There is growing evidence, that T cells are highly flexible and plastic in their gene expression and cell identity and that small variations in their gene expression profiles can govern cell fate decisions made by these cells, contradicting the theory of stable lineages or subsets (DuPage & Bluestone, 2016). Effector CD4<sup>+</sup>T cells are highly specialized and combined by their common goal: clearance of the pathogen from the body. Th1 cells produce interferon gamma (IFN $\gamma$ ) and other cytokines that activate macrophages which enables them to efficiently destroy intracellular microorganisms. Th2 cells trigger humoral immunity and are involved in allergic responses. They produce interleukin (Il) 4, Il5, Il9 and Il13 and thereby recruit and activate eosinophils, mast cells and basophils which promote barrier function at mucosal surfaces. Th17 cells secrete cytokines of the Il17 family which results in the recruitment of neutrophils to the site of infection and is part of the early adaptive immune response. (Murphy & Weaver, 2016; Zhu et al., 2010) Another crucial function of T cells is to support B cells for antibody production. Especially TFH cells can provide signals to antigen-stimulated B cells, thereby influencing their differentiation and antibody class switching (**compare chapter 1.2.3**). (Crotty, 2014)

Upon activation by antigen-engagement, some of the T and B cells differentiate into memory cells and thereby generate a long-lasting immunity. Memory T and B cells are characterized by a fast and enhanced immune response following the second exposure to their specific antigen. Summing up, a balance between effector T cells and Tregs is critical to ensure immune competence while avoiding immune pathology and autoimmunity. (Murphy & Weaver, 2016)

### **1.2.2. Mediators of immune tolerance: Regulatory T cells**

Tregs are a subset of CD4<sup>+</sup>T cells with immunosuppressive functions and play a critical role in maintaining immune homeostasis (Sharma & Rudra, 2018; Zhao et al., 2017). Tregs are diverse in their origin and either develop in the thymus (Apostolou et al., 2002; Itoh et al., 1999; Jordan et al., 2001) or are induced from naïve CD4<sup>+</sup>T cells in the periphery (Apostolou & von Boehmer, 2004; Chen et al., 2003; Kretschmer et al., 2005), however, there is so far no specific marker to distinguish between these two Treg populations. Tregs are characterized by high expression of the Il2 receptor alpha-chain (CD25) (Sakaguchi et al., 1995; Thornton & Shevach, 1998) and the expression of Forkhead box protein 3 (Foxp3) (Fontenot et al., 2003; Fontenot et al., 2005; Hori et al., 2003; Khattri et al., 2003; Roncador

et al., 2005). The latter is the lineage specifying factor and master transcription factor of Tregs which is essential for their development and function (Fontenot et al., 2003; Fontenot et al., 2005; Hori et al., 2003; Khattri et al., 2003; Roncador et al., 2005). Additionally, Cytotoxic T-lymphocyte antigen 4 (CTLA4) and Glucocorticoid-induced TNFR-related protein (GITR), are highly expressed in Tregs compared to conventional T cells (Tconv.) in a Foxp3-independent manner (Gavin et al., 2007). In the human setting, CD25 is also expressed by activated CD4<sup>+</sup>T cells and absence of the interleukin 7 receptor  $\alpha$ -chain (CD127) is used as a marker complementary to CD25 to more precisely identify human Tregs (Liu et al., 2006). Tregs are long-lived and predominantly exhibit stable Foxp3 expression. However, there is growing evidence for an unstable Treg phenotype under pro-inflammatory or pathogenic conditions. Unstable Tregs are characterized by a loss of Foxp3 expression and conversion of Tregs into ex-Tregs with acquisition of an effector T cell-like phenotype. (Dominguez-Villar & Hafler, 2018; Sakaguchi et al., 2013)

In contrast, a stable Treg phenotype is associated with Treg specific hypomethylation of the Foxp3 locus and especially with complete demethylation at the CpG-rich site of the conserved noncoding sequence 2 (CNS2) which is part of the Foxp3 locus and also known as Tregs-specific demethylated region (TSDR) (Baron et al., 2007; Polansky et al., 2008; Someya et al., 2017; Zheng et al., 2010). Thereby, the CNS2 region of the DNA is accessible for binding of transcription factors *e.g.* the runt-related transcription factor 1 (RUNX1) - core-binding factor subunit beta (CBF $\beta$ ) heterodimer which is indispensable for sustained high and stable Foxp3 expression in Tregs and their suppressive function (Kitoh et al., 2009). On the contrary, effector T cells have a completely methylated TSDR (Dominguez-Villar & Hafler, 2018; Floess et al., 2007; Polansky et al., 2008).

Foxp3<sup>+</sup>Tregs are essential for maintaining peripheral immune tolerance, prevent autoimmune diseases, such as type 1 diabetes (T1D), and are critical players in limiting chronic inflammatory diseases. Congenital deficiency in Tregs causes fatal autoimmunity in so called scurfy mice (Ramsdell & Ziegler, 2014) and Immundysregulation-Polyendokrinopathy-Enteropathy-X-chromosomal (IPEX) syndrome in humans (Bacchetta et al., 2018). Tregs act via basically four different modes of action to mediate suppression: Suppression by secretion of immunosuppressive cytokines *e.g.* Transforming growth factor- $\beta$  (TGF $\beta$ ) (Green et al., 2003), Il10 and Il35 (Wei et al., 2017); Suppression of T cell responses and death of effector T cells by cytotoxicity via secretion of granzyme B and perforin (Cao et al., 2007; Gondek et al., 2005); Suppression by disruption of the metabolic environment of the effector T cells *e.g.* by 'consuming' all surrounding Il2, a cytokine that is needed by effector T cells to survive and trigger immune responses, by high expression of CD25 (Pandiyani et al., 2007; Thornton &

Shevach, 1998) and suppression by modulation of the activity of APCs *e.g.* dendritic cells (DCs) or macrophages which are required for the activation of effector T cells (Liu et al., 2011; Misra et al., 2004; Tiemessen et al., 2007). Lymphoid Tregs, circulating Tregs and Tregs that reside in non-lymphoid tissues exhibit a high functional and phenotypic heterogeneity which is not discussed in detail here. Especially Foxp3<sup>+</sup>Tregs in VAT bear a distinct phenotype and functions beyond suppression. They were identified as critical mediators in dampening obesity-associated tissue inflammation and maintaining tissue homeostasis (**compare chapter 1.3.2.2**) (Becker et al., 2017; Panduro et al., 2016). These functions recently brought them into the limelight.

### 1.2.2.1. *In vivo* and *in vitro* Treg induction

*In vitro* Foxp3<sup>+</sup>Treg induction is commonly performed by stimulating naïve Foxp3<sup>-</sup>CD25<sup>-</sup>CD4<sup>+</sup>T cells via their TCR in the presence of TGFβ. Thereby induced Tregs lose their Foxp3 expression and their suppressive capacity upon re-stimulation in the absence of TGFβ and more importantly show a methylated TSDR which indicates that they are not stable and do not resemble *in vivo* generated Tregs. This reflects that differentiation of naïve CD4<sup>+</sup>T cells into functional Tregs can predominantly occur under conditions that simultaneously induce epigenetic fixation of the Treg phenotype by TSDR demethylation. (Floess et al., 2007; Polansky et al., 2008).

Efficient *de novo* Treg induction in the absence of TGFβ in the peripheral immune system of mice was demonstrated by several studies. This *in vivo* Treg induction was shown to be most efficient using a strong agonistic ligand for the TCR, supplied under subimmunogenic conditions, thereby avoiding general immune activation. Results of these studies additionally highlight that a weak interaction of the agonistic ligand with the TCR cannot be compensated by higher doses of the ligand. (Daniel et al., 2011; Daniel et al., 2010; Gottschalk et al., 2010; Gottschalk et al., 2012; Kretschmer et al., 2005) The group of Matthias Merkenschlager (Sauer et al., 2008) confirmed that Tregs can be *in vitro* induced in the absence of TGFβ by limiting the activity of the Phosphoinositid-3-kinase (PI3K) - Protein kinase B (Akt) - Mammalian target of rapamycin (mTOR) pathway and/or by premature deprivation of the TCR stimulus. The latter was recently confirmed by us (Serr et al., 2016a). On the contrary, continuous TCR stimulation and constitutively active PI3K-Akt-mTOR signaling antagonize Foxp3<sup>+</sup>Treg induction. Additionally, PI3K-Akt-mTOR signaling was identified to control a Treg-like transcriptional program, reflecting that this approach of *in vitro* Treg induction shares features with the development of Tregs *in vivo* (Sauer et al., 2008).

PI3K is activated by engagement of the TCR, CD28 co-stimulation, cytokine signaling *etc.* resulting in phosphorylation and activation of Akt (Merkenschlager & von Boehmer, 2010). However, Akt can also be activated independently by the costimulatory CD28 pathway (Garcon et al., 2008). Akt phosphorylates and activates mTOR, resulting in subsequent phosphorylation of Forkhead box protein O (Foxo) proteins including Foxo1 and Foxo3a and their nuclear export into the cytoplasm (Merkenschlager & von Boehmer, 2010). However, binding of Foxo1 and Foxo3a to the promotor region of Foxp3 in the nucleus is essential for the expression of Foxp3 (Kerdiles et al., 2010). Since Foxp3 is indispensable for stable and functional Tregs, Treg induction can be increased by molecules that counteract the PI3K-Akt-mTOR pathway such as phosphatase and tensin homologue (Pten), PI3K inhibitors, Akt inhibitors or mTOR inhibitors (Sauer et al., 2008). A low activity of the PI3K-Akt-mTOR pathway in activated T cells is hence associated with most efficient induction of functional Foxp3<sup>+</sup>Tregs which was confirmed by several publications (Delgoffe et al., 2009; Delgoffe et al., 2011; Haxhinasto et al., 2008; Zeng et al., 2013).

As mentioned above, TCR signaling strength and duration are critical for Treg function (Li & Rudensky, 2016). In addition to suppressing the activity of Foxo proteins via activation of Akt and subsequent negative effects on Foxp3 expression (Merkenschlager & von Boehmer, 2010), TCR stimulation was shown to, among others, activate the Transcription factors nuclear factors of activated T cells (NFATs) (Gabriel et al., 2016; Tone et al., 2008), Nuclear factor 'kappa-light-chain-enhancer' of activated B cells (NF-κB) (Long et al., 2009; Schuster et al., 2012) and Nr4a1 family of transcription factors (Nr4a1) (Sekiya et al., 2013). NFATs, NF-κB and Nr4a1 are crucial for maintenance of the Treg identity by binding to different parts of the Foxp3 locus, inducing Foxp3 expression (Gabriel et al., 2016; Long et al., 2009; Schuster et al., 2012; Sekiya et al., 2013; Tone et al., 2008). Additionally, E3 ubiquitin ligase casitas-B-lineage lymphoma protein (Cbl) b was shown to control *in vitro* and *in vivo* Treg development by tuning TCR signaling strength (Qiao et al., 2013) and Cbl-b deficiency in T cells was identified to result in defective Foxp3 induction (Harada et al., 2010). RasGRP1, a Ras-guanyl-nucleotide exchange factor, links TCR signaling with the activation of the Ras/Mitogen-activated protein kinase (MapK) signaling pathway. RasGRP1 and thus Ras/MapK signaling was shown to be important for thymic Treg development, but dispensable for the expansion and suppressive function of peripheral Tregs (Chen et al., 2008). This is in line with an increased induction of suppressive Foxp3<sup>+</sup>Tregs upon inactivation of the Ras/MapK signaling pathway in T cells (Liu et al., 2013; Luo et al., 2008). In addition to the TCR signaling strength and duration, cytokines (*e.g.* TGFβ, Tumor necrosis factor (TNF) α, IL2) critically contribute to Treg induction. IL2, the “key Treg cell growth factor”, is required for Treg survival and lineage stability (Burchill et al., 2007; Chen et al., 2011; Yao

et al., 2007). Il2 was shown to promote Foxp3<sup>+</sup>Treg induction via activation of Signal Transducers and Activators of Transcription (Stat) 5a and Stat5b (Burchill et al., 2007; Yao et al., 2007). Furthermore, Stat3 was identified as critical for Treg differentiation, Foxp3 expression and Treg function (Chaudhry et al., 2009; Pallandre et al., 2007). This highlights that Treg induction and function are tightly regulated and depend on an interplay between multiple transcription factors.

### 1.2.3. T follicular helper cells

T follicular helper (TFH) cells are a subset of CD4<sup>+</sup>T cells and belong to the group of effector T cells. TFH cells are mainly characterized by the expression of C-X-C chemokine receptor type 5 (CXCR5) (Breitfeld et al., 2000; Kim et al., 2001; Schaerli et al., 2000), the master transcription factor B cell lymphoma 6 (Bcl6) (Johnston et al., 2009; Nurieva et al., 2008; Yu et al., 2009) and by secretion of their effector cytokine Il21 (Avery et al., 2010; Linterman et al., 2010; Zotos et al., 2010).

TFH cells are specialized to provide help to follicular or germinal center (GC) B cells. GCs are compartments developed by follicles of secondary lymphoid organs (e.g. lymph nodes (LNs), tonsils, spleen), consisting of B cells, macrophages, follicular DCs, GC TFH cells and stroma. The GC reaction is a key feature of adaptive humoral immunity against foreign pathogens since the interaction of TFH cells with follicular B cells in the GCs leads to B cell maturation and the secretion of high-affinity antibodies by plasma B cells generating long-lived functional humoral immune responses and sustained immune protection. (Crotty, 2014) More specifically, GC TFH cells provide signals to GC B cells that are essential for their survival, differentiation, affinity maturation, isotype switching and high affinity antibody secretion. (Breitfeld et al., 2000; Johnston et al., 2009; Kim et al., 2017; Nurieva et al., 2008; Schaerli et al., 2000; Yu et al., 2009). Though, all above presented functions are restricted to GC TFH cells, these cells might have yet unknown additional functions outside the GCs (Crotty, 2014) e.g. in the AT.

TFH cells differentiate from CD4<sup>+</sup>T cells in a non-linear, highly complex, multifactorial process, consisting of multiple differentiation steps which are tightly regulated by various molecules and signaling cues (Crotty, 2014). Upon activation via their TCR, naïve T cells are primed towards CD4<sup>+</sup>CXCR5<sup>+</sup>ICOS<sup>+</sup>T cells that secrete Il21 (Deenick et al., 2010; Goenka et al., 2011; Langenkamp et al., 2003). The additional expression of Bcl6 depends on either transient induction by Il21 and Il6 (Eto et al., 2011; Nurieva et al., 2008; Nurieva et al., 2009) or signaling of Inducible T cell costimulator (ICOS). ICOS is highly expressed on early TFH

cells and induces Bcl6 expression by unblocking its repression by Foxo1 (Choi et al., 2011; Stone et al., 2015). Foxo1, on the other hand, can be repressed by E3 ubiquitin ligase ITCH (N. Xiao et al., 2014). ICOS also increases the production of Il21 by TFH cells (Odegard et al., 2008) and influences their differentiation and migration towards the B cell follicle via the interaction with ICOS-ligand on B cells (Akiba et al., 2005; Xu et al., 2013). The transcriptional repressor PR domain zinc finger protein 1 (Blimp1) is a negative regulator that suppresses TFH cell differentiation. Thus, Bcl6 and Blimp1 are reciprocal and antagonistic regulators of the TFH cell fate. (Crotty et al., 2010; Johnston et al., 2009) E-protein Achaete-scute complex homolog 2 (Ascl2) represents a transcription factor involved in early TFH cell differentiation (Kim et al., 2017; Liu et al., 2014). Murine studies by Liu *et al.* (Liu et al., 2014) showed that Ascl2 drives CXCR5 induction and that its expression precedes Bcl6 upregulation. Further characteristics of early TFH cell differentiation are the upregulation of Programmed cell death protein 1 (PD1) accompanied by both a downregulation of C-C chemokine receptor type 7 (CCR7) (Haynes et al., 2007; Shi et al., 2018) and cell adhesion molecule P-selectin glycoprotein ligand (PSGL1) (Hale et al., 2013; Odegard et al., 2008; Poholek et al., 2010). Bcl6 expression is closely connected with the expression of CXCR5 (Choi et al., 2011; Choi et al., 2013; Johnston et al., 2009) and PD1 (Kroenke et al., 2012; Shi et al., 2018). However, initiation of CXCR5 is feasible in the absence of Bcl6 (Liu et al., 2012).

Aforementioned TFH cell characteristics are indispensable for the migration of precursor TFH cells to the GCs in the secondary lymphoid organs and precede their interaction with B cells (Haynes et al., 2007; Odegard et al., 2008; Poholek et al., 2010). Especially the combined expression of high CXCR5 and low CCR7 levels was shown to be important for T cells to enter and accumulate at C-X-C motif chemokine 13 (CXCL13)- enriched B cell follicles enabling GC activity (Hardtke et al., 2005; Havenar-Daughton et al., 2016; Haynes et al., 2007; Tan, 2018). In the B cell follicles of the GCs, TFH cells undergo further maturation by interacting with follicular B cells. This results in continuous stimulation of precursor TFH cells and preserves their cell phenotype. (Baumjohann et al., 2013b; Choi et al., 2011; Choi et al., 2013) The maturation of TFH cells in the GCs is additionally associated with various changes in their expression of cell surface proteins, transcription factors and in their secretion of molecules (Crotty, 2014). GC-residing TFH cells for instance display much higher levels of Bcl6 than circulating precursor TFH cells (Hale et al., 2013). Additionally, they are specifically characterized by upregulation of *e.g.* SLAM-associated-protein (SAP) which is required for T to B cell adhesion, their prolonged contact and optimal TFH cell function in the GC reaction (Cannons et al., 2010; Deenick et al., 2010; Hu et al., 2013).

TFH cells underlie an enormous intrinsic heterogeneity enabling them to adapt to various environmental locations, conditions and needs and to respond against any form of pathogen (Crotty, 2014). TFH cells were examined in human tonsils (Breitfeld et al., 2000; Chtanova et al., 2004; Rasheed et al., 2006; Schaerli et al., 2000), human peripheral blood (Chtanova et al., 2004; Morita et al., 2011; Schmitt et al., 2014), the human intestinal tract (Zhou et al., 2018), murine blood and murine secondary lymphoid organs (Akiba et al., 2005; Choi et al., 2011; Weber et al., 2015). However, the designation “TFH cell” is conventionally reserved for CD4<sup>+</sup>CXCR5<sup>+</sup>T cells that are found within the GCs, while cells with a TFH profile found elsewhere are termed “precursor TFH cells” (Deenick & Ma, 2011). The frequencies of murine blood precursor TFH cells were shown to positively correlate with TFH cells in LNs (He et al., 2013). Thus, precursor TFH cells in the blood offer an excellent opportunity to study TFH cell responses in health and disease. Breitfeld *et al.* (Breitfeld et al., 2000) showed that the vast majority of human peripheral blood CD4<sup>+</sup>CD45RA<sup>-</sup>CXCR5<sup>+</sup> cells express low levels of CCR7 and high levels of PD1 and are thus precursor TFH cells. These cells were also identified as TFH cells with an antigen-experienced, memory state, since they can be readily re-activated to provide B cell help (Breitfeld et al., 2000).

There is evidence, that both human peripheral blood precursor TFH cells (Chtanova et al., 2004; Morita et al., 2011) and murine lymphatic TFH cells (Fazilleau et al., 2009) are comprised of a Th1-like, Th2-like and Th17-like subset. These subsets can be distinguished based on their cytokine profiles and the expression of C-X-C chemokine receptor type 3 (CXCR3) and C-C chemokine receptor type 6 (CCR6). CXCR3<sup>+</sup>CCR6<sup>-</sup>Th1-like TFH cells produce IFN $\gamma$ , CXCR3<sup>-</sup>CCR6<sup>-</sup>Th2-like TFH cells produce IL4, IL5 and IL13 and CXCR3<sup>-</sup>CCR6<sup>+</sup>Th17-like TFH cells are characterized by their secretion of IL17A and IL22 (Morita et al., 2011). Both Th2-like and Th17-like TFH cells can induce naïve B cells to differentiate into antibody producing plasma cells, whereas Th1-like TFH cells are inefficient B cell helpers (Bentebibel et al., 2013; Fazilleau et al., 2009; Morita et al., 2011). CD4<sup>+</sup>CXCR5<sup>+</sup>CXCR3<sup>+</sup>ICOS<sup>+</sup> precursor TFH cells, reflecting Th1-like TFH cells, were recorded to induce memory B cells, but not naïve B cells to differentiate into plasma B cells and produce high-affinity antibodies (Bentebibel et al., 2013). Thereby Th1-like TFH cells were shown to be capable to provide B cell help, although with lower efficiency than Th2- and Th17-like TFH cells (Locci et al., 2013). Th2-like and Th17-like TFH cells were additionally shown to differently regulate class switching of B cells, promoting either immunoglobulin (Ig)G and IgE responses (Th2-like) or IgG and IgA responses (Th17-like) (Fazilleau et al., 2009; Morita et al., 2011).

Given their important role in contributing to humoral immune responses and sustained immune protection, TFH cells were studied under various medical conditions such as in the context of chronic viral infection (Vella et al., 2017), vaccination (Linterman & Hill, 2016), autoimmune diseases (Scherm et al., 2016; Ueno, 2016) and recently also in the initiation and progression of autoimmune T1D due to their function of inducing high-affinity antibodies (Serr et al., 2016b). Here, increased levels of circulating precursor TFH cells were identified in children with recent onset of islet autoimmunity (Serr et al., 2016b). The limited knowledge about TFH cells in human obesity and associated T2D is presented in **chapter 1.3.2.1**.

### **1.2.3.1. *In vivo* and *in vitro* induction of TFH cells**

*In vivo* TFH cell differentiation is highly complex and research in mouse models upon immunization provides increasing knowledge about the *in vivo* TFH cell differentiation process and its regulation (Baumjohann & Ansel, 2015; Takebe et al., 2018), however TFH cell differentiation under systemic-low grade inflammation as in obesity remains to be investigated.

*In vitro* differentiation of murine naïve CD4<sup>+</sup>T cells into mature TFH cells is challenging and mainly performed using TCR-transgenic T cells, under immunizing conditions and in the presence of cytokines and neutralizing antibodies *e.g.* with IL21 and anti-IFN $\gamma$ /IL4/TGF $\beta$  (Nurieva et al., 2008) or with IL21, IL6 and anti-IFN- $\gamma$ /IL4/IL12/TGF $\beta$  (Lu et al., 2011). Kolenbrander and colleagues (Kolenbrander et al., 2018) recently showed *in vitro* TFH cell differentiation with “non-transgenic” CD4<sup>+</sup>T cells. Specifically, generation of IL21-producing CXCR5<sup>+</sup>Bcl6<sup>+</sup>TFH cells required co-culturing of “non-transgenic” CD4<sup>+</sup>T cells with DCs and B cell receptor transgenic B cells specific for the added HIV-derived virus-like particles. Results showed that thereby 10 % of the T cells differentiated into mature TFH cells (Kolenbrander et al., 2018). First efforts in murine TFH cell differentiation without immunization failed to generate mature TFH cells (Eto et al., 2011; Suto et al., 2008).

To get insights into the regulation of *in vitro* precursor TFH cell differentiation in human autoimmunity, naïve CXCR5<sup>+</sup>CD4<sup>+</sup>T cells were differentiated in the presence of autologous memory B cells, both isolated from human peripheral blood, resulting in low levels of CXCR5<sup>+</sup>CCR7<sup>low</sup>PD1<sup>hi</sup> precursor TFH cells (Serr et al., 2016b). Additionally, human *in vitro* precursor TFH cell differentiation was successful by co-culturing immunized naïve T cells and autologous memory B cells (He et al., 2013).

In summary, like Treg induction TFH cell differentiation is highly complex and signaling pathways that regulate their generation might be opposed.

#### **1.2.4. The role of miRNAs in immune activation**

MicroRNAs (miRNAs) were identified as important mediators of T cell differentiation and function and are thus critical regulators of the immune system (Baumjohann & Ansel, 2013; Cobb et al., 2006; Cobb et al., 2005; Grishok et al., 2001; Jeker & Bluestone, 2013; Monticelli, 2013).

They are small endogenously expressed, evolutionary conserved, ~22 nucleotides long, noncoding RNAs that are part of the RNA interference (RNAi) pathway (Baumjohann & Ansel, 2013; Grishok et al., 2001). Especially, miRNAs of the miRNA17~92 cluster were shown to regulate murine TFH cell differentiation and migration to the B cell follicles together with Bcl6 by repression of Retinoid-related orphan receptor  $\alpha$  (ROR $\alpha$ ) and by regulation of signaling through ICOS and PI3K/Akt (Baumjohann et al., 2013a; Kang et al., 2013). The miRNA17~92 cluster was additionally identified as highly relevant with respect to autoimmune diseases, since its overexpression leads to autoimmunity and autoantibody production (Xiao et al., 2008). The miRNA17~92 cluster is located on chromosome 13 in humans and on chromosome 14 in mice, transcribed as a single transcript and post-transcriptional processing results in six individual mature miRNAs (miRNA17, miRNA18a, miRNA19a, miRNA20a, miRNA19b and miRNA92a). This miRNA cluster is rapidly induced in activated CD4<sup>+</sup>T cells (Wu et al., 2015) and contributes to the differentiation and function of various T helper cell subsets as recently reviewed by Dirk Baumjohann (Baumjohann, 2018).

Individual miRNAs have hundreds of mRNA targets, though they induce rather modest regulation of gene and subsequent protein expression (Baek et al., 2008; Selbach et al., 2008). The interaction of miRNAs with their target mRNAs results in post-transcriptional silencing of the mRNA by its translational inhibition, deadenylation, decapping and degradation (Fabian & Sonenberg, 2012; Huntzinger & Izaurralde, 2011). Additionally, recent publications by the groups of Joan A. Seitz and Shobha Vasudevan showed that miRNAs can trigger translational upregulation of their target mRNAs under specific cellular conditions (Bukhari et al., 2016; Truesdell et al., 2012; Vasudevan et al., 2007). This adds an additional layer of complexity to the miRNA-mediated regulation of target expression. Thus, miRNAs are able to regulate complex cellular states and represent suitable candidates for immune modulating therapies that *e.g.* agonize or antagonize miRNA-mediated silencing.

Our group recently showed that high expression of miRNA92a is associated with increased frequencies of precursor TFH cells during onset of human islet autoimmunity. Additionally, we identified Krueppel-like factor 2 (Klf2) as a target of miRNA92a in regulating human precursor TFH cell induction. (Serr et al., 2016b)

The role of the miRNA17~92 cluster and especially of miRNA92a in human and murine obesity, representing a second state of immune activation, has not been investigated so far.

### 1.3. Immune-metabolic interactions in obesity

#### 1.3.1. The immunometabolism of CD4<sup>+</sup>T cells drives their function

Obesity might not only affect systemic immune-metabolic interactions, but also the cellular immunometabolism of CD4<sup>+</sup>T cells.

Naïve CD4<sup>+</sup>T cells are quiescent and largely metabolically inactive. They augment catabolic metabolic pathways and neither undergo clonal division nor secrete high levels of cytokines. These cells need no exogenous energy for *de novo* generation of DNA, lipids and proteins, but use available glucose, lipids and amino acids to maximize energy production in the form of Adenosine triphosphate (ATP) through the tricarboxylic acid (TCA) cycle and oxidative phosphorylation (OXPHOS) in the mitochondria. For energy generation via OXPHOS, electrons that are coupled with protons are transferred via the electron transport chain (ETC), a series of four transmembrane proteins (Complex I-IV). This proton transfer across the inner mitochondrial membrane creates an electrochemical proton gradient which is finally used by the ATP synthase to phosphorylate Adenosine diphosphate (ADP) to ATP. Thereby 30-36 ATP/mol glucose are generated. (Almeida et al., 2016; Park & Pan, 2015; van der Windt & Pearce, 2012)

Upon *in vitro* TCR stimulation or upon *in vivo* antigen recognition, naïve CD4<sup>+</sup>T cells rapidly get activated and undergo metabolic reprogramming in order to meet certain metabolic criteria which are required to differentiate and acquire effector functions. T cell metabolic reprogramming includes increased expression of glucose and amino acid transporters, activation of metabolic kinases (*e.g.* mTOR, Monophosphate Activated Protein Kinase (AMPK)) and transcriptional regulators (*e.g.* Proto-oncogene protein Myc, Hypoxia-inducible factor 1  $\alpha$  (HIF-1 $\alpha$ )) and an altered global gene expression profile. Importantly, changes in the cellular microenvironment such as high nutrient levels as in obesity can directly influence T cell differentiation by triggering metabolic changes and adaption in the T cell. (Almeida et al., 2016; Park & Pan, 2015; van der Windt & Pearce, 2012) AMPK is a cellular energy sensor that is activated once the cellular adenosine monophosphate (AMP)/ATP ratio increases and at least partly triggers its effects via regulation of its downstream target mTOR (Hardie et al., 2003; Xu et al., 2012). However, AMPK and mTOR are capable to antagonize each other's activity (Blagih et al., 2015). Active AMPK downregulates energy consuming metabolic pathways *e.g.* fatty acid synthesis (FAS), whilst enhancing energy generating pathways *e.g.* glycolysis. Thereby, AMPK protects the cell from suboptimal environmental conditions and ensures cell viability. (Hardie et al., 2003) Activated and effector T cells

(e.g. Th1, Th2, Th17 cells) mainly depend on aerobic glycolysis and low levels of glutaminolysis to meet their energy needs. (Almeida et al., 2016; Michalek et al., 2011; Park & Pan, 2015; van der Windt & Pearce, 2012).

The latter comprises the conversion of glutamine to  $\alpha$ -ketoglutarate in the TCA cycle in the mitochondria. Glutaminolysis is required since aerobic glycolysis was shown to be insufficient to provide the full complement of factors needed for proliferation of activated T cells. (Carr et al., 2010) In line with an active TCA cycle due to glutaminolysis in activated T cells, mitochondrial oxygen consumption was shown to be increased during T cell activation (Sena et al., 2013). This reflects that the mitochondrial metabolism plays an important role in T cell activation (Carr et al., 2010; Sena et al., 2013).

However, as mentioned above, activated T cells mainly depend on aerobic glycolysis and this pathway was shown to be enhanced by PI3K-Akt-mTOR signaling. On the contrary, fatty acid  $\beta$ -oxidation (FAO) is restrained by an active PI3K-Akt-mTOR pathway due to its inhibition of the Carnitine palmitoyl transferase I (Cpt1), a rate-limiting enzyme in FAO. (Deberardinis et al., 2006) In line with this, mTOR inhibition in T cells was shown to trigger Treg development associated with increased FAO (Delgoffe et al., 2011). Additionally, TCR/CD28 stimulation was identified as activator of downstream MapK signaling and subsequent activation of hexokinases and thus T cell specific glycolysis (Marko et al., 2010). Furthermore, the group of Erica L. Pearce (Buck et al., 2016) highlighted that mitochondrial remodeling controls metabolic reprogramming of T cells and more specifically that mitochondrial fission promotes aerobic glycolysis whilst mitochondrial fusion favors OXPHOS and FAO. The data above provides a strong link between metabolic control and differentiation of CD4<sup>+</sup>T cells.

For aerobic glycolysis in activated T cells, glucose is first imported from the extracellular space (e.g. via GLUT1) and subsequently converted into pyruvate, followed by conversion into lactate and NAD<sup>+</sup> and release of energy in the form of  $\sim 4$  ATP/mol glucose in a mitochondria-independent, aerobic process called Warburg effect, in the cytosol. (Chang et al., 2013; Frauwirth et al., 2002; Sena et al., 2013; Wang et al., 2011) The generated NAD<sup>+</sup> is required as co-factor for glycolysis (Vander Heiden et al., 2009). However, the function of the inefficient Warburg effect in activated CD4<sup>+</sup>T cells is yet incompletely understood (Almeida et al., 2016; Park & Pan, 2015; van der Windt & Pearce, 2012). Glycolytic enzymes might be metabolic checkpoints that link glycolysis with effector T cell function and changes in the activity of OXPHOS vs. aerobic glycolysis might directly affect T cell differentiation (Chang et al., 2013). Additionally, glycolytic enzymes can enter the nucleus highlighting that alterations

in the glycolytic flux might result in epigenetic changes which potentially affect the T cell phenotype (Boukouris et al., 2016). In activated, proliferating T cells, only a small part of the pyruvate is transferred into the mitochondria, converted to Acetyl-Coenzym A (Acetyl-CoA) which enters the TCA cycle to produce NADH and FADH<sub>2</sub>. NADH and FADH<sub>2</sub> are used to generate ATP by OXPHOS. (Almeida et al., 2016; Park & Pan, 2015; van der Windt & Pearce, 2012)

Despite the low OXPHOS rate, the activity of the ETC is increased in activated and proliferating T cells and a functional mitochondrial metabolism might sustain T cell activation and proliferation. (Baixauli et al., 2015; Chang et al., 2013; Frauwirth et al., 2002; Sena et al., 2013; Wang et al., 2011) Deletion of the mitochondrial transcription factor A (Tfam) in CD4<sup>+</sup>T cells resulted in mitochondrial dysfunction of these cells and an associated reduced expression of genes and proteins of the ETC accompanied by an impaired ETC function. A loss of mitochondrial electron density, a reduced mitochondrial ATP generation, lower levels of reactive oxygen species (ROS), increased energy generation by anaerobic glycolysis (assessed by the extracellular acidification rate (ECAR), an index of lactate production) and decreased energy generation by OXPHOS (assessed by the oxygen consumption rate (OCR), an indicator of OXPHOS) were identified as characteristics for the impaired ETC function in Tfam-deficient CD4<sup>+</sup>T cells. (Baixauli et al., 2015) Especially, ROS production by mitochondrial complex III, which is part of the ETC, was shown to be indispensable for T cell activation and effector T cell differentiation via NFAT activation and subsequent Il2 induction *in vitro* and *in vivo* (Sena et al., 2013). Additionally, impairments in the ETC might lead to a subsequent lower activity of the ATP synthase, resulting in both a decreased release of ATP into the extracellular space and a reduced Ca<sup>2+</sup> influx into the cell due to a lower abundance of ATP-activated Ca<sup>2+</sup>-channels. Low intracellular Ca<sup>2+</sup> levels were previously associated with impaired T cell activation. (Almeida et al., 2016; Chang et al., 2013; Ledderose et al., 2014)

On the contrary to activated and effector T cells, Tregs predominantly use FAO to meet their energy needs (Michalek et al., 2011). To this aim, fatty acids are transported into the mitochondria where they are degraded in a series of enzymatic reactions to Acetyl-CoA, NADH and FADH<sub>2</sub>. Acetyl-CoA enters the TCA cycle for further oxidation and NADH and FADH<sub>2</sub> are used for generation of ATP in the ETC and subsequent ATP synthase reaction. (Almeida et al., 2016) However, Tregs most probably have a flexible metabolic state and are not completely independent from mTOR signaling and associated glycolytic and oxidative processes which might assist them to proliferate and maintain Treg functional stability and suppressive activity (Haxhinasto et al., 2008; Michalek et al., 2011; Procaccini et al., 2016;

Zeng et al., 2013). Accordingly, *in vitro* under Treg conditions activated naïve T cells showed low rates of glycolysis and were mainly dependent on FAO (Michalek et al., 2011). However, the metabolic phenotype of Tregs is still poorly understood and especially the interaction between T cell metabolism and Treg suppressive function is yet unknown.

The highly complex immunometabolism of activated T cells and Tregs is an emerging field of current investigation and it is specifically required to understand how the metabolic phenotype *e.g.* obesity is related to the metabolic profile of CD4<sup>+</sup>T cells, their differentiation and the suppressive function of Tregs.

### 1.3.2. Mechanisms of inflammation in the VAT and its systemic effects

On the systemic level of immunometabolism, VAT inflammation and associated immune cell infiltration were identified as important drivers of the pathogenesis of obesity (**compare chapter 1.1.2**) (Kanneganti & Dixit, 2012). VAT mass was shown to be positively correlated with the disease risk for obesity and the metabolic syndrome (Lee et al., 2013), whereas, on the contrary, BAT and SAT were shown to exert beneficial effects on the metabolism (Lee et al., 2013) as exemplified by the transplantation of SAT into the VAT compartment of mice resulting in reduced adiposity and improved glucose homeostasis (Tran & Kahn, 2010).

VAT remodeling is accomplished by hyperplasia (recruitment of new adipocytes and adipocyte proliferation) and/or hypertrophy (increased size of individual adipocytes). Whilst hyperplasia is a beneficial phenomenon of adipocyte expansion, hypertrophy is accompanied by pathological, inflammatory changes with local and systemic effects due to tissue hypoxia, a shift in local immune cell polarization and release of pro-inflammatory cytokines, adipokines and other molecules (Choe et al., 2016; Osborn & Olefsky, 2012; Wang et al., 2013). VAT inflammation differs from pathogen induced acute inflammation by the absence of rubor (redness), tumor (swelling), calor (heat) and dolor (pain) (Larsen & Henson, 1983). Macrophages that engulf lipids from remnant death adipocytes (Sun et al., 2011) represent the most abundant class of immune cells in the inflamed VAT (Russo & Lumeng, 2018). They skew from an anti-inflammatory, “alternatively” activated M2-subtype with characteristic secretion of IL10- which protects adipocytes from TNF $\alpha$ -induced insulin resistance- towards a pro-inflammatory “classically activated” M1-subtype secreting TNF $\alpha$ , IL6, nitric oxide and IL1 $\beta$  *etc.* in response to *e.g.* high levels of IFN $\gamma$  (Lumeng et al., 2007; Rocha et al., 2008). Additionally, to Th1 cells, CD8<sup>+</sup>T cells, B lymphocytes, neutrophils, group 1 innate lymphoid cells (ILC1s) and mast cells accumulate in the obese VAT, whereas the number of anti-inflammatory Th2 cells and Tregs is decreased. (Choe et al., 2016; Mathis, 2013)

Enlarged adipocytes cross-talk with immune cells via soluble factors or direct cell-cell interactions (Osborn & Olefsky, 2012). They secrete pro-inflammatory cytokines such as TNF $\alpha$ , IL6, IL1 $\beta$  and monocyte chemoattractant protein 1 (MCP1) which affect adipogenesis and trigger AT inflammation. Additionally, adipocytes secrete numerous adipokines that affect insulin sensitivity such as the major drivers of the cross-talk between adipocytes and immunocytes: leptin and adiponectin (Choe et al., 2016). Leptin positively correlates with the AT mass and prevents weight gain via promoting satiety by regulating key hypothalamic circuits (Clemmensen et al., 2017). The leptin receptor is also expressed on immune cells and leptin was shown to trigger the secretion of Th1 cytokines (e.g. IFN $\gamma$ , IL2) by polarized CD4<sup>+</sup>T cells (Lord et al., 1998). Additionally, leptin was identified to promote proliferation of activated T cells (Lord et al., 1998), whilst inhibiting Treg numbers in AT. This reflects a potential mechanistic link between elevated AT mass with high numbers of activated T cells and low numbers of Treg (Matarese et al., 2010). On the contrary, anti-inflammatory adiponectin levels inversely correlate with the degree of AT inflammation, insulin resistance and glucose intolerance (Ye & Scherer, 2013). Adiponectin induces IL10 and inhibits pro-inflammatory cytokine secretion by macrophages (Kumada et al., 2004; Yamaguchi et al., 2005).

### 1.3.2.1. TFH cells in metabolic diseases

Like autoimmunity (**compare chapter 1.2.3**), obesity-associated chronic, systemic low-grade inflammation represents a state of immune activation. Thus, it might be possible to transfer gained knowledge from the autoimmune to an obesogenic setting. A limited number of publications (Q. Wang et al., 2015; Zhan et al., 2017; Zhou et al., 2018) highlights the involvement of circulating CD4<sup>+</sup>CXCR5<sup>+</sup>TFH cells in human obesity and associated T2D. Wang *et al.* (Q. Wang et al., 2015) saw a significant enrichment of CD4<sup>+</sup>CXCR5<sup>+</sup>TFH cells among circulating CD4<sup>+</sup>T cells in patients with T2D and the balance of TFH cell subsets was shifted toward the Th17-like subtype. They additionally showed that the proportion of CD4<sup>+</sup>CXCR5<sup>+</sup>TFH cells is increased in T2D patients with abdominal fat accumulation and overweight compared to normal weight T2D patients. (Q. Wang et al., 2015) Recently, Zhou *et al.* (Zhou et al., 2018) found enriched levels of IFN $\gamma$ , but not IL4 and IL17 producing mucosal TFH cells accompanied by higher IgG levels and low grade inflammation in the intestinal tract of non-obese T2D patients (Zhou et al., 2018). Furthermore, Zhan *et al.* (Zhan et al., 2017) observed a generally lower activation status of CD4<sup>+</sup>CXCR5<sup>+</sup>TFH cells with reduced pro-inflammatory cytokine secretion (IFN $\gamma$ , IL2, IL4, IL17) and elevated IL10 secretion in obese patients upon Roux-en-Y Gastric Bypass (RYGB) surgery. Enrichment of CD4<sup>+</sup>CXCR5<sup>+</sup>IL10<sup>+</sup>TFH cells was accompanied by a reduction in BMI, glycaemia and fat

mass, resulting in a downregulation of inflammation and an amelioration of obesity-related diseases upon RYGB surgery. (Zhan et al., 2017)

There is no data available yet that proves the existence of TFH cells in human or murine VAT. Additionally, it remains unclear whether these cells could be subdivided into Th-subsets compare **chapter 1.2.3**.

### **1.3.2.2. Adipose tissue residing T cells**

CD4<sup>+</sup>T cells reside in VAT, SAT and BAT and play critical roles in maintaining tissue homeostasis in mice (Choe et al., 2016; Mathis, 2013). Especially CD4<sup>+</sup>T cells were shown to control the VAT-immune crosstalk in the progression and remission of obesity-associated inflammation (Zhao et al., 2018). Several studies observed an enrichment of pro-inflammatory IFN $\gamma$  producing CD4<sup>+</sup>T cells in the obese VAT (Cheng et al., 2012; Feuerer et al., 2009; Winer et al., 2009). The increase in these cells is potentially promoted by M1-macrophages (Morris et al., 2013) or enlarged adipocytes (Deng et al., 2013) which trigger their proliferation via MHCII-mediated antigen presentation. On the contrary, T cells might respond directly to adipocyte injury, preceding innate-immune inflammation and polarization of macrophages (Deng et al., 2013; Winer et al., 2009). Different CD4<sup>+</sup>T cell subsets, such as Th1 cells and Tregs, have been detailed studied in AT inflammation, however there is no data on TFH cell yet.

Normal, lean AT is mainly populated by Th2 cells and Foxp3<sup>+</sup>Tregs, especially the latter play a critical role in ameliorating chronic VAT inflammation which contributes to AT and systemic insulin sensitivity recently reviewed by Becker *et al.* (Becker et al., 2017) and Panduro *et al.* (Panduro et al., 2016). The abundance of murine VAT Tregs is first evident at 10-15 weeks of age, comprises 40-80 % of the CD4<sup>+</sup>T cells at the age of 20-25 weeks and gradually declines from the age of 40 weeks onwards (Cipolletta et al., 2015). The fraction of Tregs within the CD4<sup>+</sup>T cell compartment is higher in VAT compared to lymphoid tissues (15-20 %) and declines with obesity progression (Deiuliis et al., 2011; Feuerer et al., 2009; Kalin et al., 2017; Winer et al., 2009). Both systemic and AT-specific ablation of Tregs was shown to exacerbate AT inflammation and dysfunction, likely by a synergistic effect on macrophages, adipocytes and other T cells (Cipolletta et al., 2012; Eller et al., 2011; Feuerer et al., 2009). On the contrary, augmentation of the Treg compartment in ob/ob mice decreased AT inflammation (Ilan et al., 2010).

VAT Tregs bear a Th2 like phenotype with high expression of Gata3, C-C chemokine receptor type 4 (CCR4) and Il10 (Cipolletta et al., 2015; Cipolletta et al., 2012; Han et al., 2015). This Th2-like phenotype might be driven by the interaction of Il33 with its receptor ST2 (Interleukin 1 receptor-like 1 (Il1rl1)), expressed by the majority of Tregs in lean VAT. The frequency of ST2<sup>+</sup>VAT Tregs was shown to be severely diminished in DIO, but could be reversed by *in vivo* administration of Il33 which additionally ameliorated VAT inflammation and increased insulin sensitivity (Han et al., 2015; Vasanthakumar et al., 2015). Il33 might together with MHCII-mediated antigen presentation contribute to the accumulation of Tregs in lean VAT (Kolodin et al., 2015). Recently the group of Diane Mathis (Li et al., 2018) showed that the formation of the VAT Treg phenotype might include an initial priming step of thymus derived Tregs in the spleen followed by migration to the non-lymphoid tissue where final diversification via epigenetic remodeling takes place. VAT Tregs are further characterized by high expression levels of the transcription factor PPAR $\gamma$  which not only represents the “master regulator” of adipocyte differentiation (Giralt & Villarroya, 2013), but was also shown to control differentiation, function and accumulation of VAT Tregs (Cipolletta et al., 2012). A Treg specific PPAR $\gamma$  depletion resulted in a loss of VAT Tregs accompanied by normal Treg levels in lymphoid tissues, whereas treatment with the PPAR $\gamma$ -agonist pioglitazone induced VAT Tregs abundance and improved AT insulin resistance in obese mice (Cipolletta et al., 2012). Both PPAR $\gamma$  and ST2 were shown to be regulated by Interferon regulatory factor 4 (IRF4) and Basic leucine zipper transcription factor (BATF) (Vasanthakumar et al., 2015). As mentioned earlier, VAT Tregs show a remarkable high production of anti-inflammatory Il10 which enable them to suppress the development of AT inflammation. However, Il10 production by VAT Tregs was shown to be reduced in obese mice. (Feuerer et al., 2009; Han et al., 2014)

VAT Tregs were shown to bear a distinct TCR repertoire compared to other Tregs which might recognize yet unknown AT-specific antigens triggering accumulation of Tregs in specific niches. Additionally, the differences in the TCR repertoires of VAT-residing Tregs and Tconv. cells imply that VAT Tregs do not differentiate from VAT Tconv. cells. (Feuerer et al., 2009)

Focusing on human VAT-residing T cells, there is no clear evidence yet that either the proportion or the phenotype of T cells is altered in obesity. Human VAT T cells might skew towards a Th1/Th17 phenotype in obesity, whilst Th2 cells and associated cytokines and transcription factors are diminished. (Deiuliis et al., 2011; Esser et al., 2013; Fabbrini et al., 2013; Ioan-Facsinay et al., 2013; McLaughlin et al., 2014; Wouters et al., 2017; Wu et al., 2018; Zeyda et al., 2011) Data is more limited and contradictory for human VAT-residing

Tregs which were shown to be both positively (Pereira et al., 2014; Zeyda et al., 2011) and negatively (Deiuliis et al., 2011; Eller et al., 2011; Feuerer et al., 2009) correlated with obesity and insulin resistance, applying gene expression analysis for *FOXP3* mRNA in total human VAT. Flow cytometry data revealed lower levels of Foxp3<sup>+</sup>Tregs in VAT of metabolically unhealthy obese individuals (Esser et al., 2013) and showed a negative correlation of VAT Foxp3<sup>+</sup>Tregs with BMI (Wu et al., 2018). Recently, Wu *et al.* (Wu et al., 2018) phenotyped Tregs from human obese VAT and showed that their gene signature is closely related to that of murine VAT-residing Tregs. However, ST2 was not detectable both via qPCR and flow cytometry (Wu et al., 2018). This is in line with the findings of Zeyda *et al.* (Zeyda et al., 2013), but contradicts the data of Vasanthakumar *et al.* (Vasanthakumar et al., 2015) showing ST2 expression on human obese VAT-residing Tregs.

Further research is needed to dissect pathways of immune regulation in murine and especially human VAT.

### 1.3.3. Insulin (receptor) signaling and insulin resistance

The anabolic peptide **hormone insulin** was discovered in 1922 by Sir Frederic Banting (Banting F. G., 1922) and belongs to a highly conserved family of sequence- and structure related, functionally distinct hormones of the insulin-like superfamily including insulin and the insulin-like growth factors IGF-I and IGF-II (Andersen et al., 2017; Shabanpoor et al., 2009). Insulin is released from the  $\beta$ -cells of the pancreas in response to elevated plasma glucose levels and is a key player for metabolic control with profound effects on cellular and whole-body carbohydrate-, lipid- and protein metabolism (Newsholme & Dimitriadis, 2001). Insulin signaling is highly complex and affects a variety of downstream signaling pathways (Araki et al., 1994; Avruch, 2007; Bouzakri et al., 2006; Gallagher & LeRoith, 2010; Taniguchi et al., 2005; Thirone et al., 2006).

In the healthy, insulin-sensitive state, insulin exerts its pleiotropic effects by binding to the **InsR** which is expressed mainly by cells of the metabolically active AT, liver and skeletal muscle (De Meyts, 2016). The InsR is a transmembrane glycoprotein of the receptor tyrosine kinase superfamily (Hubbard, 1997; Hubbard et al., 1994; Roth & Cassell, 1983; Seino et al., 1989). In human and mice, it is encoded by the *INSR* gene and exists in two isoforms (InsR-A and InsR-B) with similar physiological functions (Massague et al., 1980). The InsR has a heterodimeric structure consisting of two extracellular  $\alpha$ -subunits and two transmembrane  $\beta$ -subunits forming to monomers composed of an  $\alpha$  and  $\beta$  subunit and linked by disulfide bonds (Massague et al., 1980; Sparrow et al., 1997). Two molecules

of insulin can bind simultaneously to the dimeric structure of the alpha subunit of the InsR (Yip & Jack, 1992), initiating the activation, autophosphorylation, conformational change and internalization of the receptor and subsequent dissociation and degradation of insulin (Morcavallo et al., 2014; Ward & Lawrence, 2009). Due to their sequential and structural similarity to insulin, IGFI and IGFII are also capable to bind to the InsR and activate it, though with lower affinity (Andersen et al., 2017; Belfiore & Malaguarnera, 2011). Upon autophosphorylation of the InsR, different substrates are recruited to the tyrosine kinase domain of the  $\beta$ -subunit of the receptor resulting in their phosphorylation and activation. Depending on the recruited substrates, mainly downstream PI3K-Akt-mTOR or Ras/MapK pathway is activated. (Morcavallo et al., 2014; Ward & Lawrence, 2009) Activation of the InsR substrates (IRS) 1-6 particularly activates PI3K-Akt-mTOR signaling and evokes metabolic effects such as increased cellular glucose uptake, glycogen synthesis, lipid storage and synthesis and impaired gluconeogenesis and fatty acid oxidation in metabolically active organs (Araki et al., 1994; Bouzakri et al., 2006; Taniguchi et al., 2005; Thirone et al., 2006). On the contrary, recruitment and phosphorylation of Shc proteins mainly stimulates the Ras/MapK pathway leading to the completion of mitogenic functions such as cell proliferation (Avruch, 2007). Abnormally high insulin levels as in hyperglycemia were shown to trigger overstimulation of the mitogenic pathway (Gallagher & LeRoith, 2010).

InsR signaling and its downstream pathways are tightly controlled and regulatory mechanisms are distinct in liver, muscle and AT (De Meyts, 2016). Minor disturbances in the InsR phosphorylation cascade were shown to result in severe perturbations of the metabolism such as **insulin resistance** (Boura-Halfon & Zick, 2009; Du & Wei, 2014; Huang et al., 2009; Yazici & Sezer, 2017; Ye, 2013; Youngren, 2007) which is defined as a subnormal response of normally insulin-sensitive tissues to the hormone insulin (Yazici & Sezer, 2017; Ye, 2013). Although several obesity-associated factors were identified as causal in the pathogenesis of insulin resistance, there is no consensus for a unifying mechanism of insulin resistance yet. However, there is evidence for sexual dimorphism in insulin sensitivity with female rodents and women reflecting greater insulin sensitivity in AT, liver and muscle compared to male counterparts (Estrany et al., 2013; Garcia-Carrizo et al., 2017; Hoeg et al., 2011; Magkos et al., 2010; Masharani et al., 2009). Here, **AT insulin resistance** which might precede and contribute to insulin resistance in muscle and liver by release of FFAs (Jiao et al., 2011) is considered in more detail.

Initially, AT insulin resistance was associated with a decrease in the number of InsRs- under maintained affinity for insulin- demonstrated on plasma membranes of adipocytes from ob/ob mice (Freychet et al., 1972) and obese humans (Olefsky, 1976). This represents one

characteristic of insulin resistance. Additionally, release of pro-inflammatory TNF $\alpha$  by the chronically inflamed AT was shown to impair insulin sensitivity directly in the adipocytes either by serine phosphorylation of the IRS1 protein via the c-Jun N-terminal kinase (JNK) pathway and thus defects in the InsR downstream signaling cascade (Rui et al., 2001) or by inhibiting the activity of PPAR $\gamma$  which normally drives lipid synthesis and fat storage in cells (Ye, 2008). Isolated Foxp3<sup>+</sup>Tregs from obese VAT showed decreased Il10 and increased IFN $\gamma$  production reflecting their shift towards a Th1-like phenotype which might contribute to AT insulin resistance (Han et al., 2014). More specifically, IFN $\gamma$ , which is also secreted by other VAT-residing T cells, was shown to attenuate insulin resistance in mature human adipocytes *in vitro* via activation of JAK1-Stat1 signaling resulting in reduced activation of Akt and downregulation of IRS1, the InsR and insulin dependent glucose uptake via glucose transporter 4 (GLUT4) (McGillicuddy et al., 2009).

#### **1.3.3.1. T cell specific insulin (receptor) signaling**

The effects and regulation of insulin (receptor) signaling are cell-type dependent and the expression of the InsR by immune cells and especially by activated T cells (Han et al., 2014; Helderman & Strom, 1978; Tsai et al., 2018; Viardot et al., 2007) highlights the importance of insulin (receptor) signaling for T cell function. However, T cell specific InsR signaling is yet poorly understood, especially regarding its effect on differentiation of CD4<sup>+</sup>T cells into Foxp3<sup>+</sup>Tregs. Insulin signaling was first linked to CD4<sup>+</sup>T cell, and more specifically Treg function, by Han *et al.* (Han et al., 2014). They showed that isolated Tregs from spleens and VAT of WT mice display a reduced Il10 and an increased IFN $\gamma$  production in response to stimulation with exogenous insulin, reflecting potential impairments in their suppressive function (Han et al., 2014). On the contrary, Fischer *et al.* (Fischer et al., 2017) showed that Tregs from LNs of rats with inducible whole-body InsR deficiency were not affected in their frequency, proliferation and suppressive capacity, indicating that InsR signaling might be dispensable for Treg activity (Fischer et al., 2017). Recently, Tsai *et al.* (Tsai et al., 2018) highlighted that murine InsR-deficient CD4<sup>+</sup>T cells are more prone to differentiate into Th2 cells and Tregs under the respective polarizing conditions *in vitro*. Accordingly, they highlighted in an adoptive transfer model of colitis *in vivo* that the transfer of InsR deficient CD4<sup>+</sup>CD25<sup>-</sup>CD45RB<sup>hi</sup>T cells into RAG1-deficient hosts results in a diminished disease severity compared to the transfer of WT ctrl. cells. This was reflected by a significant reduction in pro-inflammatory CD4<sup>+</sup>T cells in the mesLNs, albeit no increase in Foxp3<sup>+</sup>Tregs was assessed. (Tsai et al., 2018) Thus, T cell specific InsR deficiency might counteract CD4<sup>+</sup>T cell-mediated inflammation *in vivo*, highlighting an anti-inflammatory effect of the T cell specific InsR deficiency with potential similar beneficial effects in the obesity setting.

#### 1.4. Objectives

Interactions between the immune and the metabolic system are critically involved in obesity development, progression, persistence and remission. However, the specific functions of immune cells and specifically CD4<sup>+</sup>T cells in this disease remain poorly understood. Investigating the effect of environmental-metabolic signaling cues on CD4<sup>+</sup>T cell frequencies, differentiation and T cell metabolism as well as on miRNA and mRNA expression might help to further dissect mechanisms that underlie immune activation vs. immune regulation in obesity. An improved understanding of mechanisms that link the metabolic and the immune system is fundamental to specifically target inflammatory effector T cells and immunoregulatory T cells (Tregs) as part of future therapeutic strategies for obesity treatment.

Therefore, the **first objective** of this thesis was to study the effect of an obesogenic environment and accompanied systemic low-grade inflammation on aberrant immune activation and specifically on inflammatory effector (precursor) TFH cell levels, since these cells can provide help to B cells and trigger the production of high-affinity antibodies. Specifically, it was the goal to investigate whether the durations of a high-fat, high-sugar (HFHS) diet has a direct impact on the abundance of TFH cells in LNs and at the site of inflammation, the non-lymphoid AT. TFH cell differentiation is regulated by miRNAs and accompanied by changes in T cell specific mRNA expression. Thus, miRNAs and mRNAs were studied to dissect potential underlying mechanisms that link environmental-metabolic signaling cues with immune responses during obesity progression. An additional goal was to study precursor TFH cells as representatives of aberrant immune activation in peripheral blood of obese humans, aiming to increase the clinical relevance of the here shown data.

The **second objective** of this thesis was to study the effect of environmental-metabolic signaling cues on CD4<sup>+</sup>T cells and especially regarding their relevance for the induction of immunoregulatory Foxp3<sup>+</sup>Tregs. The hormone insulin is crucial for metabolic control and insulin resistance in the peripheral insulin-responsive tissues is a major hallmark of obesity. Additionally, InsR signaling and stable Foxp3<sup>+</sup>Treg induction share PI3K-Akt-mTOR downstream signaling. Foxp3<sup>+</sup>Tregs are critical players in dampening tissue inflammation and contribute to tissue homeostasis highlighting their beneficial role in the obesity setting. The InsR is expressed on CD4<sup>+</sup>T cells, however, the impact of InsR signaling on the regulation of T cell activation and differentiation remains currently unclear. Therefore, the effect of insulin and genetic T cell specific InsR deficiency on *de novo* Foxp3<sup>+</sup>Treg induction from naïve CD4<sup>+</sup>T cells was studied *in vitro* during obesity development. InsR signaling is

important for whole-body glucose, lipid and energy homeostasis via acting on liver, muscle and AT. Thus, an additional goal of this thesis was to study the effect of insulin or T cell specific InsR deficiency on cellular metabolism and specifically on T cell specific glucose metabolism.

## 2. Methods

### 2.1. Blood and tissue samples from human subjects

Peripheral blood samples and biopsies from human VAT were received from the Leipzig Obesity Cohort ( $n \geq 2500$  subjects) coordinated by Prof. Matthias Blüher, Clinic for Endocrinology and Nephrology, University of Leipzig, Germany. All subjects gave written consent to the study protocols approved by the ethics committee of the University of Leipzig (Reg. no. 031-2006 and 017-12-23012012). Both caucasian females and males, aged 19 to 80 years, with a BMI from 17.1-79.1 kg/m<sup>2</sup> are included in the study. Exclusion criteria are pregnancy, acute or chronic inflammatory disease, antibodies against Glutamic acid decarboxylase, hypertension, cardiovascular or peripheral artery disease, thyroid dysfunction and alcohol or drug abuse. The study was designed to extensively characterize AT function, glucose and lipid metabolism, fat distribution and insulin sensitivity. For the here shown findings, lean, insulin-sensitive; obese, insulin-sensitive and obese, insulin-resistant subjects of the Leipzig Obesity Cohort were invited to donate a sufficient amount of blood (50 ml) and/or a VAT biopsy. Additionally, peripheral blood samples (10 ml) were received from healthy, normal weight (BMI: 18.5-25 kg/m<sup>2</sup>), caucasian subjects, aged: 20-30 years, who gave written consent to the Munich Bioresource project approved by the ethics committee of the Technical University of Munich (approval number: #5049/11).

### 2.2. Isolation of human naïve CD4<sup>+</sup>T cells and *ex vivo* precursor TFH cell staining

Peripheral blood mononuclear cells (PBMCs) were isolated from peripheral blood via density centrifugation over Ficoll Paque Plus. CD4<sup>+</sup>T cells were isolated from PBMC samples by positive enrichment using CD4 Microbeads and magnetic activated cell sorting (MACS) and CD19<sup>+</sup>B cells were enriched using CD19 Micro Beads and MACS according to the manufacturer's instructions. Cells were resuspended in HBSS<sup>+</sup> and first treated with Fc blocking reagent for 5 min at room temperature (RT), followed by staining with fluorescence-activated cell sorting (FACS) antibodies for 20 min on ice in the dark. Naïve CD4<sup>+</sup>CD3<sup>+</sup>CD45RA<sup>+</sup>CD45RO<sup>-</sup>CD127<sup>+</sup>CD25<sup>-</sup>T cells were FACS purified for *in vitro* Treg induction assays and naïve CD4<sup>+</sup>CD3<sup>+</sup>CD45RA<sup>+</sup>CD45RO<sup>-</sup>CD127<sup>+</sup>CXCR5<sup>-</sup>T cells and CD20<sup>+</sup>CD27<sup>+</sup>CD19<sup>+</sup>B cells were FACS purified for *in vitro* TFH induction assays with FACS Aria III using optimal compensation and gating settings. Dead cells were excluded based on forward (FSC) and sideward scatter (SSC) and staining with the viability dye sytox blue. For the *ex vivo* (precursor) TFH cell stainings, MACS enriched CD4<sup>+</sup>T cells were stained with the respective antibodies (**compare Table 1**) and identified as live CD4<sup>+</sup>CD3<sup>+</sup>CD45RA<sup>low</sup>CXCR5<sup>+</sup>CXCR3<sup>+</sup>CCR6<sup>-</sup> Th1-like TFH cells, live CD4<sup>+</sup>CD3<sup>+</sup>CD45RA<sup>low</sup>CXCR5<sup>+</sup>CXCR3<sup>-</sup>CCR6<sup>-</sup> Th2-like TFH cells and live

---

CD4<sup>+</sup>CD3<sup>+</sup>CD45RA<sup>low</sup>CXCR5<sup>+</sup>CXCR3<sup>-</sup>CCR6<sup>+</sup> Th17-like TFH cells. Dead cells were excluded based on FSC and SSC and staining with the viability dye eFlour450.

### 2.3. Human *in vitro* Treg induction assay

For polyclonal human *in vitro* Treg induction assays, 100 000 naïve CD4<sup>+</sup>T cells were FACS purified, resuspended in *X-VIVO* media and cultured in over-night pre-coated wells (5 µg/ml anti-CD3/ 15 µg/ml anti-CD28) in the presence of 100 U/ml IL2 with or without 100 ng/ml insulin. The cells were transferred into uncoated wells after 18 hours and cultured for additional 36 hours without further stimulation. Frequencies of *in vitro* induced live CD25<sup>hi</sup>Foxp3<sup>+</sup>Tregs were analyzed after intracellular staining with the respective antibodies (**compare Table 1**) and dead cells were excluded based on FSC and SSC and staining with the viability dye eFlour450.

### 2.4. Human *in vitro* TFH cell induction assay

Naive CD4<sup>+</sup>T cells were co-cultured with autologous B cells (ratio 1:1) in *X-VIVO* media and TFH induction was performed in presence of 5 µg/ml anti-CD3 (Okt3) and 5 µg/ml anti-CD28 (CD28.2) for five days. In some assays, Chitosan-PLGA-Nanoparticles (ratio 1:50 mimic or antagomir/nanoparticles) with or without a miRNA92a (control) mimic (0.75 ng/µl per 100,000 cells) or a miRNA92a (control) antagomir (2 ng/µl per 100,000 cells) were added. The cells were cultured in *X-VIVO* media at 37°C and 5 % CO<sub>2</sub> in the incubator. At day five the frequencies of live CD4<sup>+</sup>CD45RA<sup>-</sup>CXCR5<sup>+</sup>CCR7<sup>low</sup>PD1<sup>hi</sup> precursor TFH cells were analyzed after staining with the respective antibodies (**compare Table 1**) and dead cells were excluded based on forward (FSC) and sideward scatter (SSC) and staining with the viability dye sytox blue. Precursor TFH cells generated in presence and absence of a miRNA92a mimic were FACS purified for later gene expression analyses.

### 2.5. Mice

All mice were on C57BL/6J background. They were bred and maintained group-housed on a 12 hours/12 hours light dark cycle at 25°C under specific pathogen free conditions at the animal facility of Helmholtz Zentrum München, Germany, according to the Institutional Animal Committee Guidelines. B6.Cg-Foxp3<sup>tm2Tch/J</sup> (Foxp3-GFP) mice, B6.SJL-Ptprca<sup>Pepcb/BoyJ</sup> (WT) mice and B6.Cg-Lep<sup>ob/J</sup> (ob/ob) mice were obtained from the Jackson Laboratory. InsR TKO mice were bred by crossing mice with the InsR gene flanked by loxP sites (B6.129S4(FVB)-InsR<sup>tm1Khn/J</sup> or InsR<sup>fllox/fllox</sup>) mice, originally generated by the group of Ronald Kahn (Bruning et al., 1998) with mice in which the Cre-recombinase was expressed under

---

the control of CD4 enhancer/promotor/silencer (Tg(Cd4-cre)<sup>1</sup>Cwi/BfluJ or CD4-Cre mice). Ethical approval for breeding and experimentations performed on InsR TKO and ob/ob mice has been received by the District Government of Upper Bavaria, Munich, Germany (approval number: #ROB-55.2-2532.Vet\_02-14-33).

### 2.6. Genotyping

Genotyping of loxP sites was performed by PCR using primer sets specifically designed for InsR<sup>fllox/flox</sup> to bind to: oKAHN03: 5'- GAT GTG CAC CCC ATG TCT G-3'; oKAHN04: 5'-TCT ATC AAC CGT GCC TAG AG-3'; oKAHN05: 5'-CTG AAT AGC TGA GAC CAC AG-3' and for CD4-Cre to bind to: RO289: 5'-TGT GGC TGA TGA TCC GAA TA-3'; RO290: 5'-GCT TGC ATG ATC TCC GGT AT-3'. Ob/ob mice were genotyped by PCR applying the following primers: OB 1151: 5'-TGT CCA AGA TGG ACC AGA CTC-3' and OB 1152: 5'-ACT GGT CTG AGG CAG GGA GCA-3'.

### 2.7. Dietary challenge

Animals got *ad libitum* access to food and water. The standardized control diet (SD) consisted of 28.0 % kcal from fat, 14.0 % kcal from carbohydrates (including 8 % sucrose) and 58 % kcal from protein. The HFHS diet consisted of 58.0 % kcal from fat, 25.5 % kcal from carbohydrates (including 8 % sucrose) and 16.4 % kcal from protein. Mice were dietary challenged for 2 weeks (short-term HFHS), 8 weeks (intermediate-term HFHS), 18 weeks (long-term HFHS) and one year (sustained HFHS) starting from 8 weeks of age. The BWs of the dietary challenged mice and their corresponding controls were assessed weekly and before sacrificing the animals.

### 2.8. Glucose Tolerance Test

Mice were fasted for 6 hours prior to injection with glucose (2 g/kg BW of D-glucose in 0.9 % saline) for the GTT. Tail-blood glucose levels (mg/dl) were measured with the glucometer at the following time points: 0 (before glucose injection), 15, 30, 60, and 120 min after injection. The area under the curve (AUC) was calculated and compared between mice with different genotypes.

### 2.9. Murine cell isolation

LNs and/or spleens were collected in HBSS<sup>+</sup> and cells were isolated by mashing them through 70 µm cell strainers. For the CD4<sup>+</sup>T cell enrichment, isolated cells were treated with Fc blocking reagent in HBSS<sup>+</sup> for 10 min on ice, followed by staining with FACS antibodies

for CD44, CD25 and CD4 (CD4-Biotin) for 30 min on ice. After surface antibody staining CD4<sup>+</sup>T cells were purified based on biotin-labelled anti-CD4 antibody and MACS with streptavidin microbeads. Live naïve CD4<sup>+</sup>CD25<sup>-</sup>CD44<sup>low</sup>(Foxp3<sup>-</sup>) T cells were FACS purified from enriched CD4<sup>+</sup>T cells. Dead cells were excluded based on FSC and SSC and staining with the viability dye sytox red. VAT was collected in PBS + 0.5 % BSA and digested with 4 mg/ml Collagenase II in PBS + 0.5 % BSA supplemented with 10 mM CaCl<sub>2</sub> for 7 min at 37°C on a rotator. The cell suspensions were passed through a 200 µm nylon mesh, centrifuged to remove the SVF from adipocytes and resuspended in HBSS<sup>+</sup>. Isolated cells from VAT and unenriched, isolated cells from LNs were first treated with Fc blocking reagent in HBSS<sup>+</sup> for 10 min on ice, followed by staining with FACS antibodies for CD4, CD25 (not VAT), CD44, CD8a, CD11b, CD11c, CD14, B220 and F4/80 (sort naïve T cells) or CD4, CXCR5, CD8a, CD11b, CD11c, CD14, B220 and F4/80 (sort non-TFH and TFH cells) for 30 min on ice. Dead cells were excluded based on FSC and SSC and staining with the viability dye sytox blue. These cells were either FACS sorted as live total CD4<sup>+</sup>T cells (for RNAseq), live naïve CD4<sup>+</sup>CD25<sup>-</sup>CD44<sup>low</sup>(Foxp3<sup>-</sup>) T cells (for Treg induction assays), live CD4<sup>+</sup>CXCR5<sup>-</sup>non-TFH cells or live CD4<sup>+</sup>CXCR5<sup>+</sup>precursor TFH cells (both for mRNA analysis).

### 2.10. Murine *in vitro* Treg induction assay

For polyclonal *in vitro* Treg induction assays, 1000 (VAT) or 10 000 (LNs) murine naïve CD4<sup>+</sup>CD25<sup>-</sup>CD44<sup>low</sup>(Foxp3<sup>-</sup>) T cells were FACS purified, resuspended in RPMI medium + supplements and cultured at 37°C and 5 % CO<sub>2</sub> in the incubator in over-night pre-coated wells (5 µg/ml or 0.01 µg/ml anti-CD3e/ 5 µg/ml anti-CD28) in presence of 100 U/ml IL2 with or without 50 ng/ml insulin. In some assays 10 nmol/ml PI3K inhibitor was added to the wells after 18 hours. Unless otherwise indicated, short-term TCR stimulation was applied and cells were transferred into uncoated wells after 18 hours and cultured for additional 36 hours without further TCR stimulation. Continuously stimulated cells were cultured for 54 hours in presence of TCR stimulation and costimulation. Frequencies of *in vitro* induced Tregs were assessed by applying antibodies for CD4, CD25, CD44, CD8a, CD11b, CD11c, CD14, B220 and F4/80 and death cell exclusion marker eFlour450 for 30 min on ice following intracellular staining for Foxp3 and Ki67 and FACS analysis.

### 2.11. (Intracellular) staining of *ex vivo* Tregs and (precursor) TFH cells

To detect *ex vivo* Treg frequencies, isolated cells were stained intracellularly with Foxp3 and Ki67 following surface staining for CD4, CD25 (not VAT), CD44, CD8a, CD11b, CD11c,

CD14, B220 and F4/80. *Ex vivo* (precursor) TFH cells were identified by staining for CD4, CXCR5, PD1, CD8a, CD11b, CD11c, CD14, B220, F4/80, followed by intracellular staining for Bcl6. For the intracellular staining, cells were fixed and permeabilized using the Foxp3 Staining Buffer Set following surface staining and prior to intracellular staining with Foxp3, Ki67 and Bcl6 for 30 min on ice. Dead cells were excluded based on FSC and SSC and staining with the viability dye eFlour450. Frequencies of live CD4<sup>+</sup>CD25<sup>+</sup>Foxp3<sup>+</sup>Tregs, live CD4<sup>+</sup>CXCR5<sup>+</sup>PD1<sup>high(hi)</sup>(precursor) TFH cells and live CD4<sup>+</sup>CXCR5<sup>+</sup>PD1<sup>hi</sup>Bcl6<sup>hi</sup>TFH cells were FACS analyzed. Additionally, 2000 CD4<sup>+</sup>CD25<sup>+</sup>Foxp3<sup>+</sup>Tregs from ingLNs and 400 CD4<sup>+</sup>Foxp3<sup>+</sup>Tregs from VAT of 50 days old InsR TKO and Flox ctrl. mice were sort purified for Foxp3 CNS2 methylation analysis (**compare chapter 2.15**).

### 2.12. *In vitro* Treg re-stimulation Assay

CD4<sup>+</sup>CD25<sup>+</sup>Foxp3-GFP<sup>+</sup>Tregs were FACS purified upon *in vitro* Treg induction and 5000 Tregs/well were re-stimulated by culturing the cells in over-night pre-coated wells (5 µg/ml anti-CD3e/ 5 µg/ml anti-CD28) in RPMI medium + supplements in presence of 100 U/ml IL2 with or without 50 ng/ml insulin. After 30 hours, the frequencies of remaining CD4<sup>+</sup>CD25<sup>+</sup>Foxp3-GFP<sup>+</sup>T cells were analyzed via FACS.

### 2.13. Glucose uptake Assay

To analyze T cell specific glucose uptake 250 000 naïve CD4<sup>+</sup>CD25<sup>-</sup>CD44<sup>low</sup>T cells were FACS purified, resuspended in RPMI medium + supplements and cultured in over-night pre-coated wells (5 µg/ml anti-CD3e/ 5 µg/ml anti-CD28) in the presence of 100 U/ml IL2 and with or without 250 ng/ml insulin at 37°C and 5 % CO<sub>2</sub> for 4 hours. Thereafter, cells were transferred into uncoated wells and washed with PBS to remove remaining glucose from media. Glucose Uptake-Glo™ Assay was performed according to the manufacturer's instructions and luminescence which positively correlates with 2-Deoxyglucose uptake was measured with a Glomax Multi Detection System.

### 2.14. Gene expression analysis of mRNAs and miRNAs

Human CD4<sup>+</sup>CD45RA<sup>-</sup>CXCR5<sup>+</sup>CCR7<sup>low</sup>PD1<sup>hi</sup> precursor TFH cells, murine CD4<sup>+</sup>CXCR5<sup>+</sup>precursor TFH cells and CD4<sup>+</sup>CXCR5<sup>-</sup>non-TFH cells were sort-purified with FACS Aria III. RNA extraction was performed using the miRNeasy Micro Kit followed by either transcription into cDNA using iScript cDNA Synthesis Kit for subsequent mRNA expression analysis or by transcription into cDNA using Universal cDNA synthesis kit II for subsequent miRNA expression analysis according to the manufacturer's instructions. cDNA

from total human VAT was synthesized by the group of Prof. Matthias Blüher and was ready available at a concentration of 50 ng/ml. Real-time quantitative PCR (RT-qPCR) for mRNA expression analysis was performed with SsoFast Evagreen Supermix combined with the primers for murine *Il21*, *ICOS*, *Bcl6*, *18S*, *Histone* and human *Ascl2*, *Il21*, *ICOS*, *ITCH*, *Bcl6*, *CD4*, *Foxo1*, *Pten*, *Klf2*, *18S* and *Histone*. To quantify miRNA expression, RT-qPCR was performed with ExiLENT SYBR Green master mix combined with the LNA™ PCR primer mix for miRNA92a-3p and a primer for 5s for normalization. RT-qPCR data was normalized to the mean expression of 18S and Histone ((non-) TFH cells), to the expression of CD4 (human VAT) or to the expression of 5S (miRNA92a-3p). All RT-qPCRs were run on the CFX96 Touch Real-Time PCR Detection System and analyses were performed with Bio-Rad CFX Manager 3.1.

### 2.15. Foxp3 CNS2 methylation analysis

Sorted cells (**compare chapter 2.11**) were lysed and bisulfite converted using the EZ DNA Methylation-Direct Kit following the manufacturer's instructions. The resulting bisulfite-converted DNA (bcDNA) was used for a combination of methylation-sensitive high resolution melting (MS-HRM) analysis and subsequent Pyrosequencing as described earlier (Serr et al., 2016b; Serr et al., 2018). This bias-controlled quantitative methylation analysis was performed by first applying the SensiFAST HRM Kit and corresponding primers (forward primer: 5'-TTG GGT TTT GTT GTT ATA ATT TGA ATT TGG-3' and biotinylated reverse primer: 5'-ACC TAC CTA ATA CTC ACC AAA CAT C-3') on the CFX96 Touch Real-Time PCR System. Thereby, the bcDNA was amplified and a first estimation of the methylation status was possible. Secondly, Pyrosequencing for single CpG-site specific quantitative analysis of the methylation status of the TSDR region was performed on the PyroMark Q24 system. Therefore, PyroMark Gold Q24 Reagents were used according to the manufacturer's instructions and with a specific sequencing primer (5'-AAT TTG AAT TTG GTT AGA TTT TT-3') to cover the area of differential methylation in the first Foxp3 intron initially reported by Baron et al. (Baron et al., 2007). Pyrosequencing data are presented as means of all CpG-sites analyzed due to high homology between methylation levels of the individual sites and displayed as %.

### 2.16. RNA Sequencing

3000 CD4<sup>+</sup>T cells were FACS purified from mesLNs of InsR TKO and Flox ctrl. mice and immediately frozen at -20°C. Because of limited cell numbers, cDNA was synthesized directly using the SMARTer ultra low input RNA Kit for Sequencing-v4 according to the

manufacturer's instructions. cDNA concentration was assessed using High Sensitivity DNA Chips on an Agilent Bioanalyzer. 6 ng of cDNA were used for Library Preparation with Illumina Nextera XT DNA library preparation kit and corresponding index primers. The quality of the library was assessed with the bioanalyzer. Subsequent RNAseq was performed using HiSeq Rapid SR Cluster Kit v2 and HiSeq Rapid SBS Kit v2. Dual-indexed, multiplexed single-reads were run on an Illumina HiSeq2500 Instrument with the Sequencing Software HiSeq Control Software 2.2.70 by Dr. Christine Wurmser, Lehrstuhl für Tierzucht, Technische Universität München. Differential expression analysis of the RNAseq data was performed by Ming Wu, Institute for Animal Physiology and Immunology Weihenstephan, Technische Universität München using DESeq2 (version 1.18.1) (Love et al., 2014) with default parameters. Differences with baseMean > 50, absolute log2FoldChange > 1 and adjusted P value < 0.05 were considered as significant. Volcano plots were generated by ggplot2 (Wickham, 2016) and ggrepel (Slowikowski, 2016) and grey lines were added to illustrate the thresholds (line1: log2FoldChange = -1; line2: Log2FoldChange = 1; line 3: -log10(padj) = -log10(0.05)). Gene Set Enrichment Analysis (GSEA) was performed as described in (Sergushichev, 2016) and by using the reference databases c2 (curated gene sets), c5 (GO gene sets), c7 (immunological signatures) downloaded from <http://software.broadinstitute.org/gsea/msigdb/collections.jsp#C2>.

### 2.17. Proteomics

Total CD4<sup>+</sup>T cells from all LNs of InsR TKO and Flox ctrl. mice were MACS enriched using CD4-Biotin and streptavidin microbeads as described in **chapter 2.9** and immediately frozen in PBS. Dr. Natalie Kraemer, Institute for Diabetes and Obesity, Helmholtz Zentrum München, performed Liquid chromatography-mass spectrometry (LC-MS/MS) sample preparation, analysis and computational data analysis. To this end, T cells were lysed in SDC lysis buffer containing 4 % (w/v) SDC, 100 mM Tris-HCl (pH 8.5), heated for 5 min at 99°C, and sonicated (Branson probe sonifier, output 3-4, 50 % duty cycle, 3× 30s). Then proteins were reduced and alkylated with 10 mM tris-(2-carboxyethyl)-phosphin-hydrochlorid (TCEP), 40 mM 2-chloroacetamide(CAA)), at 45°C for 10 min in the dark. Proteins were digested with 1:50 (protein:enzyme) LysC and Trypsin at 37°C overnight and peptides were acidified to a final concentration of 1 % TFA. The peptide solution was cleared by centrifugation and loaded onto activated (30 % methanol, 1 % TFA) double layer styrenedivinylbenzene–reversed phase sulfonated STAGE tips (SDB-RPS; 3M Empore). The STAGE tips were first washed with 200 µl 0.2 % TFA, then with 200 µl 0.2% TFA and 5 % ACN. The peptides were eluted with 60 µl SDB-RPS elution buffer (80 % ACN, 5 % NH<sub>4</sub>OH) for single shot analysis. Samples were concentrated in a SpeedVac for 40 min at 45°C and dissolved in 12 µl MS loading buffer (2 % ACN, 0.1 % TFA). For LC-MS/MS

analysis peptides were loaded onto a 50 cm column with a 75  $\mu$ M inner diameter, packed in-house with 1.9  $\mu$ M C18 ReproSil particles (Dr. Maisch GmbH) at 60°C. The peptides were separated by reversed-phase chromatography using a binary buffer system consisting of 0.1 % formic acid (buffer A) and 80 % ACN in 0.1 % formic acid (buffer B). 0.5  $\mu$ g of peptides was separated on a 120 min gradient (5-30 % buffer B over 95 min, 30-60 % buffer B over 5 min) at a flowrate of 350 nl on an EASY-nLC 1200 system. MS data was acquired using a data dependent top-15 method with maximum injection time of 20 ms, a scan range of 300–1650 Th, and an AGC target of 3e6. Sequencing was performed via higher energy collisional dissociation fragmentation with a target value of 1e5, and a window of 1.4 Th. Survey scans were acquired at a resolution of 60 000. Resolution for HCD spectra was set to 15 000 with maximum ion injection time of 28 ms and an underfill ratio of either 30 % Dynamic exclusion was set to 20 s. For MS data analysis, raw mass spectrometry data was processed with MaxQuant 1.5.1.6 using default settings. False-discovery rate (FDR) at the protein, peptide and modification level was set to 0.01. Oxidized methionine (M) and acetylation (protein N-term) were selected as variable modifications, and carbamidomethyl (C) as fixed modification. Label free quantitation (LFQ) and “Match between runs” were enabled. Proteins and peptides were identified with a target-decoy approach in revert mode, using the Andromeda search engine integrated into the MaxQuant environment. Searches were performed against the mouse UniProt FASTA database (September 2014) containing 51 210 entries. Quantification of peptides and proteins was performed by MaxQuant. Bioinformatics analysis was performed with Perseus 1.5.6.2 and Microsoft Excel. Annotations were extracted from UniProtKB, Gene Ontology (GO), and the Kyoto Encyclopedia of Genes and Genomes (KEGG). Quantified proteins were filtered for at least three valid values among biological replicates in at least one of the conditions. Missing values were imputed from a normal distribution with a downshift of X and a width of Y. Significantly up-or-downregulated proteins between the three conditions were determined by Student’s t-test (P value 0.05). Hierarchical clustering and the volcano plot were performed in Perseus.

### **2.18. Immunofluorescence stainings on cytopins**

Total CD4<sup>+</sup>T cells from WT, Flox ctrl. and InsR TKO mice were negatively selected using the Dynabeads untouched CD4<sup>+</sup> mouse Kit from Invitrogen according to the manufacturer’s instructions. Briefly, non CD4<sup>+</sup>T cells are labeled by a cocktail of biotin-conjugated monoclonal antibodies against mouse: CD8a, CD11b, CD45R, CD49b, and Ter-119. Magnetically labelled non-CD4<sup>+</sup>T cells are retained at the edge of the falcon and CD4<sup>+</sup>T cells are found in the middle of the falcon. Negatively enriched CD4<sup>+</sup>T cells were either directly used or *in vitro* activated in presence of 5  $\mu$ g/ml anti-CD3e/ 5  $\mu$ g/ml anti-CD28 (and some WT

cells also in presence of insulin) for 4 hours. (Activated) T cells were washed with PBS and fixated in 4 % Roti-Histofix for 10 min at RT. Immunofluorescence stainings were performed in the lab of Dr. Benno Weigmann at the Kussmaul Campus of the University of Erlangen, Germany. Rabbit anti-mouse pS6 and GCK antibody and donkey anti-rabbit Alexa Fluor 647 antibodies were used. The cells were analyzed by confocal microscopy.

### **2.19. Statistics**

Results are presented as FACS plots, scatter plots including mean and standard error of the mean (SEM), box-and-whisker plots including all data points or as pictures of immunofluorescence stainings. Data was normalized to the assay ctrl., SD, mesLNs or housekeeping genes (18s, Histone, 5S), where appropriate. For normally distributed data unpaired or paired Student's t-test were used. The Student's t-test for unpaired values was used to compare means between independent groups (*e.g.* Treg induction InsR TKO vs. Flox ctrl. mice) and the Student's t-test for paired values was used to compare values for the same sample tested under different conditions (*e.g.* Treg induction with and without insulin). For data that was not normally distributed a nonparametric test was applied. The Wilcoxon signed-ranks test was used for samples from the same population (*e.g.* Glucose uptake of CD4<sup>+</sup>T cells with or without insulin) and the Mann-Whitney test for samples from independent populations (*e.g.* Glucose uptake of CD4<sup>+</sup>T cells from InsR TKO vs. Flox ctrl. mice). The significance levels for Student's t-tests, Wilcoxon signed-ranks test and Mann-Whitney test were set as two-tailed P values of < 0.05. To test the effect of two different variables (*e.g.* genotype and HFHS diet) a two-way ANOVA and subsequent Post-hoc Sidak's multiple comparisons test were applied. Here, the significance level was determined as adjusted P value of < 0.05. Statistical analyses were performed with the program GraphPad Prism 7 and statistical significance is shown as \*P ≤ 0.05, \*\*P ≤ 0.01, \*\*\*P ≤ 0.001, \*\*\*\*P ≤ 0.0001 or not significant (P > 0.05).

### 3. Results

Chronic, low-grade inflammation as in obesity affects (precursor) TFH cell levels and Foxp3<sup>+</sup>Treg levels in metabolic tissues as well as in peripheral blood. Additionally, their differentiation from naïve CD4<sup>+</sup>T cells, their function, their stability and their cell intrinsic metabolism might be influenced by an obesogenic environment. However, how miRNAs or metabolic signaling cues specifically trigger T cell activation vs. regulation is not yet fully understood.

#### 3.1. (Precursor) TFH cells in obesity

Until now most of the research concerning TFH cells focuses on autoimmune diseases (Scherm et al., 2016; Serr et al., 2016b), however recent evidence suggests that these cells might additionally be involved in promoting tissue and systemic inflammation. The results below indicate a potential link between an obesogenic environment and (precursor) TFH cell frequencies both in human and mice.

##### 3.1.1. MiRNA92a and obesity affect TFH cell differentiation

Our group previously investigated the role of precursor TFH cells in the onset of human islet autoimmunity and signaling pathways that regulate their differentiation. Among others, we (Serr et al., 2016b) showed that the insulin-specific target T cell population in human peripheral blood is characterized by high levels of live CD4<sup>+</sup>CD45RA<sup>-</sup>CXCR5<sup>+</sup>CCR7<sup>low</sup>PD1<sup>hi</sup> precursor TFH cells (identified as in **Figure 1A** (upper row)) during onset of human islet autoimmunity.

This identification pattern for human precursor TFH cells was applied previously by various other research groups (Breitfeld et al., 2000; Haynes et al., 2007; He et al., 2013). Additionally, precursor TFH cells can be identified as live CD4<sup>+</sup>CD45RA<sup>-</sup>CXCR5<sup>+</sup>PD1<sup>+</sup>TFH cells (**Figure 1A** (lower row)) (Serr et al., 2016b) as also shown by (Baumjohann et al., 2013a; Kang et al., 2013; Ma & Deenick, 2017). MiRNAs of the miR-17~92 cluster were shown to promote TFH cell differentiation and function, GC formation and antibody responses (Baumjohann et al., 2013a; Kang et al., 2013).

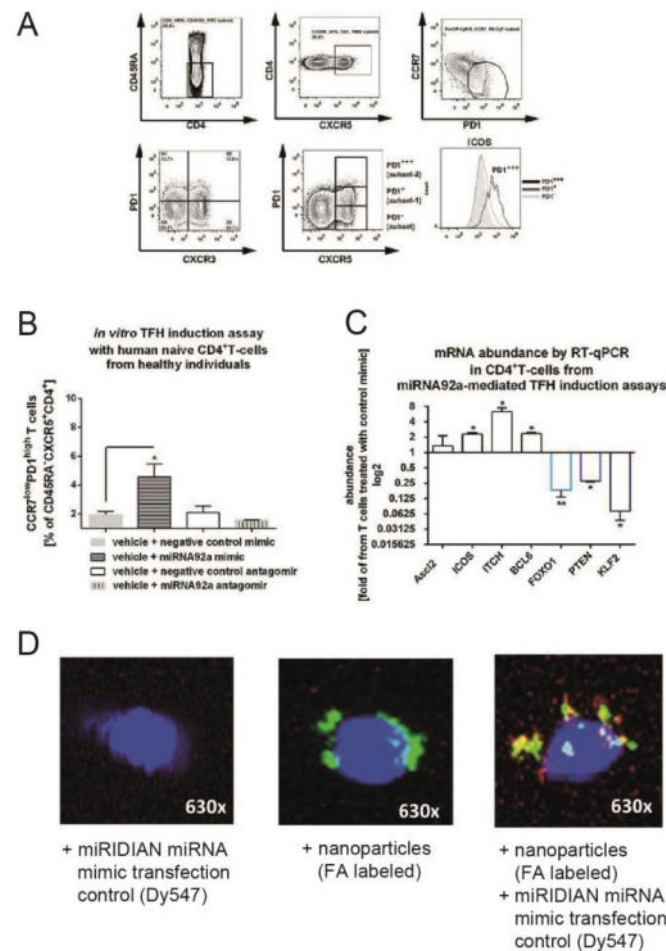


**Figure 1: MiRNA92a affects human precursor TFH cell induction *in vitro*.** (A) Representative FACS plots for the identification of CD4<sup>+</sup>CD45RA<sup>-</sup>CXCR5<sup>+</sup>CCR7<sup>low</sup>PD1<sup>hi</sup>T cells (upper) and CXCR5<sup>+</sup>PD1<sup>-</sup>, CXCR5<sup>+</sup>PD1<sup>+</sup> and CXCR5<sup>+</sup>PD1<sup>+++</sup>T cells (lower). (B) Precursor TFH cell induction using human naïve CD4<sup>+</sup>T cells from healthy individuals in the presence of memory B cells with or without a miRNA92a mimic, a miRNA92a antagomir, or respective negative control mimics or antagomirs. Summary graphs are shown for frequencies of CCR7<sup>low</sup>PD1<sup>hi</sup> cells presented as percentages of CXCR5<sup>+</sup>CD45RA<sup>-</sup>CD4<sup>+</sup>T cells. Data represents the mean ± SEM. \*P < 0.05 (C) mRNA abundance of predicted signaling pathways controlled by miRNA92a from CD4<sup>+</sup>T cells of precursor TFH cell induction assays in the presence of a miRNA92a mimic quantified by RT-qPCR analyses. Results are shown in abundance as the fold of T cells treated with negative miRNA mimic controls. Data represents the mean ± SEM from duplicate wells of four independent experiments. \*P < 0.05; \*\*P < 0.01. (D) Assessment of uptake, intracellular colocalization of FA-labeled nanoparticles, and Dy457-labeled transfection control miRNA mimic in CD4<sup>+</sup>T cells upon stimulation with anti-CD3/anti-CD28 by confocal microscopy. **Graphs as published in Serr et al. (Serr et al., 2016b). The corresponding graphs are shown there in Figure 5A, 5C and S3.**

We provided evidence that miRNA92a mediates human precursor TFH cell induction and showed that the abundance of this miRNA in CD4<sup>+</sup>T cells positively correlates with precursor TFH cell frequencies in peripheral blood (Serr et al., 2016b). *In vitro* precursor TFH cell induction assays co-culturing naïve CD4<sup>+</sup>CXCR5<sup>+</sup>T cells with autologous memory CD19<sup>+</sup>B cells in the presence of anti-CD3/CD28 for 5 days and with or without a miRNA92a mimic or miRNA92a antagomir, confirmed a role of miRNA92a for precursor TFH cell differentiation. A miRNA92a mimic significantly increased the frequencies of *in vitro* induced precursor TFH

cells, whilst incubation with a miRNA92a antagomir reversed this effect (**Figure 1B**). The miRNA92a mimic or antagomir were delivered using chitosan-coated poly (D,L-lactide-coglycolide) (PLGA) nanoparticles (Ravi Kumar et al., 2004) and confocal microscopy proved uptake, intracellular localization of labeled nanoparticles and delivery of fluorescently labeled control miRNAs into CD4<sup>+</sup>T cells as shown in **Figure 1D**.

FACS purified CD4<sup>+</sup>T cells at day 5 of *in vitro* precursor TFH cell differentiation assay showed that a miRNA92a mimic can modulate mRNA expression of its potential targets (**Figure 1C**). MiRNA92a increased mRNA expression of the early TFH cell marker *Ascl2* and significantly elevated mRNA levels of the TFH cell markers *ICOS*, *ITCH* and *Bcl6*. On the contrary, mRNA expression of negative regulators of T cell activation and TFH differentiation, namely *Foxo1*, *Pten* and *Klf2*, were significantly reduced in these cells. (**Figure 1** is published in (Serr et al., 2016b))

These results highlight an important role for precursor TFH cells during human islet autoimmunity and T1D. However, the function of TFH cells in metabolic diseases such as obesity and T2D remains unclear. Thus, the influence of an obesogenic environment on miRNA92a mediated (precursor) TFH cell differentiation and (precursor) TFH cell abundance in murine lymphoid tissues and in metabolically active, non-lymphoid ATs was examined. These results are shown below.

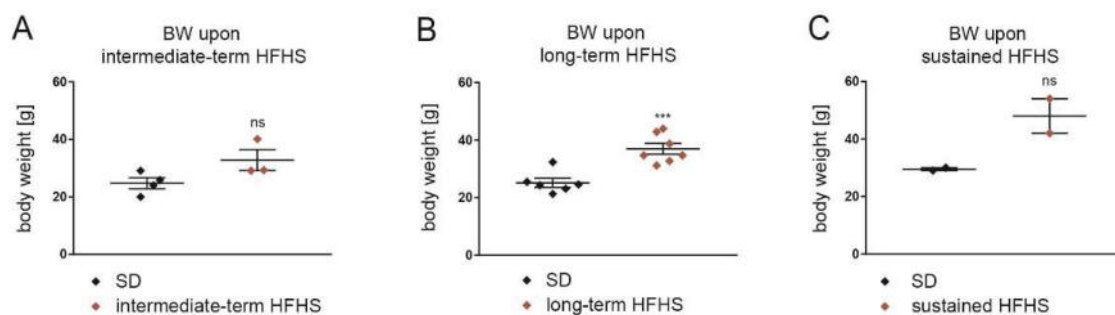


**Figure 2: BW upon different durations of a HFHS diet.** (A-C) BW in gram of mice exposed to a SD (n=4/6/2 mice) vs. (A) an intermediate-term HFHS diet (n=3 mice) vs. (B) a long-term HFHS diet (n=7 mice) vs. (C) a sustained HFHS diet (n=2 mice). Data is presented as scatter plots including all data points and mean ± SEM. ns P > 0.05, \*\*\*P ≤ 0.001 as determined by unpaired t-test. (SD: black diamonds, different HFHS: dark red diamonds).

First, non-TFH cells and precursor TFH cells were isolated from mesLN of mice exposed to either a SD or long-term HFHS diet. In addition to immunological analyses, metabolic parameters such as BW were assessed. **Figure 2B** shows the BWs of the used mice at the

day of sacrifice. Mice exposed to a long-term HFHS diet were significantly heavier than the corresponding control mice (SD:  $25.21 \pm 1.557$  g, long-term HFHS  $37.01 \pm 1.883$  g, \*\*\*P = 0.0006).

MesLNs and not inguinal (ingLNs) were used for these experiments because of their location close to the metabolically more active VAT. Murine precursor TFH cells were identified as live  $CD4^+CXCR5^+PD1^+$ T cells as shown in **Figure 3** and non-TFH cells were gated as  $CD4^+CXCR5^-$ T cells.

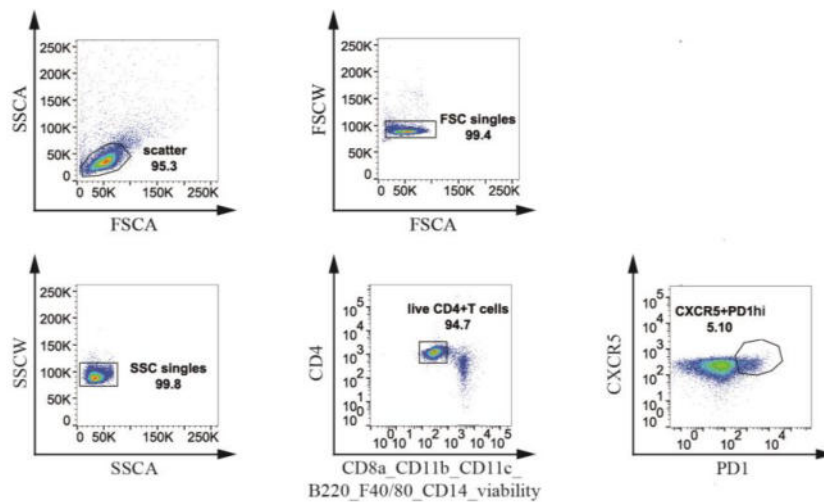


**Figure 3: Representative FACS plots for the identification of murine live  $CD4^+CXCR5^+(PD1^{hi})$  TFH cells.** Lymphocytes are first identified based on their size followed by doublet exclusion. Live  $CD4^+$ T cells are determined by a panel of exclusion markers (CD8a, CD11b, CD11c, B220, F40/80, CD14) and dead cell exclusion marker eFlour450. TFH cells are classified as live  $CD4^+CXCR5^+(PD1^{hi})$ T cells.

The influence of an obesogenic environment on T cell-intrinsic miRNA92a levels was assessed by measuring miRNA92a expression in precursor TFH cells and non-TFH cells isolated from mesLNs via RT-qPCR (**Figure 4**). MiRNA92a abundance was similar in non-TFH cells and precursor TFH cells independent of the dietary regimen (**Figure 4A+B**) (SD: non-TFH cells:  $11.22 \pm 0.816$ , precursor TFH cells:  $9.99 \pm 1.475$ , ns P = 0.2096 vs. long-term HFHS: non-TFH cells:  $9.02 \pm 0.830$ , precursor TFH cells:  $9.27 \pm 1.885$ , ns P = 0.8744). Moreover, a long-term HFHS diet did not result in changes in miRNA92a expression levels in both non-TFH cells (**Figure 4C**) (SD:  $9.99 \pm 1.475$ , long-term HFHS:  $9.27 \pm 1.885$ , ns P = 0.6121) and precursor TFH cells (**Figure 4D**) (SD:  $11.22 \pm 0.816$ , long-term HFHS:  $9.02 \pm 0.692$ , ns P = 0.0627). This indicates that an obesogenic environment might not trigger differentiation of  $CD4^+$ T cells into (precursor) TFH cells, at least not via increasing the expression of miRNA92a.

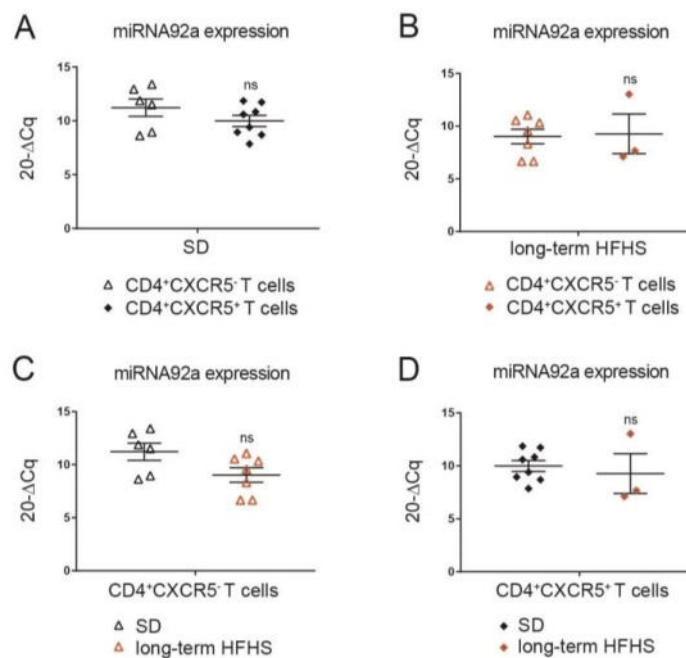


**Figure 4: miRNA92a expression in murine precursor TFH vs. non-TFH cells from mesLNs upon a long-term HFHS diet.** (A+B) miRNA92a expression in CD4<sup>+</sup>CXCR5<sup>+</sup> precursor TFH cells and CD4<sup>+</sup>CXCR5<sup>-</sup> non-TFH cells upon (A) a SD or (B) a long-term HFHS diet. (C+D) Diet depended changes in miRNA92a expression in (C) CD4<sup>+</sup>CXCR5<sup>-</sup> non-TFH cells and (D) CD4<sup>+</sup>CXCR5<sup>+</sup> precursor TFH cells. MiRNA92a expression as quantified by RT-qPCR analyses and normalized to the expression of 5s. Data is presented as scatter plots including all data points and mean  $\pm$  SEM. ns  $P > 0.05$  as determined by unpaired t-test. (n=3-8 mice, CD4<sup>+</sup>CXCR5<sup>-</sup> non-TFH cells (SD: black triangles, long-term HFHS: dark red triangles), CD4<sup>+</sup>CXCR5<sup>+</sup> precursor TFH cells (SD: black diamonds, long-term HFHS: dark red diamonds))

To test whether a high calorie environment affects mRNA expression of genes associated with TFH cell differentiation independent from miRNA92a induction, RT-qPCR was performed to measure mRNA abundance of *Il21*, *ICOS* and *Bcl6* in the identical non-TFH cells and precursor TFH cells isolated from mesLNs that were previously used for miRNA analysis. All analyzed genes showed, although mostly not significant, a tendency towards a higher expression in precursor TFH compared to non-TFH cells (**Figure 5**). Upon SD, *Il21* and *Bcl6* expression were significantly higher in CD4<sup>+</sup>CXCR5<sup>+</sup> precursor TFH cells compared to the corresponding non-TFH cells (**Figure 5A+C**) (*Il21*: 1.43 fold increase, \* $P = 0.0118$  and *Bcl6*: 1.54 fold increase, \* $P = 0.0267$ ), whilst *ICOS* levels were not changed in both T cell subsets (**Figure 5B**) (ns  $P = 0.3926$ ). Precursor TFH cells from mesLNs of mice exposed to a HFHS diet showed a significantly higher expression of *Il21* compared to non-TFH cells from HFHS mice (**Figure 5A**) (1.43 fold increase, \* $P = 0.0155$ ). This increase in *Il21* expression was similar to the increase seen in precursor TFH cells compared to non-TFH cells from SD mice. *ICOS* and *Bcl6* expression were not affected by the obesogenic environment (**Figure 5B+C**) (*ICOS* ns  $P = 0.0737$ , *Bcl6* ns  $P = 0.2116$ ).

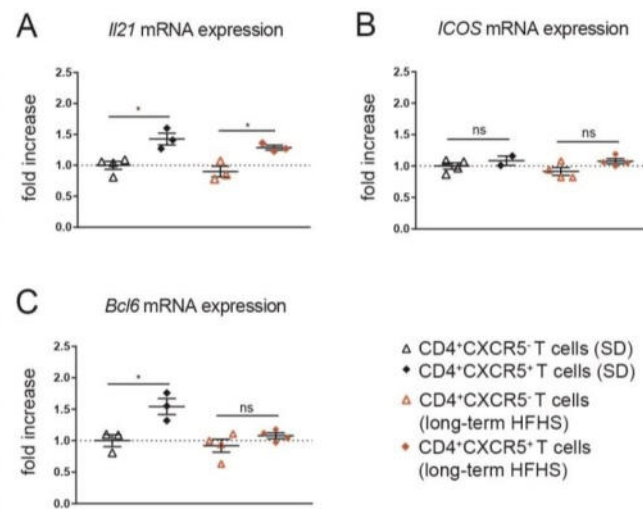


**Figure 5: mRNA expression of genes associated with TFH cell differentiation.** (A-C) mRNA expression of (A) *Ii21*, (B) *ICOS* and (C) *Bcl6* in CD4<sup>+</sup>CXCR5<sup>+</sup> precursor TFH cells vs. CD4<sup>+</sup>CXCR5<sup>-</sup> non-TFH cells upon a SD or long-term HFHS diet. Gene expression as quantified by RT-qPCR analyses and normalized to the mean expression of the housekeeping genes *Histone* and *18S*. Data is presented relative to the mRNA expression in CD4<sup>+</sup>CXCR5<sup>-</sup> non-TFH cells upon SD. Data is shown as scatter plots including all data points and mean ± SEM. ns P > 0.05, \*P ≤ 0.05 as determined by unpaired t-test. (n=3-4 mice, CD4<sup>+</sup>CXCR5<sup>-</sup> non-TFH cells (SD: black triangles, long-term HFHS: dark red triangles), CD4<sup>+</sup>CXCR5<sup>+</sup> precursor TFH cells (SD: black diamonds, long-term HFHS: dark red diamonds))

miRNA and mRNA expression analyses in precursor TFH cells and non-TFH cells gave no indication that obesity impacts TFH cells differentiation and abundance. To confirm these findings on the cellular level, next, (precursor) TFH cell frequencies were assessed in lymphoid and non-lymphoid tissues.

To better understand the link between the initiation and progression of obesity and TFH cell abundance, the frequencies of live CXCR5<sup>+</sup>PD<sup>hi</sup> precursor TFH cells [% of live CD4<sup>+</sup>T cells] (**Figure 3**) were assessed in both ingLNs and mesLNs of mice exposed to either a SD or different durations of a HFHS diet (**Figure 6**).

The BWs of all used mice are shown in **Figure 2**. As already mentioned, exposure to a long-term HFHS significantly increased the BW of the used mice (**Figure 2B**). Although not significantly due to the small sample number, the BWs of mice exposed to an intermediate-term HFHS diet (**Figure 2A**) and sustained HFHS diet (**Figure 2C**) were also increased (SD: 24.75 ± 1.901 g, intermediate-term HFHS 32.83 ± 3.634 g, ns P = 0.0860 vs. SD: 29.50 ± 0.500 g, sustained HFHS: 48.00 ± 6 g, ns P = 0.0920).

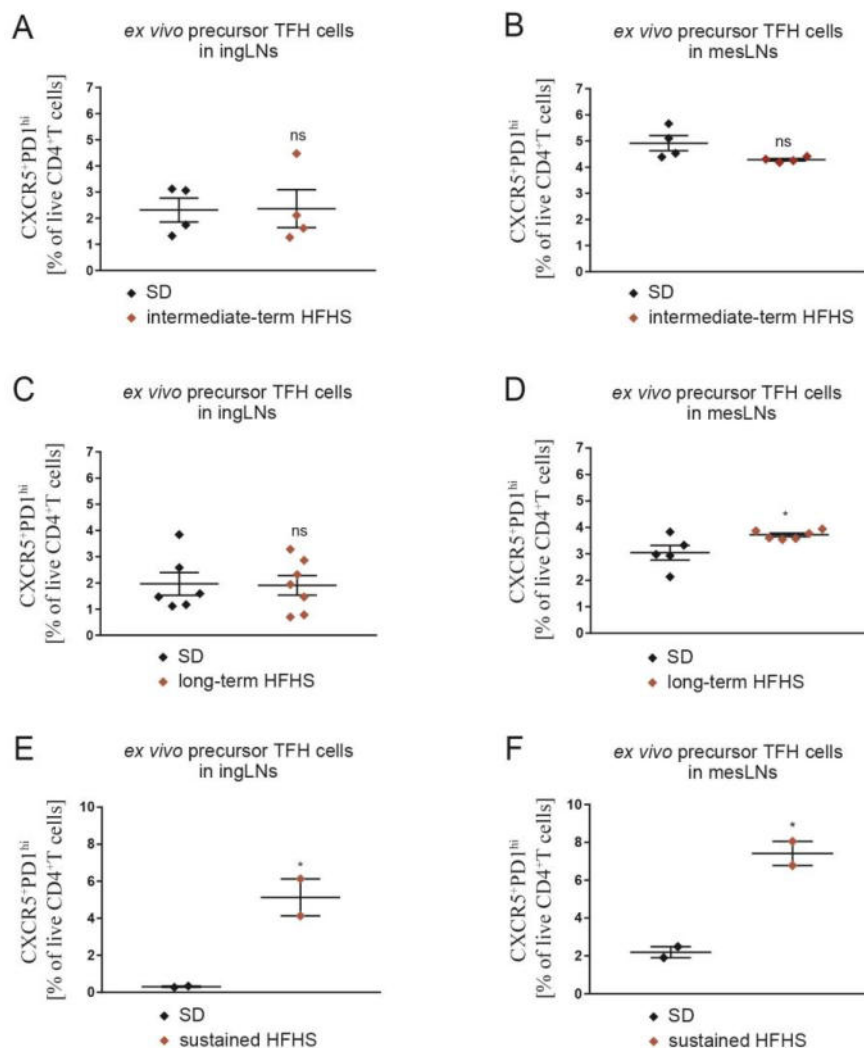


**Figure 6: Ex vivo (precursor) TFH cell frequencies in ingLNs and mesLNs are influenced by the progression of obesity.** (A-F) Frequencies of live CD4<sup>+</sup>CXCR5<sup>+</sup>PD1<sup>hi</sup> precursor TFH cells in ingLNs and mesLNs upon (A+B) an intermediate-term HFHS diet, (C+D) a long-term HFHS diet, (E+F) a sustained HFHS diet. Data is shown as scatter plots including all data points and mean  $\pm$  SEM. ns  $P > 0.05$ , \* $P \leq 0.05$  as determined by unpaired t-test. (n=2-7 mice, SD: black diamonds, intermediate-term HFHS/ long-term HFHS/ sustained HFHS: dark red diamonds)

The frequencies of precursor TFH cells in ingLNs and mesLNs showed marked variation upon dietary challenge. Exposure to both an intermediate-term and a long-term HFHS diet induced no changes in precursor TFH cell frequencies in ingLNs (**Figure 6A+C**) (SD:  $2.31 \pm 0.459$ , intermediate-term HFHS:  $2.36 \pm 0.720$ , ns  $P = 0.9531$  and SD:  $1.96 \pm 0.434$ , long-term HFHS:  $1.91 \pm 0.374$ , ns  $P = 0.9238$ ).

However, precursor TFH cell levels in mesLNs did change differently upon an intermediate-term and a long-term HFHS diet (**Figure 6B+D**). There was a marginal reduction in precursor TFH cells in mesLNs upon an intermediate-term HFHS diet (**Figure 6B**) (SD:  $4.92 \pm 0.291$ , intermediate-term HFHS:  $4.29 \pm 0.048$ , ns  $P = 0.0745$ ) and significantly more precursor TFH cells upon a long-term HFHS diet (**Figure 6D**) (SD:  $3.04 \pm 0.279$ , long-term HFHS:  $3.72 \pm 0.068$ , \* $P = 0.0298$ ). Preliminary data showed that the frequencies of CXCR5<sup>+</sup>PD<sup>hi</sup> precursor TFH cells [% of live CD4<sup>+</sup>T cells] were significantly higher in both ingLNs and mesLNs upon one year exposure to a high caloric environment (**Figure 6E+F**) (ingLNs: SD:  $0.31 \pm 0.035$ , sustained HFHS:  $5.13 \pm 1.000$ , \* $P = 0.0404$ , mesLNs: SD:  $2.20 \pm 0.295$ , sustained HFHS:  $7.42 \pm 0.635$ , \* $P = 0.0175$ ).

To analyze whether the frequencies of TFH cells are similarly or even more prominently influenced by an obese, hyperphagic, hyperinsulinemic and hyperglycemic environment, TFH cell levels were assessed in mesLNs of genetically obese ob/ob mice. In contrast to DIO mice, genetically obese ob/ob mice develop severe obesity and peripheral insulin resistance (in the under healthy conditions insulin-sensitive tissues liver, muscle and AT) due a spontaneous, autosomal recessive, non-sense C to T mutation in codon 105 of the leptin gene and not due to increased food consumption. This mutation not only triggers obesity development in ob/ob mice, but also has multiple known and unknown other molecular and cellular effects. Thus, direct comparison of results from DIO mice and ob/ob mice should be avoided.

As expected, ob/ob mice had a significantly higher BW than their corresponding WT ctrls. (**Figure 7A**) (WT ctrl.:  $32.36 \pm 0.452$  g vs. ob/ob:  $46.51 \pm 0.695$  g, \*\*\*\* $P < 0.0001$ ). Frequencies of CXCR5<sup>+</sup>PD<sup>hi</sup> precursor TFH cells [% of live CD4<sup>+</sup>T cells] (gated as in **Figure 7B, left FACS Plot**) were unchanged in WT ctrl. vs. ob/ob mice (**Figure 7C**) (WT ctrl.:  $3.80 \pm 0.529$  vs. ob/ob:  $4.01 \pm 0.481$ , ns  $P = 0.7727$ ). Given the role of *Bcl6* as marker for more differentiated, mature, GC TFH cells (Hale et al., 2013), this marker was included for more specific flow cytometric analysis of TFH cells. Identification of GC-like TFH cells by gating for CD4<sup>+</sup>CXCR5<sup>+</sup>PD<sup>hi</sup>TFH cells with high expression of *Bcl6* (**Figure 7B, right FACS Plot**) depicted significantly higher levels of these TFH cells in mesLNs of ob/ob mice (**Figure 7D**) (*Bcl6*<sup>hi</sup>TFH cells [% of live CD4<sup>+</sup>CXCR5<sup>+</sup>PD1<sup>hi</sup>T cells] WT ctrl.:  $7.32 \pm 1.093$  vs. ob/ob:  $16.23 \pm 2.213$ , \*\* $P = 0.0023$ ).

The data shown here provides evidence for a positive correlation between obesity development and CD4<sup>+</sup>CXCR5<sup>+</sup>PD1<sup>hi</sup>(*Bcl6*<sup>hi</sup>) (precursor) TFH cell levels in lymphoid tissues, though, data is characterized by a great heterogeneity.

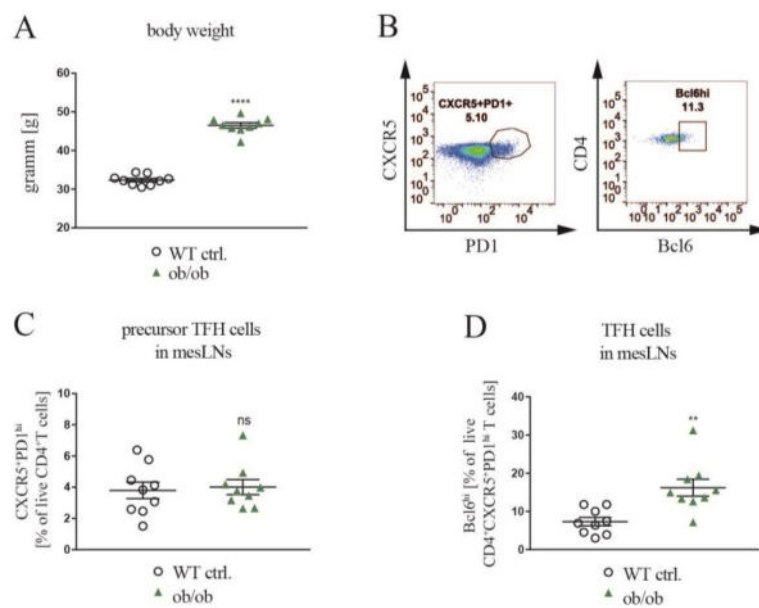


**Figure 7: (Precursor) TFH cells in mesLNs of genetically obese ob/ob mice.** (A) Assessed BW in WT ctrl. and ob/ob mice at the day of sacrifice. (B) Identification of CXCR5+PD1<sup>hi</sup> precursor TFH cells and CXCR5+PD1<sup>hi</sup>Bcl6<sup>hi</sup>TFH cells. (C+D) Frequencies of (C) precursor TFH cells and (D) TFH cells in mesLNs of WT ctrl. vs. ob/ob mice. Data is presented as scatter plots including all data points and mean  $\pm$  SEM (A+C+D) or FACS Plots (B). ns  $P > 0.05$ , \*\* $P \leq 0.01$ , \*\*\*\* $P \leq 0.0001$  as determined by unpaired t-test. (n=9 mice/ genotype, WT ctrl.: black circles, ob/ob: green triangles)

To answer the question whether TFH cells play an important role outside the lymphoid organs, in non-lymphoid tissues *e.g.* the AT, next TFH cell frequencies in BAT, SAT and particularly in VAT were assessed, to dissect the contribution of TFH cells to obesity-associated inflammation.

Our group previously showed (Kalin et al., 2017) that immune cell populations within metabolically active tissues alter during exposure to a HFHS diet. Specifically, we showed that the frequency of anti-inflammatory Foxp3<sup>+</sup>Tregs [% of total CD4<sup>+</sup>T cells] were decreased in BAT, SAT and VAT upon a long-term HFHS diet. Moreover, the impairments in response to the high caloric environment were highest and significant in VAT (**Figure 8A**) (Figure 1N in (Kalin et al., 2017)). Pro-inflammatory TFH cells were shown to antagonize Treg function in multiple signaling pathways. Thus, it is highly relevant to analyze TFH cell frequency in tissues that were shown to harbor decreasing numbers of Tregs in response to an obesogenic environment.

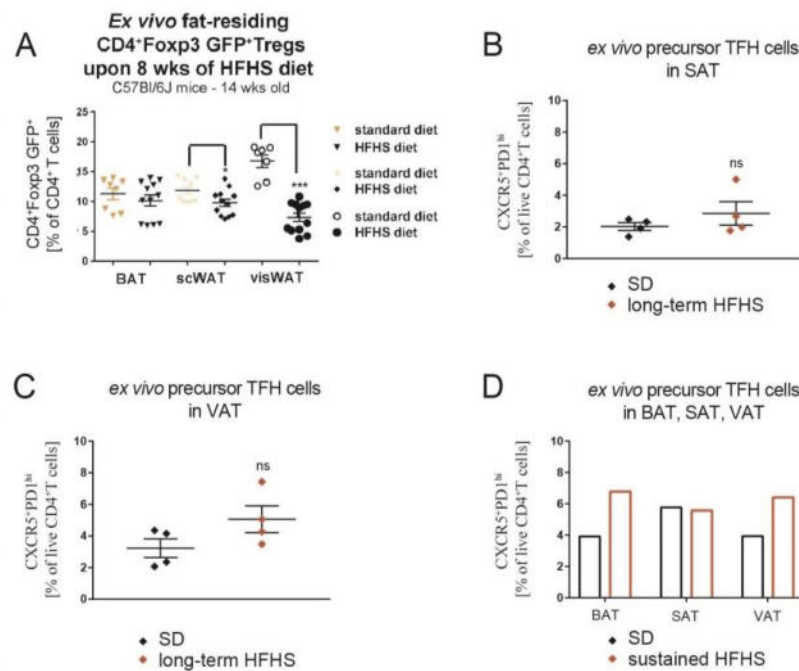


**Figure 8: Frequencies of *ex vivo* Foxp3<sup>+</sup>Tregs and precursor TFH cells in murine ATs upon a HFHS diet.** (A) Depicted are *ex vivo* fat-residing CD4<sup>+</sup>CD25<sup>+</sup>Foxp3<sup>+</sup> Tregs of 14 week old C57BL/6J animals that were on a HFHS diet for 8 weeks. n=4 per group. Data is presented as scatter plots including all data points and mean  $\pm$  SEM (\*\*P < 0.001). Graph as published in Kälén *et al.* (Kalin *et al.*, 2017). The corresponding graph is shown in Figure 1N. (B+C) *Ex vivo* fat-residing precursor CXCR5<sup>+</sup>PD1<sup>hi</sup>TFH cells in (B) SAT and (C) VAT of n=4 mice upon a long-term HFHS diet. (D) *Ex vivo* fat-residing precursor CXCR5<sup>+</sup>PD1<sup>hi</sup>TFH cells from BAT, SAT and VAT of n=1 mouse upon one year of a HFHS diet. Data is presented as scatter plots including all data points and mean  $\pm$  SEM (B+C) or bar chart (D). ns P > 0.05 as determined by paired t-test (B+C). (D) The shown preliminary data has a limited number of biological replicates, therefore, no statistics were possible. (SD: black diamonds, HFHS: diet red diamonds)

CD4<sup>+</sup>CXCR5<sup>+</sup>PD1<sup>hi</sup> precursor TFH cells were isolated from BAT, SAT and VAT to analyze whether their abundance is affected by an obesogenic environment. CXCR5<sup>+</sup>PD1<sup>hi</sup> precursor TFH cells [% of live CD4<sup>+</sup>T cells] showed a tendency towards a higher expression in SAT (**Figure 8B**) and VAT (**Figure 8C**) upon a long-term HFHS diet (SAT: SD: 2.03  $\pm$  0.247, long-term HFHS: 2.56  $\pm$  0.741, ns P = 0.3287 vs. VAT: SD: 3.23  $\pm$  0.593, long-term HFHS: 5.06  $\pm$  0.854, ns P = 0.1285). Preliminary data applying mice exposed to a sustained HFHS diet of one year showed that the increase in CD4<sup>+</sup>CXCR5<sup>+</sup>PD1<sup>hi</sup> precursor TFH cells might positively correlate with the duration of the HFHS diet. Additionally, the effects of a sustained HFHS diet might be most prominent in BAT and VAT (**Figure 8D**) (no statistics possible).

### 3.1.2. Preliminary data: TFH cells in human obesity

In order to translate the above shown preliminary data from mice to humans and to investigate a potential effect of an obesogenic environment on TFH cell frequencies in human peripheral blood, a limited number of peripheral blood samples from lean, insulin-sensitive (BMI:  $23.0 \pm 0 \text{ kg/m}^2$ ) vs. obese, insulin-sensitive (BMI:  $46.2 \pm 0 \text{ kg/m}^2$ ) vs. obese, insulin-resistant (BMI:  $50.2 \pm 0.97 \text{ kg/m}^2$ ) patients (**Figure 9A**, no statistics possible due to a low sample number) was available for analysis, resulting in the below shown preliminary data.

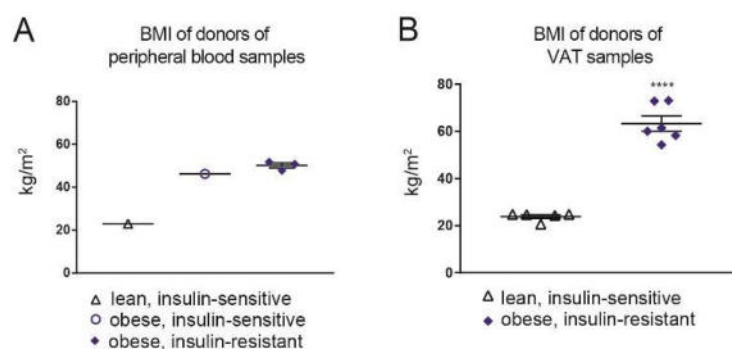


**Figure 9: BMI of lean and obese individuals.** (A) BMI of one lean, insulin-sensitive vs. one obese, insulin-sensitive vs. three obese, insulin-resistant individual(s) that donated peripheral blood (B) BMI of lean, insulin-sensitive (n=5) vs. obese, insulin-resistant (n=6) individuals that donated VAT. Data is presented as scatter plots including all data points and mean  $\pm$  SEM. \*\*\*\*P  $\leq$  0.0001 as determined by unpaired t-test. (lean, insulin-sensitive: blue triangles, obese, insulin-sensitive: blue circles, obese, insulin-resistant: blue diamonds)

Human peripheral blood precursor TFH cells might comprise of a CXCR3<sup>+</sup>CCR6<sup>-</sup>Th1-like, CXCR3<sup>-</sup>CCR6<sup>-</sup>Th2-like and CXCR3<sup>-</sup>CCR6<sup>+</sup>Th17-like precursor TFH cell subset, all capable to provide B cell help, though with different efficiency (Bentebibel et al., 2013; Chtanova et al., 2004; Fazilleau et al., 2009; Locci et al., 2013; Morita et al., 2011). A representative gating strategy for the subclassification of human peripheral blood precursor TFH cells is shown in **Figure 10A**.

Precursor TFH cell levels with a Th1-like cytokine profile were highest in lean, insulin-sensitive individuals and similarly lower in both obesity groups (**Figure 10B**). Th2-like precursor TFH cells were decreasing with the appearance of obesity and were lowest in obese, insulin-resistant individuals (**Figure 10C**). In contrast, precursor TFH cells with a Th17-like cytokine profile increased from lean, insulin-sensitive to obese, insulin-sensitive to obese, insulin-resistant individuals (**Figure 10D**).

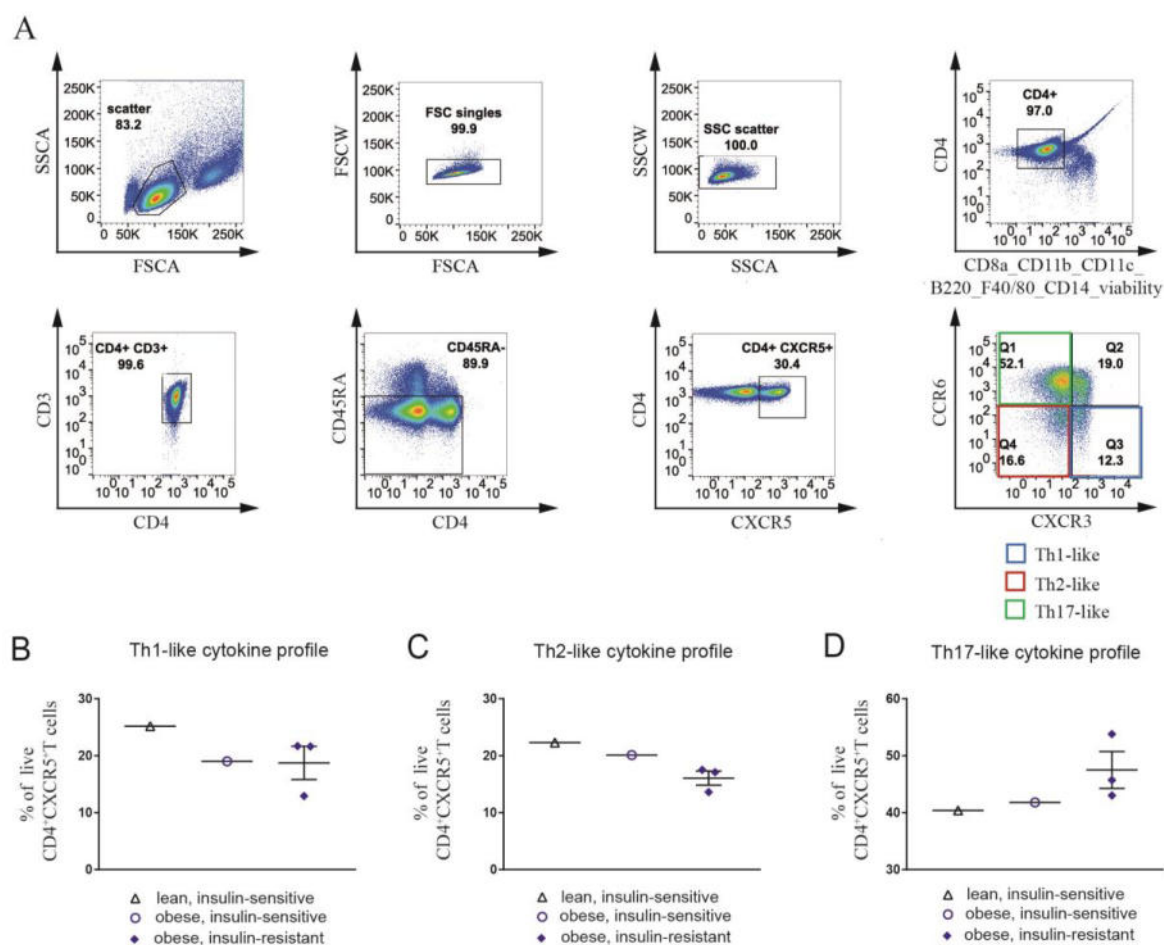


**Figure 10: Preliminary data: Analysis of precursor TFH cells in peripheral blood during human obesity.** (A) Representative FACS plots for the identification of CD4<sup>+</sup>CD45RA<sup>-</sup>CXCR5<sup>+</sup> precursor TFH cells and their Th1-like, Th2-like and Th17-like subsets. (B-D) Frequencies of the precursor TFH cell subpopulations with (B) a Th1-like cytokine profile, (C) a Th2-like cytokine profile and (D) a Th17-like cytokine profile presented as % of CD4<sup>+</sup>CXCR5<sup>+</sup>TFH cells in human peripheral blood of one lean, insulin-sensitive vs. one obese, insulin-sensitive vs. three obese, insulin-resistant individual(s). Data is presented as (A) FACS Plots or (B-D) scatter plots including all data points and mean  $\pm$  SEM. The shown preliminary data has a limited number of biological replicates; therefore no statistics were possible. (lean, insulin-sensitive: black triangles, obese, insulin-sensitive: blue circles, obese, insulin-resistant: blue diamonds)

To further support the initial findings indicating altered precursor TFH cell frequencies in human peripheral blood due to an obesogenic environment, mRNA expression analysis was performed on total human VAT from lean, insulin-sensitive (BMI:  $23.87 \pm 0.793 \text{ kg/m}^2$ ) vs. obese, insulin-resistant (BMI:  $63.30 \pm 3.194 \text{ kg/m}^2$ ) individuals. The BMIs of the individuals that donated VAT are shown in **Figure 9B**. As expected, obese, insulin-resistant individuals had a significantly higher BMI than lean, insulin-sensitive individuals (lean, insulin-sensitive:  $23.87 \pm 0.793 \text{ kg/m}^2$ , obese, insulin-resistant:  $63.3 \pm 3.194 \text{ kg/m}^2$ , \*\*\*\* $P \leq 0.0001$ ).

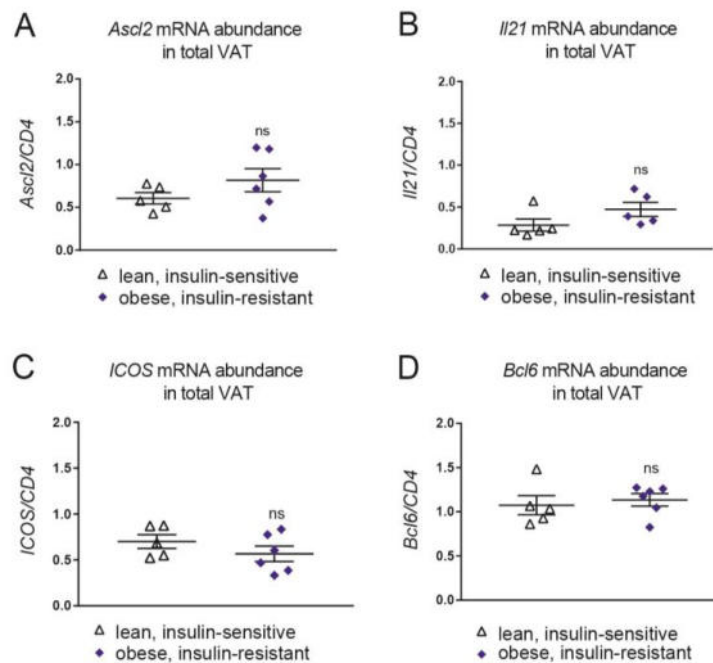


**Figure 11: Initial results: mRNA expression of genes associated with TFH cell differentiation in total human VAT.** mRNA expression of (A) *Ascl2*, (B) *Il21*, (C) *ICOS* and (D) *Bcl6* in human total VAT of lean, insulin-sensitive (n=5) vs. obese, insulin-resistant individuals (n=6). Gene expression as quantified by RT-qPCR analyses and normalized to CD4. Data is presented as scatter plots including all data points and mean ± SEM. ns P > 0.05 as determined by unpaired t-test. (lean, insulin-sensitive: black triangles, obese, insulin-sensitive: blue circles, obese, insulin-resistant: blue diamonds)

Initial analysis of *Ascl2*, *Il21*, *ICOS* and *Bcl6* mRNA expression in total human VAT, showed a tendency towards a higher abundance of *Ascl2* and *Il21* (relative to the expression of CD4) in the VAT of obese, insulin-resistant individuals (**Figure 11A+B**) (*Ascl2*: lean: 0.606 ± 0.067, obese: 0.817 ± 0.135, ns P = 0.2221, *Il21*: lean: 0.285 ± 0.073, obese: 0.427 ± 0.118, ns P = 0.1312), whilst *Bcl6* expression remained unaffected (**Figure 11D**) (*Bcl6*: lean: 1.08 ± 0.0108, obese: 1.14 ± 0.071, ns P = 0.6421). On the contrary, *ICOS* showed a tendency towards a lower expression in VAT of obese, insulin-resistant individuals compared to the lean, insulin-sensitive controls (**Figure 11C**) (*ICOS*: lean: 0.701 ± 0.075, obese: 0.567 ± 0.084, ns P = 0.2790).

### 3.2. Insulin (receptor) signaling and its effects on *de novo* Treg induction

The second main focus of this thesis was to assess the contribution of metabolic signaling cues to the function of CD4<sup>+</sup>T cells and in particular to dissect their relevance for the induction of immunoregulatory Foxp3<sup>+</sup>Tregs. Given its pivotal role for metabolic control, specifically the effect of the hormone insulin was investigated.

#### 3.2.1. Insulin impairs *de novo* Foxp3<sup>+</sup>Treg induction

First, the role of CD4<sup>+</sup>T cell specific insulin signaling in guiding Foxp3<sup>+</sup>Treg induction and function was investigated. To this end, Tregs were *in vitro* induced from sort-purified naïve CD4<sup>+</sup>T cells applying short-term TCR stimulation provided under subimmunogenic conditions in continuous presence of IL2 and insulin. This polyclonal induction assay was previously shown by us (Serr et al., 2016a) and others (Fontenot et al., 2003; Sauer et al., 2008) to result in highest levels of Foxp3<sup>+</sup>Tregs. Previously, our group also identified an improved Treg induction capacity when modifying and thereby reducing TCR signaling strength, though maintaining all stimuli for the whole assay (referred to as low dose, continuous TCR stimulation) (Serr et al., 2016a). Since both Treg induction with short-term TCR stimulation and with low dose, continuous TCR stimulation were shown to result in high Treg frequencies, here, both methods were applied for Treg induction in presence of insulin (**Figure 12C+D**) and compared regarding the effect of insulin on resulting Treg frequencies.

Titration of human recombinant insulin (10, 25, 50, 75, 100 ng/ml insulin) in *in vitro* Treg induction assays applying short-term TCR stimulation showed that 50 ng/ml insulin have the most prominent effect on resulting Treg frequencies (data not shown). Treg induction with 50 ng/ml insulin significantly impaired the differentiation of naïve CD4<sup>+</sup>T cells from lean C57BL/6J mice into Foxp3<sup>+</sup>CD25<sup>hi</sup>Tregs *in vitro* both under short-term TCR stimulation (**Figure 12B+C**) (normalized to the assay ctrl.: assay ctrl.  $100 \pm 1.124$  vs. insulin  $84.44 \pm 1.306$ , \*\*\*\* $P \leq 0.0001$ ) and under low dose, continuous TCR stimulation (**Figure 12D**) (normalized to the assay ctrl.: assay ctrl.  $100 \pm 1.361$  vs. insulin  $72.39 \pm 2.228$ , \*\*\*\* $P \leq 0.0001$ ). In the latter, impairments in Treg induction capacity were more prominent and accompanied by a significant increase in CD4<sup>+</sup>T cells expressing the proliferation marker Ki67 (Ki67<sup>+</sup>T cells [% of live CD4<sup>+</sup>T cells]: assay ctrl.  $92.13 \pm 1.437$  vs. insulin  $94.13 \pm 1.114$ , \*\* $P = 0.0045$ ).

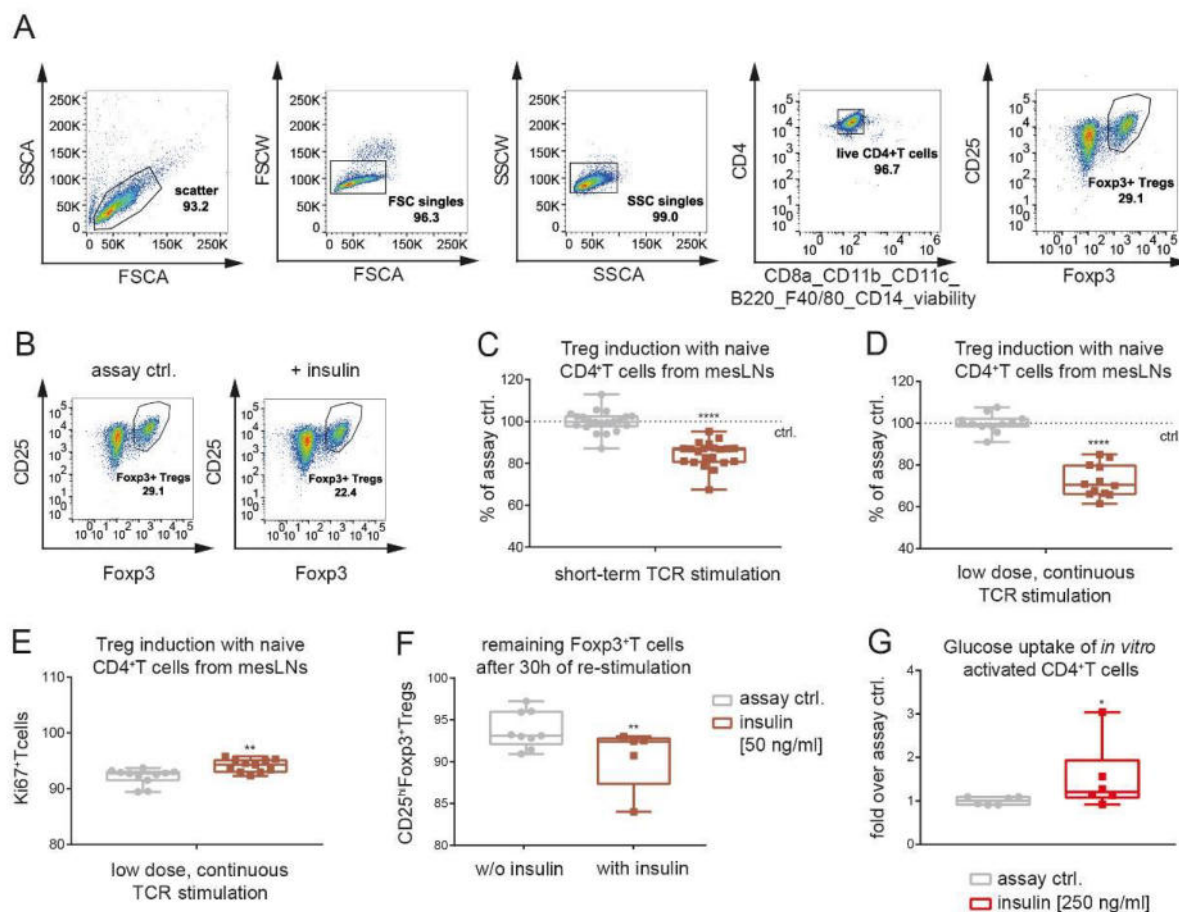


**Figure 12: Insulin affects *in vitro* CD25<sup>hi</sup>Foxp3<sup>+</sup>Treg induction, T cell proliferation, Treg stability and T cell specific glucose uptake.** (A) Identification of *in vitro* induced murine Tregs. (B+C) Representative FACS plots (B) and frequencies of *in vitro* induced CD25<sup>hi</sup>Foxp3<sup>+</sup>Tregs (n=8 mice/ 2-3 technical replicates) (C) In presence and absence of 50 ng/ml insulin using short-term TCR stimulation. (D) Tregs frequencies using low dose, continuous TCR stimulation (n=4 mice/ 3 technical replicates). (E) Frequencies of CD4<sup>+</sup>Ki67<sup>+</sup>T cells (at day 3 of Treg induction, as in (D)). (F) Analysis of remaining Foxp3<sup>+</sup>T cells after *in vitro* induction from naïve CD4<sup>+</sup>T cells of all LNs of Foxp3-GFP mice and re-stimulation for 30 h (hours) in presence or absence of 50 ng/ml insulin (n=8 mice pooled/ 5 or 9 technical replicates). (F) Glucose uptake measured by luminescence in FACS purified naïve CD4<sup>+</sup>T cells from all LNs and spleen of n=3 mice (2 technical replicates) upon *in vitro* activation with or without 250 ng/ml insulin for 4 hours at 37°C and 5 % CO<sub>2</sub>. Data is presented as box-and-whisker plots including all data points (C-G). Data in C+D is normalized to assay ctrl. \*P ≤ 0.05, \*\*P ≤ 0.01, \*\*\*\*P ≤ 0.0001 as determined by paired t-test (C-F) or Wilcoxon matched-pairs signed rank test (G). (assay ctrl.: grey dots, 50 ng/ml insulin: dark red squares, 250 ng/ml insulin: red squares)

These insulin-mediated impairments in Treg induction, raise the question whether insulin similarly affects Treg stability. Of note, re-stimulation of *in vitro* induced Foxp3<sup>+</sup>T cells from total LNs showed that a significantly higher percentage of Tregs that were both induced and re-stimulated in the presence of insulin lost their Foxp3 expression (**Figure 12F**). This indicates a reduced stability of their Treg phenotype (Tregs [% of live CD4<sup>+</sup>T cells]: w/o insulin 93.72 ± 0.721 vs. with insulin 90.52 ± 1.676, P = 0.0089).

To more specifically integrate the findings that insulin does interfere with *de novo* Treg induction into the field of immunometabolism, the next aim was to investigate metabolic characteristics of T cells involved in the regulation of T cell activation, proliferation and Treg

induction. Once CD4<sup>+</sup>T cells get activated, they switch their energy supply and mainly depend on aerobic glycolysis (Almeida et al., 2016; Michalek et al., 2011; Park & Pan, 2015; van der Windt & Pearce, 2012). Thus, *in vitro* activation of naïve CD4<sup>+</sup>T cells by anti-CD3e/CD28 and insulin (as in Treg induction assays) that precedes their differentiation into Foxp3<sup>+</sup>Tregs might trigger adaptations of the CD4<sup>+</sup>T cell-intrinsic metabolism. A luminescence-based assay showed that insulin (the concentration was adjusted to the cell number resulting in 250 ng/ml insulin) significantly increased glucose uptake by CD4<sup>+</sup>T cells that were previously activated for 4 hours (**Figure 12G**) (fold increase in glucose uptake, assay ctrl.:  $1.00 \pm 0.036$ , insulin:  $1.512 \pm 0.317$ , \* $P = 0.0313$ ).

The hormone insulin was previously shown to trigger its metabolic effect (partly) by signaling via the PI3K-Akt-mTOR pathway in metabolically active tissue such as the AT (Araki et al., 1994; Bouzakri et al., 2006; Taniguchi et al., 2005; Thirone et al., 2006). In line with these findings, *in vitro* activation and insulin stimulation of CD4<sup>+</sup>T cells resulted in an significantly increased expression of phosphorylated ribosomal protein S6 kinase (pS6) assessed by immunofluorescence microscopy (**Figure 13A**) (w/o insulin:  $3.67 \pm 0.333$ , with insulin:  $10.33 \pm 1.430$ , \*\* $P = 0.0071$ ). Likewise, an significantly increased expression of Glucokinase (GCK) was identified upon insulin activation of CD4<sup>+</sup>T cells (**Figure 13B**) (w/o insulin:  $4.60 \pm 1.208$ , with insulin:  $13.20 \pm 2.223$ , \*\* $P = 0.0026$ ).

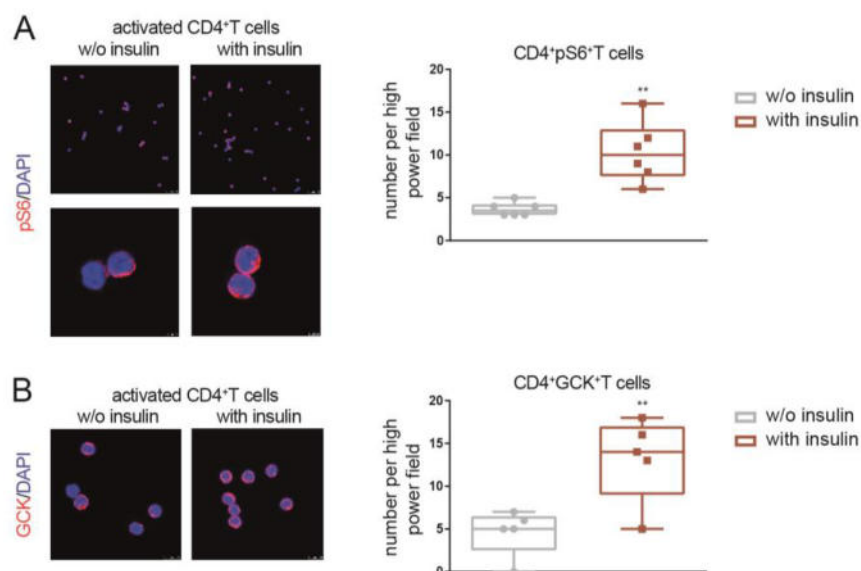


**Figure 13: Insulin affects targets downstream of InsR signaling.** (A-B) Representative immunofluorescence stainings on cytopsmen from *in vitro* in presence or absence of 250 ng/ml insulin activated CD4<sup>+</sup>T cells of WT mice stained for (A) pS6 and (B) GCK. Respective summary graphs show the number of positive CD4<sup>+</sup>T cells/high power field for each antibody. \*\* $P \leq 0.01$  as determined by paired t-test. Data in the graphs is presented as box-and-whisker plots including all data points. (assay ctrl.: grey dots, 250 ng/ml insulin: red squares)

Next, to study the translational relevance of the findings above for human physiology, the impact of insulin and downstream InsR signaling on human CD4<sup>+</sup>T cell activation and differentiation was investigated. Human Tregs were gated as CD4<sup>+</sup>CD3<sup>+</sup>CD127<sup>lo</sup>CD25<sup>hi</sup>Foxp3<sup>+</sup>T cells (as shown in the FACS Plots in **Figure 14A**) and 100 ng/ml insulin were identified as most suitable concentration for human Treg induction experiments (data for 50 and 150 ng/ml insulin is not shown). Treg induction with 100 ng/ml insulin significantly impaired the differentiation of naïve CD4<sup>+</sup>T cells from human peripheral blood of female individuals (**Figure 14B**) (normalized to the assay ctrl.: assay ctrl.  $100 \pm 1.497$  vs. insulin  $94.9 \pm 1.050$ , \* $P = 0.0366$ ). However, this concentration of insulin was not sufficient to reduce *in vitro* Treg induction starting with naïve CD4<sup>+</sup>T cells from peripheral blood of male subjects (**Figure 14C**) (normalized to the assay ctrl.: assay ctrl.  $100 \pm 1.416$  vs. insulin  $101 \pm 3.347$ , ns  $P = 0.3772$ ).

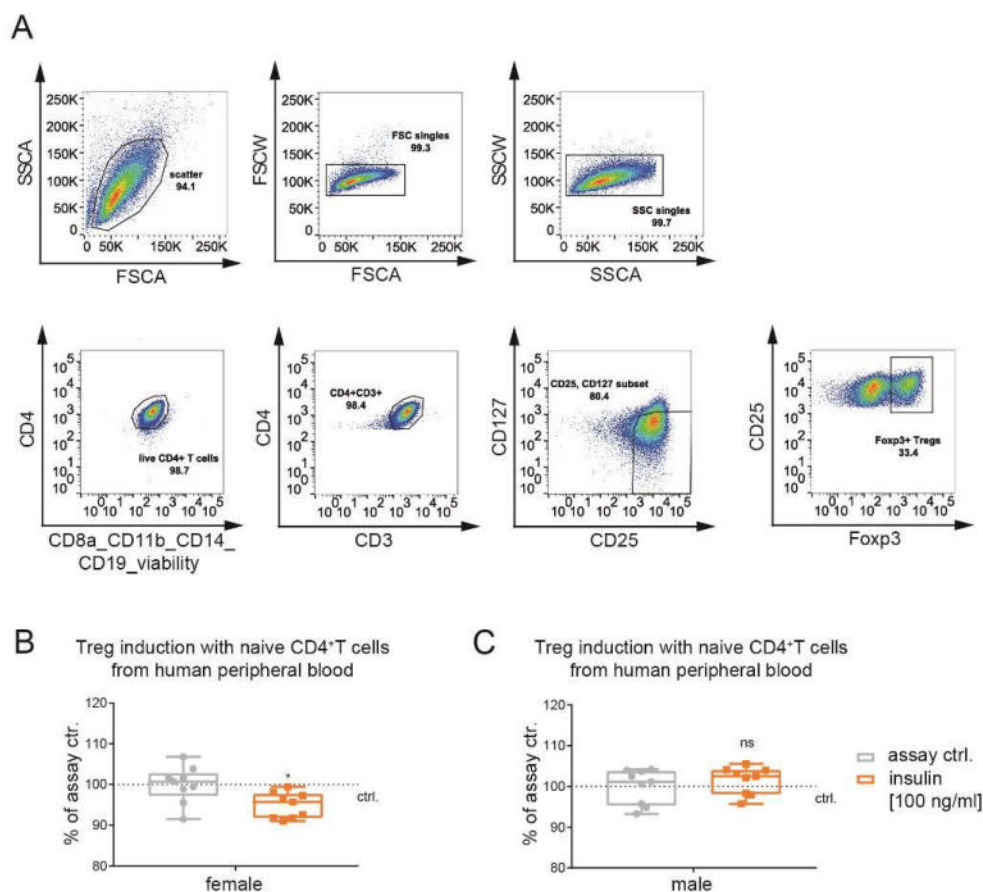


**Figure 14: The effect of insulin on human *in vitro* Treg induction is sex dependent.** (A) Representative FACS plots for the identification of *in vitro* induced human Tregs. (B+C) Frequencies of induced CD127<sup>lo</sup>CD25<sup>hi</sup>Foxp3<sup>+</sup>Tregs using naïve CD4<sup>+</sup>T cells from human peripheral blood of (B) n=3 females (3 technical replicates/each) or (C) n=3 males (3 technical replicates/each) with or without 100 ng/ml insulin. Data is normalized to assay ctrl. and presented as box-and-whisker plots including all data points. ns  $P > 0.05$ , \* $P \leq 0.05$  as determined by paired t-test. (assay ctrl.:grey dots, 100 ng/ml insulin: orange squares)

To combine insulin-mediated impairments in Treg induction with obesity-associated negative metabolic effects and to assess whether CD4<sup>+</sup>T cells get insulin-resistant similarly to

peripheral metabolically active tissues in ob/ob and DIO mice, *in vitro* Treg induction with naïve CD4<sup>+</sup>T cells from mesLNs of genetically obese ob/ob and DIO mice was performed. Insulin similarly and significantly lowered Treg induction capacity using naïve CD4<sup>+</sup>T cells from both ob/ob mice (**Figure 15**) (normalized to own assay ctrl., WT ctrl.: assay ctrl.  $100 \pm 1.499$  vs. insulin  $86.14 \pm 1.384$ , ob/ob: assay ctrl.  $100 \pm 1.201$  vs. insulin  $87.96 \pm 1.192$ , both \*\*\*\*P < 0.0001) and mice that were exposed to a SD, a short-term HFHS diet, a long-term HFHS diet or a sustained HFHS diet (**Figure 17A-C**). Specifically, insulin-mediated impairments in Treg induction were comparable when using T cells from ob/ob mice and their corresponding WT ctrls. (**Figure 15**). The mean BW of these mice and their corresponding controls is shown in **Figure 7A**.

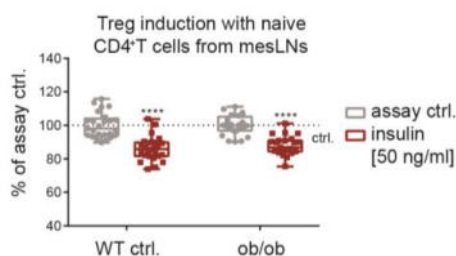


**Figure 15: The effect of insulin on *in vitro* Treg induction is maintained in genetic obesity.** (A) *In vitro* Treg induction with naïve CD4<sup>+</sup>T cells from genetically obese ob/ob mice and respective WT ctrl. mice in the presence or absence of 50 ng/ml insulin (n=14 mice per genotype/ 1-3 technical replicates). Data is normalized to the assay ctrl. and presented as box-and-whisker plots including all data points. \*\*\*\*P ≤ 0.0001 as determined by 2way ANOVA and Sidak's multiple comparison test. (assay ctrl.: grey dots, 50 ng/ml: dark red squares)

In DIO mice, a short-term HFHS diet did not markedly change their BW (**Figure 16A**) (SD:  $22.97 \pm 0.805$ , short-term HFHS:  $23.71 \pm 0.756$ , ns P = 0.7561). On the contrary, a long-term HFHS diet (**Figure 16B**) and sustained HFHS (**Figure 16C**) significantly increased the BW of the respective mice compared to their controls (SD:  $23.70 \pm 0.5070$ , long-term HFHS:  $28.93 \pm 1.353$ , \*P = 0.013 vs. SD:  $38.07 \pm 2.2452$ , sustained HFHS:  $57.25 \pm 0.250$ , \*\*P = 0.0071).

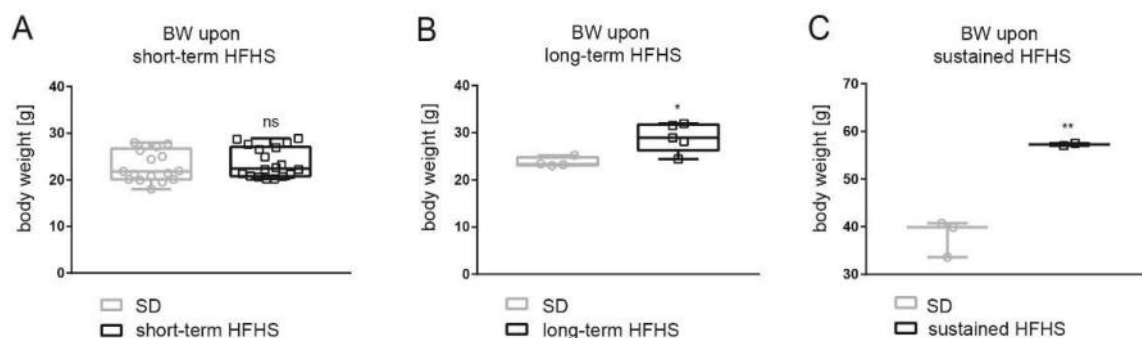


**Figure 16: BW upon different durations of a HFHS diet.** (A-C) BW of mice exposed to a SD vs. (A) a short-term HFHS diet (n=18 per group) vs. (B) a long-term HFHS diet (n=4-5 per group) vs. (C) a sustained HFHS diet (n=2-3 per group) in gram. Data is presented as box-and-whisker plots including all data points. ns  $P > 0.05$ , \* $P \leq 0.05$ , \*\* $P \leq 0.01$  as determined by unpaired t-test. (SD: grey circles, different HFHS diets: black squares)

Although insulin impaired Treg induction capacity using naïve CD4<sup>+</sup>T cells from all applied DIO models (**Figure 17A-C**), the extent of these impairments was dependent on the duration of the HFHS diet.

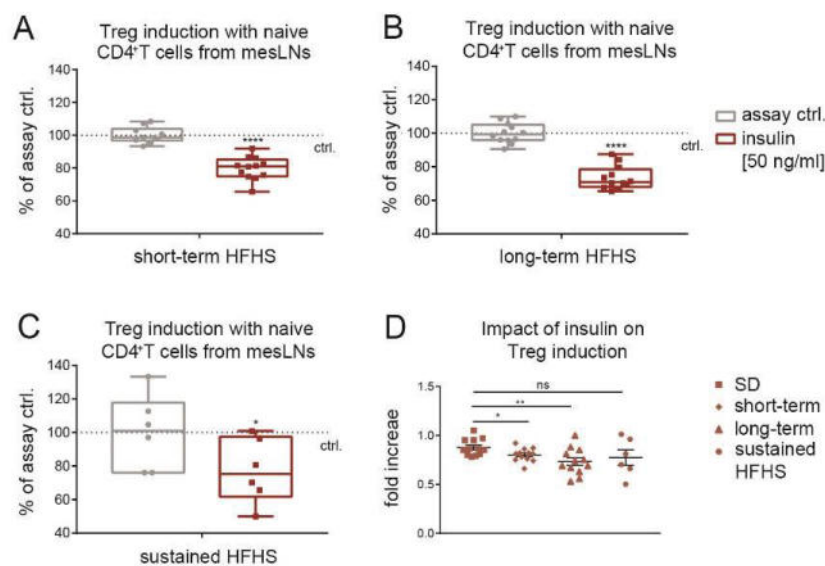


**Figure 17: The effect of insulin on *in vitro* Treg induction is maintained in dietary induced obesity.** (A-C) *In vitro* Treg induction in presence or absence of 50 ng/ml insulin using naive CD4<sup>+</sup>T cells from WT mice exposed to (A) a short-term HFHS diet (n=18 mice per group/ 6 mice were pooled and 4 technical replicates are shown), (B) a long-term HFHS diet (n=4 mice per group) or (C) a sustained HFHS diet (n=2 mice per group/ 2-3 technical replicates). (assay ctrl.: grey dots, 50 ng/ml: dark red squares (D) Net effect of insulin on *in vitro* Treg induction, represented as fold change in Treg frequency relative to SD. (SD: dark red squares, short-term HFHS: dark red diamonds, long-term HFHS: dark red triangles and sustained HFHS diet: red dots) ns  $P > 0.05$ , \* $P \leq 0.05$ , \*\* $P \leq 0.01$ , \*\*\* $P \leq 0.0001$  as determined by paired t-test (A-C) or unpaired t-test (D).

The net effect of insulin significantly decreased from SD to short-term HFHS diet (\* $P = 0.0232$ ) and from SD to long-term HFHS diet (\*\* $P = 0.0051$ ), whilst stagnating from SD to sustained HFHS diet (ns  $P = 0.1271$ ) (**Figure 17D**) (data is normalized to the

corresponding assay ctrls., SD:  $0.88 \pm 0.024$ , short-term HFHS:  $0.80 \pm 0.068$ , long-term HFHS:  $0.73 \pm 0.039$ , sustained HFHS:  $0.77 \pm 0.079$ ).

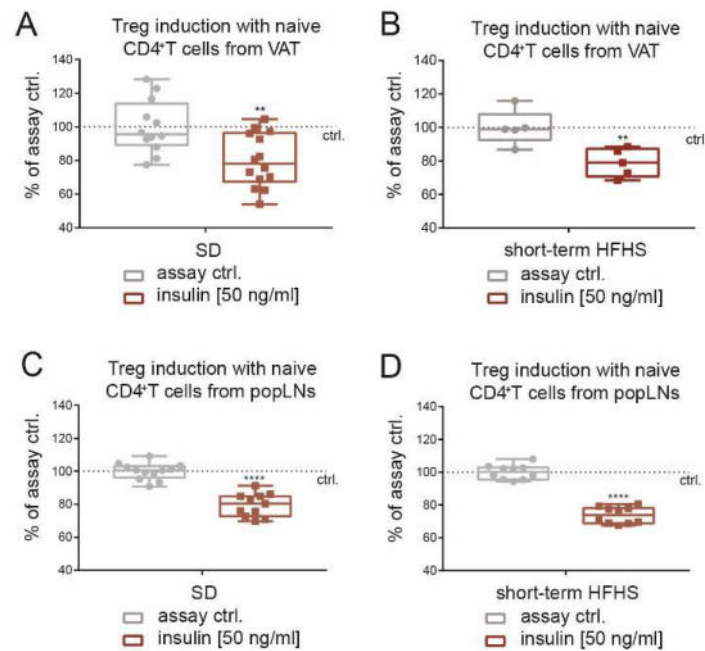


**Figure 18: Naïve CD4<sup>+</sup>T cells from VAT and popliteal LNs (popLNs) of obese mice remain insulin-sensitive upon DIO.** (A+B) *In vitro* Treg induction using VAT-residing naïve CD4<sup>+</sup>T cells of WT mice exposed to (A) a SD or (B) a short-term HFHS diet (n=18 mice per group/ 6 mice were pooled and 1-5 technical replicates are shown) (C+D) *In vitro* Treg induction using naïve T cells from popLNs of WT mice exposed to (C) a SD or (D) a short-term HFHS diet (n=18 mice per group/ 6 mice were pooled and 3-4 technical replicates are shown). Data is normalized to the assay ctrl. and presented as box-and-whisker plots including all data points. \*\*P ≤ 0.01, \*\*\*\*P ≤ 0.0001 as determined by paired t-test. (assay ctrl.: grey dots, 50 ng/ml: dark red squares)

Tregs are critical players in dampening tissue inflammation and maintaining tissue homeostasis, especially in the metabolically relevant tissues such as the ATs and the muscles. Therefore, it is highly relevant to investigate the effect of insulin on AT-residing CD4<sup>+</sup>T cells and CD4<sup>+</sup>T cells from popliteal LNs (popLNs) located in the fat pad of the leg muscle. Importantly, insulin likewise significantly impaired *in vitro* Treg induction using naïve CD4<sup>+</sup>T cells from VAT and popLNs (**Figure 18A+C**) (normalized to the own assay ctrl., VAT: assay ctrl.:  $100.00 \pm 4.573$  vs. insulin  $80.01 \pm 4.232$ , \*\*P = 0.0064; popLNs: assay ctrl.  $100 \pm 1.397$  vs. insulin  $73.76 \pm 1.589$ , \*\*\*\*P ≤ 0.0001). This effect was maintained when mice were exposed to a short-term HFHS diet (**Figure 18B+D**) (normalized to the own assay ctrl., VAT: assay ctrl.  $100 \pm 4.636$  vs. insulin  $78.99 \pm 3.773$ , \*\*P = 0.0009; popLNs: assay ctrl.  $100 \pm 1.457$  vs. insulin  $79.56 \pm 2.106$ , \*\*\*\*P ≤ 0.0001).

### 3.2.2. A T cell-specific loss of InsR expression enhances *de novo* Foxp3<sup>+</sup>Treg induction

To more mechanistically dissect the role of T cell specific InsR signaling in guiding Treg induction, proliferation and T cell-intrinsic metabolism, CD4-Cre mice were crossed with InsR<sup>flox/flox</sup> mice. Thereby obtained mice have a T cell-specific loss of the InsR (InsR TKO mice), as identified by PCR and Gel electrophoresis (**Figure 19A**).

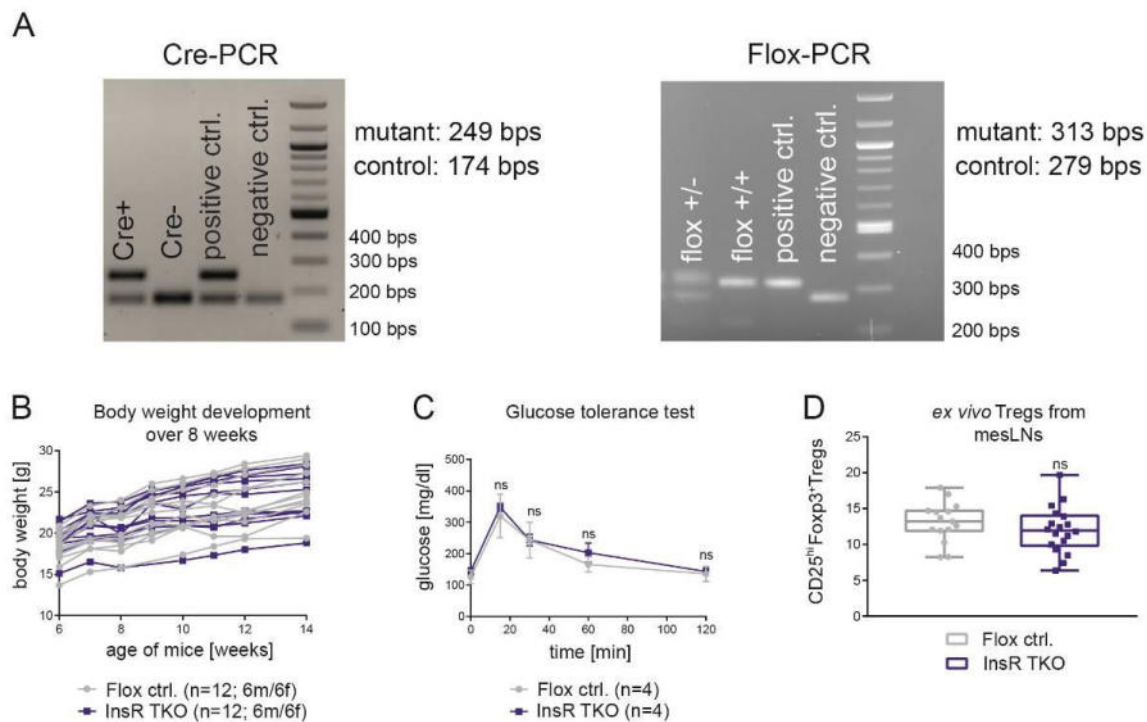


**Figure 19: Characterization of mice with a T cell specific loss of the InsR.** (A) Representative gel electrophoresis to identify the T cell specific InsR knockout via PCR (InsR TKO = Cre<sup>+</sup>flox<sup>+/+</sup>, Flox ctrl. = Cre<sup>-</sup>flox<sup>+/+</sup>). (B) BW curves from n=6 mice per genotype and sex over 8 weeks starting from 6 weeks of age until 14 weeks of age. (C) Glucose tolerance test with n=4 mice per genotype (all females) at the age of 24 weeks. (D) Analysis of *ex vivo* Treg frequencies in mesLNs of InsR TKO and Flox ctrl. mice (n=15 mice per genotype) presented as box-and-whisker plot including all data points. ns P > 0.05 as determined by unpaired t-tests. (Flox ctrl.: grey dots, InsR TKO: blue squares)

InsR TKO mice showed normal BW development (**Figure 19B**) and normal glucose tolerance (**Figure 19C**) compared to the corresponding Flox ctrls. *Ex vivo* Foxp3<sup>+</sup>Treg frequencies were not affected by the knockout (**Figure 19D**) (Flox ctrl.: 13.09 ± 0.720, InsR TKO: 12.02 ± 0.766, ns P = 0.3226).

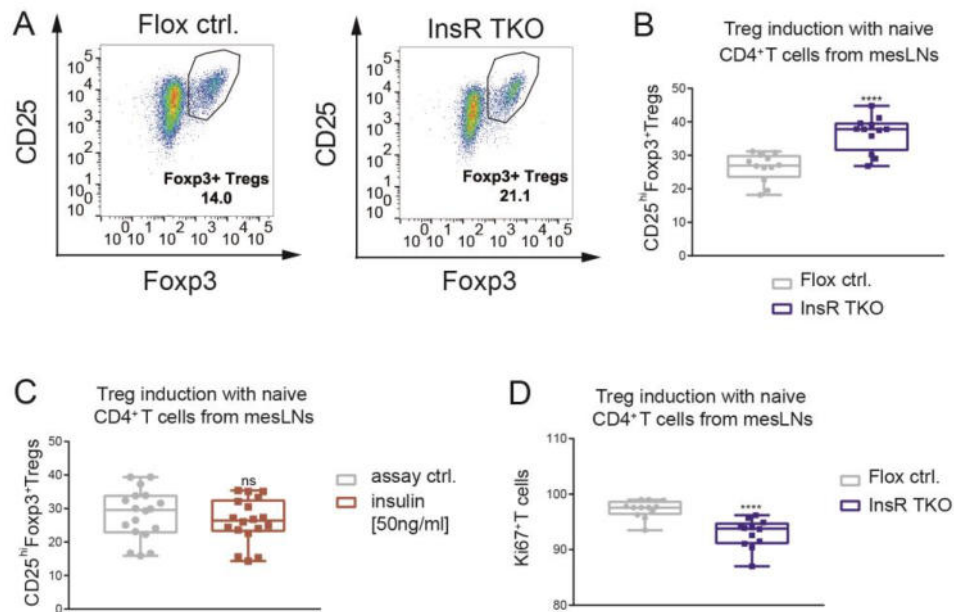


**Figure 20: A T cell specific loss of the InsR affects *in vitro* Treg induction and T cell proliferation.** (A) Identification of *in vitro* induced Tregs from naïve CD4<sup>+</sup>T cells of InsR TKO vs. Flox ctrl. mice. (B+D) Frequencies of (B) CD25<sup>hi</sup>Foxp3<sup>+</sup>Tregs and (D) CD4<sup>+</sup>Ki67<sup>+</sup>T cells at day 3 of *in vitro* Treg induction (n=4 mice per genotype/ 3 technical replicates). (C) *In vitro* Treg induction in presence or absence of 50 ng/ml insulin using naïve CD4<sup>+</sup>T cells from InsR TKO mice (n=6/ 2-3 technical replicates). Data is presented as box-and-whisker plots including all data points. ns P > 0.05, \*\*\*\*P ≤ 0.0001 as determined by (B+D) unpaired t-test and (C) paired t-test. (assay ctrl. or Flox ctrl.: grey dots, 50 ng/ml: dark red squares, InsR TKO: blue squares)

Since stable Treg induction and InsR signaling share downstream pathways (Delgoffe et al., 2009; Delgoffe et al., 2011; Haxhinasto et al., 2008; Morcavallo et al., 2014; Ward & Lawrence, 2009; Zeng et al., 2013), the effect of a T cell specific loss of the InsR might oppose incubation of T cells with insulin regarding to Treg induction, function and T cell-intrinsic metabolism. To get further insights into CD4<sup>+</sup>T cell specific InsR signaling, naïve CD4<sup>+</sup>T cells from mesLN of InsR TKO mice were used for *in vitro* Treg induction. Remarkably, the loss of the InsR on CD4<sup>+</sup>T cells significantly increased Foxp3<sup>+</sup>Treg induction capacity [% of CD4<sup>+</sup>T cells] compared to Flox ctrls. (**Figure 20A+B**) (Flox ctrl.:  $26.37 \pm 1.219$  vs. InsR TKO:  $36.46 \pm 1.518$ , \*\*\*\*P ≤ 0.0001). As expected, insulin did not interfere with *in vitro* Treg induction [% of CD4<sup>+</sup>T cells] using naïve CD4<sup>+</sup>T cells from InsR TKO mice (**Figure 20C**) (assay ctrl.:  $23.18 \pm 1.755$  vs. insulin:  $26.31 \pm 1.567$ , ns P = 0.4303). The enhanced Foxp3<sup>+</sup>Treg induction using InsR-deficient T cells was accompanied by a reduced frequency of Ki67<sup>+</sup>T cells [% of live CD4<sup>+</sup>T cells] (**Figure 20D**) (Flox ctrl.:  $97.3 \pm 0.454$  vs. InsR TKO  $92.93 \pm 0.746$ , \*\*\*\*P ≤ 0.0001).

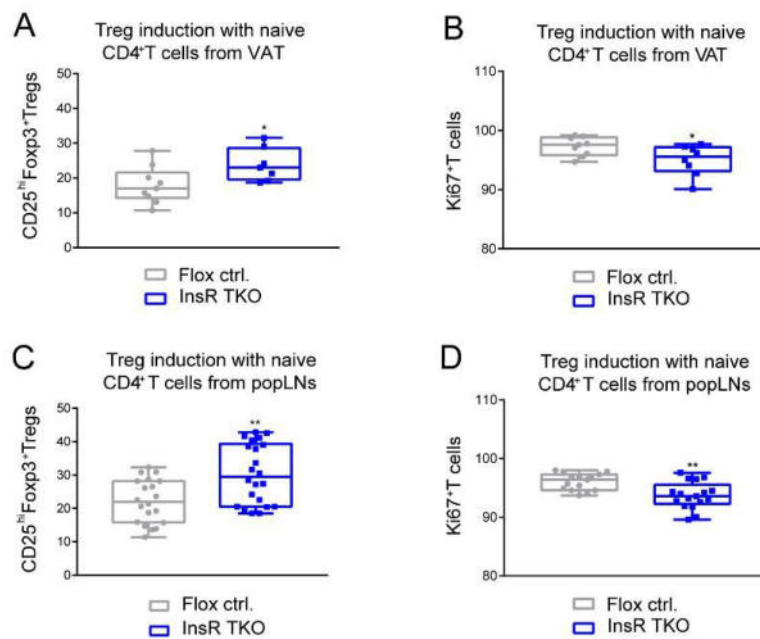


**Figure 21: A T cell specific loss of the InsR affects *in vitro* Tregs induction and T cell proliferation using naïve CD4<sup>+</sup>T cells from VAT and popLNs.** (A+C) Frequencies of CD25<sup>hi</sup>Foxp3<sup>+</sup>Tregs and (B+D) CD4<sup>+</sup>Ki67<sup>+</sup>T cells at day 3 of *in vitro* Treg induction using naïve CD4<sup>+</sup>T cells from (A+B) VAT (n=4 mice per genotype/ 1-3 technical replicates) or (C+D) popLNs (n=4 mice per genotype/ 3-6 technical replicates). Data is presented as box-and-whisker plots including all data points. \*P ≤ 0.05, \*\*P ≤ 0.01 as determined by unpaired t-test. (Flox ctrl.: grey dots, InsR TKO: blue squares)

Next, the influence of InsR deficiency on *in vitro* Treg induction and T cell proliferation of CD4<sup>+</sup>T cells from metabolically more active VAT and popLNs was determined. These cells depicted a significantly higher Treg induction capacity (**Figure 21A+C**) accompanied by a decreased number of proliferating CD4<sup>+</sup>Ki67<sup>+</sup>T cells (**Figure 21B+D**) compared to the respective Flox ctrls. (Foxp3<sup>+</sup>Tregs [% of CD4<sup>+</sup>T cells]: VAT: Flox ctrl.: 17.94 ± 1.783 vs. InsR TKO 23.84 ± 1.829, \*P = 0.0397, popLNs: Flox ctrl.: 22.15 ± 1.472 vs. InsR TKO 30.33 ± 1.900, \*\*P = 0.0020, Ki67<sup>+</sup>T cells [% of CD4<sup>+</sup>T cells]: VAT: Flox ctrl. 97.31 ± 0.526 vs. InsR TKO 95.00 ± 0.550, \*P = 0.0402, popLNs: Flox ctrl 96.02 ± 0.366 vs. InsR TKO 99.71 ± 0.550, \*\*P = 0.0021). However, the net beneficial effect of the knockout on Treg induction was varying. Specifically, the net effect of the InsR TKO was most prominent and significantly higher in CD4<sup>+</sup>T cells from VAT compared to mesLNs (**Figure 23A**) (\*P = 0.0206). There was no difference in the net increase in Treg induction capacity between CD4<sup>+</sup>T cells from mesLNs and popLNs (**Figure 23A**) (ns P = 0.5233) (normalized to the corresponding Flox ctrl., mesLNs: 1.32 ± 0.056, popLNs: 1.43 ± 0.071, VAT: 1.66 ± 0.106).

Similarly to insulin, T cell specific InsR deficiency might trigger the shown effects by-at least partly- acting on downstream PI3K-Akt-mTOR signaling or proteins that are involved in energy generation via glycolysis. Immunofluorescence stainings on cytopins from CD4<sup>+</sup>T cells of InsR TKO mice showed significant lower levels of pS6 downstream of the PI3K-Akt-mTOR signaling pathway (**Figure 22A**) (Flox ctrl.:  $48.75 \pm 2.358$ , InsR TKO:  $36.25 \pm 3.705$ , \*P = 0.0293) and significantly reduced levels of GCK compared to the corresponding Flox ctrl. (**Figure 22B**) (Flox ctrl.:  $93.25 \pm 5.121$ , InsR TKO:  $76.25 \pm 3.838$ , \*P = 0.0377).

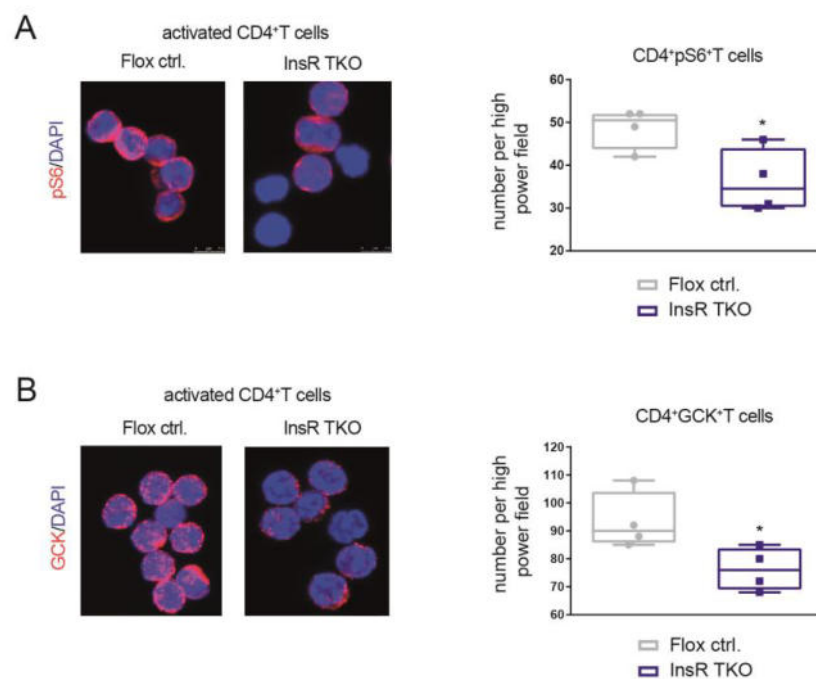


**Figure 22: InsR deficiency and its effects on downstream signaling pathways.** (A+B) Representative immunofluorescence stainings on cytopins from CD4<sup>+</sup>T cells of Flox ctrl. and InsR TKO mice stained for (A) pS6 and (B) GCK. Respective summary graphs show the number of positive CD4<sup>+</sup>T cells/high power field for each antibody. \*P ≤ 0.05 as determined by unpaired t-test. Data in graphs is presented as box-and-whisker plots including all data points. (Flox ctrl.: grey dots, InsR TKO: blue squares)

Additionally, activated CD4<sup>+</sup>T cells from InsR TKO mice showed significantly lower glucose uptake compared to the Flox ctrls. (**Figure 23B**) (fold increase in glucose uptake, Flox ctrl.:  $1.00 \pm 0.044$ , InsR TKO  $0.64 \pm 0.090$ , \*\*P = 0.0042).

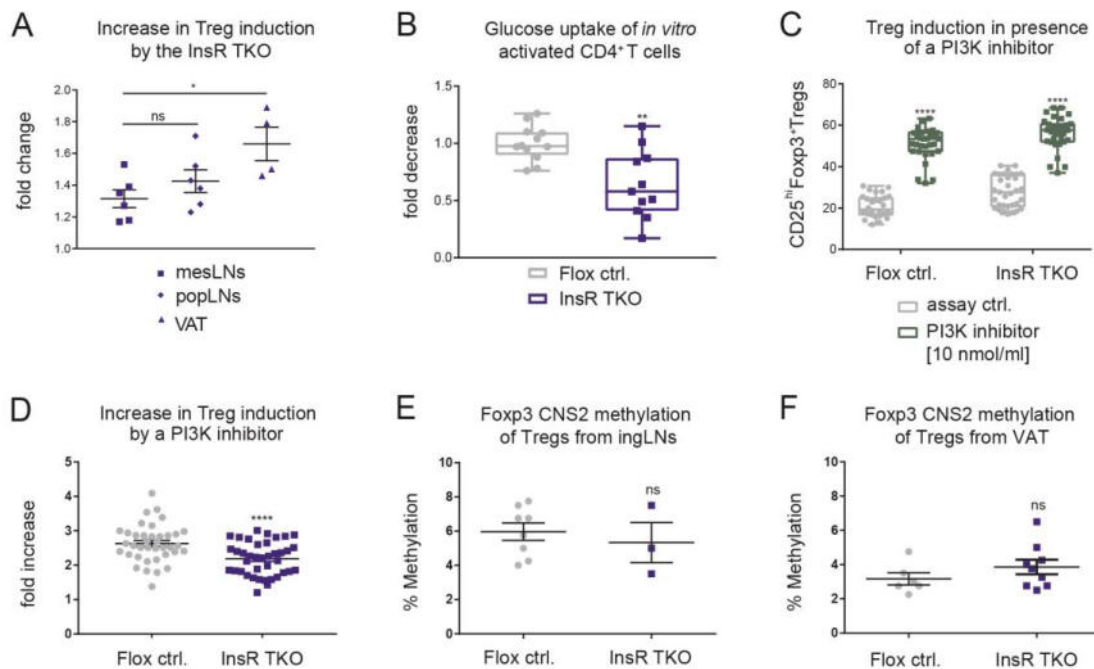


**Figure 23: The effect of the InsR TKO depends on the T cell environment, glucose uptake and PI3K activation.** (A) Net effect of a T cell specific InsR knockout on *in vitro* induced Treg frequencies comparing Treg induction with naïve CD4<sup>+</sup>T cells from mesLN, popLN and VAT (n=2 mice per genotype/ 2-3 replicates). (mesLN: blue squares, popLN: blue diamonds, VAT: blue triangles). (B) Glucose uptake in FACS purified naïve CD4<sup>+</sup>T cells from all LN and spleens of n=4 mice per genotype (2-3 technical replicates/each) (InsR TKO vs. Flox ctrl. mice) upon *in vitro* activation for 4 hours at 37°C and 5 % measured by luminescence. (C) *In vitro* Treg induction with naïve CD4<sup>+</sup>T cells from mesLN of InsR TKO and Flox ctrl. mice in presence or absence of 10 nmol/ml PI3K inhibitor. (D) Net effect of a PI3K inhibitor on Treg induction comparing InsR TKO and Flox ctrl. mice (n=11 mice per genotype/ 2-3 technical replicates). (E+F) Foxp3 CNS2 methylation in CD25<sup>+</sup>Foxp3<sup>+</sup>Tregs from (E) ingLN and (F) VAT (n=3-9 mice per genotype). Data is presented as scatter plots including all data points and mean ± SEM (A+D-F) and box-and-whisker plots including all data points (B+C). ns P > 0.05, \*P ≤ 0.05, \*\*P ≤ 0.01, \*\*\*\*P ≤ 0.0001 as determined by unpaired t-test (A+E+F), Mann Whitney test (B), 2way ANOVA and Sidak's multiple comparisons test (C) or paired t-test (D). (Flox ctrl.: grey dots, InsR TKO: blue squares, PI3K inhibitor: dark green squares)

Given the important role of the PI3K-Akt-mTOR pathway for stable and functional Foxp3<sup>+</sup>Treg induction (Delgoffe et al., 2009; Delgoffe et al., 2011; Haxhinasto et al., 2008; Sauer et al., 2008; Zeng et al., 2013), the next goal was to assess whether the observed effects of the InsR knockout are exclusively caused by a lower activity of this pathway. To this end *in vitro* Treg induction was performed in the presence of the PI3K inhibitor LY294002. As naïve CD4<sup>+</sup>T cells of Flox ctrl. mice, CD4<sup>+</sup>T cells of InsR TKO mice responded to the PI3K inhibitor with significantly increased Foxp3<sup>+</sup>Treg induction levels [% of CD4<sup>+</sup>T cells] (**Figure 23C**) (Flox ctrl.: assay ctrl.: 20.82 ± 0.921, PI3K inh.: 51.23 ± 1.349, InsR TKO: assay ctrl.: 28.00 ± 1.325, PI3K inh.: 56.16 ± 1.349, both \*\*\*\*P ≤ 0.0001). However, the net effect of the PI3K inhibitor on Treg induction was significantly lower in the InsR TKO (**Figure 23D**) (fold increase, Flox ctrl.: 2.63 ± 0.088, InsR TKO: 2.19 ± 0.077, \*\*\*\*P ≤ 0.0001).

Next, to analyze whether the InsR TKO affects besides T cell differentiation and function also stability of *ex vivo* Foxp3<sup>+</sup>Tregs, methylation analysis of the *FOXP3* CNS2 TSDR was performed with Foxp3<sup>+</sup>Tregs isolated from ingLNs or VAT of InsR TKO mice. These Tregs depicted no differences concerning their methylation status of the *FOXP3* locus (**Figure 23E+F**) (ingLNs: Flox ctrl.:  $5.97 \pm 0.510$ , InsR TKO:  $5.33 \pm 1.167$ , ns  $P = 0.5689$ , VAT: Flox ctrl.:  $3.17 \pm 0.358$ , InsR TKO:  $3.86 \pm 0.4272$ , ns  $P = 0.2696$ ), reflecting an unaffected Treg stability.

As a next step, InsR TKO and Flox ctrl. mice were exposed to a long-term HFHS diet to investigate whether CD4<sup>+</sup>T cells of these mice are affected by an obesogenic environment. Flox ctrl. and InsR TKO mice showed likewise a significant BW gain upon dietary challenge and the BWs of SD and long-term HFHS diet mice were comparable at the day of sacrifice (**Figure 24**) (Flox ctrl.: SD:  $23.41 \pm 0.347$ , long-term HFHS:  $28.91 \pm 0.155$ , \*\* $P = 0.0072$  vs. InsR TKO: SD:  $23.76 \pm 0.346$ , long-term HFHS:  $29.06 \pm 1.634$ , \* $P = 0.0213$ ).

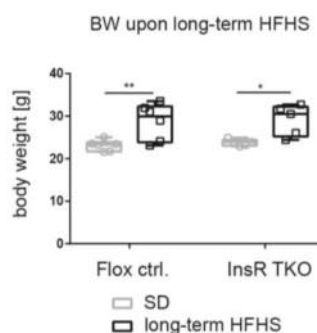


**Figure 24: BW of InsR TKO vs. Flox ctrl. mice upon a long-term HFHS diet.** BW of mice exposed to a SD vs. a long-term HFHS diet in gram. Data is presented as box-and-whisker plots including all data points. \* $P \leq 0.05$ , \*\* $P \leq 0.01$  as determined by unpaired t-test. (SD: grey circles, different HFHS diets: black squares)

As under SD conditions (**Figure 20A+B** and **Figure 21A**), *in vitro* Foxp3<sup>+</sup>Treg induction [% of CD4<sup>+</sup>T cells] was significantly higher using naïve CD4<sup>+</sup>T cells from mesLNs or VAT of InsR TKO mice exposed to a long-term HFHS diet (**Figure 25A+C**) (mesLNs: Flox ctrl.:  $20.98 \pm 1.404$ , InsR TKO:  $26.91 \pm 1.877$ , \* $P = 0.0150$ , VAT: Flox ctrl.:  $16.08 \pm 0.954$ , InsR TKO:  $21.63 \pm 1.494$ , \*\* $P = 0.0041$ ). The representative FACS plots for identification of Foxp3<sup>+</sup>Tregs from VAT are shown in **Figure 25B**.

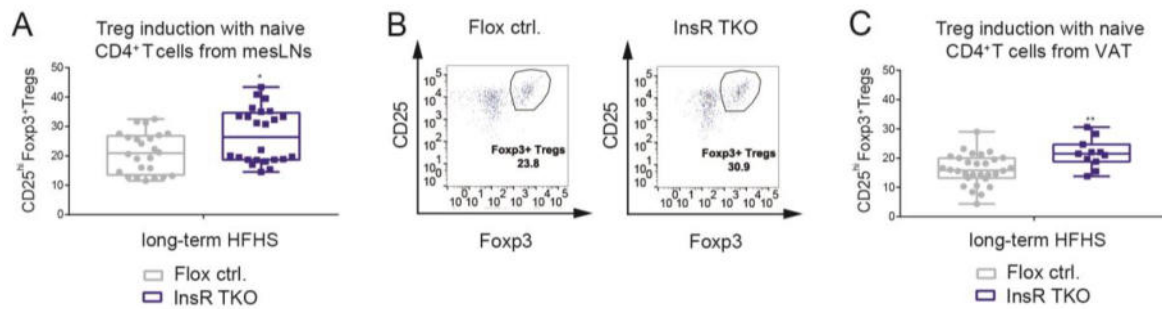


**Figure 25: The effect of a T cell specific InsR knockout on Treg induction upon DIO.** (A+C) *In vitro* Treg induction using naïve CD4<sup>+</sup>T cells from (A) mesLN (n=10 mice per genotype/ 2-3 technical replicates) or (C) VAT (n=6 mice per genotype/ 1-5 technical replicates) of InsR TKO and Flox ctrl. mice exposed to a long-term HFHS diet. (B) Representative FACS plots for *in vitro* Treg induction assays with naïve CD4<sup>+</sup>T cells isolated from VAT of InsR TKO or Flox ctrl. mice. Data is presented as box-and-whisker plots including all data points (A+C). \*P ≤ 0.05, \*\*P ≤ 0.01 as determined by unpaired t-test (A+C). (Flox ctrl.: grey dots, InsR TKO: blue squares)

To mechanistically dissect the underlying mechanisms that trigger Foxp3<sup>+</sup>Treg induction, inhibit Ki67<sup>+</sup>T cell proliferation and diminish glucose uptake of CD4<sup>+</sup>T cells from InsR TKO mice, RNA-based next-generation sequencing (RNA-Seq) analysis of total CD4<sup>+</sup>T cell from mesLN of InsR TKO and Flox ctrl. mice was performed.

In total, 569 genes were significantly changed as a consequence of the T cell-specific InsR deficiency. Among them, 358 genes were significantly downregulated, whereas 211 genes were significantly higher expressed by CD4<sup>+</sup>T cells of the InsR TKO mice. As highlighted in the volcano plots, these differently expressed genes belong to the InsR signaling pathway (**Figure 26A**), the PI3K-Akt-mTOR pathway (**Figure 26C**) or the Ras/MapK pathway (**Figure 26D**). Additionally, a Gene Set Enrichment Analysis (GSEA) enrichment score plot for 11 annotated, individual genes of the InsR signaling pathway (*Ppp1cc*, *Inpp5k*, *Elk1*, *Gsk3*, *Rptor*, *Eif4e2*, *Prkag2*, *Prkar2a*, *Pygb*, *Flot1*, *Ppp1r3e*) is shown in (**Figure 26B**) and reveals a downregulation of this pathway.

Of note, CD4<sup>+</sup>T cells from InsR TKO mice showed significantly lower expression of relevant genes of the PI3K-Akt-mTOR and the Ras/MapK pathway. These include glycogen synthase kinase 3 beta (*Gsk3b*), regulatory-associated protein of mTORC1 (Raptor) *Rptor*, cAMP responsive element binding protein 3 (*Creb3*), the G1 phase kinase cell division protein kinase 6 (*Cdk6*), activating transcription factor 4 (*Atf4*), protein tyrosine phosphatase, non-receptor type 11 (*Ptpn11*) and growth arrest and DNA damage inducible beta (*Gadd45β*). A lower abundance of each of these genes supports Foxp3<sup>+</sup>Treg induction.

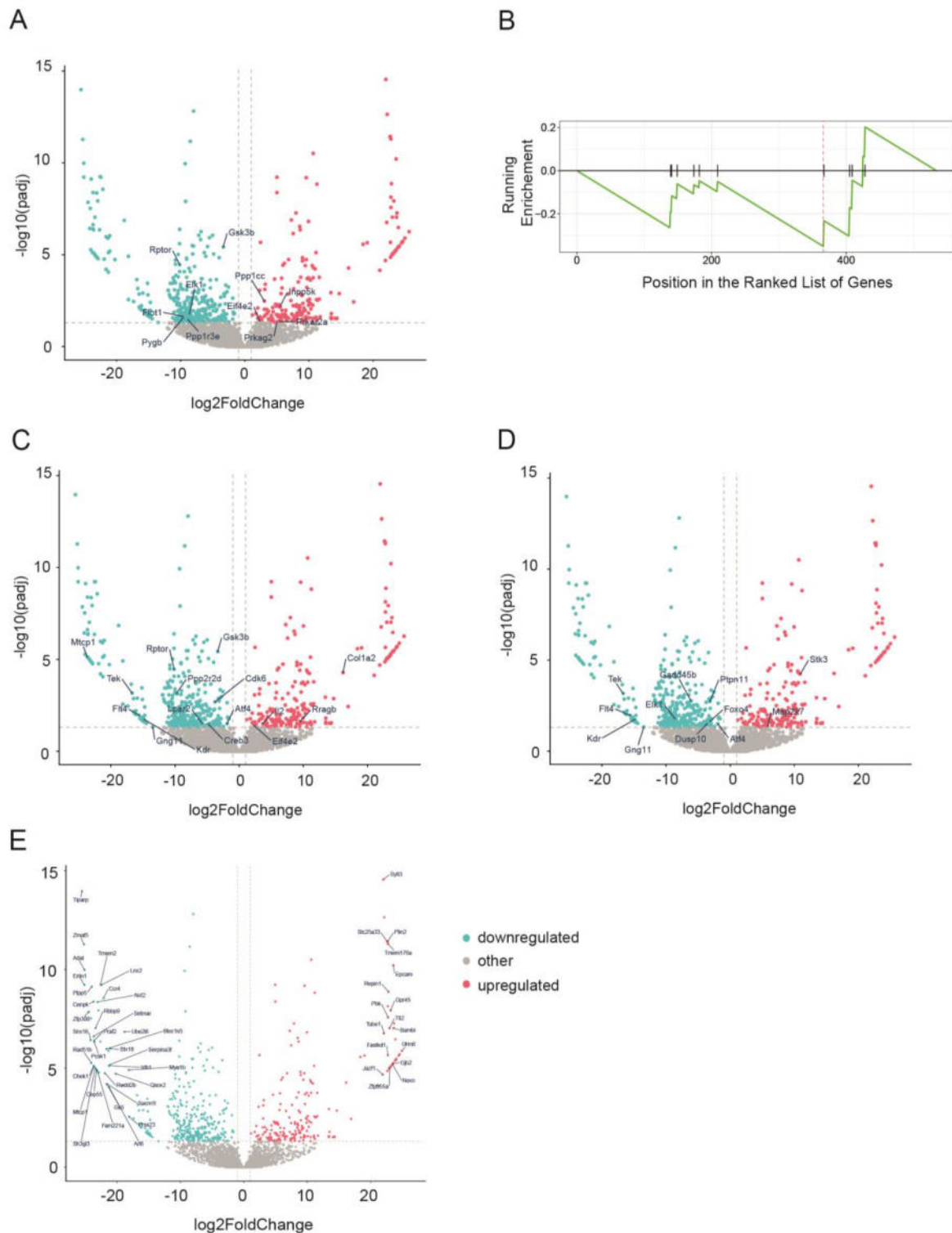


**Figure 26: Transcriptomic Analysis of CD4<sup>+</sup>T cells from InsR TKO vs. Flox ctrl. mice.** Significantly differentially expressed genes in the CD4<sup>+</sup>T cells of the InsR TKO compared to the Flox ctrl. mice are highlighted in the volcano plots and belong to either (A) the InsR signaling pathway, (C) the PI3K-Akt-mTOR signaling pathway, (D) the Ras/MapK signaling pathway or (E) the 40 most up- and down-regulated genes (predicted genes are not shown). Significant genes in the volcano plots were defined by baseMean > 50 and absolute log<sub>2</sub>FoldChange > 1 and adjusted P value < 0.05 using DESeq2 Differential expression analysis (Love et al., 2014). (Upregulated genes (red dots), downregulated genes (blue dots), other (grey dots), thresholds (grey lines; line1: log<sub>2</sub>FoldChange = -1; line2: Log<sub>2</sub>FoldChange = 1; line 3: -log<sub>10</sub>(padj) = -log<sub>10</sub>(0.05))). (B) Gene Set Enrichment Analysis (GSEA) enrichment score plot for 11 annotated, individual genes of the InsR signaling pathway (*Ppp1cc*, *Inpp5k*, *Elk1*, *Gsk3*, *Rptor*, *Eif4e2*, *Prkag2*, *Prkar2a*, *Pygb*, *Flot1*, *Ppp1r3e*) which are represented by black vertical bars in the middle of the plot.

Next, to further dissect the effect of T cell specific InsR signaling on *in vitro* Treg induction, the 40 most up- and downregulated genes (**Figure 26E**) (predicted genes are not shown) were identified in CD4<sup>+</sup>T cells from InsR TKO vs. Flox ctrl. mice. Specifically, *Tiparp* (TCDD-inducible poly-ADP-ribose polymerase) was identified as most prominently downregulated gene in InsR-deficient T cells. This gene is a target of the transcription factor Ahr (aryl hydrocarbon receptor) and regulates its activity via a negative feedback loop through mono-ADP-ribosylation (Engin et al., 2015). Additionally, CD4<sup>+</sup>T cells from InsR TKO mice revealed, among others, reduced expression of Glycerokinase 5 (*Gk5*), relevant for the synthesis of glycerophospholipids (Wieland & Suyter, 1957) and Checkpoint kinase 1 (*Chk1*), a dynamic positive regulator of NFATs activity in T cells (Gabriel et al., 2016; Tone et al., 2008). These genes further support Foxp3<sup>+</sup>Treg induction capacity by contributing to a lower intrinsic activation and proliferation status of the InsR-deficient T cells.

As a next step, the proteome composition of CD4<sup>+</sup>T cells from total LNs of InsR TKO vs. Flox ctrl. mice was analyzed applying quantitative mass spectrometry-based proteomics (Meissner & Mann, 2014). Here, in total 4585 proteins were significantly changed in the InsR-deficient T cells. Among them 2320 proteins were significantly lower, and 2265 proteins were significantly higher expressed in the InsR TKO cells. Specifically, unsupervised hierarchical clustering conditions revealed up-regulation of several GO terms related to negative regulators of T cell activation and immune system process such as Proteasomal ubiquitin receptor *Adrm1* and Bone marrow stromal antigen 2 (*Bst2*) (**Figure 27**). Moreover, proteins relevant for Foxp3<sup>+</sup>Treg induction from naïve CD4<sup>+</sup>T cells lacking InsR expression were also upregulated *e.g.* Casitas B-lineage Lymphoma (*Cbl*), *Stat3*, *Stat5a*, *Stat5b* and *Pten* (**Figure 27**). Of note, proteomic analyses highlight metabolic manipulations of CD4<sup>+</sup>T cells from InsR TKO mice. Specifically, expression of proteins of the ETC including *Etfb*, *Fdxr*, *Sdha*, *Cyc1*, *Dld*, *Ndufv1*, *Ndufa2*, *Ndufa6*, *Ndufa8* and *Ndufa10* was significantly reduced in InsR-deficient T cells. More specifically, the downregulated proteins of the ETC are components of the NADH dehydrogenase (Complex I: NADH dehydrogenase [ubiquinone] 1 alpha subcomplex subunit (*Ndufa*) 2, 6, 8, 10 and NADH dehydrogenase [ubiquinone] flavoprotein (*Ndufv*) 1), Succinate dehydrogenase (Complex II: Succinate dehydrogenase complex, subunit A (*Sdha*)), Cytochrome c reductase (Complex III: Cytochrome c1 (*Cyc1*)) or are electron transfer proteins (Electron transfer flavoprotein subunit beta (*Etfb*), Adrenodoxin reductase (*Adxr* or *Fdxr*)) (Kyōto University, 1995). Additionally, Dihydrolipoyl dehydrogenase (*Dld*) is indispensable for the function of various oxidative enzyme complexes (Odievre et al., 2005). In line with this, RNAseq revealed significant reduced levels of *ldh1* in InsR-deficient T cells. The gene Isocitrate dehydrogenase (*ldh1*) encodes an

enzyme of the TCA cycle and its activity is important for subsequent OXPHOS (Almeida et al., 2016; Park & Pan, 2015; van der Windt & Pearce, 2012).

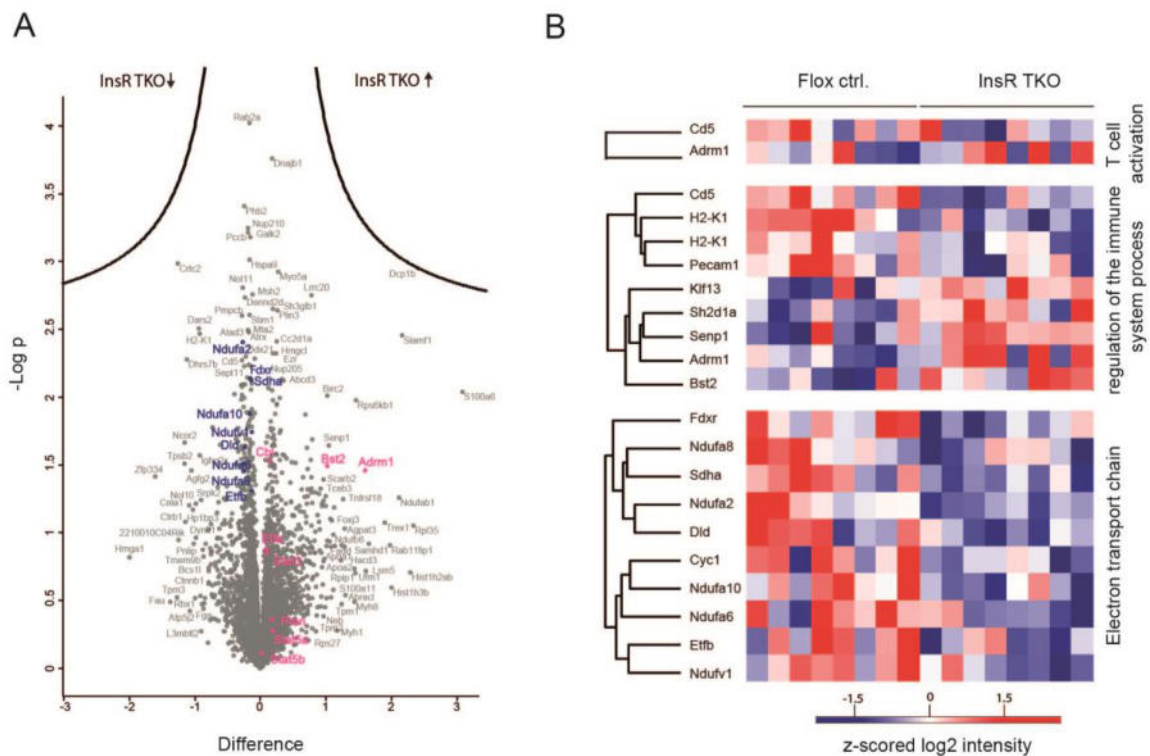


**Figure 27: Proteomic Analysis of CD4<sup>+</sup>T cells from InsR TKO vs. Flox ctrl. mice.** (A) Volcano plot of all quantified proteins with at least three valid values in one condition. Selected downregulated proteins in the CD4<sup>+</sup>T cells from InsR TKO mice are indicated in blue, selected up-regulated proteins in pink. (B) Hierarchical clustering of label-free quantified intensities of significantly changed proteins ( $P < 0.05$ ) of the indicated GOBP-annotations.

Thus, proteomic (and transcriptomic) data suggests that the T cell-specific InsR deficiency disrupts mitochondrial ETC integrity in CD4<sup>+</sup>T cells which potentially affects OXPHOS, subsequent mitochondrial ATP generation and the generation of ROS.

## 4. Discussion

Systemic low-grade inflammation and associated defects in immune homeostasis are major characteristics of obesity, the metabolic syndrome and its progression to T2D. A better understanding of the cellular and systemic immune-metabolic interactions in the development, progression, persistence and remission of obesity is pivotal for the development of novel therapeutic strategies that specifically target immune cell populations to limit inflammatory processes. Specifically, pro-inflammatory CD4<sup>+</sup>CXCR5<sup>+</sup>(PD1<sup>hi</sup>Bcl6<sup>hi</sup>) effector TFH cells and suppressive, anti-inflammatory regulatory Foxp3<sup>+</sup>Tregs are critical mediators of immune activation versus immune regulation, however, the mechanisms that link an obesogenic environment with alterations in their abundance, functionality and immunometabolism are yet poorly understood and are in the focus of the present thesis.

### 4.1 (Precursor) TFH cells in obesity

Given their important role in the autoimmune setting (Scherm et al., 2016; Serr et al., 2016b; Ueno, 2016), the first aim of this thesis was to dissect the contribution of (precursor) TFH cells to obesity-associated inflammatory processes. Commonly, CD4<sup>+</sup>CXCR5<sup>+</sup>(Bcl6<sup>hi</sup>) T cells that are found within the GCs are defined as “TFH cells”, whereas CD4<sup>+</sup>CXCR5<sup>+</sup>PD1<sup>hi</sup>T cells with a TFH cell profile found elsewhere are defined as precursor TFH cells (Crotty, 2014; Deenick & Ma, 2011). So far, the role of these cells in obesity and more specifically in AT inflammation was not investigated and there is no prove for AT-residing (precursor) TFH cells in both health and obesity. Thus, investigation of (precursor) TFH cells in the context of obesity-associated chronic, low-grade inflammation systemically and directly in the VAT is of great interest. Accumulation of VAT-residing pathogenic B cells upon 4 weeks of a high-fat diet (HFD) (corresponding to the short-term HFHS diet in this thesis) and their production of IgG antibodies were previously identified as critical players for VAT inflammation and especially insulin resistance (Winer et al., 2011). Thus, (precursor) TFH cells might be equally important for VAT inflammation due to their capability to provide B cell help and to induce antibody responses (Breitfeld et al., 2000; Johnston et al., 2009; Nurieva et al., 2008; Schaerli et al., 2000; Yu et al., 2009). Winer *et al.* (Winer et al., 2011) specifically showed that pathogenic IgG antibodies that might drive AT inflammation (Harmon et al., 2016) are not detectable after 3-6 weeks of a HFD (corresponding to the short-term HFHS diet in this thesis), but appear late in disease progression after 14-18 weeks of a HFD (corresponding to the long-term HFHS diet in this thesis). Hence, (precursor) TFH cells might be equally late contributors to the obesity pathology.

The results presented in this thesis show that an intermediate-term HFHS diet (8 weeks) was insufficient to significantly raise the number of CD4<sup>+</sup>CXCR5<sup>+</sup>PD1<sup>hi</sup> (precursor) TFH cells in

both ingLNs and mesLNs, but resulted in highly heterogeneous frequencies of these cells. However, in line with the previously identified increased number of pathogenic VAT-residing B cells upon long-term exposure to a high calorie environment (Winer et al., 2011), there was a significant increase in CD4<sup>+</sup>CXCR5<sup>+</sup>PD1<sup>hi</sup> precursor TFH cells in mesLNs, but not ingLNs, of WT mice exposed to a long-term HFHS diet (18 weeks). This increase in precursor TFH cells in mesLNs might be due to their location in close proximity to the VAT which represents the metabolically active obesity-associated site of inflammation. However, precursor TFH cell frequencies were rather low and contributed to only 2-5 % of the live CD4<sup>+</sup>T cell compartment. Preliminary data from mice exposed to a sustained HFHS diet (one year) revealed most prominent effects and significantly **increased CD4<sup>+</sup>CXCR5<sup>+</sup>PD1<sup>hi</sup> precursor TFH cell levels in both ingLNs and mesLNs**. Precursor TFH cells were detectable in ingLNs and mesLNs of all applied SD and HFHS diet mice, but their frequencies depicted a high heterogeneity. This might on the one hand be attributed to the enormous intrinsic heterogeneity of TFH cells and the difficulty to use adequate TFH cell markers, since the identification of (precursor) TFH cell is inconsistent in literature (Crotty, 2014). On the other hand, and from an experimental point of view, TFH cells populations showed a high heterogeneity between biological replicates and their abundance was extremely low. This resulted in difficulties to identify and sort purify TFH cells. However and importantly, the findings from long-term and sustained HFHS diet experiments in this thesis are supported by **a significant increase in fully committed, more mature, GC-like CD4<sup>+</sup>CXCR5<sup>+</sup>PD1<sup>hi</sup>Bcl6<sup>hi</sup>TFH cells in mesLNs of genetically obese ob/ob mice**.

DIO and ob/ob mice show similar phenotypic characteristics and traits such as obesity and peripheral insulin resistance. Importantly, the results in this thesis revealed a similar positive correlation between their obese phenotype and *ex vivo* (precursor) TFH cell levels in mesLNs. Nevertheless, research with these two obesity mouse models should not be reduced to a single pathophysiologic entity and direct comparison of results from DIO and ob/ob mice should be avoided. In DIO models, obesity development positively correlates with the amount and composition of the digested food and DIO largely reflects the pathogenesis of human obesity with respect to its slow progression in BW gain and the development of insulin resistance. However, the obtained results from DIO studies must be transferred with caution to humans. Reasons for the lack of transferability include a diminished complexity and variety of murine HFHS diets compared to human diets (Kleinert et al., 2018). Additionally, in humans, the intake of fat is remarkably consistent across age and BMI and accounts for ~30 % of their daily calories (Vadiveloo et al., 2014), whereas DIO is mainly induced by diets that contain a high fat content with 40 % to 60 % of the calories from fat (Kleinert et al., 2018), including the here applied diet (58 % of the calories from fat and

sucrose). On the contrary, the ob/ob polymorphism not only triggers obesity development, but also has multiple known and unknown other molecular and cellular effects. Thus, DIO and ob/ob mice represent suitable mouse models to study (precursor) TFH cells in both DIO and genetic obesity.

In order to investigate a possible correlation between **TFH cell levels and human obesity**, TFH cells can be assessed in human peripheral blood samples from lean vs. obese individuals with different states of insulin sensitivity. These samples offer a valuable resource for studying immune-metabolic signaling cues that are involved in immune activation vs. immune tolerance in human obesity because of their easy accessibility and the positive correlation between murine and human blood precursor TFH cell frequencies and TFH cells in lymphoid tissues (He et al., 2013; Heit et al., 2017; Schaerli et al., 2000; Simpson et al., 2010). Likewise, blood circulating precursor TFH cells might positively correlate with AT-residing (precursor) TFH cells. Additionally, since human VAT-residing precursor TFH cells might (at least partly) be recruited from the circulation to the ATs, peripheral blood leucocytes might reflect a surrogate readout for the VAT immune cell profile (McLaughlin et al., 2014; Pecht et al., 2014; Wouters et al., 2017). Nevertheless, gained knowledge from peripheral blood must be considered with caution when drawing conclusions for the human AT immune cell profile from it and the relation between blood precursor TFH cell frequencies and AT-residing TFH cells has to be further investigated. Additionally, it is important to apply suitable markers to detect (precursor) TFH cells directly in the VAT, since obesity-associated changes in immune cell populations might be restricted to TFH cell subsets (Th1-like, Th2-like and Th17-like subset) and undetectable in the “global” TFH cell pool. Specifically, imbalances in peripheral blood precursor TFH cell subsets were previously identified in several diseases including a skewing of TFH cell subsets towards Th2 and Th17-like TFH cells in osteosarcoma patients (H. Xiao et al., 2014), an increase in Th2-like TFH cells in recent onset of T1D autoimmunity (Serr et al., 2016b) and a shift towards Th17-like TFH cells in T2D patients (Q. Wang et al., 2015).

In line with these previous studies, the results of the present thesis reveal a disbalance in precursor TFH cell subsets upon obesity or/and insulin-resistance when comparing live CD4<sup>+</sup>CD45RA<sup>-</sup>CXCR5<sup>+</sup>T cells with either a Th1-like (CXCR3<sup>+</sup>CCR6<sup>-</sup>), a Th2-like (CXCR3<sup>-</sup>CCR6<sup>-</sup>) or a Th17-like (CXCR3<sup>-</sup>CCR6<sup>+</sup>) profile in the peripheral blood of lean, insulin-sensitive vs. obese, insulin-sensitive vs. obese, insulin-resistant individuals. Specifically, **the peripheral blood of obese, insulin-resistant individuals was enriched in Th17-like precursor TFH cells**, whereas Th1-like and Th2-like cells were rather decreased. This is in line with the results from Wang *et al.* (Q. Wang et al., 2015) showing a significant

increase in circulating Th17-like precursor TFH cells and a significant decrease in Th1-like precursor TFH cells in insulin-resistant T2D patients compared to healthy controls. Additionally, the researchers showed highest levels of Th17-like precursor TFH cells in T2D patients with abdominal fat accumulation and overweight (BMI < 30 kg/m<sup>2</sup>) (Q. Wang et al., 2015). This highlights that Th17-like precursor TFH cells might already be highly relevant in the presence of overweight, potentially reflecting an early time point of obesity development associated with only minor metabolic changes. This increase in Th17-like precursor TFH cells seems to persist in obesity (with a BMI > 46 kg/m<sup>2</sup>) as highlighted in the present thesis. Th17-like precursor TFH cells are efficient B cell helpers and can induce naïve B cells to differentiate into antibody producing plasma cells. More specifically, Th17-like precursor TFH cells were shown to regulate class switching of B cells, promoting IgG and IgA responses. (Fazilleau et al., 2009; Morita et al., 2011) Especially, IgG antibodies were previously identified to drive AT inflammation (Harmon et al., 2016). Additionally, Th17-like precursor TFH cells might trigger the obesity pathology by secreting pro-inflammatory IL17A (Morita et al., 2011). This supports the here shown data suggesting that high levels of Th17-like precursor TFH cells might particularly take part in the pathogenesis of obesity and associated chronic inflammation. On the contrary, Th1-like precursor TFH cells were shown to be less efficient B cell helpers by only inducing memory B cells (Bentebibel et al., 2013). Thus, they are less effective in contributing to the humoral immune response and might therefore be less important for obesity-associated inflammatory immune responses, reflected by their lower abundance in obese individuals shown here. However, the mechanisms that underlie obesity-mediated TFH cell dysregulation remain unclear and the here shown data has to be further confirmed, especially regarding the individual and joint contribution of obesity and insulin resistance to the precursor TFH cell subset levels in human peripheral blood. Thereby, the important roles of the different TFH cell subsets can be further dissected. Especially the contribution of Th2-like TFH cells to human obesity needs to be clarified, since this cell population was shown to be slightly increased in overweight individuals (Q. Wang et al., 2015), whilst the data of this thesis indicates a reduction in Th2-like precursor TFH cells in obese, insulin-resistant individuals. Furthermore, the assessment of (precursor) TFH cells directly in the inflamed VAT of lean vs. obese humans might provide further insights into the role of (precursor) TFH cells in obesity.

Unfortunately, human VAT is hardly accessible especially in lean individuals, representing the required control group. Additionally, the here identified precursor TFH cell levels in human peripheral blood and murine LNs contributed to only 2-5 % of live CD4<sup>+</sup>T cell compartment and levels might be equally low in human VAT and thus hardly detectable in a small amount of VAT biopsy. To broaden the scope of human research and to overcome the

limitations of clinical investigation, mouse models were applied and TFH cells were assessed directly in the ATs of lean vs. obese mice. Here, at the site of inflammation (VAT), changes in TFH cell levels might be more consistent than in LNs and AT-residing TFH cells might either represent blood derived precursor TFH cells or TFH cells derived from the GCs of the lymphoid tissues. However, their origin is yet unknown and their characterization is limited to the results shown in this thesis. AT-residing TFH cells were similarly to circulating TFH cells named “precursor TFH cells”. In non-lymphoid structures such as the ATs, precursor TFH cells might reside in ectopic germinal centers (GC-like, “tertiary lymphoid organ-like” structures) (Aloisi & Pujol-Borrell, 2006). These might result from lymphoid neogenesis which can be induced during chronic inflammatory processes and their formation is reversible (Aloisi & Pujol-Borrell, 2006; Nosalski & Guzik, 2017; Salomonsson et al., 2003). Ectopic GCs were previously identified in *e.g.* perivascular AT (Nosalski & Guzik, 2017). The data shown here gives no information about the localization of AT-residing (precursor) TFH cells and does not directly support the existence of ectopic GCs in the ATs (*e.g.* Bcl6 expression was not assessed in AT-residing precursor TFH cells). However, the coexistence of pathogenic B cell, pathogenic IgG antibodies (Winer et al., 2011) and (precursor) TFH cells in the ATs indicates the possible occurrence of a GC reaction directly in the AT and might thus give a hint for the existence of ectopic GCs. However, the VAT-residing pathogenic B cells (CD19<sup>+</sup>B cells with differently expressed immunoglobins depending on the B cell subtype) identified by Winer *et al.* (Winer et al., 2011) do not correspond to GC B cells, since GC B cells were previously characterized as CD19<sup>+</sup>(CD20<sup>+</sup>)GL7<sup>+</sup>Fas<sup>+</sup>(B220<sup>+</sup>PNA<sup>+</sup>) B cells (Johnston et al., 2009; Nurieva et al., 2008; Shinall et al., 2000; C. J. Wang et al., 2015). Additionally, Winer *et al.* (Winer et al., 2011) showed a preferred localization of pathogenic B cells to regions of “crown like structures”. Thus, precursor TFH cells might also reside in such structures surrounding predominantly death adipocytes (Cinti et al., 2005; Coats et al., 2017; Feuerer et al., 2009). Furthermore, precursor TFH cells could reside in milky spots (tiny white-colored areas of lymphoid tissue) (Rangel-Moreno et al., 2009) or might be dispersed through the AT (Kolodin et al., 2015).

In line with the data from LNs, AT-residing (precursor) TFH cell frequencies depicted a certain heterogeneity. Although, blood contaminations were strictly avoided, they could contribute to a small part of this heterogeneity. The identification of a yet unknown VAT-specific TFH cell marker and the assessment of TFH cell numbers per gram AT, instead of the here analyzed frequencies relative to the total number of CD4<sup>+</sup>T cells, might result in more constant results. Additionally, changes in (precursor) TFH cell levels in response to a HFHS diet and chronic, low-grade inflammation might be minor compared to the effects seen upon acute or high-grade inflammation (Crotty, 2014; Scherm et al., 2016; Ueno, 2016) or

immunization (Baumjohann & Ansel, 2015; Takebe et al., 2018) which is applied in most studies targeting TFH cells. Nevertheless, the preliminary data of this thesis shows that similarly to the effects seen in mesLNs upon a long-term HFHS diet, **CD4<sup>+</sup>CXCR5<sup>+</sup>PD1<sup>hi</sup> precursor TFH cells were**, although not significantly, increased in murine SAT and VAT. In VAT, this effect was even more prominent upon one year of a HFHS diet. Our group previously showed that Treg levels are significantly decreased in murine VAT and SAT and slightly decreased in BAT upon an intermediate-term HFHS diet (Kalin et al., 2017). This reduction in suppressive, anti-inflammatory Tregs might make the ATs more permissive for pro-inflammatory cells, like TFH cells, and is in line with the here shown results. Tregs and (precursor) TFH cells have opposing roles and functions and signaling cues such as miRNAs might be beneficial for the differentiation and function of one cell population, whilst having negative effects on the other cell population.

miRNAs were previously highlighted to be involved in T cell differentiation and function (Baumjohann & Ansel, 2013; Cobb et al., 2006; Cobb et al., 2005; Grishok et al., 2001; Jeker & Bluestone, 2013; Monticelli, 2013; Serr et al., 2016b; Serr et al., 2018) and in obesity-associated immune-metabolic processes (Deiuliis, 2016; Heneghan et al., 2011; Kloting et al., 2009). Our group recently showed that high expression of miRNA92a, a miRNA of the miRNA17~92 cluster, is associated with increased frequencies of peripheral blood precursor TFH cells during onset of human islet autoimmunity (Serr et al., 2016b). MiRNAs of this cluster were also shown to be highly relevant for promoting obesity progression (Deiuliis, 2016). Specifically, miRNA17-5p expression was shown to be decreased in omental AT of obese (Heneghan et al., 2011) and T2D patients (Kloting et al., 2009) compared to healthy controls. Additionally, Kloting *et al.* (Kloting et al., 2009) reported a negative correlation between miRNA17-5p expression and VAT mass. Hence, miRNAs of the miRNA17~92 cluster, including miRNA92a, represent potential **immune-metabolic signaling cues** linking obesity with increased TFH cell levels. As mentioned above, a long-term HFHS diet was associated with increased (precursor) TFH cell levels representing an ideal time point for tissue biopsies and subsequent cell sorting and gene expression analysis. Of note, there were no observable changes in miRNA92a expression in this thesis when comparing CD4<sup>+</sup>CXCR5<sup>+</sup> precursor TFH or CD4<sup>+</sup>CXCR5<sup>-</sup> non-TFH cells from mesLNs of mice exposed to a SD with equivalent cells of mice exposed to a long-term HFHS diet. Thus, miRNA92a could not be confirmed as important for linking obesity-associated chronic, low-grade inflammation with increased (precursor) TFH cell levels and other yet unidentified immune-metabolic signaling cues (*e.g.* other miRNAs, cytokines, adipokines, FFA, hormones) might be involved in the disease pathology.

Various stages of TFH cell differentiation and maturation were characterized by the expression of different TFH cell markers in the literature (Crotty, 2014). A long-term HFHS diet might not only affect TFH cell quantities but might also influence the differentiation and maturation of these cells represented in their mRNA expression profiles. **Gene expression analyses** in the aforementioned precursor TFH vs. non-TFH cells from SD vs. long-term HFHS diet mice revealed no significant effect of the obesogenic environment on the expression of TFH cell markers. This might be attributed to the previously mentioned heterogeneity of TFH cells and low frequencies. Additionally, the duration of the HFHS diet was probably insufficient and differences in TFH cell markers might be clearer on the protein level. However, the here performed gene expression analyses **confirmed the TFH cell phenotype** with (significant) higher expression of *Il21*, *ICOS* and *Bcl6* in precursor TFH cells compared to non-TFH cells from SD mice. *Il21* and *ICOS* were significantly higher expressed in precursor TFH cells compared to non-TFH cells upon a long-term HFHS diet, whereas *Bcl6* expression remained unchanged. This is surprising, since Bcl6 is the master transcription factor and regulator of differentiation and function of TFH cells (Johnston et al., 2009; Nurieva et al., 2009; Yu et al., 2009) and its expression is expected to be high in these cells. *Bcl6* mRNA quantity was previously shown to be a poor indicator for Bcl6 protein expression and function due to its high posttranscriptional modulation (Allman et al., 1996; Kitano et al., 2011). Thus, Bcl6 protein expression might differ from mRNA expression and might be potentially increased in TFH cells from long-term HFHS diet mice. Additional, gene expression analyses of transcription factors which are important for TFH cell differentiation and function such as *Pdcd1* (encodes PD1), *CCR7*, *Ascl2*, *ITCH*, *Foxo1*, *Pten* and *Klf2* would help to more specifically dissect the role of (precursor) TFH cells and to determine (precursor) TFH cell characteristics in obesity.

Furthermore, differences in the expression of miRNA92a and TFH cell markers might be more prominent in precursor TFH vs. non-TFH cells isolated directly from the inflamed VAT upon dietary challenge. To this aim, gene expression analyses with human total VAT biopsies from lean vs. obese individuals with different states of insulin sensitivity were performed. The mean BMI of lean individuals that donated VAT biopsies for the here shown experiments was 23.2 kg/m<sup>2</sup> and was thus at the upper limit of normal weight (BMI of normal weight: 18.5 – 25 kg/m<sup>2</sup>). On the contrary, obese donors had a mean BMI of 63.3 kg/m<sup>2</sup> representing highly obese individuals, since obesity is defined as a BMI  $\geq$  30 kg/m<sup>2</sup>. Given the large differences in BMI between lean and obese donors, obesity-associated changes in gene expression in total human VAT might be highly prominent but could be biased by an immune overactivation by the extremely obese state. Additionally, obesity-associated changes in gene expression during obesity progression could not be assessed. Above

---

mentioned VAT biopsies were used for analyses of TFH cell-associated genes (*Ascl2*, *Il21*, *ICOS*, *Bcl6*) and data was normalized to the expression of the T cell marker CD4. This method was previously applied by the group of Diane Mathis (Feuerer et al., 2009) showing the ratio of Foxp3/CD4 expression in human AT. However, in this way generated results cannot be equated with T cell specific variations in gene expression, but allow an assumption. On the contrary to the gene expression analyses from murine LNs in which obesity-associated inflammatory signaling cues did not significantly influence the expression of TFH cell markers, VAT biopsies from obese, insulin-resistant individuals showed increased, albeit not significant, expression of the TFH cell markers *Ascl2* and *Il21* compared to lean, insulin-sensitive controls. In contrast, the expression of the TFH cell markers *ICOS* and *Bcl6* was not affected in the present thesis. However, the here shown gene expression analyses of TFH cell markers in total VAT might be biased due to their co-expression by other AT-residing cells such as *Il21* expression by Th1 and Th17 cells (Chtanova et al., 2004; Revu et al., 2018) or *Bcl6* mRNA expression on human GC B cells (Kitano et al., 2011; Mages et al., 2000). Furthermore, analyses must be confirmed on CD4<sup>+</sup>T cells isolated from human VAT, where changes in gene expression might be more prominent and more specific and extended by the use of additional TFH cell markers. Nevertheless, the increased expression of *Ascl2* and *Il21* in VAT of obese, insulin-resistant individuals might represent a weak indicator for higher precursor TFH cell levels in obese VAT, which is in line with the above discussed cellular data indicating higher precursor TFH cell levels in murine VAT upon a long-term and a sustained HFHS diet. Additionally, this data extends the yet limited knowledge about the contribution of immune-metabolic interactions to obesity-associated VAT inflammation in humans which might be similar to the murine setting (Aron-Wisniewsky et al., 2009; Deiuliis et al., 2011; Fabbrini et al., 2013; Feuerer et al., 2009; Ioan-Facsinay et al., 2013; McLaughlin et al., 2014; Pereira et al., 2014; Travers et al., 2015; Wentworth et al., 2010; Wouters et al., 2017; Wu et al., 2018; Zeyda et al., 2011).

Importantly, the data of this thesis reflects a potentially important role for pro-inflammatory (precursor) TFH cells in both human and murine obesity which might be opposed to that of anti-inflammatory Tregs. A better understanding of the underlying immune-metabolic signaling cues that trigger the differentiation, proliferation and function of CD4<sup>+</sup>T cells in the obese setting is highly important, since signaling pathways might be inversely regulated in the cell fate of (precursor) TFH cells and Tregs.

## 4.2 Insulin (receptor) signaling and its effects on *de novo* Treg induction

Obesity progression is associated with deficiencies in AT-residing Tregs (Deiuliis et al., 2011; Feuerer et al., 2009; Kalin et al., 2017; Winer et al., 2009). This might be either due to an inhibition of local *de novo* Treg induction resulting from obesity-associated immune activation and pathological changes such as hyperinsulinemia, alterations in Treg homing or a combination of both mechanisms. Albeit emerging data highlights the plasticity of AT-residing T cells and Tregs in response to a HFHS diet, so far nothing is known about the induction of Tregs from CD4<sup>+</sup>T cells in the presence of insulin or hyperinsulinemia. Here, an important role of T cell-specific InsR signaling for Foxp3<sup>+</sup>Treg induction from naïve CD4<sup>+</sup>T cells was identified both in health and obesity. This is of great interest since an increase in peripheral Tregs and specifically in VAT-residing Tregs might trigger an anti-inflammatory skew of the adaptive immune response with beneficial effects on systemic and local inflammation.

Specifically, the data of this thesis demonstrates that **exogenous insulin results in a significant reduction of the *in vitro* Foxp3<sup>+</sup>Treg induction** capacity when using naïve CD4<sup>+</sup>T cells from mesLNs (closely located to the metabolically active VAT), directly from the VAT or from popLNs (located in the fat pad of the knee which is in close proximity to the metabolically active muscles). Likewise, insulin interfered with human Foxp3<sup>+</sup>Treg induction. Accordingly, an improved Treg induction capacity due to the absence of insulin (receptor) signaling was proven in this thesis using naïve CD4<sup>+</sup>T cells from LNs and VAT of mice with a T cell specific InsR deficiency (InsR TKO mice).

InsR TKO mice display a powerful genetic mouse model that allows to mechanistically dissect T cell specific insulin (receptor) signaling. Here, for the first time, T cell specific insulin (receptor) signaling and its effects on T cell activation, differentiation, Treg induction and T cell intrinsic immune-metabolic adaptations were assessed. Insulin stimulation did not interfere with Foxp3<sup>+</sup>Treg induction in absence of InsR expression. This verifies the functionality of the InsR TKO and reflects the specificity of insulin binding to its receptor. Minor variations in Treg induction by insulin using InsR TKO cells might be attributed to insulin binding to IGF1 and IGFII receptor with lower affinity which might alter downstream signaling pathways that affect Treg induction (Andersen et al., 2017; De Meyts & Whittaker, 2002; Morcavallo et al., 2014). As mentioned above, the data of this thesis shows **a beneficial effect of the InsR TKO on *in vitro* Treg induction**. Specifically, the net effect of the InsR deficiency on Treg induction was slightly higher when using T cells from popLNs and significantly higher when using T cells isolated from VAT compared to mesLNs. Despite normalization to the respective controls, this might be partly attributed to the tissue-dependent, different cell numbers used for Treg induction assays. Importantly, VAT-residing CD4<sup>+</sup>T cells might be more sensitive to

changes of immune-metabolic signaling cues (e.g. InsR signaling) than CD4<sup>+</sup>T cells from metabolically less active LNs. Hence, CD4<sup>+</sup>T cells from VAT of Flox ctrl. mice might more rapidly upregulate InsR expression upon activation than CD4<sup>+</sup>T cells from popLNs and mesLNs of these mice. This might lead to a high difference in intrinsic T cell activation between VAT-residing CD4<sup>+</sup>T cells from Flox ctrl. and InsR TKO mice, accompanied by the observed highest difference in Treg induction in this thesis.

The here applied *in vitro* Treg induction- using short-term or limited TCR/CD28 stimulation with a strong agonistic ligand in presence of exogenous IL2 and in the absence of TGFβ provided under subimmunogenic conditions- was previously shown to result in a highly efficient Foxp3<sup>+</sup>Treg induction with only limited proliferation (Daniel et al., 2011; Daniel et al., 2010; Kalin et al., 2017; Sauer et al., 2008; Serr et al., 2016a; Serr et al., 2018; von Boehmer & Daniel, 2013). A purity control of isolated naïve CD4<sup>+</sup>T cells (> 98 % purity) ruled out that the here observed changes in Treg induction were due to an expansion of pre-existing (Foxp3<sup>+</sup>)CD25<sup>+</sup>Tregs. Additionally, proliferation of newly induced Tregs was assessed by labelling with Ki67 which represents a cell cycle-associated nuclear protein. In the here shown data, Treg induction efficiency in the presence of insulin or in the absence of the InsR was inversely correlated with the amount of proliferating CD4<sup>+</sup>Ki67<sup>+</sup>T cells. This **inverse correlation of Foxp3<sup>+</sup>Tregs and proliferating CD4<sup>+</sup>Ki67<sup>+</sup>T cells** might result from different activation levels of pathways downstream of insulin (receptor) signaling. Transcriptomic analyses of CD4<sup>+</sup>T cells from InsR TKO mice revealed a significant downregulation of the **InsR signaling pathway** and a marked reduction of the **Ras/MapK** and the **PI3K-Akt-mTOR signaling pathway** compared to CD4<sup>+</sup>T cells from Flox ctrls. Both the Ras/MapK and the PI3K-Akt-mTOR signaling pathway lie downstream of InsR signaling and all three pathways were previously shown to link immune-metabolic processes in T cells (Deberardinis et al., 2006; Fischer et al., 2017; Han et al., 2014; Li & Rudensky, 2016; Tsai et al., 2018). A lower activity of the Ras/MapK signaling pathway was previously associated with less mitogenic effects (Avruch, 2007) including the here observed lower proliferative capacity of T cells from InsR TKO mice. On the contrary, abnormally high insulin levels as in hyperinsulinemia are associated with an overstimulation of the mitogenic pathway (Gallagher & LeRoith, 2010) and the here performed Treg induction in presence of insulin might be accompanied by elevated levels of CD4<sup>+</sup>Ki67<sup>+</sup>T cells due to a higher activity of the Ras/MapK signaling pathway. Importantly, the availability of insulin or the expression of the InsR on CD4<sup>+</sup>T cells regulate the signaling intensity of the insulin (receptor) pathway and the downstream Ras/MapK and PI3K-Akt-mTOR signaling pathway, resulting in either increased Foxp3<sup>+</sup>Treg induction or CD4<sup>+</sup>Ki67<sup>+</sup>T cell proliferation. The highly complex Foxp3<sup>+</sup>Treg induction is additionally regulated by signaling mechanisms upstream of the aforementioned pathways

such as the **signal strength of TCR stimulation** (Li & Rudensky, 2016) and more specifically by varying anti-CD3 concentrations and the duration of the TCR stimulus (Serr et al., 2018). In this thesis, insulin mediated impairments in Treg induction were more prominent once Treg induction was performed with continuous low dose TCR stimulation, supporting the notion that the immune-metabolic effect of insulin on Treg induction can be additionally influenced by the TCR signal strength.

Previous studies have highlighted the importance of proteins that limit PI3K-Akt-mTOR signaling (e.g. Pten) for Treg induction (Battaglia et al., 2005; Delgoffe et al., 2009; Delgoffe et al., 2011; Haxhinasto et al., 2008; Sauer et al., 2008). Sauer *et al.* (Sauer et al., 2008) specifically showed that *in vitro* Treg induction is increased in the presence of a PI3K inhibitor (LY294002), an Akt inhibitor (Akti-1/2) or a mTOR inhibitor (Rapamycin). These compounds were shown to limit the activity of the PI3K-Akt-mTOR pathway and to result in high levels of Foxp3<sup>+</sup>Tregs (Sauer et al., 2008). This is in line with the here shown enhanced Treg induction using InsR-deficient T cells and the reduced gene expression of components of the PI3K-Akt-mTOR signaling pathway in InsR TKO cells identified by RNAseq. The lower activity of the PI3K-Akt-mTOR pathway was confirmed by immunofluorescence stainings on cytopins from *in vitro* activated CD4<sup>+</sup>T cells reflecting less abundance of pS6, a direct target of the mTOR-regulated p70 S6 kinase S6K1 (Saxton & Sabatini, 2017). On the contrary, insulin increased pS6 levels which is associated with a sustained activation of the PI3K-Akt-mTOR pathway (Saxton & Sabatini, 2017) and the here observed lower Treg induction capacity in the presence of insulin. Partial inhibition of the PI3K-Akt-mTOR pathway by applying a **PI3K inhibitor (LY294002) similarly increased Treg induction using naïve CD4<sup>+</sup>T cells from InsR TKO and Flox ctrl. mice**, however, the net increase was significantly lower in the InsR TKO cells. Thus, T cells from these mice might be less responsive to attenuations of PI3K-Akt-mTOR signaling, potentially due to their already intrinsically lower activity of this pathway. Furthermore, the additional increase of the already high Treg induction capacity by the PI3K inhibitor using InsR TKO cells suggests that other signaling cascades than solely the PI3K-Akt-mTOR pathway downstream of the InsR are involved in the lower intrinsic activation of these cells.

A combination of **transcriptomic and proteomic data** in this thesis **uncovered a lower intrinsic activation state of CD4<sup>+</sup>T cells from InsR TKO mice as key beneficial driver for Foxp3<sup>+</sup>Treg induction**. *Chek1*, *CCR4*, *Gk5* and *Tiparp* were among the 40 most significant downregulated genes in the InsR TKO cells. *Chek1* was previously identified as dynamic positive regulator of NFAT activity in Jurkat cells (Gabriel et al., 2016) and NFAT proteins are crucial for maintenance of the Treg cell identity by binding to different parts of the Foxp3

locus, inducing Foxp3 expression (Gabriel et al., 2016; Tone et al., 2008). C-C chemokine receptor type 4 (*CCR4*), the high affinity receptor for Ccl17 and Ccl22, was shown to be not expressed on resting (naïve and memory) T cells. However, its expression immediately increases upon T cell activation and was shown to be highest and most functional in finally differentiated Th2 cells. (Morimoto et al., 2005) *Gk5* synthesizes the generation of glycerophospholipids (Wieland & Suyter, 1957) which are basic components of plasma membranes and their synthesis is increased upon T cell activation and proliferation due an increasing membrane surface (Almeida et al., 2016; Park & Pan, 2015; van der Windt & Pearce, 2012). *Tiparp* is a target of the transcription factor Ahr and regulates its activity via a negative feedback loop. Ahr was shown to respond to endogenous kynurenine, resulting from the oxidation of the essential amino acid tryptophan, with the generation of Tregs whilst inhibiting Th1-, Th2- and Th17-differentiation and T cell proliferation. (Engin et al., 2015; Zhou, 2016) Thus, low levels of *Tiparp* gene expression in CD4<sup>+</sup>T cells from InsR TKO mice might point towards a higher intrinsic Ahr activity and associated benefits for Treg induction. (Engin et al., 2015; Zhou, 2016). In addition to the reduced levels of *Tiparp*, decreased gene expression of *Gsk3b*, *Atf4* and *GADD45β* in T cells were previously associated with benefits for Treg induction and Foxp3 expression and these genes were additionally downregulated in InsR-deficient T cells. Specifically, low levels of *Gsk3b* were previously identified as beneficial for T cell differentiation into Foxp3<sup>+</sup>Tregs potentially via regulation of β-catenin (Ding et al., 2008; Neal & Clipstone, 2001). Likewise, *Atf4* deletion in CD4<sup>+</sup>T cells resulted in increased *Foxp3* mRNA levels when CD4<sup>+</sup>T cells were cultured under Tregs conditions (Yang et al., 2018). Furthermore, *Gadd45β*<sup>-/-</sup> mice showed a greater number of Tregs in their spleens and IFNγ and Il17 production of T cells isolated from these mice was significantly reduced (Luo et al., 2011). The low intrinsic activation status of InsR-deficient T cells is supported by the proteomic analysis in this thesis. Specifically, protein expression of both negative regulators of T cell activation and the immune system process (*Adrm1* and *Bst2*) and proteins that are relevant for Foxp3<sup>+</sup>Treg induction (*Cbl*, *Stat3*, *Stat5a*, *Stat5b* and *Pten*) were significantly increased in CD4<sup>+</sup>T cells from InsR TKO mice. Specifically, *Cbl-b* was shown to control *in vitro* and *in vivo* Treg development by tuning TCR signaling strength (Qiao et al., 2013) and *Cbl-b* deficiency in T cells was shown to result in defective Foxp3 induction (Harada et al., 2010). Additionally, Il2-mediated activation of *Stat5a* and *Stat5b* (Burchill et al., 2007; Yao et al., 2007) and an active *Stat3* signaling were identified as critical for Treg differentiation, Foxp3 expression and Treg function (Chaudhry et al., 2009; Pallandre et al., 2007). Furthermore, *Pten* counteracts the activity of the PI3K-Akt-mTOR pathway with beneficial effects on Treg induction (Sauer et al., 2008). This reflects an additional layer of a lower intrinsic activation status of the InsR TKO cells and highlights that T cells are skewed towards a Th2/Treg phenotype in absence of InsR signaling.

---

As shortly mentioned in the beginning of the discussion and in line with the murine data, the human data of this thesis highlights that **naïve CD4<sup>+</sup>T cells isolated from human peripheral blood of healthy, lean females react to insulin with a significant decrease in Treg induction** capacity. Importantly, human T cell specific insulin sensitivity appears to be influenced by the gender. Naïve CD4<sup>+</sup>T cells isolated from peripheral blood of males did not respond with decreased Treg levels to equal amounts of insulin than used for Treg induction from females, but maintained their Treg induction capacity. This is in line with a previously identified sexual dimorphism in insulin sensitivity with female rodents and women reflecting greater insulin sensitivity in AT, liver and muscle compared to male counterparts (Estrany et al., 2013; Garcia-Carrizo et al., 2017; Hoeg et al., 2011; Magkos et al., 2010; Masharani et al., 2009). Additionally, GWAS showed that gender differences are rather the norm than the exception in the susceptibility to obesity and T2D and the disease development (Parks et al., 2015). However, the murine experiments in this thesis showed no observable inter-gender difference in the insulin sensitivity of murine T cells and insulin-mediated impairments in Treg induction where not affected by the gender (pooled data from both sexes is shown in this thesis).

In addition to the gender and more importantly, obesity might affect Treg induction and T cell specific insulin sensitivity. However, although isolated from an inflammatory setting, T cells from obese mice maintained their differentiation potential into Tregs which was already previously assessed by us (Kalin et al., 2017). Additionally and of great relevance, in the present thesis obesity did not interfere with T cell-specific insulin-sensitivity. Specifically, insulin-mediated impairments in Treg induction were maintained upon a short-term HFHS diet (2 weeks) and gradually increased with obesity progression using mesLNs of mice exposed to a short-term, a long-term (18 weeks) and a sustained HFHS diet, resembling the pathogenesis of human obesity progression (Kleinert et al., 2018). Data from genetically obese *ob/ob* mice highlights similar insulin-induced impairments in Treg induction capacity compared to the corresponding lean controls. These maintained insulin-mediated impairments in Treg induction and their gradual intensification with obesity progression might be attributed to a higher intrinsic activation and associated accelerated InsR upregulation by *in vitro* activated naïve CD4<sup>+</sup>T cells from obese mice triggered by obesity-associated pathological processes. A positive correlation of the T cell specific InsR expression with obesity (progression) could be one potential explanation for the increasing or higher responsiveness of T cells to insulin in obese mice. Unfortunately, T cell specific InsR expression could not be assessed in the present work due to the unavailability of a FACS-proved specific InsR antibody. It remains open, whether CD4<sup>+</sup>T cells isolated from VAT or

---

popLNs show similar or even increased insulin responsiveness upon exposure to a long-term or sustained HFHS diet or when isolated from ob/ob mice.

Considering the entire murine body, the duration of DIO was previously shown to progressively increase hyperinsulinemia, accompanied by a worsening of whole-body insulin resistance. Already one week of a HFHS diet was identified to slightly increase insulin levels and decrease insulin sensitivity. After a long-term HFHS diet, obesity is normally manifested and among others characterized by peripheral insulin resistance and hyperinsulinemia. (Speakman et al., 2007; Winzell & Ahren, 2004) In line with this, genetically obese ob/ob mice are insulin-resistant in the peripheral insulin-sensitive tissues and metabolic alterations were previously shown to be already completely present starting from week 6 of age (Soli et al., 1975). Importantly, the here used naïve CD4<sup>+</sup>T cells are mainly derived from body compartments that are relevant for the body's metabolic control (VAT and muscle) or closely located to metabolically active tissues (mesLNs, popLNs) and were therefore suspected to be affected by obesity-associated insulin resistance. Thus, although the here used **DIO and ob/ob mice are insulin-resistant in the peripheral, normally insulin-sensitive tissues (AT, muscle and liver), CD4<sup>+</sup>T cells isolated from their LNs (and VAT) remain insulin-sensitive** as indicated by decreased Treg induction capacities in the presence of insulin in this thesis. Thus, obesity-associated pathological processes might not diminish T cell specific insulin (receptor) signaling. In ob/ob mice, whole-body leptin deficiency might lead to T cell-intrinsic pathological changes apart from T cell-specific insulin resistance. The hormone leptin was previously shown to activate PI3K-Akt-mTOR signaling associated with decreased Treg levels and diminished Treg function (Iikuni et al., 2008; Procaccini et al., 2010; Taleb et al., 2007). Thus, leptin deficiency in ob/ob mice might be associated with a low activity of this pathway and might positively contribute to the here assessed Treg induction capacity starting from naïve CD4<sup>+</sup>T cells. Since ob/ob mice more resemble the state of leptin deficiency than obesity (Zhang et al., 1994), studies with these mice provide only a limited understanding of mechanisms and effects of obesity on immune cell function. Additionally, results from ob/ob mice are hardly transferable to murine DIO and the human obesity setting, since both DIO mice and obese humans are characterized by elevated leptin levels contributing to systemic low-grade inflammation (Iikuni et al., 2008), whereas leptin-deficient ob/ob mice are associated with an increased risk for infections due to reduced cell-mediated immune responses (Taleb et al., 2007; Zhang et al., 1994). However, it was previously shown that the expression of the InsR in ob/ob mice is not regulated by genetics, but rather by obesity itself, at least in the liver (Soli et al., 1975). Hence, InsR expression and signaling in CD4<sup>+</sup>T cells from ob/ob mice might also be regulated by obesity, making this mouse model more valuable for the here presented research. Thus, both DIO and ob/ob mice represent powerful models

to study the effect of obesity and insulin on Treg induction and the adaptive immune response.

Further experiments might help to confirm the here shown data and to especially verify maintained insulin sensitivity of CD4<sup>+</sup>T cells isolated from metabolically relevant body compartments of obese mice and humans. Specifically, Treg induction assays with naïve CD4<sup>+</sup>T cells from peripheral blood or even VAT of obese humans that are either insulin-sensitive or insulin-resistant in the peripheral tissues would help to verify gained knowledge from the murine setting in the human system. To prove maintained T cell specific insulin sensitivity in obese mice and humans independently from Treg induction, these cells could be stimulated with exogenous insulin and subsequent quantitative assessment of the InsR levels by Western Plot would provide information about the insulin sensitivity of these cells. Furthermore, Treg induction experiments with T cells from peripheral blood of males and higher levels of insulin need to be conducted to get better insights into the sex-dependent insulin sensitivity of T cells isolated from human peripheral blood.

Recently, Tsai *et al.* (Tsai et al., 2018) highlighted that murine InsR-deficient CD4<sup>+</sup>T cells are more prone to differentiate into anti-inflammatory Th2 cells than their corresponding controls under the respective polarizing conditions *in vitro*. This strengthens the here shown data, revealing an increased differentiation of InsR-deficient naïve CD4<sup>+</sup>T cells into anti-inflammatory Tregs. Accordingly, Tsai *et al.* (Tsai et al., 2018) highlighted in an adoptive transfer model of colitis *in vivo* that the transfer of InsR-deficient CD4<sup>+</sup>CD25<sup>-</sup>CD45RB<sup>hi</sup> T cells into RAG1-deficient hosts results in a diminished disease severity compared to the transfer of WT ctrl. cells. This was reflected by a significant reduction in pro-inflammatory CD4<sup>+</sup>T cells in the mesLNs. (Tsai et al., 2018) Thus, T cell specific InsR deficiency might counteract CD4<sup>+</sup>T cell-mediated inflammation *in vivo*, highlighting an anti-inflammatory effect of the T cell specific InsR deficiency with potential similar beneficial effects in the obesity setting. Indeed, **exposure of InsR TKO mice to a long-term HFHS diet maintained increased *in vitro* Treg induction capacity** using naïve CD4<sup>+</sup>T cells from mesLNs and VAT of these mice. This reflects that the beneficial effect of the InsR deficiency on Treg induction is not disturbed by pathological processes of an obesogenic environment. For further research it is of great interest to investigate the *in vivo* effect of the InsR TKO, especially under obese conditions. To this end, initially *ex vivo* Treg frequencies in different body compartments and particularly in VAT and muscle of InsR TKO mice need to be assessed and confirmed under SD and HFHS diet conditions.

---

From an immune-metabolic perspective insulin (receptor) signaling might be additionally to T cell differentiation- highly important for the function and cell-intrinsic metabolism of CD4<sup>+</sup>T cell and Foxp3<sup>+</sup>Tregs. Like (activated) CD4<sup>+</sup>T cells, their Foxp3<sup>+</sup>Treg subpopulation might be sensitive to insulin. Specifically, insulin (receptor) signaling might be highly important for *in vitro* activation and differentiation of isolated CD4<sup>+</sup>T cell into Foxp3<sup>+</sup>Tregs, indicated by the previously shown increased expression of the InsR upon T cell activation (Han et al., 2014; Helderman & Strom, 1978; Tsai et al., 2018; Viardot et al., 2007) and the insulin mediated impairments in *in vitro* Treg induction shown in this thesis. *In vitro* Treg induction starting from isolated naïve CD4<sup>+</sup>T cells and re-stimulation of the resulting *in vitro* differentiated Foxp3<sup>+</sup>Tregs, both in presence of insulin, resulted in impaired Treg levels as highlighted in the present thesis. This reflects that insulin reduces the **stability of Foxp3<sup>+</sup>Treg phenotype in re-stimulation assays**. However, *in vitro* induced Foxp3<sup>+</sup>Tregs might similarly to *ex vivo* Tregs show a low or no expression of the InsR. Thus, the observed defects in Treg stability in the re-stimulation assays of this thesis might be more attributed to insulin-mediated impairments in Treg induction than to the effect of insulin on differentiated Foxp3<sup>+</sup>Tregs.

Activation of **murine CD4<sup>+</sup>T cells** affects their **metabolism** which in turn influences their differentiation and function (Almeida et al., 2016; Park & Pan, 2015; van der Windt & Pearce, 2012). As mentioned above, murine and human CD4<sup>+</sup>T cell activation was previously shown to be accompanied by an upregulation of the InsR (Han et al., 2014; Helderman & Strom, 1978; Tsai et al., 2018; Viardot et al., 2007). Thus, insulin might be equally important for facilitated glucose uptake by CD4<sup>+</sup>T cells than it is for *e.g.* glucose uptake by adipocytes. Inducible silencing of whole-body InsR signaling in rats was previously identified to impair glucose uptake and glycolysis in activated CD4<sup>+</sup>T cells via downregulation of compounds of the PI3K-Akt-mTOR and Ras/MapK pathway (Fischer et al., 2017). Here, glucose uptake was assessed in T cells upon *in vitro* activation for 4 hours under identical conditions than in Treg induction assays. This represents a time point in which the cells have not yet proliferated and thereby confounding effects of proliferation are eliminated, enabling adequate investigation of changes in the metabolism of activated T cells (Almeida et al., 2016; Park & Pan, 2015; van der Windt & Pearce, 2012). Accordingly, the data of this thesis shows that InsR deficiency in murine CD4<sup>+</sup>T cells impairs cellular **glucose uptake**, whilst activation of WT CD4<sup>+</sup>T cells in presence of insulin led to the opposite effect. This is in line with previous findings from Tsai *et al.* (Tsai et al., 2018) and results were confirmed and extended regarding their relevance for Treg induction in the present thesis. Additionally, immunofluorescence stainings showed higher levels of **GCK** expression on *in vitro* activated CD4<sup>+</sup>T cells in presence of insulin, whilst GCK expression was reduced in InsR deficient T cells compared to the respective controls. GCK is a hexokinase that phosphorylates glucose

to glucose-6-phosphat in the first step of glycolysis. Hence, the expression of this enzyme by T cells indicates their glycolytic activity. This is in line with previous studies showing that the glycolytic flux in CD4<sup>+</sup>T is triggered by an increased expression of glycolytic enzymes (Hsu et al., 2018; Peng et al., 2016; Tsai et al., 2018; Wang et al., 2011) such as Hexokinase II (HkII) (Tsai et al., 2018; Wang et al., 2011), Phosphofruktokinase (Pfk) (Hsu et al., 2018; Tsai et al., 2018) and Lactate dehydrogenase alpha (Ldha) (Peng et al., 2016; Tsai et al., 2018). The results of this thesis highlight that the T cell specific glucose metabolism is regulated by the InsR and GCK, however, the expression of GLUTs, variations in passive glucose uptake and alterations in the expression of other glycolytic enzymes *etc.* contribute with great probability also to the observed effects.

From an immune-metabolic perspective, a combination of **transcriptomic and proteomic analyses** in this thesis provides further insights into the metabolic manipulation of CD4<sup>+</sup>T cells through their InsR deficiency. RNAseq revealed significant reduced levels of *ldh1* in InsR-deficient T cells. The gene Isocitrate dehydrogenase (*ldh1*) encodes an enzyme of the TCA cycle which was previously shown to be highly active in naïve T cells since they mainly depend on OXPHOS for energy generation (Almeida et al., 2016; Park & Pan, 2015; van der Windt & Pearce, 2012). Additionally, proteins of the ETC (Etfb, Fdxr, Sdha, Cyc1, Dld, Ndufv1, Ndufa2, Ndufa6, Ndufa8 and Ndufa10) were significantly downregulated in CD4<sup>+</sup>T cells from InsR TKO mice and these proteins are presented throughout the ETC, reflecting a potential impaired ETC function in these cells. Furthermore, Dihydrolipoyl dehydrogenase (Dld) is indispensable for the function of various oxidative enzyme complexes. (Odievre et al., 2005) Thus, reduced levels of Dld might result in a lower activity of the TCA cycle and hence less electrons that are bound to the coenzymes NADH and FADH<sub>2</sub> and transferred to the ETC. This might contribute to a decreased proton gradient across the inner mitochondrial membrane and an associated impaired ETC activity. A reduced expression of proteins of the ETC was previously associated with an impaired ETC function, a loss of mitochondrial electron density, a reduced mitochondrial ATP generation, lower levels of ROS, an increased energy generation by anaerobic glycolysis, a decreased energy generation by OXPHOS and an overall T cell specific mitochondrial dysfunction in mice with a T cell specific Tfam-deficiency (Baixauli et al., 2015). Especially, ROS production by mitochondrial complex III was identified to be indispensable for the activation of NFATs and subsequent T cell activation and effector T cell differentiation (Sena et al., 2013). Thus, the here observed reduced levels of Cyc1 might result in a lower activity of complex III accompanied by reduced levels of ROS and potential impairments in T cell activation. Importantly, impairments in the ETC might finally result in a lower activity of the ATP synthase resulting in both a decreased release of ATP into the extracellular space and a reduced Ca<sup>2+</sup> influx into the cell due to a

lower abundance of ATP-activated  $\text{Ca}^{2+}$ -channels. Low intracellular  $\text{Ca}^{2+}$  levels were previously associated with impaired T cell activation. (Almeida et al., 2016; Chang et al., 2013; Ledderose et al., 2014) Importantly, the here observed downregulation of ETC-associated proteins and *Idh1* gene expression in InsR-deficient T cells represents an additional feature of their low intrinsic activation status. The here analyzed  $\text{CD4}^+$ T cells from InsR TKO mice mainly consist of naïve T cells which depend on OXPHOS to meet their energy need. Thus, less OXPHOS in these cells might either indicate an overall lower metabolic activity of these cells or enhanced energy generation independently from OXPHOS.

To further mechanistically dissect how InsR signaling guides *de novo* Treg induction, the transcriptomic and proteomic data in this thesis needs to be validated and addressed in future studies by *e.g.* Seahorse analyses, *in vitro* Treg induction assays with compounds that specifically target these genes and proteins or gene expression analyses in different  $\text{CD4}^+$ T cell populations.

### 4.3 Conclusions and outlook

In summary, the data of this thesis extend our current knowledge of immune-metabolic interactions that are involved in immune activation vs. immune tolerance in murine and human obesity. More specifically, this thesis provides first evidence for the involvement of pro-inflammatory (precursor) TFH cell in the obesity pathology and links the disease with increased (precursor) TFH cell levels or at least alterations in their frequencies in the periphery and in the inflamed VAT of both humans and mice. Additionally, supraphysiological amounts of insulin were shown to impair *in vitro* induction of anti-inflammatory, suppressive  $\text{Foxp3}^+$ Tregs using naïve  $\text{CD4}^+$ T cells from lean humans and lean and obese mice, reflecting T cell specific insulin sensitivity. Surprisingly, besides their insulin resistance in the peripheral, metabolically active, normally insulin resistant tissues (AT, liver and muscle), DIO and ob/ob mice remain insulin-sensitive at the T cell level, reflected by the sustained negative effect of insulin on Treg induction. On the contrary, InsR deficiency in T cells was associated with a lower intrinsic activation status and a pro-tolerogenic signaling network that supports  $\text{Foxp3}^+$ Treg induction with potential beneficial effects on the obesity setting.

In conclusion, the results of this thesis highlight the complexity of obesity focusing on immune-metabolic interactions and especially obesity-associated metabolic signaling cues that are involved in the pathophysiology of the disease. Specifically, the here shown data provides an improved understanding of insulin (receptor) signaling affecting *in vitro*  $\text{Foxp3}^+$ Treg induction. Thereby gained knowledge is highly valuable to better understand

disease settings in which Treg induction is beneficial (*e.g.* obesity) or in which Tregs are undesirable (*e.g.* cancer). Last but not least, a better understanding of CD4<sup>+</sup>T cell activation and differentiation as well as an extended knowledge about immune-metabolic characteristics and functions of CD4<sup>+</sup>T cells and especially anti-inflammatory, suppressive Tregs and pro-inflammatory TFH cells might contribute to the understanding of the obesity pathology and may help to develop future treatment approaches which could specifically target these cells at the site of inflammation.

## 5. References

- Akiba, H., Takeda, K., Kojima, Y., Usui, Y., Harada, N., Yamazaki, T., Ma, J., Tezuka, K., Yagita, H., & Okumura, K. (2005). The role of ICOS in the CXCR5+ follicular B helper T cell maintenance in vivo. *J Immunol*, *175*(4), 2340-2348.
- Allman, D., Jain, A., Dent, A., Maile, R. R., Selvaggi, T., Kehry, M. R., & Staudt, L. M. (1996). BCL-6 expression during B-cell activation. *Blood*, *87*(12), 5257-5268.
- Almeida, L., Lochner, M., Berod, L., & Sparwasser, T. (2016). Metabolic pathways in T cell activation and lineage differentiation. *Semin Immunol*, *28*(5), 514-524. doi:10.1016/j.smim.2016.10.009
- Aloisi, F., & Pujol-Borrell, R. (2006). Lymphoid neogenesis in chronic inflammatory diseases. *Nat Rev Immunol*, *6*(3), 205-217. doi:10.1038/nri1786
- Andersen, M., Norgaard-Pedersen, D., Brandt, J., Pettersson, I., & Slaaby, R. (2017). IGF1 and IGF2 specificities to the two insulin receptor isoforms are determined by insulin receptor amino acid 718. *PLoS One*, *12*(6), e0178885. doi:10.1371/journal.pone.0178885
- Apostolou, I., Sarukhan, A., Klein, L., & von Boehmer, H. (2002). Origin of regulatory T cells with known specificity for antigen. *Nat Immunol*, *3*(8), 756-763. doi:10.1038/ni816
- Apostolou, I., & von Boehmer, H. (2004). In vivo instruction of suppressor commitment in naive T cells. *J Exp Med*, *199*(10), 1401-1408. doi:10.1084/jem.20040249
- Araki, E., Lipes, M. A., Patti, M. E., Bruning, J. C., Haag, B., 3rd, Johnson, R. S., & Kahn, C. R. (1994). Alternative pathway of insulin signalling in mice with targeted disruption of the IRS-1 gene. *Nature*, *372*(6502), 186-190. doi:10.1038/372186a0
- Aron-Wisnewsky, J., Tordjman, J., Poitou, C., Darakhshan, F., Hugol, D., Basdevant, A., Aissat, A., Guerre-Millo, M., & Clement, K. (2009). Human adipose tissue macrophages: m1 and m2 cell surface markers in subcutaneous and omental depots and after weight loss. *J Clin Endocrinol Metab*, *94*(11), 4619-4623. doi:10.1210/jc.2009-0925
- Avery, D. T., Deenick, E. K., Ma, C. S., Suryani, S., Simpson, N., Chew, G. Y., Chan, T. D., Palendira, U., Bustamante, J., Boisson-Dupuis, S., Choo, S., Bleasel, K. E., Peake, J., King, C., French, M. A., Engelhard, D., Al-Hajjar, S., Al-Muhsen, S., Magdorf, K., Roesler, J., Arkwright, P. D., Hissaria, P., Riminton, D. S., Wong, M., Brink, R., Fulcher, D. A., Casanova, J. L., Cook, M. C., & Tangye, S. G. (2010). B cell-intrinsic signaling through IL-21 receptor and STAT3 is required for establishing long-lived antibody responses in humans. *J Exp Med*, *207*(1), 155-171. doi:10.1084/jem.20091706
- Avruch, J. (2007). MAP kinase pathways: the first twenty years. *Biochim Biophys Acta*, *1773*(8), 1150-1160. doi:10.1016/j.bbamcr.2006.11.006
- Bacchetta, R., Barzaghi, F., & Roncarolo, M. G. (2018). From IPEX syndrome to FOXP3 mutation: a lesson on immune dysregulation. *Ann N Y Acad Sci*, *1417*(1), 5-22. doi:10.1111/nyas.13011
- Baek, D., Villén, J., Shin, C., Camargo, F. D., Gygi, S. P., & Bartel, D. P. (2008). The impact of microRNAs on protein output. *Nature*, *455*(7209), 64-71.
- Baixaulli, F., Acin-Perez, R., Villarroya-Beltri, C., Mazzeo, C., Nunez-Andrade, N., Gabande-Rodriguez, E., Ledesma, M. D., Blazquez, A., Martin, M. A., Falcon-Perez, J. M., Redondo, J. M., Enriquez, J. A., & Mittelbrunn, M. (2015). Mitochondrial Respiration Controls Lysosomal Function during Inflammatory T Cell Responses. *Cell Metab*, *22*(3), 485-498. doi:10.1016/j.cmet.2015.07.020
- Banting F. G., B. C. H., Collip J. B., Campbell W. R., Fletcher A. A., MacLeod J. J. R., Noble E. C. . (1922). The effect produced on diabetes by extracts of pancreas. *Trans. Assoc. Am. Physicians*(37), 337-347.
- Baron, U., Floess, S., Wiczorek, G., Baumann, K., Grutzkau, A., Dong, J., Thiel, A., Boeld, T. J., Hoffmann, P., Edinger, M., Turbachova, I., Hamann, A., Olek, S., & Huehn, J. (2007). DNA demethylation in the human FOXP3 locus discriminates regulatory T

- cells from activated FOXP3(+) conventional T cells. *Eur J Immunol*, 37(9), 2378-2389. doi:10.1002/eji.200737594
- Battaglia, M., Stabilini, A., & Roncarolo, M. G. (2005). Rapamycin selectively expands CD4+CD25+FoxP3+ regulatory T cells. *Blood*, 105(12), 4743-4748. doi:10.1182/blood-2004-10-3932
- Baumjohann, D. (2018). Diverse functions of miR-17-92 cluster microRNAs in T helper cells. *Cancer Lett*, 423, 147-152. doi:10.1016/j.canlet.2018.02.035
- Baumjohann, D., & Ansel, K. M. (2013). MicroRNA-mediated regulation of T helper cell differentiation and plasticity. *Nat Rev Immunol*, 13(9), 666-678. doi:10.1038/nri3494
- Baumjohann, D., & Ansel, K. M. (2015). Tracking early T follicular helper cell differentiation in vivo. *Methods Mol Biol*, 1291, 27-38. doi:10.1007/978-1-4939-2498-1\_3
- Baumjohann, D., Kageyama, R., Clingan, J. M., Morar, M. M., Patel, S., de Kouchkovsky, D., Bannard, O., Bluestone, J. A., Matloubian, M., Ansel, K. M., & Jeker, L. T. (2013a). The microRNA cluster miR-17 approximately 92 promotes TFH cell differentiation and represses subset-inappropriate gene expression. *Nat Immunol*, 14(8), 840-848. doi:10.1038/ni.2642
- Baumjohann, D., Preite, S., Reboldi, A., Ronchi, F., Ansel, K. M., Lanzavecchia, A., & Sallusto, F. (2013b). Persistent antigen and germinal center B cells sustain T follicular helper cell responses and phenotype. *Immunity*, 38(3), 596-605. doi:10.1016/j.immuni.2012.11.020
- Becker, M., Levings, M. K., & Daniel, C. (2017). Adipose-tissue regulatory T cells: Critical players in adipose-immune crosstalk. *Eur J Immunol*, 47(11), 1867-1874. doi:10.1002/eji.201646739
- Belfiore, A., & Malaguarnera, R. (2011). Insulin receptor and cancer. *Endocr Relat Cancer*, 18(4), R125-147. doi:10.1530/ERC-11-0074
- Bentebibel, S. E., Lopez, S., Obermoser, G., Schmitt, N., Mueller, C., Harrod, C., Flano, E., Mejias, A., Albrecht, R. A., Blankenship, D., Xu, H., Pascual, V., Banchereau, J., Garcia-Sastre, A., Palucka, A. K., Ramilo, O., & Ueno, H. (2013). Induction of ICOS+CXCR3+CXCR5+ TH cells correlates with antibody responses to influenza vaccination. *Sci Transl Med*, 5(176), 176ra132. doi:10.1126/scitranslmed.3005191
- Blagih, J., Coulombe, F., Vincent, E. E., Dupuy, F., Galicia-Vazquez, G., Yurchenko, E., Raissi, T. C., van der Windt, G. J., Viollet, B., Pearce, E. L., Pelletier, J., Piccirillo, C. A., Krawczyk, C. M., Divangahi, M., & Jones, R. G. (2015). The energy sensor AMPK regulates T cell metabolic adaptation and effector responses in vivo. *Immunity*, 42(1), 41-54. doi:10.1016/j.immuni.2014.12.030
- Boukouris, A. E., Zervopoulos, S. D., & Michelakis, E. D. (2016). Metabolic Enzymes Moonlighting in the Nucleus: Metabolic Regulation of Gene Transcription. *Trends Biochem Sci*, 41(8), 712-730. doi:10.1016/j.tibs.2016.05.013
- Boura-Halfon, S., & Zick, Y. (2009). Phosphorylation of IRS proteins, insulin action, and insulin resistance. *Am J Physiol Endocrinol Metab*, 296(4), E581-591. doi:10.1152/ajpendo.90437.2008
- Bouzakri, K., Zachrisson, A., Al-Khalili, L., Zhang, B. B., Koistinen, H. A., Krook, A., & Zierath, J. R. (2006). siRNA-based gene silencing reveals specialized roles of IRS-1/Akt2 and IRS-2/Akt1 in glucose and lipid metabolism in human skeletal muscle. *Cell Metab*, 4(1), 89-96. doi:10.1016/j.cmet.2006.04.008
- Breitfeld, D., Ohl, L., Kremmer, E., Ellwart, J., Sallusto, F., Lipp, M., & Forster, R. (2000). Follicular B helper T cells express CXC chemokine receptor 5, localize to B cell follicles, and support immunoglobulin production. *J Exp Med*, 192(11), 1545-1552.
- Brestoff, J. R., Kim, B. S., Saenz, S. A., Stine, R. R., Monticelli, L. A., Sonnenberg, G. F., Thome, J. J., Farber, D. L., Lutfy, K., Seale, P., & Artis, D. (2015). Group 2 innate lymphoid cells promote beiging of white adipose tissue and limit obesity. *Nature*, 519(7542), 242-246. doi:10.1038/nature14115
- Bruning, J. C., Michael, M. D., Winnay, J. N., Hayashi, T., Horsch, D., Accili, D., Goodyear, L. J., & Kahn, C. R. (1998). A muscle-specific insulin receptor knockout exhibits features

- of the metabolic syndrome of NIDDM without altering glucose tolerance. *Mol Cell*, 2(5), 559-569.
- Buck, M. D., O'Sullivan, D., Klein Geltink, R. I., Curtis, J. D., Chang, C. H., Sanin, D. E., Qiu, J., Kretz, O., Braas, D., van der Windt, G. J., Chen, Q., Huang, S. C., O'Neill, C. M., Edelson, B. T., Pearce, E. J., Sesaki, H., Huber, T. B., Rambold, A. S., & Pearce, E. L. (2016). Mitochondrial Dynamics Controls T Cell Fate through Metabolic Programming. *Cell*, 166(1), 63-76. doi:10.1016/j.cell.2016.05.035
- Bukhari, S. I. A., Truesdell, S. S., Lee, S., Kollu, S., Classon, A., Boukhali, M., Jain, E., Mortensen, R. D., Yanagiya, A., Sadreyev, R. I., Haas, W., & Vasudevan, S. (2016). A Specialized Mechanism of Translation Mediated by FXR1a-Associated MicroRNP in Cellular Quiescence. *Mol Cell*, 61(5), 760-773. doi:10.1016/j.molcel.2016.02.013
- Burchill, M. A., Yang, J., Vogtenhuber, C., Blazar, B. R., & Farrar, M. A. (2007). IL-2 receptor beta-dependent STAT5 activation is required for the development of Foxp3+ regulatory T cells. *J Immunol*, 178(1), 280-290.
- Cannons, J. L., Qi, H., Lu, K. T., Dutta, M., Gomez-Rodriguez, J., Cheng, J., Wakeland, E. K., Germain, R. N., & Schwartzberg, P. L. (2010). Optimal germinal center responses require a multistage T cell:B cell adhesion process involving integrins, SLAM-associated protein, and CD84. *Immunity*, 32(2), 253-265. doi:10.1016/j.immuni.2010.01.010
- Cao, X., Cai, S. F., Fehniger, T. A., Song, J., Collins, L. I., Piwnicka-Worms, D. R., & Ley, T. J. (2007). Granzyme B and perforin are important for regulatory T cell-mediated suppression of tumor clearance. *Immunity*, 27(4), 635-646. doi:10.1016/j.immuni.2007.08.014
- Carr, E. L., Kelman, A., Wu, G. S., Gopaul, R., Senkevitch, E., Aghvanyan, A., Turay, A. M., & Frauwirth, K. A. (2010). Glutamine uptake and metabolism are coordinately regulated by ERK/MAPK during T lymphocyte activation. *J Immunol*, 185(2), 1037-1044. doi:10.4049/jimmunol.0903586
- Chang, C. H., Curtis, J. D., Maggi, L. B., Jr., Faubert, B., Villarino, A. V., O'Sullivan, D., Huang, S. C., van der Windt, G. J., Blagih, J., Qiu, J., Weber, J. D., Pearce, E. J., Jones, R. G., & Pearce, E. L. (2013). Posttranscriptional control of T cell effector function by aerobic glycolysis. *Cell*, 153(6), 1239-1251. doi:10.1016/j.cell.2013.05.016
- Chaudhry, A., Rudra, D., Treuting, P., Samstein, R. M., Liang, Y., Kas, A., & Rudensky, A. Y. (2009). CD4+ regulatory T cells control TH17 responses in a Stat3-dependent manner. *Science*, 326(5955), 986-991. doi:10.1126/science.1172702
- Chen, Q., Kim, Y. C., Laurence, A., Punkosdy, G. A., & Shevach, E. M. (2011). IL-2 controls the stability of Foxp3 expression in TGF-beta-induced Foxp3+ T cells in vivo. *J Immunol*, 186(11), 6329-6337. doi:10.4049/jimmunol.1100061
- Chen, W., Jin, W., Hardegen, N., Lei, K. J., Li, L., Marinos, N., McGrady, G., & Wahl, S. M. (2003). Conversion of peripheral CD4+CD25- naive T cells to CD4+CD25+ regulatory T cells by TGF-beta induction of transcription factor Foxp3. *J Exp Med*, 198(12), 1875-1886. doi:10.1084/jem.20030152
- Chen, X., Priatel, J. J., Chow, M. T., & Teh, H. S. (2008). Preferential development of CD4 and CD8 T regulatory cells in RasGRP1-deficient mice. *J Immunol*, 180(9), 5973-5982.
- Cheng, X., Wang, J., Xia, N., Yan, X. X., Tang, T. T., Chen, H., Zhang, H. J., Liu, J., Kong, W., Sjöberg, S., Folco, E., Libby, P., Liao, Y. H., & Shi, G. P. (2012). A guanidine-rich regulatory oligodeoxynucleotide improves type-2 diabetes in obese mice by blocking T-cell differentiation. *EMBO Mol Med*, 4(10), 1112-1125. doi:10.1002/emmm.201201272
- Chin, S. H., Kahathuduwa, C. N., & Binks, M. (2016). Physical activity and obesity: what we know and what we need to know. *Obes Rev*, 17(12), 1226-1244. doi:10.1111/obr.12460
- Choe, S. S., Huh, J. Y., Hwang, I. J., Kim, J. I., & Kim, J. B. (2016). Adipose Tissue Remodeling: Its Role in Energy Metabolism and Metabolic Disorders. *Front Endocrinol (Lausanne)*, 7, 30. doi:10.3389/fendo.2016.00030

- Choi, Y. S., Kageyama, R., Eto, D., Escobar, T. C., Johnston, R. J., Monticelli, L., Lao, C., & Crotty, S. (2011). ICOS receptor instructs T follicular helper cell versus effector cell differentiation via induction of the transcriptional repressor Bcl6. *Immunity*, *34*(6), 932-946. doi:10.1016/j.immuni.2011.03.023
- Choi, Y. S., Yang, J. A., Yusuf, I., Johnston, R. J., Greenbaum, J., Peters, B., & Crotty, S. (2013). Bcl6 expressing follicular helper CD4 T cells are fate committed early and have the capacity to form memory. *J Immunol*, *190*(8), 4014-4026. doi:10.4049/jimmunol.1202963
- Chtanova, T., Tangye, S. G., Newton, R., Frank, N., Hodge, M. R., Rolph, M. S., & Mackay, C. R. (2004). T follicular helper cells express a distinctive transcriptional profile, reflecting their role as non-Th1/Th2 effector cells that provide help for B cells. *J Immunol*, *173*(1), 68-78.
- Cinti, S., Mitchell, G., Barbatelli, G., Murano, I., Ceresi, E., Faloia, E., Wang, S., Fortier, M., Greenberg, A. S., & Obin, M. S. (2005). Adipocyte death defines macrophage localization and function in adipose tissue of obese mice and humans. *J Lipid Res*, *46*(11), 2347-2355. doi:10.1194/jlr.M500294-JLR200
- Cipolletta, D., Cohen, P., Spiegelman, B. M., Benoist, C., & Mathis, D. (2015). Appearance and disappearance of the mRNA signature characteristic of Treg cells in visceral adipose tissue: age, diet, and PPARgamma effects. *Proc Natl Acad Sci U S A*, *112*(2), 482-487. doi:10.1073/pnas.1423486112
- Cipolletta, D., Feuerer, M., Li, A., Kamei, N., Lee, J., Shoelson, S. E., Benoist, C., & Mathis, D. (2012). PPAR-gamma is a major driver of the accumulation and phenotype of adipose tissue Treg cells. *Nature*, *486*(7404), 549-553. doi:10.1038/nature11132
- Clemmensen, C., Muller, T. D., Woods, S. C., Berthoud, H. R., Seeley, R. J., & Tschop, M. H. (2017). Gut-Brain Cross-Talk in Metabolic Control. *Cell*, *168*(5), 758-774. doi:10.1016/j.cell.2017.01.025
- Coats, B. R., Schoenfelt, K. Q., Barbosa-Lorenzi, V. C., Peris, E., Cui, C., Hoffman, A., Zhou, G., Fernandez, S., Zhai, L., Hall, B. A., Haka, A. S., Shah, A. M., Reardon, C. A., Brady, M. J., Rhodes, C. J., Maxfield, F. R., & Becker, L. (2017). Metabolically Activated Adipose Tissue Macrophages Perform Detrimental and Beneficial Functions during Diet-Induced Obesity. *Cell Rep*, *20*(13), 3149-3161. doi:10.1016/j.celrep.2017.08.096
- Cobb, B. S., Hertweck, A., Smith, J., O'Connor, E., Graf, D., Cook, T., Smale, S. T., Sakaguchi, S., Livesey, F. J., Fisher, A. G., & Merckenschlager, M. (2006). A role for Dicer in immune regulation. *J Exp Med*, *203*(11), 2519-2527. doi:10.1084/jem.20061692
- Cobb, B. S., Nesterova, T. B., Thompson, E., Hertweck, A., O'Connor, E., Godwin, J., Wilson, C. B., Brockdorff, N., Fisher, A. G., Smale, S. T., & Merckenschlager, M. (2005). T cell lineage choice and differentiation in the absence of the RNase III enzyme Dicer. *J Exp Med*, *201*(9), 1367-1373. doi:10.1084/jem.20050572
- Coleman, D. L. (1978). Obese and diabetes: two mutant genes causing diabetes-obesity syndromes in mice. *Diabetologia*, *14*(3), 141-148.
- Collaborators, G. B. D. O., Afshin, A., Forouzanfar, M. H., Reitsma, M. B., Sur, P., Estep, K., Lee, A., Marczak, L., Mokdad, A. H., Moradi-Lakeh, M., Naghavi, M., Salama, J. S., Vos, T., Abate, K. H., Abbafati, C., Ahmed, M. B., Al-Aly, Z., Alkerwi, A., Al-Raddadi, R., Amare, A. T., Amberbir, A., Amegah, A. K., Amini, E., Amrock, S. M., Anjana, R. M., Arnlov, J., Asayesh, H., Banerjee, A., Barac, A., Baye, E., Bennett, D. A., Beyene, A. S., Biadgilign, S., Biryukov, S., Bjertness, E., Boneya, D. J., Campos-Nonato, I., Carrero, J. J., Cecilio, P., Cercy, K., Ciobanu, L. G., Cornaby, L., Damtew, S. A., Dandona, L., Dandona, R., Dharmaratne, S. D., Duncan, B. B., Eshrati, B., Esteghamati, A., Feigin, V. L., Fernandes, J. C., Furst, T., Gebrehiwot, T. T., Gold, A., Gona, P. N., Goto, A., Habtewold, T. D., Hadush, K. T., Hafezi-Nejad, N., Hay, S. I., Horino, M., Islami, F., Kamal, R., Kasaeian, A., Katikireddi, S. V., Kengne, A. P., Kesavachandran, C. N., Khader, Y. S., Khang, Y. H., Khubchandani, J., Kim, D., Kim, Y. J., Kinfu, Y., Kosen, S., Ku, T., Defo, B. K., Kumar, G. A., Larson, H. J., Leinsalu,

- M., Liang, X., Lim, S. S., Liu, P., Lopez, A. D., Lozano, R., Majeed, A., Malekzadeh, R., Malta, D. C., Mazidi, M., McAlinden, C., McGarvey, S. T., Mengistu, D. T., Mensah, G. A., Mensink, G. B. M., Mezgebe, H. B., Mirrakhimov, E. M., Mueller, U. O., Noubiap, J. J., Obermeyer, C. M., Ogbo, F. A., Owolabi, M. O., Patton, G. C., Pourmalek, F., Qorbani, M., Rafay, A., Rai, R. K., Ranabhat, C. L., Reinig, N., Safiri, S., Salomon, J. A., Sanabria, J. R., Santos, I. S., Sartorius, B., Sawhney, M., Schmidhuber, J., Schutte, A. E., Schmidt, M. I., Sepanlou, S. G., Shamsizadeh, M., Sheikhabaie, S., Shin, M. J., Shiri, R., Shiue, I., Roba, H. S., Silva, D. A. S., Silverberg, J. I., Singh, J. A., Stranges, S., Swaminathan, S., Tabares-Seisdedos, R., Tadese, F., Tedla, B. A., Tegegne, B. S., Terkawi, A. S., Thakur, J. S., Tonelli, M., Topor-Madry, R., Tyrovolas, S., Ukwaja, K. N., Uthman, O. A., Vaezghasemi, M., Vasankari, T., Vlassov, V. V., Vollset, S. E., Weiderpass, E., Werdecker, A., Wesana, J., Westerman, R., Yano, Y., Yonemoto, N., Yonga, G., Zaidi, Z., Zenebe, Z. M., Zipkin, B., & Murray, C. J. L. (2017). Health Effects of Overweight and Obesity in 195 Countries over 25 Years. *N Engl J Med*, *377*(1), 13-27. doi:10.1056/NEJMoa1614362
- Collet, J. P. (2000). [Limitations of clinical trials]. *Rev Prat*, *50*(8), 833-837.
- Cox, J., & Mann, M. (2009). Computational principles of determining and improving mass precision and accuracy for proteome measurements in an Orbitrap. *J Am Soc Mass Spectrom*, *20*(8), 1477-1485. doi:10.1016/j.jasms.2009.05.007
- Crotty, S. (2014). T follicular helper cell differentiation, function, and roles in disease. *Immunity*, *41*(4), 529-542. doi:10.1016/j.immuni.2014.10.004
- Crotty, S., Johnston, R. J., & Schoenberger, S. P. (2010). Effectors and memories: Bcl-6 and Blimp-1 in T and B lymphocyte differentiation. *Nat Immunol*, *11*(2), 114-120. doi:10.1038/ni.1837
- Daley, S. R., Teh, C., Hu, D. Y., Strasser, A., & Gray, D. H. D. (2017). Cell death and thymic tolerance. *Immunol Rev*, *277*(1), 9-20. doi:10.1111/imr.12532
- Daniel, C., Weigmann, B., Bronson, R., & von Boehmer, H. (2011). Prevention of type 1 diabetes in mice by tolerogenic vaccination with a strong agonist insulin mimotope. *J Exp Med*, *208*(7), 1501-1510. doi:10.1084/jem.20110574
- Daniel, C., Wennhold, K., Kim, H. J., & von Boehmer, H. (2010). Enhancement of antigen-specific Treg vaccination in vivo. *Proc Natl Acad Sci U S A*, *107*(37), 16246-16251. doi:10.1073/pnas.1007422107
- De Meyts, P. (2016). *The Insulin Receptor and Its Signal Transduction Network* (L. De Groot, G. Chrousos, & K. Dungan Eds.): Endotext [Internet].
- De Meyts, P., & Whittaker, J. (2002). Structural biology of insulin and IGF1 receptors: implications for drug design. *Nat Rev Drug Discov*, *1*(10), 769-783. doi:10.1038/nrd917
- Deberardinis, R. J., Lum, J. J., & Thompson, C. B. (2006). Phosphatidylinositol 3-kinase-dependent modulation of carnitine palmitoyltransferase 1A expression regulates lipid metabolism during hematopoietic cell growth. *J Biol Chem*, *281*(49), 37372-37380. doi:10.1074/jbc.M608372200
- Deenick, E. K., Chan, A., Ma, C. S., Gatto, D., Schwartzberg, P. L., Brink, R., & Tangye, S. G. (2010). Follicular helper T cell differentiation requires continuous antigen presentation that is independent of unique B cell signaling. *Immunity*, *33*(2), 241-253. doi:10.1016/j.immuni.2010.07.015
- Deenick, E. K., & Ma, C. S. (2011). The regulation and role of T follicular helper cells in immunity. *Immunology*, *134*(4), 361-367. doi:10.1111/j.1365-2567.2011.03487.x
- Deiuliis, J., Shah, Z., Shah, N., Needleman, B., Mikami, D., Narula, V., Perry, K., Hazey, J., Kampfrath, T., Kollengode, M., Sun, Q., Satoskar, A. R., Lumeng, C., Moffatt-Bruce, S., & Rajagopalan, S. (2011). Visceral adipose inflammation in obesity is associated with critical alterations in tregulatory cell numbers. *PLoS One*, *6*(1), e16376. doi:10.1371/journal.pone.0016376
- Deiuliis, J. A. (2016). MicroRNAs as regulators of metabolic disease: pathophysiologic significance and emerging role as biomarkers and therapeutics. *Int J Obes (Lond)*, *40*(1), 88-101. doi:10.1038/ijo.2015.170

- Delgoffe, G. M., Kole, T. P., Zheng, Y., Zarek, P. E., Matthews, K. L., Xiao, B., Worley, P. F., Kozma, S. C., & Powell, J. D. (2009). The mTOR kinase differentially regulates effector and regulatory T cell lineage commitment. *Immunity*, *30*(6), 832-844. doi:10.1016/j.immuni.2009.04.014
- Delgoffe, G. M., Pollizzi, K. N., Waickman, A. T., Heikamp, E., Meyers, D. J., Horton, M. R., Xiao, B., Worley, P. F., & Powell, J. D. (2011). The kinase mTOR regulates the differentiation of helper T cells through the selective activation of signaling by mTORC1 and mTORC2. *Nat Immunol*, *12*(4), 295-303. doi:10.1038/ni.2005
- Deng, T., Lyon, C. J., Minze, L. J., Lin, J., Zou, J., Liu, J. Z., Ren, Y., Yin, Z., Hamilton, D. J., Reardon, P. R., Sherman, V., Wang, H. Y., Phillips, K. J., Webb, P., Wong, S. T., Wang, R. F., & Hsueh, W. A. (2013). Class II major histocompatibility complex plays an essential role in obesity-induced adipose inflammation. *Cell Metab*, *17*(3), 411-422. doi:10.1016/j.cmet.2013.02.009
- Ding, Y., Shen, S., Lino, A. C., Curotto de Lafaille, M. A., & Lafaille, J. J. (2008). Beta-catenin stabilization extends regulatory T cell survival and induces anergy in nonregulatory T cells. *Nat Med*, *14*(2), 162-169. doi:10.1038/nm1707
- Dominguez-Villar, M., & Hafler, D. A. (2018). Regulatory T cells in autoimmune disease. *Nat Immunol*, *19*(7), 665-673. doi:10.1038/s41590-018-0120-4
- Du, Y., & Wei, T. (2014). Inputs and outputs of insulin receptor. *Protein Cell*, *5*(3), 203-213. doi:10.1007/s13238-014-0030-7
- DuPage, M., & Bluestone, J. A. (2016). Harnessing the plasticity of CD4(+) T cells to treat immune-mediated disease. *Nat Rev Immunol*, *16*(3), 149-163. doi:10.1038/nri.2015.18
- Ehrlich, P. (1906). *Collected studies on immunity*. New York: J. Wiley & sons.
- Eller, K., Kirsch, A., Wolf, A. M., Sopper, S., Tagwerker, A., Stanzl, U., Wolf, D., Patsch, W., Rosenkranz, A. R., & Eller, P. (2011). Potential role of regulatory T cells in reversing obesity-linked insulin resistance and diabetic nephropathy. *Diabetes*, *60*(11), 2954-2962. doi:10.2337/db11-0358
- Engin, A., Engin, A. B., Becker, K., Engin, E. D., Murakami, Y., Unluturk, U., Oxenkrug, G., Cardinali, D. P., Kokturk, O., Haznedaroglu, I. C., & Kesikli, S. (2015). *Tryptophan Metabolism: Implications for Biological Processes, Health and Disease* (A. Engin & A. B. Engin Eds. Vol. 1): Humana Press.
- Esser, N., L'Homme, L., De Roover, A., Kohnen, L., Scheen, A. J., Moutschen, M., Piette, J., Legrand-Poels, S., & Paquot, N. (2013). Obesity phenotype is related to NLRP3 inflammasome activity and immunological profile of visceral adipose tissue. *Diabetologia*, *56*(11), 2487-2497. doi:10.1007/s00125-013-3023-9
- Estrany, M. E., Proenza, A. M., Gianotti, M., & Llado, I. (2013). High-fat diet feeding induces sex-dependent changes in inflammatory and insulin sensitivity profiles of rat adipose tissue. *Cell Biochem Funct*, *31*(6), 504-510. doi:10.1002/cbf.2927
- Eto, D., Lao, C., DiToro, D., Barnett, B., Escobar, T. C., Kageyama, R., Yusuf, I., & Crotty, S. (2011). IL-21 and IL-6 are critical for different aspects of B cell immunity and redundantly induce optimal follicular helper CD4 T cell (T<sub>fh</sub>) differentiation. *PLoS One*, *6*(3), e17739. doi:10.1371/journal.pone.0017739
- Fabbrini, E., Cella, M., McCartney, S. A., Fuchs, A., Abumrad, N. A., Pietka, T. A., Chen, Z., Finck, B. N., Han, D. H., Magkos, F., Conte, C., Bradley, D., Fraterrigo, G., Eagon, J. C., Patterson, B. W., Colonna, M., & Klein, S. (2013). Association between specific adipose tissue CD4+ T-cell populations and insulin resistance in obese individuals. *Gastroenterology*, *145*(2), 366-374 e361-363. doi:10.1053/j.gastro.2013.04.010
- Fabian, M. R., & Sonenberg, N. (2012). The mechanics of miRNA-mediated gene silencing: a look under the hood of miRISC. *Nat Struct Mol Biol*, *19*(6), 586-593. doi:10.1038/nsmb.2296
- Fazilleau, N., Mark, L., McHeyzer-Williams, L. J., & McHeyzer-Williams, M. G. (2009). Follicular helper T cells: lineage and location. *Immunity*, *30*(3), 324-335. doi:10.1016/j.immuni.2009.03.003

- Feuerer, M., Herrero, L., Cipolletta, D., Naaz, A., Wong, J., Nayer, A., Lee, J., Goldfine, A. B., Benoist, C., Shoelson, S., & Mathis, D. (2009). Lean, but not obese, fat is enriched for a unique population of regulatory T cells that affect metabolic parameters. *Nat Med*, *15*(8), 930-939. doi:10.1038/nm.2002
- Fischer, H. J., Sie, C., Schumann, E., Witte, A. K., Dressel, R., van den Brandt, J., & Reichardt, H. M. (2017). The Insulin Receptor Plays a Critical Role in T Cell Function and Adaptive Immunity. *J Immunol*, *198*(5), 1910-1920. doi:10.4049/jimmunol.1601011
- Floess, S., Freyer, J., Siewert, C., Baron, U., Olek, S., Polansky, J., Schlawe, K., Chang, H. D., Bopp, T., Schmitt, E., Klein-Hessling, S., Serfling, E., Hamann, A., & Huehn, J. (2007). Epigenetic control of the foxp3 locus in regulatory T cells. *PLoS Biol*, *5*(2), e38. doi:10.1371/journal.pbio.0050038
- Fontenot, J. D., Gavin, M. A., & Rudensky, A. Y. (2003). Foxp3 programs the development and function of CD4+CD25+ regulatory T cells. *Nat Immunol*, *4*(4), 330-336. doi:10.1038/ni904
- Fontenot, J. D., Rasmussen, J. P., Williams, L. M., Dooley, J. L., Farr, A. G., & Rudensky, A. Y. (2005). Regulatory T cell lineage specification by the forkhead transcription factor foxp3. *Immunity*, *22*(3), 329-341. doi:10.1016/j.immuni.2005.01.016
- Frauwirth, K. A., Riley, J. L., Harris, M. H., Parry, R. V., Rathmell, J. C., Plas, D. R., Elstrom, R. L., June, C. H., & Thompson, C. B. (2002). The CD28 signaling pathway regulates glucose metabolism. *Immunity*, *16*(6), 769-777.
- Frayling, T. M., Timpson, N. J., Weedon, M. N., Zeggini, E., Freathy, R. M., Lindgren, C. M., Perry, J. R., Elliott, K. S., Lango, H., Rayner, N. W., Shields, B., Harries, L. W., Barrett, J. C., Ellard, S., Groves, C. J., Knight, B., Patch, A. M., Ness, A. R., Ebrahim, S., Lawlor, D. A., Ring, S. M., Ben-Shlomo, Y., Jarvelin, M. R., Sovio, U., Bennett, A. J., Melzer, D., Ferrucci, L., Loos, R. J., Barroso, I., Wareham, N. J., Karpe, F., Owen, K. R., Cardon, L. R., Walker, M., Hitman, G. A., Palmer, C. N., Doney, A. S., Morris, A. D., Smith, G. D., Hattersley, A. T., & McCarthy, M. I. (2007). A common variant in the FTO gene is associated with body mass index and predisposes to childhood and adult obesity. *Science*, *316*(5826), 889-894. doi:10.1126/science.1141634
- Freychet, P., Laudat, M. H., Laudat, P., Rosselin, G., Kahn, C. R., Gorden, P., & Roth, J. (1972). Impairment of insulin binding to the fat cell plasma membrane in the obese hyperglycemic mouse. *FEBS Lett*, *25*(2), 339-342.
- Gabriel, C. H., Gross, F., Karl, M., Stephanowitz, H., Hennig, A. F., Weber, M., Gryzik, S., Bachmann, I., Hecklau, K., Wienands, J., Schuchhardt, J., Herzel, H., Radbruch, A., Krause, E., & Baumgrass, R. (2016). Identification of Novel Nuclear Factor of Activated T Cell (NFAT)-associated Proteins in T Cells. *J Biol Chem*, *291*(46), 24172-24187. doi:10.1074/jbc.M116.739326
- Gallagher, E. J., & LeRoith, D. (2010). The proliferating role of insulin and insulin-like growth factors in cancer. *Trends Endocrinol Metab*, *21*(10), 610-618. doi:10.1016/j.tem.2010.06.007
- Garcia-Carrizo, F., Priego, T., Szostaczk, N., Palou, A., & Pico, C. (2017). Sexual Dimorphism in the Age-Induced Insulin Resistance, Liver Steatosis, and Adipose Tissue Function in Rats. *Front Physiol*, *8*, 445. doi:10.3389/fphys.2017.00445
- Garcon, F., Patton, D. T., Emery, J. L., Hirsch, E., Rottapel, R., Sasaki, T., & Okkenhaug, K. (2008). CD28 provides T-cell costimulation and enhances PI3K activity at the immune synapse independently of its capacity to interact with the p85/p110 heterodimer. *Blood*, *111*(3), 1464-1471. doi:10.1182/blood-2007-08-108050
- Garris, D. R., & Garris, B. L. (2004). Cytochemical analysis of pancreatic islet hypercytolipidemia following diabetes (db/db) and obese (ob/ob) mutation expression: influence of genomic background. *Pathobiology*, *71*(5), 231-240. doi:10.1159/000080056
- Gavin, M. A., Rasmussen, J. P., Fontenot, J. D., Vasta, V., Manganiello, V. C., Beavo, J. A., & Rudensky, A. Y. (2007). Foxp3-dependent programme of regulatory T-cell differentiation. *Nature*, *445*(7129), 771-775. doi:10.1038/nature05543

- Giralt, M., & Villarroya, F. (2013). White, brown, beige/brite: different adipose cells for different functions? *Endocrinology*, *154*(9), 2992-3000. doi:10.1210/en.2013-1403
- Goenka, R., Barnett, L. G., Silver, J. S., O'Neill, P. J., Hunter, C. A., Cancro, M. P., & Laufer, T. M. (2011). Cutting edge: dendritic cell-restricted antigen presentation initiates the follicular helper T cell program but cannot complete ultimate effector differentiation. *J Immunol*, *187*(3), 1091-1095. doi:10.4049/jimmunol.1100853
- Gondek, D. C., Lu, L. F., Quezada, S. A., Sakaguchi, S., & Noelle, R. J. (2005). Cutting edge: contact-mediated suppression by CD4+CD25+ regulatory cells involves a granzyme B-dependent, perforin-independent mechanism. *J Immunol*, *174*(4), 1783-1786.
- Gottschalk, R. A., Corse, E., & Allison, J. P. (2010). TCR ligand density and affinity determine peripheral induction of Foxp3 in vivo. *J Exp Med*, *207*(8), 1701-1711. doi:10.1084/jem.20091999
- Gottschalk, R. A., Hathorn, M. M., Beuneu, H., Corse, E., Dustin, M. L., Altan-Bonnet, G., & Allison, J. P. (2012). Distinct influences of peptide-MHC quality and quantity on in vivo T-cell responses. *Proc Natl Acad Sci U S A*, *109*(3), 881-886. doi:10.1073/pnas.1119763109
- Grant, R. W., & Dixit, V. D. (2015). Adipose tissue as an immunological organ. *Obesity (Silver Spring)*, *23*(3), 512-518. doi:10.1002/oby.21003
- Green, E. A., Gorelik, L., McGregor, C. M., Tran, E. H., & Flavell, R. A. (2003). CD4+CD25+ T regulatory cells control anti-islet CD8+ T cells through TGF-beta-TGF-beta receptor interactions in type 1 diabetes. *Proc Natl Acad Sci U S A*, *100*(19), 10878-10883. doi:10.1073/pnas.1834400100
- Grishok, A., Pasquinelli, A. E., Conte, D., Li, N., Parrish, S., Ha, I., Baillie, D. L., Fire, A., Ruvkun, G., & Mello, C. C. (2001). Genes and mechanisms related to RNA interference regulate expression of the small temporal RNAs that control *C. elegans* developmental timing. *Cell*, *106*(1), 23-34.
- Hale, J. S., Youngblood, B., Latner, D. R., Mohammed, A. U., Ye, L., Akondy, R. S., Wu, T., Iyer, S. S., & Ahmed, R. (2013). Distinct memory CD4+ T cells with commitment to T follicular helper- and T helper 1-cell lineages are generated after acute viral infection. *Immunity*, *38*(4), 805-817. doi:10.1016/j.immuni.2013.02.020
- Han, J. M., Patterson, S. J., Speck, M., Ehses, J. A., & Levings, M. K. (2014). Insulin inhibits IL-10-mediated regulatory T cell function: implications for obesity. *J Immunol*, *192*(2), 623-629. doi:10.4049/jimmunol.1302181
- Han, J. M., Wu, D., Denroche, H. C., Yao, Y., Verchere, C. B., & Levings, M. K. (2015). IL-33 Reverses an Obesity-Induced Deficit in Visceral Adipose Tissue ST2+ T Regulatory Cells and Ameliorates Adipose Tissue Inflammation and Insulin Resistance. *J Immunol*, *194*(10), 4777-4783. doi:10.4049/jimmunol.1500020
- Harada, Y., Harada, Y., Elly, C., Ying, G., Paik, J. H., DePinho, R. A., & Liu, Y. C. (2010). Transcription factors Foxo3a and Foxo1 couple the E3 ligase Cbl-b to the induction of Foxp3 expression in induced regulatory T cells. *J Exp Med*, *207*(7), 1381-1391. doi:10.1084/jem.20100004
- Hardie, D. G., Scott, J. W., Pan, D. A., & Hudson, E. R. (2003). Management of cellular energy by the AMP-activated protein kinase system. *FEBS Lett*, *546*(1), 113-120.
- Hardtke, S., Ohl, L., & Forster, R. (2005). Balanced expression of CXCR5 and CCR7 on follicular T helper cells determines their transient positioning to lymph node follicles and is essential for efficient B-cell help. *Blood*, *106*(6), 1924-1931. doi:10.1182/blood-2004-11-4494
- Harmon, D. B., Srikakulapu, P., Kaplan, J. L., Oldham, S. N., McSkimming, C., Garmey, J. C., Perry, H. M., Kirby, J. L., Prohaska, T. A., Gonen, A., Hallowell, P., Schirmer, B., Tsimikas, S., Taylor, A. M., Witztum, J. L., & McNamara, C. A. (2016). Protective Role for B-1b B Cells and IgM in Obesity-Associated Inflammation, Glucose Intolerance, and Insulin Resistance. *Arterioscler Thromb Vasc Biol*, *36*(4), 682-691. doi:10.1161/ATVBAHA.116.307166

- Hatting, M., Tavares, C. D. J., Sharabi, K., Rines, A. K., & Puigserver, P. (2018). Insulin regulation of gluconeogenesis. *Ann N Y Acad Sci*, *1411*(1), 21-35. doi:10.1111/nyas.13435
- Havenar-Daughton, C., Lindqvist, M., Heit, A., Wu, J. E., Reiss, S. M., Kendric, K., Belanger, S., Kasturi, S. P., Landais, E., Akondy, R. S., McGuire, H. M., Bothwell, M., Vagefi, P. A., Scully, E., Investigators, I. P. C. P., Tomaras, G. D., Davis, M. M., Poignard, P., Ahmed, R., Walker, B. D., Pulendran, B., McElrath, M. J., Kaufmann, D. E., & Crotty, S. (2016). CXCL13 is a plasma biomarker of germinal center activity. *Proc Natl Acad Sci U S A*, *113*(10), 2702-2707. doi:10.1073/pnas.1520112113
- Haxhinasto, S., Mathis, D., & Benoist, C. (2008). The AKT-mTOR axis regulates de novo differentiation of CD4<sup>+</sup>Foxp3<sup>+</sup> cells. *J Exp Med*, *205*(3), 565-574. doi:10.1084/jem.20071477
- Haynes, N. M., Allen, C. D., Lesley, R., Ansel, K. M., Killeen, N., & Cyster, J. G. (2007). Role of CXCR5 and CCR7 in follicular Th cell positioning and appearance of a programmed cell death gene-1high germinal center-associated subpopulation. *J Immunol*, *179*(8), 5099-5108.
- He, J., Tsai, L. M., Leong, Y. A., Hu, X., Ma, C. S., Chevalier, N., Sun, X., Vandenberg, K., Rockman, S., Ding, Y., Zhu, L., Wei, W., Wang, C., Karnowski, A., Belz, G. T., Ghali, J. R., Cook, M. C., Riminton, D. S., Veillette, A., Schwartzberg, P. L., Mackay, F., Brink, R., Tangye, S. G., Vinuesa, C. G., Mackay, C. R., Li, Z., & Yu, D. (2013). Circulating precursor CCR7(lo)PD-1(hi) CXCR5(+) CD4(+) T cells indicate Tfh cell activity and promote antibody responses upon antigen reexposure. *Immunity*, *39*(4), 770-781. doi:10.1016/j.immuni.2013.09.007
- Heit, A., Schmitz, F., Gerdt, S., Flach, B., Moore, M. S., Perkins, J. A., Robins, H. S., Aderem, A., Spearman, P., Tomaras, G. D., De Rosa, S. C., & McElrath, M. J. (2017). Vaccination establishes clonal relatives of germinal center T cells in the blood of humans. *J Exp Med*, *214*(7), 2139-2152. doi:10.1084/jem.20161794
- Helderman, J. H., & Strom, T. B. (1978). Specific insulin binding site on T and B lymphocytes as a marker of cell activation. *Nature*, *274*(5666), 62-63.
- Heneghan, H. M., Miller, N., McAnena, O. J., O'Brien, T., & Kerin, M. J. (2011). Differential miRNA expression in omental adipose tissue and in the circulation of obese patients identifies novel metabolic biomarkers. *J Clin Endocrinol Metab*, *96*(5), E846-850. doi:10.1210/jc.2010-2701
- Himms-Hagen, J., & Desautels, M. (1978). A mitochondrial defect in brown adipose tissue of the obese (ob/ob) mouse: reduced binding of purine nucleotides and a failure to respond to cold by an increase in binding. *Biochem Biophys Res Commun*, *83*(2), 628-634.
- Hoeg, L. D., Sjoberg, K. A., Jeppesen, J., Jensen, T. E., Frosig, C., Birk, J. B., Bisiani, B., Hiscock, N., Pilegaard, H., Wojtaszewski, J. F., Richter, E. A., & Kiens, B. (2011). Lipid-induced insulin resistance affects women less than men and is not accompanied by inflammation or impaired proximal insulin signaling. *Diabetes*, *60*(1), 64-73. doi:10.2337/db10-0698
- Hong, J., Stubbins, R. E., Smith, R. R., Harvey, A. E., & Nunez, N. P. (2009). Differential susceptibility to obesity between male, female and ovariectomized female mice. *Nutr J*, *8*, 11. doi:10.1186/1475-2891-8-11
- Hori, S., Nomura, T., & Sakaguchi, S. (2003). Control of regulatory T cell development by the transcription factor Foxp3. *Science*, *299*(5609), 1057-1061. doi:10.1126/science.1079490
- Hsu, W. C., Chen, M. Y., Hsu, S. C., Huang, L. R., Kao, C. Y., Cheng, W. H., Pan, C. H., Wu, M. S., Yu, G. Y., Hung, M. S., Leu, C. M., Tan, T. H., & Su, Y. W. (2018). DUSP6 mediates T cell receptor-engaged glycolysis and restrains TFH cell differentiation. *Proc Natl Acad Sci U S A*, *115*(34), E8027-E8036. doi:10.1073/pnas.1800076115
- Hu, J., Havenar-Daughton, C., & Crotty, S. (2013). Modulation of SAP dependent T:B cell interactions as a strategy to improve vaccination. *Curr Opin Virol*, *3*(3), 363-370. doi:10.1016/j.coviro.2013.05.015

- Huang, S. M., Hancock, M. K., Pitman, J. L., Orth, A. P., & Gekakis, N. (2009). Negative regulators of insulin signaling revealed in a genome-wide functional screen. *PLoS One*, *4*(9), e6871. doi:10.1371/journal.pone.0006871
- Hubbard, S. R. (1997). Crystal structure of the activated insulin receptor tyrosine kinase in complex with peptide substrate and ATP analog. *EMBO J*, *16*(18), 5572-5581. doi:10.1093/emboj/16.18.5572
- Hubbard, S. R., Wei, L., Ellis, L., & Hendrickson, W. A. (1994). Crystal structure of the tyrosine kinase domain of the human insulin receptor. *Nature*, *372*(6508), 746-754. doi:10.1038/372746a0
- Huntzinger, E., & Izaurralde, E. (2011). Gene silencing by microRNAs: contributions of translational repression and mRNA decay. *Nat Rev Genet*, *12*(2), 99-110. doi:10.1038/nrg2936
- IDF. (2006). The International Diabetes Federation (IDF) consensus worldwide definition of the metabolic syndrom [Press release]. Retrieved from <https://www.idf.org/component/attachments/attachments.html?id=705&task=download>
- Ilikuni, N., Lam, Q. L., Lu, L., Matarese, G., & La Cava, A. (2008). Leptin and Inflammation. *Curr Immunol Rev*, *4*(2), 70-79. doi:10.2174/157339508784325046
- Ilan, Y., Maron, R., Tukpah, A. M., Maioli, T. U., Murugaiyan, G., Yang, K., Wu, H. Y., & Weiner, H. L. (2010). Induction of regulatory T cells decreases adipose inflammation and alleviates insulin resistance in ob/ob mice. *Proc Natl Acad Sci U S A*, *107*(21), 9765-9770. doi:10.1073/pnas.0908771107
- Ingalls, A. M., Dickie, M. M., & Snell, G. D. (1996). Obese, a new mutation in the house mouse. *Obes Res*, *4*(1), 101.
- Ioan-Facsinay, A., Kwekkeboom, J. C., Westhoff, S., Giera, M., Rombouts, Y., van Harmelen, V., Huizinga, T. W., Deelder, A., Kloppenburg, M., & Toes, R. E. (2013). Adipocyte-derived lipids modulate CD4+ T-cell function. *Eur J Immunol*, *43*(6), 1578-1587. doi:10.1002/eji.201243096
- Itoh, M., Takahashi, T., Sakaguchi, N., Kuniyasu, Y., Shimizu, J., Otsuka, F., & Sakaguchi, S. (1999). Thymus and autoimmunity: production of CD25+CD4+ naturally anergic and suppressive T cells as a key function of the thymus in maintaining immunologic self-tolerance. *J Immunol*, *162*(9), 5317-5326.
- Jeker, L. T., & Bluestone, J. A. (2013). MicroRNA regulation of T-cell differentiation and function. *Immunol Rev*, *253*(1), 65-81. doi:10.1111/imr.12061
- Jiang, S. Z., Lu, W., Zong, X. F., Ruan, H. Y., & Liu, Y. (2016). Obesity and hypertension. *Exp Ther Med*, *12*(4), 2395-2399. doi:10.3892/etm.2016.3667
- Jiao, P., Ma, J., Feng, B., Zhang, H., Diehl, J. A., Chin, Y. E., Yan, W., & Xu, H. (2011). FFA-induced adipocyte inflammation and insulin resistance: involvement of ER stress and IKKbeta pathways. *Obesity (Silver Spring)*, *19*(3), 483-491. doi:10.1038/oby.2010.200
- Johnston, R. J., Poholek, A. C., DiToro, D., Yusuf, I., Eto, D., Barnett, B., Dent, A. L., Craft, J., & Crotty, S. (2009). Bcl6 and Blimp-1 are reciprocal and antagonistic regulators of T follicular helper cell differentiation. *Science*, *325*(5943), 1006-1010. doi:10.1126/science.1175870
- Jordan, M. S., Boesteanu, A., Reed, A. J., Petrone, A. L., Hohenbeck, A. E., Lerman, M. A., Naji, A., & Caton, A. J. (2001). Thymic selection of CD4+CD25+ regulatory T cells induced by an agonist self-peptide. *Nat Immunol*, *2*(4), 301-306. doi:10.1038/86302
- Kalin, S., Becker, M., **Ott, V. B.**, Serr, I., Hosp, F., Mollah, M. M. H., Keipert, S., Lamp, D., Rohner-Jeanraud, F., Flynn, V. K., Scherm, M. G., Nascimento, L. F. R., Gerlach, K., Popp, V., Dietzen, S., Bopp, T., Krishnamurthy, P., Kaplan, M. H., Serrano, M., Woods, S. C., Tripal, P., Palmisano, R., Jastroch, M., Bluher, M., Wolfrum, C., Weigmann, B., Ziegler, A. G., Mann, M., Tschop, M. H., & Daniel, C. (2017). A Stat6/Pten Axis Links Regulatory T Cells with Adipose Tissue Function. *Cell Metab*, *26*(3), 475-492 e477. doi:10.1016/j.cmet.2017.08.008
- Kang, S. G., Liu, W. H., Lu, P., Jin, H. Y., Lim, H. W., Shepherd, J., Fremgen, D., Verdin, E., Oldstone, M. B., Qi, H., Teijaro, J. R., & Xiao, C. (2013). MicroRNAs of the miR-17

- approximately 92 family are critical regulators of T(FH) differentiation. *Nat Immunol*, 14(8), 849-857. doi:10.1038/ni.2648
- Kanneganti, T. D., & Dixit, V. D. (2012). Immunological complications of obesity. *Nat Immunol*, 13(8), 707-712. doi:10.1038/ni.2343
- Kappler, J. W., Roehm, N., & Marrack, P. (1987). T cell tolerance by clonal elimination in the thymus. *Cell*, 49(2), 273-280.
- Kerdiles, Y. M., Stone, E. L., Beisner, D. R., McGargill, M. A., Ch'en, I. L., Stockmann, C., Katayama, C. D., & Hedrick, S. M. (2010). Foxo transcription factors control regulatory T cell development and function. *Immunity*, 33(6), 890-904. doi:10.1016/j.immuni.2010.12.002
- Khattri, R., Cox, T., Yasayko, S. A., & Ramsdell, F. (2003). An essential role for Scurfin in CD4+CD25+ T regulatory cells. *Nat Immunol*, 4(4), 337-342. doi:10.1038/ni909
- Kim, C. H., Rott, L. S., Clark-Lewis, I., Campbell, D. J., Wu, L., & Butcher, E. C. (2001). Subspecialization of CXCR5+ T cells: B helper activity is focused in a germinal center-localized subset of CXCR5+ T cells. *J Exp Med*, 193(12), 1373-1381.
- Kim, S. M., Kwon, J. E., Park, J. S., Seo, H. B., Jung, K. A., Moon, Y. M., Lee, J., Kwok, S. K., Cho, M. L., & Park, S. H. (2017). Achaete-scute complex homologue 2 accelerates the development of Sjogren's syndrome-like disease in the NOD/ShiLtJ mouse. *Immunol Lett*, 190, 26-33. doi:10.1016/j.imlet.2017.07.010
- Kisielow, P., Bluthmann, H., Staerz, U. D., Steinmetz, M., & von Boehmer, H. (1988). Tolerance in T-cell-receptor transgenic mice involves deletion of nonmature CD4+8+ thymocytes. *Nature*, 333(6175), 742-746. doi:10.1038/333742a0
- Kitano, M., Moriyama, S., Ando, Y., Hikida, M., Mori, Y., Kurosaki, T., & Okada, T. (2011). Bcl6 protein expression shapes pre-germinal center B cell dynamics and follicular helper T cell heterogeneity. *Immunity*, 34(6), 961-972. doi:10.1016/j.immuni.2011.03.025
- Kitoh, A., Ono, M., Naoe, Y., Ohkura, N., Yamaguchi, T., Yaguchi, H., Kitabayashi, I., Tsukada, T., Nomura, T., Miyachi, Y., Taniuchi, I., & Sakaguchi, S. (2009). Indispensable role of the Runx1-Cbfbeta transcription complex for in vivo-suppressive function of FoxP3+ regulatory T cells. *Immunity*, 31(4), 609-620. doi:10.1016/j.immuni.2009.09.003
- Kleinert, M., Clemmensen, C., Hofmann, S. M., Moore, M. C., Renner, S., Woods, S. C., Huypens, P., Beckers, J., de Angelis, M. H., Schurmann, A., Bakhti, M., Klingenspor, M., Heiman, M., Cherrington, A. D., Ristow, M., Lickert, H., Wolf, E., Havel, P. J., Muller, T. D., & Tschop, M. H. (2018). Animal models of obesity and diabetes mellitus. *Nat Rev Endocrinol*. doi:10.1038/nrendo.2017.161
- Klop, B., Elte, J. W., & Cabezas, M. C. (2013). Dyslipidemia in obesity: mechanisms and potential targets. *Nutrients*, 5(4), 1218-1240. doi:10.3390/nu5041218
- Kloting, N., Berthold, S., Kovacs, P., Schon, M. R., Fasshauer, M., Ruschke, K., Stumvoll, M., & Bluher, M. (2009). MicroRNA expression in human omental and subcutaneous adipose tissue. *PLoS One*, 4(3), e4699. doi:10.1371/journal.pone.0004699
- Kolenbrander, A., Grewe, B., Nemazee, D., Uberla, K., & Temchura, V. (2018). Generation of T follicular helper cells in vitro: requirement for B-cell receptor cross-linking and cognate B- and T-cell interaction. *Immunology*, 153(2), 214-224. doi:10.1111/imm.12834
- Kolodin, D., van Panhuys, N., Li, C., Magnuson, A. M., Cipolletta, D., Miller, C. M., Wagers, A., Germain, R. N., Benoist, C., & Mathis, D. (2015). Antigen- and cytokine-driven accumulation of regulatory T cells in visceral adipose tissue of lean mice. *Cell Metab*, 21(4), 543-557. doi:10.1016/j.cmet.2015.03.005
- Konige, M., Wang, H., & Sztalryd, C. (2014). Role of adipose specific lipid droplet proteins in maintaining whole body energy homeostasis. *Biochim Biophys Acta*, 1842(3), 393-401. doi:10.1016/j.bbadis.2013.05.007
- Kretschmer, K., Apostolou, I., Hawiger, D., Khazaie, K., Nussenzweig, M. C., & von Boehmer, H. (2005). Inducing and expanding regulatory T cell populations by foreign antigen. *Nat Immunol*, 6(12), 1219-1227. doi:10.1038/ni1265

- Kroenke, M. A., Eto, D., Locci, M., Cho, M., Davidson, T., Haddad, E. K., & Crotty, S. (2012). Bcl6 and Maf cooperate to instruct human follicular helper CD4 T cell differentiation. *J Immunol*, *188*(8), 3734-3744. doi:10.4049/jimmunol.1103246
- Kumada, M., Kihara, S., Ouchi, N., Kobayashi, H., Okamoto, Y., Ohashi, K., Maeda, K., Nagaretani, H., Kishida, K., Maeda, N., Nagasawa, A., Funahashi, T., & Matsuzawa, Y. (2004). Adiponectin specifically increased tissue inhibitor of metalloproteinase-1 through interleukin-10 expression in human macrophages. *Circulation*, *109*(17), 2046-2049. doi:10.1161/01.CIR.0000127953.98131.ED
- Kyōto University. (1995). Kyoto Encyclopedia of Genes and Genomes (KEGG): map00195 (Bioinformatics resource for deciphering the genome). retrieved from <https://www.genome.jp/kegg/> (02-01-2019)
- Langenkamp, A., Nagata, K., Murphy, K., Wu, L., Lanzavecchia, A., & Sallusto, F. (2003). Kinetics and expression patterns of chemokine receptors in human CD4+ T lymphocytes primed by myeloid or plasmacytoid dendritic cells. *Eur J Immunol*, *33*(2), 474-482. doi:10.1002/immu.200310023
- Larsen, G. L., & Henson, P. M. (1983). Mediators of inflammation. *Annu Rev Immunol*, *1*, 335-359. doi:10.1146/annurev.iy.01.040183.002003
- Ledderose, C., Bao, Y., Lidicky, M., Zipperle, J., Li, L., Strasser, K., Shapiro, N. I., & Junger, W. G. (2014). Mitochondria are gate-keepers of T cell function by producing the ATP that drives purinergic signaling. *J Biol Chem*, *289*(37), 25936-25945. doi:10.1074/jbc.M114.575308
- Lee, M. J., Wu, Y., & Fried, S. K. (2013). Adipose tissue heterogeneity: implication of depot differences in adipose tissue for obesity complications. *Mol Aspects Med*, *34*(1), 1-11. doi:10.1016/j.mam.2012.10.001
- Lee, M. W., Odegaard, J. I., Mukundan, L., Qiu, Y., Molofsky, A. B., Nussbaum, J. C., Yun, K., Locksley, R. M., & Chawla, A. (2015). Activated type 2 innate lymphoid cells regulate beige fat biogenesis. *Cell*, *160*(1-2), 74-87. doi:10.1016/j.cell.2014.12.011
- Lee, P. P., Fitzpatrick, D. R., Beard, C., Jessup, H. K., Lehar, S., Makar, K. W., Perez-Melgosa, M., Sweetser, M. T., Schlissel, M. S., Nguyen, S., Cherry, S. R., Tsai, J. H., Tucker, S. M., Weaver, W. M., Kelso, A., Jaenisch, R., & Wilson, C. B. (2001). A critical role for Dnmt1 and DNA methylation in T cell development, function, and survival. *Immunity*, *15*(5), 763-774.
- Li, C., DiSpirito, J. R., Zemmour, D., Spallanzani, R. G., Kuswanto, W., Benoist, C., & Mathis, D. (2018). TCR Transgenic Mice Reveal Stepwise, Multi-site Acquisition of the Distinctive Fat-Treg Phenotype. *Cell*, *174*(2), 285-299 e212. doi:10.1016/j.cell.2018.05.004
- Li, M. O., & Rudensky, A. Y. (2016). T cell receptor signalling in the control of regulatory T cell differentiation and function. *Nat Rev Immunol*, *16*(4), 220-233. doi:10.1038/nri.2016.26
- Lidell, M. E., Betz, M. J., Dahlqvist Leinhard, O., Heglind, M., Elander, L., Slawik, M., Mussack, T., Nilsson, D., Romu, T., Nuutila, P., Virtanen, K. A., Beuschlein, F., Persson, A., Borga, M., & Enerback, S. (2013). Evidence for two types of brown adipose tissue in humans. *Nat Med*, *19*(5), 631-634. doi:10.1038/nm.3017
- Linterman, M. A., Beaton, L., Yu, D., Ramiscal, R. R., Srivastava, M., Hogan, J. J., Verma, N. K., Smyth, M. J., Rigby, R. J., & Vinuesa, C. G. (2010). IL-21 acts directly on B cells to regulate Bcl-6 expression and germinal center responses. *J Exp Med*, *207*(2), 353-363. doi:10.1084/jem.20091738
- Linterman, M. A., & Hill, D. L. (2016). Can follicular helper T cells be targeted to improve vaccine efficacy? *F1000Res*, *5*. doi:10.12688/f1000research.7388.1
- Liu, G., Ma, H., Qiu, L., Li, L., Cao, Y., Ma, J., & Zhao, Y. (2011). Phenotypic and functional switch of macrophages induced by regulatory CD4+CD25+ T cells in mice. *Immunol Cell Biol*, *89*(1), 130-142. doi:10.1038/icb.2010.70
- Liu, H., Yao, S., Dann, S. M., Qin, H., Elson, C. O., & Cong, Y. (2013). ERK differentially regulates Th17- and Treg-cell development and contributes to the pathogenesis of colitis. *Eur J Immunol*, *43*(7), 1716-1726. doi:10.1002/eji.201242889

- Liu, J., Divoux, A., Sun, J., Zhang, J., Clement, K., Glickman, J. N., Sukhova, G. K., Wolters, P. J., Du, J., Gorgun, C. Z., Doria, A., Libby, P., Blumberg, R. S., Kahn, B. B., Hotamisligil, G. S., & Shi, G. P. (2009). Genetic deficiency and pharmacological stabilization of mast cells reduce diet-induced obesity and diabetes in mice. *Nat Med*, *15*(8), 940-945. doi:10.1038/nm.1994
- Liu, W., Putnam, A. L., Xu-Yu, Z., Szot, G. L., Lee, M. R., Zhu, S., Gottlieb, P. A., Kapranov, P., Gingeras, T. R., Fazekas de St Groth, B., Clayberger, C., Soper, D. M., Ziegler, S. F., & Bluestone, J. A. (2006). CD127 expression inversely correlates with FoxP3 and suppressive function of human CD4+ T reg cells. *J Exp Med*, *203*(7), 1701-1711. doi:10.1084/jem.20060772
- Liu, X., Chen, X., Zhong, B., Wang, A., Wang, X., Chu, F., Nurieva, R. I., Yan, X., Chen, P., van der Flier, L. G., Nakatsukasa, H., Neelapu, S. S., Chen, W., Clevers, H., Tian, Q., Qi, H., Wei, L., & Dong, C. (2014). Transcription factor achaete-scute homologue 2 initiates follicular T-helper-cell development. *Nature*, *507*(7493), 513-518. doi:10.1038/nature12910
- Liu, X., Yan, X., Zhong, B., Nurieva, R. I., Wang, A., Wang, X., Martin-Orozco, N., Wang, Y., Chang, S. H., Esplugues, E., Flavell, R. A., Tian, Q., & Dong, C. (2012). Bcl6 expression specifies the T follicular helper cell program in vivo. *J Exp Med*, *209*(10), 1841-1852, S1841-1824. doi:10.1084/jem.20120219
- Locci, M., Havenar-Daughton, C., Landais, E., Wu, J., Kroenke, M. A., Arlehamn, C. L., Su, L. F., Cubas, R., Davis, M. M., Sette, A., Haddad, E. K., International, A. V. I. P. C. P. I., Poignard, P., & Crotty, S. (2013). Human circulating PD-1+CXCR3-CXCR5+ memory Tfh cells are highly functional and correlate with broadly neutralizing HIV antibody responses. *Immunity*, *39*(4), 758-769. doi:10.1016/j.immuni.2013.08.031
- Long, M., Park, S. G., Strickland, I., Hayden, M. S., & Ghosh, S. (2009). Nuclear factor-kappaB modulates regulatory T cell development by directly regulating expression of Foxp3 transcription factor. *Immunity*, *31*(6), 921-931. doi:10.1016/j.immuni.2009.09.022
- Lord, G. M., Matarese, G., Howard, J. K., Baker, R. J., Bloom, S. R., & Lechler, R. I. (1998). Leptin modulates the T-cell immune response and reverses starvation-induced immunosuppression. *Nature*, *394*(6696), 897-901. doi:10.1038/29795
- Loten, E. G., Rabinovitch, A., & Jeanrenaud, B. (1974). In vivo studies on lipogenesis in obese hyperglycaemic (ob-ob) mice: possible role of hyperinsulinaemia. *Diabetologia*, *10*(1), 45-52.
- Love, M. I., Huber, W., & Anders, S. (2014). Moderated estimation of fold change and dispersion for RNA-seq data with DESeq2. *Genome Biol*, *15*(12), 550. doi:10.1186/s13059-014-0550-8
- Lu, K. T., Kanno, Y., Cannons, J. L., Handon, R., Bible, P., Elkhouloun, A. G., Anderson, S. M., Wei, L., Sun, H., O'Shea, J. J., & Schwartzberg, P. L. (2011). Functional and epigenetic studies reveal multistep differentiation and plasticity of in vitro-generated and in vivo-derived follicular T helper cells. *Immunity*, *35*(4), 622-632. doi:10.1016/j.immuni.2011.07.015
- Lumeng, C. N., Bodzin, J. L., & Saltiel, A. R. (2007). Obesity induces a phenotypic switch in adipose tissue macrophage polarization. *J Clin Invest*, *117*(1), 175-184. doi:10.1172/JCI29881
- Luo, X., Zhang, Q., Liu, V., Xia, Z., Pothoven, K. L., & Lee, C. (2008). Cutting edge: TGF-beta-induced expression of Foxp3 in T cells is mediated through inactivation of ERK. *J Immunol*, *180*(5), 2757-2761.
- Luo, Y., Boyle, D. L., Hammaker, D., Edgar, M., Franzoso, G., & Firestein, G. S. (2011). Suppression of collagen-induced arthritis in growth arrest and DNA damage-inducible protein 45beta-deficient mice. *Arthritis Rheum*, *63*(10), 2949-2955. doi:10.1002/art.30497
- Ma, C. S., & Deenick, E. K. (2017). The circulating life of a memory T-follicular helper cell. *Clin Transl Immunology*, *6*(5), e141. doi:10.1038/cti.2017.17

- Macotela, Y., Boucher, J., Tran, T. T., & Kahn, C. R. (2009). Sex and depot differences in adipocyte insulin sensitivity and glucose metabolism. *Diabetes*, *58*(4), 803-812. doi:10.2337/db08-1054
- Mages, H. W., Hutloff, A., Heuck, C., Buchner, K., Himmelbauer, H., Oliveri, F., & Kroccek, R. A. (2000). Molecular cloning and characterization of murine ICOS and identification of B7h as ICOS ligand. *Eur J Immunol*, *30*(4), 1040-1047. doi:10.1002/(SICI)1521-4141(200004)30:4<1040::AID-IMMU1040>3.0.CO;2-6
- Magkos, F., Wang, X., & Mittendorfer, B. (2010). Metabolic actions of insulin in men and women. *Nutrition*, *26*(7-8), 686-693. doi:10.1016/j.nut.2009.10.013
- Mann, A., Thompson, A., Robbins, N., & Blomkalns, A. L. (2014). Localization, identification, and excision of murine adipose depots. *J Vis Exp*(94). doi:10.3791/52174
- Marko, A. J., Miller, R. A., Kelman, A., & Frauwirth, K. A. (2010). Induction of glucose metabolism in stimulated T lymphocytes is regulated by mitogen-activated protein kinase signaling. *PLoS One*, *5*(11), e15425. doi:10.1371/journal.pone.0015425
- Martyniak, K., & Masternak, M. M. (2017). Changes in adipose tissue cellular composition during obesity and aging as a cause of metabolic dysregulation. *Exp Gerontol*, *94*, 59-63. doi:10.1016/j.exger.2016.12.007
- Masharani, U., Goldfine, I. D., & Youngren, J. F. (2009). Influence of gender on the relationship between insulin sensitivity, adiposity, and plasma lipids in lean nondiabetic subjects. *Metabolism*, *58*(11), 1602-1608. doi:10.1016/j.metabol.2009.05.012
- Massague, J., Pilch, P. F., & Czech, M. P. (1980). Electrophoretic resolution of three major insulin receptor structures with unique subunit stoichiometries. *Proc Natl Acad Sci U S A*, *77*(12), 7137-7141.
- Matarese, G., Procaccini, C., De Rosa, V., Horvath, T. L., & La Cava, A. (2010). Regulatory T cells in obesity: the leptin connection. *Trends Mol Med*, *16*(6), 247-256. doi:10.1016/j.molmed.2010.04.002
- Mathis, D. (2013). Immunological goings-on in visceral adipose tissue. *Cell Metab*, *17*(6), 851-859. doi:10.1016/j.cmet.2013.05.008
- McGillicuddy, F. C., Chiquoine, E. H., Hinkle, C. C., Kim, R. J., Shah, R., Roche, H. M., Smyth, E. M., & Reilly, M. P. (2009). Interferon gamma attenuates insulin signaling, lipid storage, and differentiation in human adipocytes via activation of the JAK/STAT pathway. *J Biol Chem*, *284*(46), 31936-31944. doi:10.1074/jbc.M109.061655
- McLaughlin, T., Liu, L. F., Lamendola, C., Shen, L., Morton, J., Rivas, H., Winer, D., Tolentino, L., Choi, O., Zhang, H., Hui Yen Chng, M., & Engleman, E. (2014). T-cell profile in adipose tissue is associated with insulin resistance and systemic inflammation in humans. *Arterioscler Thromb Vasc Biol*, *34*(12), 2637-2643. doi:10.1161/ATVBAHA.114.304636
- Medrikova, D., Jilkova, Z. M., Bardova, K., Janovska, P., Rossmeisl, M., & Kopecky, J. (2012). Sex differences during the course of diet-induced obesity in mice: adipose tissue expandability and glycemic control. *Int J Obes (Lond)*, *36*(2), 262-272. doi:10.1038/ijo.2011.87
- Meissner, F., & Mann, M. (2014). Quantitative shotgun proteomics: considerations for a high-quality workflow in immunology. *Nat Immunol*, *15*(2), 112-117. doi:10.1038/ni.2781
- Merkenschlager, M., & von Boehmer, H. (2010). PI3 kinase signalling blocks Foxp3 expression by sequestering Foxo factors. *J Exp Med*, *207*(7), 1347-1350. doi:10.1084/jem.20101156
- Michalek, R. D., Gerriets, V. A., Jacobs, S. R., Macintyre, A. N., MacIver, N. J., Mason, E. F., Sullivan, S. A., Nichols, A. G., & Rathmell, J. C. (2011). Cutting edge: distinct glycolytic and lipid oxidative metabolic programs are essential for effector and regulatory CD4+ T cell subsets. *J Immunol*, *186*(6), 3299-3303. doi:10.4049/jimmunol.1003613
- Misra, N., Bayry, J., Lacroix-Desmazes, S., Kazatchkine, M. D., & Kaveri, S. V. (2004). Cutting edge: human CD4+CD25+ T cells restrain the maturation and antigen-presenting function of dendritic cells. *J Immunol*, *172*(8), 4676-4680.

- Monticelli, S. (2013). MicroRNAs in T helper cell differentiation and plasticity. *Semin Immunol*, 25(4), 291-298. doi:10.1016/j.smim.2013.10.015
- Morcavallo, A., Stefanello, M., Iozzo, R. V., Belfiore, A., & Morrione, A. (2014). Ligand-mediated endocytosis and trafficking of the insulin-like growth factor receptor I and insulin receptor modulate receptor function. *Front Endocrinol (Lausanne)*, 5, 220. doi:10.3389/fendo.2014.00220
- Morimoto, Y., Bian, Y., Gao, P., Yashiro-Ohtani, Y., Zhou, X. Y., Ono, S., Nakahara, H., Kogo, M., Hamaoka, T., & Fujiwara, H. (2005). Induction of surface CCR4 and its functionality in mouse Th2 cells is regulated differently during Th2 development. *J Leukoc Biol*, 78(3), 753-761. doi:10.1189/jlb.0305139
- Morita, R., Schmitt, N., Bentebibel, S. E., Ranganathan, R., Bourdery, L., Zurawski, G., Foucat, E., Dullaers, M., Oh, S., Sabzghabaei, N., Lavecchio, E. M., Punaro, M., Pascual, V., Banchereau, J., & Ueno, H. (2011). Human blood CXCR5(+)/CD4(+) T cells are counterparts of T follicular cells and contain specific subsets that differentially support antibody secretion. *Immunity*, 34(1), 108-121. doi:10.1016/j.immuni.2010.12.012
- Morris, D. L., Cho, K. W., Delproposto, J. L., Oatmen, K. E., Geletka, L. M., Martinez-Santibanez, G., Singer, K., & Lumeng, C. N. (2013). Adipose tissue macrophages function as antigen-presenting cells and regulate adipose tissue CD4+ T cells in mice. *Diabetes*, 62(8), 2762-2772. doi:10.2337/db12-1404
- Moticka, E. J. (2016). *Chapter 2 - Hallmarks of the Adaptive Immune Responses*: Elsevier.
- Murphy, K., & Weaver, C. (2016). *Janeway's Immunobiology* (Vol. 9th revised edition): Norton & Company.
- Neal, J. W., & Clipstone, N. A. (2001). Glycogen synthase kinase-3 inhibits the DNA binding activity of NFATc. *J Biol Chem*, 276(5), 3666-3673. doi:10.1074/jbc.M004888200
- Newsholme, E. A., & Dimitriadis, G. (2001). Integration of biochemical and physiologic effects of insulin on glucose metabolism. *Exp Clin Endocrinol Diabetes*, 109 Suppl 2, S122-134. doi:10.1055/s-2001-18575
- Nishikawa, S., Yasoshima, A., Doi, K., Nakayama, H., & Uetsuka, K. (2007). Involvement of sex, strain and age factors in high fat diet-induced obesity in C57BL/6J and BALB/cA mice. *Exp Anim*, 56(4), 263-272.
- Nishimura, S., Manabe, I., Nagasaki, M., Eto, K., Yamashita, H., Ohsugi, M., Otsu, M., Hara, K., Ueki, K., Sugiura, S., Yoshimura, K., Kadowaki, T., & Nagai, R. (2009). CD8+ effector T cells contribute to macrophage recruitment and adipose tissue inflammation in obesity. *Nat Med*, 15(8), 914-920. doi:10.1038/nm.1964
- Nosalski, R., & Guzik, T. J. (2017). Perivascular adipose tissue inflammation in vascular disease. *Br J Pharmacol*, 174(20), 3496-3513. doi:10.1111/bph.13705
- Nurieva, R. I., Chung, Y., Hwang, D., Yang, X. O., Kang, H. S., Ma, L., Wang, Y. H., Watowich, S. S., Jetten, A. M., Tian, Q., & Dong, C. (2008). Generation of T follicular helper cells is mediated by interleukin-21 but independent of T helper 1, 2, or 17 cell lineages. *Immunity*, 29(1), 138-149. doi:10.1016/j.immuni.2008.05.009
- Nurieva, R. I., Chung, Y., Martinez, G. J., Yang, X. O., Tanaka, S., Matskevitch, T. D., Wang, Y. H., & Dong, C. (2009). Bcl6 mediates the development of T follicular helper cells. *Science*, 325(5943), 1001-1005. doi:10.1126/science.1176676
- O'Rahilly, S. (2009). Human genetics illuminates the paths to metabolic disease. *Nature*, 462(7271), 307-314. doi:10.1038/nature08532
- Odegard, J. M., Marks, B. R., DiPlacido, L. D., Poholek, A. C., Kono, D. H., Dong, C., Flavell, R. A., & Craft, J. (2008). ICOS-dependent extrafollicular helper T cells elicit IgG production via IL-21 in systemic autoimmunity. *J Exp Med*, 205(12), 2873-2886. doi:10.1084/jem.20080840
- Odievre, M. H., Chretien, D., Munnich, A., Robinson, B. H., Dumoulin, R., Masmoudi, S., Kadhom, N., Rotig, A., Rustin, P., & Bonnefont, J. P. (2005). A novel mutation in the dihydrolipoamide dehydrogenase E3 subunit gene (DLD) resulting in an atypical form of alpha-ketoglutarate dehydrogenase deficiency. *Hum Mutat*, 25(3), 323-324. doi:10.1002/humu.9319

- Olefsky, J. M. (1976). Decreased insulin binding to adipocytes and circulating monocytes from obese subjects. *J Clin Invest*, *57*(5), 1165-1172. doi:10.1172/JCI108384
- Osborn, O., & Olefsky, J. M. (2012). The cellular and signaling networks linking the immune system and metabolism in disease. *Nat Med*, *18*(3), 363-374. doi:10.1038/nm.2627
- Pallandre, J. R., Brillard, E., Crehange, G., Radlovic, A., Remy-Martin, J. P., Saas, P., Rohrlich, P. S., Pivot, X., Ling, X., Tiberghien, P., & Borg, C. (2007). Role of STAT3 in CD4+CD25+FOXP3+ regulatory lymphocyte generation: implications in graft-versus-host disease and antitumor immunity. *J Immunol*, *179*(11), 7593-7604.
- Pandiyani, P., Zheng, L., Ishihara, S., Reed, J., & Lenardo, M. J. (2007). CD4+CD25+Foxp3+ regulatory T cells induce cytokine deprivation-mediated apoptosis of effector CD4+ T cells. *Nat Immunol*, *8*(12), 1353-1362. doi:10.1038/ni1536
- Panduro, M., Benoist, C., & Mathis, D. (2016). Tissue Tregs. *Annu Rev Immunol*, *34*, 609-633. doi:10.1146/annurev-immunol-032712-095948
- Park, B. V., & Pan, F. (2015). Metabolic regulation of T cell differentiation and function. *Mol Immunol*, *68*(2 Pt C), 497-506. doi:10.1016/j.molimm.2015.07.027
- Parks, B. W., Sallam, T., Mehrabian, M., Psychogios, N., Hui, S. T., Norheim, F., Castellani, L. W., Rau, C. D., Pan, C., Phun, J., Zhou, Z., Yang, W. P., Neuhaus, I., Gargalovic, P. S., Kirchgessner, T. G., Graham, M., Lee, R., Tontonoz, P., Gerszten, R. E., Hevener, A. L., & Lusis, A. J. (2015). Genetic architecture of insulin resistance in the mouse. *Cell Metab*, *21*(2), 334-347. doi:10.1016/j.cmet.2015.01.002
- Pecht, T., Gutman-Tirosh, A., Bashan, N., & Rudich, A. (2014). Peripheral blood leucocyte subclasses as potential biomarkers of adipose tissue inflammation and obesity subphenotypes in humans. *Obes Rev*, *15*(4), 322-337. doi:10.1111/obr.12133
- Peng, M., Yin, N., Chhangawala, S., Xu, K., Leslie, C. S., & Li, M. O. (2016). Aerobic glycolysis promotes T helper 1 cell differentiation through an epigenetic mechanism. *Science*, *354*(6311), 481-484. doi:10.1126/science.aaf6284
- Pereira, S., Teixeira, L., Aguilar, E., Oliveira, M., Savassi-Rocha, A., Pelaez, J. N., Capettini, L., Diniz, M. T., Ferreira, A., & Alvarez-Leite, J. (2014). Modulation of adipose tissue inflammation by FOXP3+ Treg cells, IL-10, and TGF-beta in metabolically healthy class III obese individuals. *Nutrition*, *30*(7-8), 784-790. doi:10.1016/j.nut.2013.11.023
- Poholek, A. C., Hansen, K., Hernandez, S. G., Eto, D., Chandele, A., Weinstein, J. S., Dong, X., Odegard, J. M., Kaech, S. M., Dent, A. L., Crotty, S., & Craft, J. (2010). In vivo regulation of Bcl6 and T follicular helper cell development. *J Immunol*, *185*(1), 313-326. doi:10.4049/jimmunol.0904023
- Polansky, J. K., Kretschmer, K., Freyer, J., Floess, S., Garbe, A., Baron, U., Olek, S., Hamann, A., von Boehmer, H., & Huehn, J. (2008). DNA methylation controls Foxp3 gene expression. *Eur J Immunol*, *38*(6), 1654-1663. doi:10.1002/eji.200838105
- Procaccini, C., Carbone, F., Di Silvestre, D., Brambilla, F., De Rosa, V., Galgani, M., Faicchia, D., Marone, G., Tramontano, D., Corona, M., Alviggi, C., Porcellini, A., La Cava, A., Mauri, P., & Matarese, G. (2016). The Proteomic Landscape of Human Ex Vivo Regulatory and Conventional T Cells Reveals Specific Metabolic Requirements. *Immunity*, *44*(2), 406-421. doi:10.1016/j.immuni.2016.01.028
- Procaccini, C., De Rosa, V., Galgani, M., Abanni, L., Cali, G., Porcellini, A., Carbone, F., Fontana, S., Horvath, T. L., La Cava, A., & Matarese, G. (2010). An oscillatory switch in mTOR kinase activity sets regulatory T cell responsiveness. *Immunity*, *33*(6), 929-941. doi:10.1016/j.immuni.2010.11.024
- Qiao, G., Zhao, Y., Li, Z., Tang, P. Q., Langdon, W. Y., Yang, T., & Zhang, J. (2013). T cell activation threshold regulated by E3 ubiquitin ligase Cbl-b determines fate of inducible regulatory T cells. *J Immunol*, *191*(2), 632-639. doi:10.4049/jimmunol.1202068
- Radtke, F., MacDonald, H. R., & Tacchini-Cottier, F. (2013). Regulation of innate and adaptive immunity by Notch. *Nat Rev Immunol*, *13*(6), 427-437. doi:10.1038/nri3445
- Ramsdell, F., & Ziegler, S. F. (2014). FOXP3 and scurfy: how it all began. *Nat Rev Immunol*, *14*(5), 343-349. doi:10.1038/nri3650

- Rangel-Moreno, J., Moyron-Quiroz, J. E., Carragher, D. M., Kusser, K., Hartson, L., Moquin, A., & Randall, T. D. (2009). Omental milky spots develop in the absence of lymphoid tissue-inducer cells and support B and T cell responses to peritoneal antigens. *Immunity*, *30*(5), 731-743. doi:10.1016/j.immuni.2009.03.014
- Rasheed, A. U., Rahn, H. P., Sallusto, F., Lipp, M., & Muller, G. (2006). Follicular B helper T cell activity is confined to CXCR5(hi)ICOS(hi) CD4 T cells and is independent of CD57 expression. *Eur J Immunol*, *36*(7), 1892-1903. doi:10.1002/eji.200636136
- Ravi Kumar, M. N., Bakowsky, U., & Lehr, C. M. (2004). Preparation and characterization of cationic PLGA nanospheres as DNA carriers. *Biomaterials*, *25*(10), 1771-1777.
- Redinger, R. N. (2007). The pathophysiology of obesity and its clinical manifestations. *Gastroenterol Hepatol (N Y)*, *3*(11), 856-863.
- Revu, S., Wu, J., Henkel, M., Rittenhouse, N., Menk, A., Delgoffe, G. M., Poholek, A. C., & McGeachy, M. J. (2018). IL-23 and IL-1beta Drive Human Th17 Cell Differentiation and Metabolic Reprogramming in Absence of CD28 Costimulation. *Cell Rep*, *22*(10), 2642-2653. doi:10.1016/j.celrep.2018.02.044
- Rocha, V. Z., Folco, E. J., Sukhova, G., Shimizu, K., Gotsman, I., Vernon, A. H., & Libby, P. (2008). Interferon-gamma, a Th1 cytokine, regulates fat inflammation: a role for adaptive immunity in obesity. *Circ Res*, *103*(5), 467-476. doi:10.1161/CIRCRESAHA.108.177105
- Roncador, G., Brown, P. J., Maestre, L., Hue, S., Martinez-Torrecuadrada, J. L., Ling, K. L., Pratap, S., Toms, C., Fox, B. C., Cerundolo, V., Powrie, F., & Banham, A. H. (2005). Analysis of FOXP3 protein expression in human CD4+CD25+ regulatory T cells at the single-cell level. *Eur J Immunol*, *35*(6), 1681-1691. doi:10.1002/eji.200526189
- Rosen, E. D., & Spiegelman, B. M. (2014). What we talk about when we talk about fat. *Cell*, *156*(1-2), 20-44. doi:10.1016/j.cell.2013.12.012
- Roth, R. A., & Cassell, D. J. (1983). Insulin receptor: evidence that it is a protein kinase. *Science*, *219*(4582), 299-301.
- Rothwell, N. J., & Stock, M. J. (1997). A role for brown adipose tissue in diet-induced thermogenesis. *Obes Res*, *5*(6), 650-656.
- Rui, L., Aguirre, V., Kim, J. K., Shulman, G. I., Lee, A., Corbould, A., Dunaif, A., & White, M. F. (2001). Insulin/IGF-1 and TNF-alpha stimulate phosphorylation of IRS-1 at inhibitory Ser307 via distinct pathways. *J Clin Invest*, *107*(2), 181-189. doi:10.1172/JCI10934
- Russo, L., & Lumeng, C. N. (2018). Properties and functions of adipose tissue macrophages in obesity. *Immunology*. doi:10.1111/imm.13002
- Rutkowski, J. M., Stern, J. H., & Scherer, P. E. (2015). The cell biology of fat expansion. *J Cell Biol*, *208*(5), 501-512. doi:10.1083/jcb.201409063
- Sakaguchi, S., Sakaguchi, N., Asano, M., Itoh, M., & Toda, M. (1995). Immunologic self-tolerance maintained by activated T cells expressing IL-2 receptor alpha-chains (CD25). Breakdown of a single mechanism of self-tolerance causes various autoimmune diseases. *J Immunol*, *155*(3), 1151-1164.
- Sakaguchi, S., Vignali, D. A., Rudensky, A. Y., Niec, R. E., & Waldmann, H. (2013). The plasticity and stability of regulatory T cells. *Nat Rev Immunol*, *13*(6), 461-467. doi:10.1038/nri3464
- Salomonsson, S., Jonsson, M. V., Skarstein, K., Brokstad, K. A., Hjelmstrom, P., Wahren-Herlenius, M., & Jonsson, R. (2003). Cellular basis of ectopic germinal center formation and autoantibody production in the target organ of patients with Sjogren's syndrome. *Arthritis Rheum*, *48*(11), 3187-3201. doi:10.1002/art.11311
- Sauer, B., & Henderson, N. (1988). Site-specific DNA recombination in mammalian cells by the Cre recombinase of bacteriophage P1. *Proc Natl Acad Sci U S A*, *85*(14), 5166-5170.
- Sauer, S., Bruno, L., Hertweck, A., Finlay, D., Leleu, M., Spivakov, M., Knight, Z. A., Cobb, B. S., Cantrell, D., O'Connor, E., Shokat, K. M., Fisher, A. G., & Merckenschlager, M. (2008). T cell receptor signaling controls Foxp3 expression via PI3K, Akt, and mTOR. *Proc Natl Acad Sci U S A*, *105*(22), 7797-7802. doi:10.1073/pnas.0800928105

- Saxton, R. A., & Sabatini, D. M. (2017). mTOR Signaling in Growth, Metabolism, and Disease. *Cell*, 168(6), 960-976. doi:10.1016/j.cell.2017.02.004
- Schaerli, P., Willimann, K., Lang, A. B., Lipp, M., Loetscher, P., & Moser, B. (2000). CXC chemokine receptor 5 expression defines follicular homing T cells with B cell helper function. *J Exp Med*, 192(11), 1553-1562.
- Scherm, M. G., **Ott, V. B.**, & Daniel, C. (2016). Follicular Helper T Cells in Autoimmunity. *Curr Diab Rep*, 16(8), 75. doi:10.1007/s11892-016-0770-2
- Schmitt, N., Bentebibel, S. E., & Ueno, H. (2014). Phenotype and functions of memory Tfh cells in human blood. *Trends Immunol*, 35(9), 436-442. doi:10.1016/j.it.2014.06.002
- Schuster, M., Glaubien, R., Plaza-Sirvent, C., Schreiber, L., Annemann, M., Floess, S., Kuhl, A. A., Clayton, L. K., Sparwasser, T., Schulze-Osthoff, K., Pfeffer, K., Huehn, J., Siegmund, B., & Schmitz, I. (2012). I $\kappa$ B(N $\kappa$ ) protein mediates regulatory T cell development via induction of the Foxp3 transcription factor. *Immunity*, 37(6), 998-1008. doi:10.1016/j.immuni.2012.08.023
- Seino, S., Seino, M., Nishi, S., & Bell, G. I. (1989). Structure of the human insulin receptor gene and characterization of its promoter. *Proc Natl Acad Sci U S A*, 86(1), 114-118.
- Sekiya, T., Kashiwagi, I., Yoshida, R., Fukaya, T., Morita, R., Kimura, A., Ichinose, H., Metzger, D., Chambon, P., & Yoshimura, A. (2013). Nr4a receptors are essential for thymic regulatory T cell development and immune homeostasis. *Nat Immunol*, 14(3), 230-237. doi:10.1038/ni.2520
- Selbach, M., Schwanhauser, B., Thierfelder, N., Fang, Z., Khanin, R., & Rajewsky, N. (2008). Widespread changes in protein synthesis induced by microRNAs. *Nature*, 455(7209), 58-63. doi:10.1038/nature07228
- Sena, L. A., Li, S., Jairaman, A., Prakriya, M., Ezponda, T., Hildeman, D. A., Wang, C. R., Schumacker, P. T., Licht, J. D., Perlman, H., Bryce, P. J., & Chandel, N. S. (2013). Mitochondria are required for antigen-specific T cell activation through reactive oxygen species signaling. *Immunity*, 38(2), 225-236. doi:10.1016/j.immuni.2012.10.020
- Sergushichev, A. (2016). An algorithm for fast preranked gene set enrichment analysis using cumulative statistic calculation. *BioRxiv*. doi: <https://doi.org/10.1101/060012>
- Serr, I., Furst, R. W., Achenbach, P., Scherm, M. G., Gokmen, F., Haupt, F., Sedlmeier, E. M., Knopff, A., Shultz, L., Willis, R. A., Ziegler, A. G., & Daniel, C. (2016a). Type 1 diabetes vaccine candidates promote human Foxp3(+)Treg induction in humanized mice. *Nat Commun*, 7, 10991. doi:10.1038/ncomms10991
- Serr, I., Furst, R. W., **Ott, V. B.**, Scherm, M. G., Nikolaev, A., Gokmen, F., Kalin, S., Zillmer, S., Bunk, M., Weigmann, B., Kunschke, N., Loretz, B., Lehr, C. M., Kirchner, B., Haase, B., Pfaffl, M., Waisman, A., Willis, R. A., Ziegler, A. G., & Daniel, C. (2016b). miRNA92a targets KLF2 and the phosphatase PTEN signaling to promote human T follicular helper precursors in T1D islet autoimmunity. *Proc Natl Acad Sci U S A*, 113(43), E6659-E6668. doi:10.1073/pnas.1606646113
- Serr, I., Scherm, M. G., Zahm, A. M., Schug, J., Flynn, V. K., Hippich, M., Kalin, S., Becker, M., Achenbach, P., Nikolaev, A., Gerlach, K., Liebsch, N., Loretz, B., Lehr, C. M., Kirchner, B., Spornraft, M., Haase, B., Segars, J., Kuper, C., Palmisano, R., Waisman, A., Willis, R. A., Kim, W. U., Weigmann, B., Kaestner, K. H., Ziegler, A. G., & Daniel, C. (2018). A miRNA181a/NFAT5 axis links impaired T cell tolerance induction with autoimmune type 1 diabetes. *Sci Transl Med*, 10(422). doi:10.1126/scitranslmed.aag1782
- Shabanpoor, F., Separovic, F., & Wade, J. D. (2009). The human insulin superfamily of polypeptide hormones. *Vitam Horm*, 80, 1-31. doi:10.1016/S0083-6729(08)00601-8
- Sharma, A., & Rudra, D. (2018). Emerging Functions of Regulatory T Cells in Tissue Homeostasis. *Front Immunol*, 9, 883. doi:10.3389/fimmu.2018.00883
- Shi, J., Hou, S., Fang, Q., Liu, X., Liu, X., & Qi, H. (2018). PD-1 Controls Follicular T Helper Cell Positioning and Function. *Immunity*, 49(2), 264-274 e264. doi:10.1016/j.immuni.2018.06.012

- Shinall, S. M., Gonzalez-Fernandez, M., Noelle, R. J., & Waldschmidt, T. J. (2000). Identification of murine germinal center B cell subsets defined by the expression of surface isotypes and differentiation antigens. *J Immunol*, *164*(11), 5729-5738.
- Simpson, N., Gatenby, P. A., Wilson, A., Malik, S., Fulcher, D. A., Tangye, S. G., Manku, H., Vyse, T. J., Roncador, G., Huttley, G. A., Goodnow, C. C., Vinuesa, C. G., & Cook, M. C. (2010). Expansion of circulating T cells resembling follicular helper T cells is a fixed phenotype that identifies a subset of severe systemic lupus erythematosus. *Arthritis Rheum*, *62*(1), 234-244. doi:10.1002/art.25032
- Slowikowski, K. (2016). ggrepel: Repulsive text and label geoms for 'ggplot2' (Version R package version 0.6 5.11).
- Smith-Garvin, J. E., Koretzky, G. A., & Jordan, M. S. (2009). T cell activation. *Annu Rev Immunol*, *27*, 591-619. doi:10.1146/annurev.immunol.021908.132706
- Soli, A. H., Kahn, C. R., Neville, D. M., Jr., & Roth, J. (1975). Insulin receptor deficiency in genetic and acquired obesity. *J Clin Invest*, *56*(4), 769-780. doi:10.1172/JCI108155
- Someya, K., Nakatsukasa, H., Ito, M., Kondo, T., Tateda, K. I., Akanuma, T., Koya, I., Sanosaka, T., Kohyama, J., Tsukada, Y. I., Takamura-Enya, T., & Yoshimura, A. (2017). Improvement of Foxp3 stability through CNS2 demethylation by TET enzyme induction and activation. *Int Immunol*, *29*(8), 365-375. doi:10.1093/intimm/dxx049
- Sparrow, L. G., McKern, N. M., Gorman, J. J., Strike, P. M., Robinson, C. P., Bentley, J. D., & Ward, C. W. (1997). The disulfide bonds in the C-terminal domains of the human insulin receptor ectodomain. *J Biol Chem*, *272*(47), 29460-29467.
- Speakman, J., Hambly, C., Mitchell, S., & Krol, E. (2007). Animal models of obesity. *Obes Rev*, *8 Suppl 1*, 55-61. doi:10.1111/j.1467-789X.2007.00319.x
- Stone, Erica L., Pepper, M., Katayama, Carol D., Kerdiles, Yann M., Lai, C.-Y., Emslie, E., Lin, Yin C., Yang, E., Goldrath, Ananda W., Li, Ming O., Cantrell, Doreen A., & Hedrick, Stephen M. (2015). ICOS Coreceptor Signaling Inactivates the Transcription Factor FOXO1 to Promote Tfh Cell Differentiation. *Immunity*, *42*(2), 239-251.
- Sun, K., Kusminski, C. M., & Scherer, P. E. (2011). Adipose tissue remodeling and obesity. *J Clin Invest*, *121*(6), 2094-2101. doi:10.1172/JCI45887
- Surwit, R. S., Kuhn, C. M., Cochrane, C., McCubbin, J. A., & Feinglos, M. N. (1988). Diet-induced type II diabetes in C57BL/6J mice. *Diabetes*, *37*(9), 1163-1167.
- Suto, A., Kashiwakuma, D., Kagami, S., Hirose, K., Watanabe, N., Yokote, K., Saito, Y., Nakayama, T., Grusby, M. J., Iwamoto, I., & Nakajima, H. (2008). Development and characterization of IL-21-producing CD4+ T cells. *J Exp Med*, *205*(6), 1369-1379. doi:10.1084/jem.20072057
- Takebe, T., Sakamoto, K., Higami, Y., & Harada, Y. (2018). A novel mouse model for tracking the fate of CXCR5-expressing T cells. *Biochem Biophys Res Commun*, *495*(2), 1642-1647. doi:10.1016/j.bbrc.2017.12.029
- Taleb, S., Herbin, O., Ait-Oufella, H., Verreth, W., Gourdy, P., Barateau, V., Merval, R., Esposito, B., Clement, K., Holvoet, P., Tedgui, A., & Mallat, Z. (2007). Defective leptin/leptin receptor signaling improves regulatory T cell immune response and protects mice from atherosclerosis. *Arterioscler Thromb Vasc Biol*, *27*(12), 2691-2698. doi:10.1161/ATVBAHA.107.149567
- Talukdar, S., Oh, D. Y., Bandyopadhyay, G., Li, D., Xu, J., McNelis, J., Lu, M., Li, P., Yan, Q., Zhu, Y., Ofrecio, J., Lin, M., Brenner, M. B., & Olefsky, J. M. (2012). Neutrophils mediate insulin resistance in mice fed a high-fat diet through secreted elastase. *Nat Med*, *18*(9), 1407-1412. doi:10.1038/nm.2885
- Tan, S., Lai, Tang, Xie, Xu, Wei, Zhang, Yang and Wu. (2018). Regulative role of the CXCL13-CXCR5 axis in the tumor microenvironment. *Oxford Precision Clinical Medicine*, *1*(1), 49-56. doi:10.1093/pcmedi/pby006
- Taniguchi, C. M., Ueki, K., & Kahn, R. (2005). Complementary roles of IRS-1 and IRS-2 in the hepatic regulation of metabolism. *J Clin Invest*, *115*(3), 718-727. doi:10.1172/JCI23187

- Templeman, N. M., Skovso, S., Page, M. M., Lim, G. E., & Johnson, J. D. (2017). A causal role for hyperinsulinemia in obesity. *J Endocrinol*, *232*(3), R173-R183. doi:10.1530/JOE-16-0449
- Thirone, A. C., Huang, C., & Klip, A. (2006). Tissue-specific roles of IRS proteins in insulin signaling and glucose transport. *Trends Endocrinol Metab*, *17*(2), 72-78. doi:10.1016/j.tem.2006.01.005
- Thornton, A. M., & Shevach, E. M. (1998). CD4+CD25+ immunoregulatory T cells suppress polyclonal T cell activation in vitro by inhibiting interleukin 2 production. *J Exp Med*, *188*(2), 287-296.
- Tiemessen, M. M., Jagger, A. L., Evans, H. G., van Herwijnen, M. J., John, S., & Taams, L. S. (2007). CD4+CD25+Foxp3+ regulatory T cells induce alternative activation of human monocytes/macrophages. *Proc Natl Acad Sci U S A*, *104*(49), 19446-19451. doi:10.1073/pnas.0706832104
- Tone, Y., Furuuchi, K., Kojima, Y., Tykocinski, M. L., Greene, M. I., & Tone, M. (2008). Smad3 and NFAT cooperate to induce Foxp3 expression through its enhancer. *Nat Immunol*, *9*(2), 194-202. doi:10.1038/ni1549
- Tran, T. T., & Kahn, C. R. (2010). Transplantation of adipose tissue and stem cells: role in metabolism and disease. *Nat Rev Endocrinol*, *6*(4), 195-213. doi:10.1038/nrendo.2010.20
- Travers, R. L., Motta, A. C., Betts, J. A., Bouloumie, A., & Thompson, D. (2015). The impact of adiposity on adipose tissue-resident lymphocyte activation in humans. *Int J Obes (Lond)*, *39*(5), 762-769. doi:10.1038/ijo.2014.195
- Truesdell, S. S., Mortensen, R. D., Seo, M., Schroeder, J. C., Lee, J. H., LeTonqueze, O., & Vasudevan, S. (2012). MicroRNA-mediated mRNA translation activation in quiescent cells and oocytes involves recruitment of a nuclear microRNP. *Sci Rep*, *2*, 842. doi:10.1038/srep00842
- Tsai, S., Clemente-Casares, X., Zhou, A. C., Lei, H., Ahn, J. J., Chan, Y. T., Choi, O., Luck, H., Woo, M., Dunn, S. E., Engleman, E. G., Watts, T. H., Winer, S., & Winer, D. A. (2018). Insulin Receptor-Mediated Stimulation Boosts T Cell Immunity during Inflammation and Infection. *Cell Metab*. doi:10.1016/j.cmet.2018.08.003
- Tyanova, S., Temu, T., Sinitcyn, P., Carlson, A., Hein, M. Y., Geiger, T., Mann, M., & Cox, J. (2016). The Perseus computational platform for comprehensive analysis of (prote)omics data. *Nat Methods*, *13*(9), 731-740. doi:10.1038/nmeth.3901
- Ueno, H. (2016). T follicular helper cells in human autoimmunity. *Curr Opin Immunol*, *43*, 24-31. doi:10.1016/j.coi.2016.08.003
- Vadiveloo, M., Scott, M., Quatromoni, P., Jacques, P., & Parekh, N. (2014). Trends in dietary fat and high-fat food intakes from 1991 to 2008 in the Framingham Heart Study participants. *Br J Nutr*, *111*(4), 724-734. doi:10.1017/S0007114513002924
- van der Klaauw, A. A., & Farooqi, I. S. (2015). The hunger genes: pathways to obesity. *Cell*, *161*(1), 119-132. doi:10.1016/j.cell.2015.03.008
- van der Windt, G. J., & Pearce, E. L. (2012). Metabolic switching and fuel choice during T-cell differentiation and memory development. *Immunol Rev*, *249*(1), 27-42. doi:10.1111/j.1600-065X.2012.01150.x
- Vander Heiden, M. G., Cantley, L. C., & Thompson, C. B. (2009). Understanding the Warburg effect: the metabolic requirements of cell proliferation. *Science*, *324*(5930), 1029-1033. doi:10.1126/science.1160809
- Vasanthakumar, A., Moro, K., Xin, A., Liao, Y., Gloury, R., Kawamoto, S., Fagarasan, S., Mielke, L. A., Afshar-Sterle, S., Masters, S. L., Nakae, S., Saito, H., Wentworth, J. M., Li, P., Liao, W., Leonard, W. J., Smyth, G. K., Shi, W., Nutt, S. L., Koyasu, S., & Kallies, A. (2015). The transcriptional regulators IRF4, BATF and IL-33 orchestrate development and maintenance of adipose tissue-resident regulatory T cells. *Nat Immunol*, *16*(3), 276-285. doi:10.1038/ni.3085
- Vasudevan, S., Tong, Y., & Steitz, J. A. (2007). Switching from repression to activation: microRNAs can up-regulate translation. *Science*, *318*(5858), 1931-1934. doi:10.1126/science.1149460

- Vella, L. A., Herati, R. S., & Wherry, E. J. (2017). CD4(+) T Cell Differentiation in Chronic Viral Infections: The Tfh Perspective. *Trends Mol Med*, 23(12), 1072-1087. doi:10.1016/j.molmed.2017.10.001
- Viardot, A., Grey, S. T., Mackay, F., & Chisholm, D. (2007). Potential antiinflammatory role of insulin via the preferential polarization of effector T cells toward a T helper 2 phenotype. *Endocrinology*, 148(1), 346-353. doi:10.1210/en.2006-0686
- von Boehmer, H., & Daniel, C. (2013). Therapeutic opportunities for manipulating T(Reg) cells in autoimmunity and cancer. *Nat Rev Drug Discov*, 12(1), 51-63. doi:10.1038/nrd3683
- Wang, C. J., Heuts, F., Ovcinnikovs, V., Wardzinski, L., Bowers, C., Schmidt, E. M., Kogimtzis, A., Kenefeck, R., Sansom, D. M., & Walker, L. S. (2015). CTLA-4 controls follicular helper T-cell differentiation by regulating the strength of CD28 engagement. *Proc Natl Acad Sci U S A*, 112(2), 524-529. doi:10.1073/pnas.1414576112
- Wang, Q., Zhai, X., Chen, X., Lu, J., Zhang, Y., & Huang, Q. (2015). Dysregulation of circulating CD4+CXCR5+ T cells in type 2 diabetes mellitus. *APMIS*, 123(2), 146-151. doi:10.1111/apm.12330
- Wang, Q. A., Tao, C., Gupta, R. K., & Scherer, P. E. (2013). Tracking adipogenesis during white adipose tissue development, expansion and regeneration. *Nat Med*, 19(10), 1338-1344. doi:10.1038/nm.3324
- Wang, R., Dillon, C. P., Shi, L. Z., Milasta, S., Carter, R., Finkelstein, D., McCormick, L. L., Fitzgerald, P., Chi, H., Munger, J., & Green, D. R. (2011). The transcription factor Myc controls metabolic reprogramming upon T lymphocyte activation. *Immunity*, 35(6), 871-882. doi:10.1016/j.immuni.2011.09.021
- Ward, C. W., & Lawrence, M. C. (2009). Ligand-induced activation of the insulin receptor: a multi-step process involving structural changes in both the ligand and the receptor. *Bioessays*, 31(4), 422-434. doi:10.1002/bies.200800210
- Weber, J. P., Fuhrmann, F., Feist, R. K., Lahmann, A., Al Baz, M. S., Gentz, L. J., Vu Van, D., Mages, H. W., Haftmann, C., Riedel, R., Grun, J. R., Schuh, W., Kroczeck, R. A., Radbruch, A., Mashreghi, M. F., & Hutloff, A. (2015). ICOS maintains the T follicular helper cell phenotype by down-regulating Kruppel-like factor 2. *J Exp Med*, 212(2), 217-233. doi:10.1084/jem.20141432
- Wei, X., Zhang, J., Gu, Q., Huang, M., Zhang, W., Guo, J., & Zhou, X. (2017). Reciprocal Expression of IL-35 and IL-10 Defines Two Distinct Effector Treg Subsets that Are Required for Maintenance of Immune Tolerance. *Cell Rep*, 21(7), 1853-1869. doi:10.1016/j.celrep.2017.10.090
- Weisberg, S. P., McCann, D., Desai, M., Rosenbaum, M., Leibel, R. L., & Ferrante, A. W., Jr. (2003). Obesity is associated with macrophage accumulation in adipose tissue. *J Clin Invest*, 112(12), 1796-1808. doi:10.1172/JCI19246
- Wentworth, J. M., Naselli, G., Brown, W. A., Doyle, L., Phipson, B., Smyth, G. K., Wabitsch, M., O'Brien, P. E., & Harrison, L. C. (2010). Pro-inflammatory CD11c+CD206+ adipose tissue macrophages are associated with insulin resistance in human obesity. *Diabetes*, 59(7), 1648-1656. doi:10.2337/db09-0287
- West, D. B., Boozer, C. N., Moody, D. L., & Atkinson, R. L. (1992). Dietary obesity in nine inbred mouse strains. *Am J Physiol*, 262(6 Pt 2), R1025-1032. doi:10.1152/ajpregu.1992.262.6.R1025
- WHO. (2017). Fact Sheet- Obesity and overweight. Retrieved from <http://www.who.int/mediacentre/factsheets/fs311/en/#.WndJn7pL5Ck.email>
- Wickham, H. (2016). *ggplot2: Elegant Graphics for Data Analysis*.
- Wieland, O., & Suyter, M. (1957). [Glycerokinase; isolation and properties of the enzyme]. *Biochem Z*, 329(4), 320-331.
- Winer, D. A., Winer, S., Shen, L., Wadia, P. P., Yantha, J., Paltser, G., Tsui, H., Wu, P., Davidson, M. G., Alonso, M. N., Leong, H. X., Glassford, A., Caimol, M., Kenkel, J. A., Tedder, T. F., McLaughlin, T., Miklos, D. B., Dosch, H. M., & Engleman, E. G. (2011). B cells promote insulin resistance through modulation of T cells and production of pathogenic IgG antibodies. *Nat Med*, 17(5), 610-617. doi:10.1038/nm.2353

- Winer, S., Chan, Y., Paltser, G., Truong, D., Tsui, H., Bahrami, J., Dorfman, R., Wang, Y., Zielenski, J., Mastronardi, F., Maezawa, Y., Drucker, D. J., Engleman, E., Winer, D., & Dosch, H. M. (2009). Normalization of obesity-associated insulin resistance through immunotherapy. *Nat Med*, *15*(8), 921-929. doi:10.1038/nm.2001
- Winzell, M. S., & Ahren, B. (2004). The high-fat diet-fed mouse: a model for studying mechanisms and treatment of impaired glucose tolerance and type 2 diabetes. *Diabetes*, *53 Suppl 3*, S215-219.
- Wouters, K., Gaens, K., Bijnen, M., Verboven, K., Jocken, J., Wetzels, S., Wijnands, E., Hansen, D., van Greevenbroek, M., Duijvestijn, A., Biessen, E. A., Blaak, E. E., Stehouwer, C. D., & Schalkwijk, C. G. (2017). Circulating classical monocytes are associated with CD11c(+) macrophages in human visceral adipose tissue. *Sci Rep*, *7*, 42665. doi:10.1038/srep42665
- Wu, D., Han, J. M., Yu, X., Lam, A. J., Hoeppli, R. E., Pesenacker, A. M., Huang, Q., Chen, V., Speake, C., Yorke, E., Nguyen, N., Sampath, S., Harris, D., & Levings, M. K. (2018). Characterization of regulatory T cells in obese omental adipose tissue in humans. *Eur J Immunol*. doi:10.1002/eji.201847570
- Wu, D., Molofsky, A. B., Liang, H. E., Ricardo-Gonzalez, R. R., Jouihan, H. A., Bando, J. K., Chawla, A., & Locksley, R. M. (2011). Eosinophils sustain adipose alternatively activated macrophages associated with glucose homeostasis. *Science*, *332*(6026), 243-247. doi:10.1126/science.1201475
- Wu, J., Bostrom, P., Sparks, L. M., Ye, L., Choi, J. H., Giang, A. H., Khandekar, M., Virtanen, K. A., Nuutila, P., Schaart, G., Huang, K., Tu, H., van Marken Lichtenbelt, W. D., Hoeks, J., Enerback, S., Schrauwen, P., & Spiegelman, B. M. (2012). Beige adipocytes are a distinct type of thermogenic fat cell in mouse and human. *Cell*, *150*(2), 366-376. doi:10.1016/j.cell.2012.05.016
- Wu, T., Wieland, A., Lee, J., Hale, J. S., Han, J. H., Xu, X., & Ahmed, R. (2015). Cutting Edge: miR-17-92 Is Required for Both CD4 Th1 and T Follicular Helper Cell Responses during Viral Infection. *J Immunol*, *195*(6), 2515-2519. doi:10.4049/jimmunol.1500317
- Xiao, C., Srinivasan, L., Calado, D. P., Patterson, H. C., Zhang, B., Wang, J., Henderson, J. M., Kutok, J. L., & Rajewsky, K. (2008). Lymphoproliferative disease and autoimmunity in mice with increased miR-17-92 expression in lymphocytes. *Nat Immunol*, *9*(4), 405-414. doi:10.1038/ni1575
- Xiao, H., Luo, G., Son, H., Zhou, Y., & Zheng, W. (2014). Upregulation of peripheral CD4+CXCR5+ T cells in osteosarcoma. *Tumour Biol*, *35*(6), 5273-5279. doi:10.1007/s13277-014-1686-6
- Xiao, N., Eto, D., Elly, C., Peng, G., Crotty, S., & Liu, Y. C. (2014). The E3 ubiquitin ligase Itch is required for the differentiation of follicular helper T cells. *Nat Immunol*, *15*(7), 657-666. doi:10.1038/ni.2912
- Xing, Y., & Hogquist, K. A. (2012). T-cell tolerance: central and peripheral. *Cold Spring Harb Perspect Biol*, *4*(6). doi:10.1101/cshperspect.a006957
- Xu, H., Barnes, G. T., Yang, Q., Tan, G., Yang, D., Chou, C. J., Sole, J., Nichols, A., Ross, J. S., Tartaglia, L. A., & Chen, H. (2003). Chronic inflammation in fat plays a crucial role in the development of obesity-related insulin resistance. *J Clin Invest*, *112*(12), 1821-1830. doi:10.1172/JCI19451
- Xu, H., Li, X., Liu, D., Li, J., Zhang, X., Chen, X., Hou, S., Peng, L., Xu, C., Liu, W., Zhang, L., & Qi, H. (2013). Follicular T-helper cell recruitment governed by bystander B cells and ICOS-driven motility. *Nature*, *496*(7446), 523-527. doi:10.1038/nature12058
- Xu, J., Ji, J., & Yan, X. H. (2012). Cross-talk between AMPK and mTOR in regulating energy balance. *Crit Rev Food Sci Nutr*, *52*(5), 373-381. doi:10.1080/10408398.2010.500245
- Yamaguchi, N., Argueta, J. G., Masuhiro, Y., Kagishita, M., Nonaka, K., Saito, T., Hanazawa, S., & Yamashita, Y. (2005). Adiponectin inhibits Toll-like receptor family-induced signaling. *FEBS Lett*, *579*(30), 6821-6826. doi:10.1016/j.febslet.2005.11.019
- Yang, X., Xia, R., Yue, C., Zhai, W., Du, W., Yang, Q., Cao, H., Chen, X., Obando, D., Zhu, Y., Chen, X., Chen, J. J., Piganelli, J., Wipf, P., Jiang, Y., Xiao, G., Wu, C., Jiang, J.,

- & Lu, B. (2018). ATF4 Regulates CD4(+) T Cell Immune Responses through Metabolic Reprogramming. *Cell Rep*, 23(6), 1754-1766. doi:10.1016/j.celrep.2018.04.032
- Yang, Y., Smith, D. L., Jr., Keating, K. D., Allison, D. B., & Nagy, T. R. (2014). Variations in body weight, food intake and body composition after long-term high-fat diet feeding in C57BL/6J mice. *Obesity (Silver Spring)*, 22(10), 2147-2155. doi:10.1002/oby.20811
- Yao, Z., Kanno, Y., Kerényi, M., Stephens, G., Durant, L., Watford, W. T., Laurence, A., Robinson, G. W., Shevach, E. M., Moriggl, R., Hennighausen, L., Wu, C., & O'Shea, J. J. (2007). Nonredundant roles for Stat5a/b in directly regulating Foxp3. *Blood*, 109(10), 4368-4375. doi:10.1182/blood-2006-11-055756
- Yazici, D., & Sezer, H. (2017). Insulin Resistance, Obesity and Lipotoxicity. *Adv Exp Med Biol*, 960, 277-304. doi:10.1007/978-3-319-48382-5\_12
- Ye, J. (2008). Regulation of PPARgamma function by TNF-alpha. *Biochem Biophys Res Commun*, 374(3), 405-408. doi:10.1016/j.bbrc.2008.07.068
- Ye, J. (2013). Mechanisms of insulin resistance in obesity. *Front Med*, 7(1), 14-24. doi:10.1007/s11684-013-0262-6
- Ye, R., & Scherer, P. E. (2013). Adiponectin, driver or passenger on the road to insulin sensitivity? *Mol Metab*, 2(3), 133-141. doi:10.1016/j.molmet.2013.04.001
- Yip, C. C., & Jack, E. (1992). Insulin receptors are bivalent as demonstrated by photoaffinity labeling. *J Biol Chem*, 267(19), 13131-13134.
- Youngren, J. F. (2007). Regulation of insulin receptor function. *Cell Mol Life Sci*, 64(7-8), 873-891. doi:10.1007/s00018-007-6359-9
- Yu, D., Rao, S., Tsai, L. M., Lee, S. K., He, Y., Sutcliffe, E. L., Srivastava, M., Linterman, M., Zheng, L., Simpson, N., Ellyard, J. I., Parish, I. A., Ma, C. S., Li, Q. J., Parish, C. R., Mackay, C. R., & Vinuesa, C. G. (2009). The transcriptional repressor Bcl-6 directs T follicular helper cell lineage commitment. *Immunity*, 31(3), 457-468. doi:10.1016/j.immuni.2009.07.002
- Zeng, H., Yang, K., Cloer, C., Neale, G., Vogel, P., & Chi, H. (2013). mTORC1 couples immune signals and metabolic programming to establish T(reg)-cell function. *Nature*, 499(7459), 485-490. doi:10.1038/nature12297
- Zeyda, M., Huber, J., Prager, G., & Stulnig, T. M. (2011). Inflammation correlates with markers of T-cell subsets including regulatory T cells in adipose tissue from obese patients. *Obesity (Silver Spring)*, 19(4), 743-748. doi:10.1038/oby.2010.123
- Zeyda, M., Wernly, B., Demyanets, S., Kaun, C., Hammerle, M., Hantusch, B., Schranz, M., Neuhofer, A., Itariu, B. K., Keck, M., Prager, G., Wojta, J., & Stulnig, T. M. (2013). Severe obesity increases adipose tissue expression of interleukin-33 and its receptor ST2, both predominantly detectable in endothelial cells of human adipose tissue. *Int J Obes (Lond)*, 37(5), 658-665. doi:10.1038/ijo.2012.118
- Zhan, J., Huang, L., Ma, H., Chen, H., Yang, Y., Tan, S., Song, W., Zhao, W., & Dai, X. (2017). Reduced inflammatory responses of follicular helper T cell promote the development of regulatory B cells after Roux-en-Y gastric bypass. *Clin Exp Pharmacol Physiol*, 44(5), 556-565. doi:10.1111/1440-1681.12740
- Zhang, Y., Proenca, R., Maffei, M., Barone, M., Leopold, L., & Friedman, J. M. (1994). Positional cloning of the mouse obese gene and its human homologue. *Nature*, 372(6505), 425-432. doi:10.1038/372425a0
- Zhao, H., Liao, X., & Kang, Y. (2017). Tregs: Where We Are and What Comes Next? *Front Immunol*, 8, 1578. doi:10.3389/fimmu.2017.01578
- Zhao, Y., Lin, L., Li, J., Xiao, Z., Chen, B., Wan, L., Li, M., Wu, X., Hin Cho, C., & Shen, J. (2018). CD4(+) T cells in obesity and obesity-associated diseases. *Cell Immunol*, 332, 1-6. doi:10.1016/j.cellimm.2018.08.013
- Zheng, Y., Josefowicz, S., Chaudhry, A., Peng, X. P., Forbush, K., & Rudensky, A. Y. (2010). Role of conserved non-coding DNA elements in the Foxp3 gene in regulatory T-cell fate. *Nature*, 463(7282), 808-812. doi:10.1038/nature08750
- Zhou, J., Wang, Y., He, Y., Gao, Y., Wan, R., Cai, M., Li, W., Chen, R., Walker, E., Zhai, X., & Wang, Q. (2018). Non-obese type 2 diabetes patients present intestinal B cell

- dysregulations associated with hyperactive intestinal Tfh cells. *Mol Immunol*, 97, 27-32. doi:10.1016/j.molimm.2018.03.008
- Zhou, L. (2016). AHR Function in Lymphocytes: Emerging Concepts. *Trends Immunol*, 37(1), 17-31. doi:10.1016/j.it.2015.11.007
- Zhu, J., Yamane, H., & Paul, W. E. (2010). Differentiation of effector CD4 T cell populations (\*). *Annu Rev Immunol*, 28, 445-489. doi:10.1146/annurev-immunol-030409-101212
- Zotos, D., Coquet, J. M., Zhang, Y., Light, A., D'Costa, K., Kallies, A., Corcoran, L. M., Godfrey, D. I., Toellner, K. M., Smyth, M. J., Nutt, S. L., & Tarlinton, D. M. (2010). IL-21 regulates germinal center B cell differentiation and proliferation through a B cell-intrinsic mechanism. *J Exp Med*, 207(2), 365-378. doi:10.1084/jem.20091777

## 6. Permissions

### Proceedings of the National Academy of Sciences (PNAS)

Serr, I., Furst, R.W., **Ott, V.B.**, Scherm, M.G., Nikolaev, A., Gokmen, F., Kalin, S., Zillmer, S., Bunk, M., Weigmann, B., et al. (2016). miRNA92a targets KLF2 and the phosphatase Pten signaling to promote human T follicular helper precursors in T1D islet autoimmunity. *Proc Natl Acad Sci U S A* 113, E6659-E6668.

**PNAS authors need not obtain permission for the following cases:** 1) to use their original figures or tables in their future works; 2) ... **3) to include their papers as part of their dissertations;** or 4) **to use all or part of their articles in printed compilations of their own works.** The full journal reference must be cited and, for articles published in volumes 90–105 (1993–2008), "Copyright (copyright year) National Academy of Sciences" (Retrieved from [https://www.google.com/url?sa=t&rct=j&q=&esrc=s&source=web&cd=1&ved=2ahUKEwiYrsOfntbeAhXDGCwKHdq\\_D98QFjAAegQIAhAC&url=http%3A%2F%2Fdigitalcommons.library.tmc.edu%2Fcgi%2Fviewcontent.cgi%3Ffilename%3D3%26article%3D1168%26context%3Dutgsbs\\_dissertations%26type%3Dadditional&usq=AOvVaw3\\_wfsrdPoOSbVt-uLs3lxP](https://www.google.com/url?sa=t&rct=j&q=&esrc=s&source=web&cd=1&ved=2ahUKEwiYrsOfntbeAhXDGCwKHdq_D98QFjAAegQIAhAC&url=http%3A%2F%2Fdigitalcommons.library.tmc.edu%2Fcgi%2Fviewcontent.cgi%3Ffilename%3D3%26article%3D1168%26context%3Dutgsbs_dissertations%26type%3Dadditional&usq=AOvVaw3_wfsrdPoOSbVt-uLs3lxP) (11/15/2018))

### Cell Metabolism

Kalin, S., Becker, M., **Ott, V.B.**, Serr, I., Hosp, F., Mollah, M.M.H., Keipert, S., Lamp, D., Rohner-Jeanrenaud, F., Flynn, V.K., et al. (2017). A Stat6/Pten Axis Links Regulatory T Cells with Adipose Tissue Function. *Cell Metab* 26, 475-492 e477.

As an author, you (or your employer or institution) may do the following:

- ...
- **Include the article in full or in part in a thesis or dissertation (provided that this is not to be published commercially)**
- ...

(Retrieved from <https://www.cell.com/trends/editorial-policies> (11/15/2018))

## 7. Attachment: Overview of the used Material

**Table 1: Used Material**

|  | Source          | Catalog No. or<br>Primer Sequence |
|--|-----------------|-----------------------------------|
| <b>Isolation of human naïve CD4<sup>+</sup>T cells</b> |                 |                                   |
| BD Vacutainer Tubes                                    | BD              | #368480                           |
| BD Vacutainer Safety-Lock blood donation system        | BD              | #367282                           |
| Ficoll Paque Plus                                      | Th. Geyer       | #AM/17144003/00000<br>1           |
| CD4 Microbeads human                                   | Miltenyi Biotec | #130-045-101                      |
| CD19 Microbeads human                                  | Miltenyi Biotec | #130-050-301                      |
| LS-columns   | Miltenyi Biotec | #130-042-401                      |
| <b>Antibodies and Fc-Block (human samples)</b>         |                 |                                   |
| Fc-Block   | BioLegend       | #422302                           |
| CD45RA FITC (Clone: HI100)                             | BioLegend       | #304106                           |
| CD25 (II-2Ra) APC (Clone: 2A3)                         | BD              | #340907                           |
| CD3 PerCPCy5.5 (Clone: HIT3a)                          | BioLegend       | #300328                           |
| CD45RO APC-Cy7 (Clone: UCHL1)                          | BD Pharmingen   | #561137                           |
| CD4 AmCyan (Clone: RPA-T4)                             | BD Horizon      | #560768                           |
| CD127 (II-7Ra) PE-Cy7 (Clone: A019D5)                  | BioLegend       | #351320                           |
| CXCR5 (CD185) APC (Clone: J252D4)                      | BioLegend       | #356907                           |

|   |                   |              |
|---|-------------------|--------------|
| PD1 (CD279) PerCP-Cy5.5 (Clone: EH12.1)                 | BD Pharmingen     | #561273      |
| CCR7 Pe-Cy7 (Clone: G043H7)                             | BioLegend         | #353226      |
| CCR6 (CD196) PE-Cy7 (Clone: G034E3)                     | BioLegend         | #353418      |
| CXCR3 (CD183) PerCP-Cy5.5 (Clone: G025H7)               | BioLegend         | #323714      |
| CD8a DAPI (Clone: RPA-T8)                               | BioLegend         | #301006      |
| CD11b DAPI (Clone: ICRF44)                              | BioLegend         | #301315      |
| CD14 DAPI (Clone: HCD14)                                | BioLegend         | #325616      |
| CD19 DAPI (Clone: HIB19)                                | BioLegend         | #302224      |
| Foxp3 PE (Clone: 236A/E7)                               | eBioscience       | #12-4777-42  |
| Ki-67 Qdot (Clone: 16A8)                                | BioLegend         | #652413      |
| Purified CD3 (Clone: UCHT1)                             | BioLegend         | #300432      |
| Purified CD28 (Clone:CD28.2)                            | BioLegend         | #302923      |
| Purified CD3 (Clone: Okt3)                              | BioLegend         | #317304      |
| <b>Isolation of murine naïve CD4<sup>+</sup>T cells</b> |                   |              |
| 70 µm cell strainers                                    | Fisher Scientific | #FALC352350  |
| Streptavidin Microbeads                                 | Miltenyi          | #130-048-101 |
| Collagenase type II                                     | Sigma-Aldrich     | #C6885-5G    |
| 200µm neoLab-Siebgewebe                                 | NeoLab            | #41413       |
| LS-Columns  | Miltenyi Biotec   | #130-042-401 |

|   |               |             |
|---|---------------|-------------|
| Dynabeads untouched CD4+ mouse                  | Invitrogen    | #11415D     |
| <b>Antibodies and Fc-Block (murine samples)</b> |               |             |
| Fc-Block (Clone: 2.4G2)                         | BD Pharmingen | #553142     |
| CD25 PerCP-Cy5.5 (Clone: PC61)                  | Biolegend     | #102030     |
| CD4 Biotin (Clone: GK1.5)                       | Biolegend     | #100404     |
| CD44 PE (Clone: IM7)                            | Biolegend     | #122014     |
| CD4 Alexa Fluor 700 (Clone: RM4-5)              | eBioscience   | #56-0042    |
| CXCR5 (CD185) PerCP-Cy5.5 (Clone: L138D7)       | BioLegend     | #L138D7     |
| PD1 APC-Cy7 (Clone: 29F.1A12)                   | eBioscience   | #47-9985-80 |
| CD8a Pacific Blue (Clone: 53-6.7)               | Biolegend     | #100725     |
| CD11b Pacific Blue (Clone: M1/70)               | Biolegend     | #101224     |
| CD11c Brilliant Violet 421 (Clone: N418)        | Biolegend     | #117330     |
| B220 Pacific Blue (Clone: RA3-6B2)              | Biolegend     | #103227     |
| F4/80 Pacific Blue (Clone: BM8)                 | Biolegend     | #123124     |
| CD14 V450 (Clone: rmC5-3)                       | BD Bioscience | #560639     |
| Bcl6 Alexa Fluor 647 (Clone: K112-91)           | BD Pharmingen | #561525     |
| Foxp3 FITC (Clone: FJK-16s)                     | eBioscience   | #11-5773-82 |
| Ki67 APC (Clone: 16A8)                          | Biolegend     | #652406     |
| CD3e (Clone: 145-2C11)                          | BD Pharmingen | #553057;    |

|   |                          |              |
|---|--------------------------|--------------|
| CD28 (Clone: 37.51)                                     | BD Pharmingen            | #553294      |
| <b>Intracellular staining</b>                           |                          |              |
| Foxp3 Staining Buffer Set                               | eBioscience              | #00-5523-00  |
| <b>Death cell exclusion markers</b>                     |                          |              |
| sytox red   | Thermo Fisher Scientific | #S34859      |
| sytox blue  | Thermo Fisher Scientific | #S34857      |
| Fixable viability dye eFlour450                         | eBioscience              | #65-0863-18  |
| <b><i>in vitro</i> TFH induction assays</b>             |                          |              |
| miRCURY LNA™ microRNA Mimic, hsa-miR-92a-3p, 5 nmol     | Exiqon                   | #472171-001  |
| miRCURY LNA™ microRNA inhibitor, hsa-miR-92a-3p, 5 nmol | Exiqon                   | #4100969-001 |
| <b><i>in vitro</i> Treg induction assays</b>            |                          |              |
| human recombinant IL2                                   | PeproTech                | #200-02      |
| human recombinant insulin                               | Sigma-Aldrich            | #I9278       |
| PI3K inhibitor (LY294002)                               | Peprotech                | #1543664     |
| 96-well suspension culture plate with U-Bottom          | Greiner Bio-One          | #650185      |
| <b>Buffers and Media</b>                                |                          |              |
| <b>HBSS<sup>+</sup></b>                                 |                          |              |
| Hanks' Balanced Salt Solution                           | Sigma-Aldrich            | #H6648       |
| Fetal Calf Serum (FCS) (5%)                             | PAA                      | #A15-151     |

|  |                          |               |
|--|--------------------------|---------------|
| HEPES (10 mM)                                  | Biochrom AG              | #L1613        |
| <b>PBS+0,5% BSA</b>                            |                          |               |
| DPBS<br>(Dulbecco's Phosphate-Buffered Saline) | Life Technologies        | #14190-094    |
| BSA  | Sigma-Aldrich            | #A790650G     |
| <b>MACS-PBS</b>                                |                          |               |
| DPBS<br>(Dulbecco's Phosphate-Buffered Saline) | Life Technologies        | #14190-094    |
| BSA  | Sigma-Aldrich            | #A790650G     |
| Ethylenediaminetetraacetic acid                | VWR                      | #45001-122    |
| <b>X-VIVO media (human)</b>                    |                          |               |
| X-VIVO Media                                   | Lonza                    | #BE04-418Q    |
| Human Serum                                    | Biochrom                 | #S01049.2-0.1 |
| Penicillin and streptavidin                    | Sigma-Aldrich            | #P4333        |
| sodium pyruvate                                | Sigma-Aldrich            | #S8636        |
| non-essential amino acids                      | Biochrom                 | #K0293        |
| GlutaMAX™ Supplement                           | Life Technologies        | #35050-038    |
| <b>RPMI Medium + Supplements (murin)</b>       |                          |               |
| RPMI media                                     | Thermo Fisher Scientific | #61870036     |
| FCS (Fetal Calf Serum) "GOLD"                  | Biowest                  | #S1810-500    |
| b-mercaptoethanol                              | Biozol Diagnostica       | #5-69F00-E    |

|   |                    |                                |
|---|--------------------|--------------------------------|
| non-essential amino acids   | Biochrom           | #K0293                         |
| sodium pyruvate   | Sigma-Aldrich      | #S8636                         |
| Penicillin and streptavidin                                       | Sigma-Aldrich      | #P4333                         |
| <b>Mice</b>   |                    |                                |
| B6.Cg-Foxp3 <sup>tm2Tch/J</sup> (Foxp3-GFP)                       | Jackson Laboratory | #006772                        |
| B6.SJL-Ptprca <sup>Pepcb/BoyJ</sup> (WT)                          | Jackson Laboratory | #002014                        |
| B6.Cg-Lep <sup>ob/J</sup> (ob/ob)                                 | Jackson Laboratory | #000632                        |
| B6.129S4(FVB)-Insr <sup>tm1Khn/J</sup> (InsR <sup>flx/flx</sup> ) | Jackson Laboratory | #006955                        |
| Tg(Cd4-cre)1Cwi/BfluJ (CD4Cre)                                    | Jackson Laboratory | #017336                        |
| <b>Genotyping via PCR</b>   |                    |                                |
| oKAHN03   | Sigma              | GAT GTG CAC CCC<br>ATG TCT G-3 |
| oKAHN04   | Sigma              | TCT ATC AAC CGT<br>GCC TAG AG  |
| oKAHN05   | Sigma              | CTG AAT AGC TGA<br>GAC CAC AG  |
| RO290   | Sigma              | GCT TGC ATG ATC<br>TCC GGT AT  |
| OB 1151   | Sigma              | TGT CCA AGA TGG<br>ACC AGA CTC |
| OB 1152   | Sigma              | ACT GGT CTG AGG<br>CAG GGA GCA |
| Proteinase K  | Thermo Fisher      | #10181030                      |
| Taq DNA Polymerase  | VWR International  | #01-1040                       |

|  |                     |           |
|--|---------------------|-----------|
| Midori Green                                   | Biozym              | #617004   |
| Gel Loading Dye, Blue                          | New England Biolabs | #B7021 S  |
| DNA-Leiter: DNA Ladder 100 bp                  | New England Biolabs | #N3231 L  |
| <b>Murine diet</b>                             |                     |           |
| Standard diet                                  | Altromin            | #1314     |
| high-fat, high-sugar (HFHS) diet               | Research Diets      | #D12331   |
| <b>GTT</b>                                     |                     |           |
| D(+)-Glucose                                   | Carl Roth           | #HN06.1   |
| Glucometer Accu-Chek Aviva                     | Roche Diabetes Care | #06114986 |
| ACCU CHEK Aviva Teststreifen                   | Roche Diabetes Care | #6114963  |
| Disposable needles                             | Neopoint            | #L10103   |
| <b>Glucose uptake Assay</b>                    |                     |           |
| Glucose Uptake-Glo™ Assay                      | Promega             | #J1341    |
| 96-well microplates for luminescence detection | Greiner             | #655073   |
| <b>RT-qPCR</b>                                 |                     |           |
| Hard- Shell PCR Plates, 96- well               | Bio-Rad             | #HSP9655  |
| Seals for PCR Plates                           | Bio-Rad             | #MSB 1001 |
| <b>RNA isolation</b>                           |                     |           |
| miRNeasy Micro Kit (50)                        | Qiagen              | #217084   |

| <b>mRNA analysis</b>                      |                            |   |
|---|----------------------------|---|
| iScript Advanced cDNA Synthesis Kit       | Biorad                     | #172-5038   |
| SsoFast EvaGreen Supermix 5x 5ml          | Bio-Rad                    | #172-5204   |
| <b>mRNA Primers</b>                       |                            |   |
| Murine/Human Ascl2                        | Bio-Rad                    | #10025636   |
| QuantiTect Primer Assay murine/human Bcl6 | Qiagen                     | #QT00079233   |
| QuantiTect Primer Assay human ITCH        | Qiagen                     | #QT00077812   |
| QuantiTect Primer Assay human Foxo1       | Qiagen                     | #QT00044247   |
| QuantiTect Primer Assay murine/human Pten | Qiagen                     | #QT01115135   |
| QuantiTect Primer Assay human Klf2        | Qiagen                     | #QT00204729   |
| Murine ICOS                               | self-designed,<br>Eurofins | fwd.: GCA CGA CCC<br>TAA CGG TGA AT;<br>rev.: GAA AAC TGG<br>CCA ACG TGC TT |
| Human ICOS                                | self-designed,<br>Eurofins | fwd.: GCA CGA CCC<br>TAA CGG TGA AT;<br>rev.: GAA AAC TGG<br>CCA ACG TGC TT |
| Murine/Human Il21                         | self-designed,<br>Eurofins | fwd.: CTC CCA AGG<br>TCA AGA TCG CC;<br>rev.: TGG CAG AAA<br>TTC AGG GAC CA |
| QuantiTect Primer Assay murine/human 18S  | Qiagen                     | #QT00199367   |
| Murine/Human Histone                      | self-designed,<br>Eurofins | fwd: ACT GGC TAC<br>AAA AGC CG;<br>rev:CTT GCC TCC<br>TGC AAA GCA C         |

| <b>miRNA analysis</b>  |                 |   |
|--|-----------------|---|
| Universal cDNA Synthesis Kit II  | Exiqon          | #203301   |
| ExiLENT SYBR® Green master mix   | Exiqon          | #203403   |
| <b>miRNA Primers</b>   |                 |   |
| mmu-miR-92a-3p LNA™ PCR primer set, UniRT                                | Exiqon          | #205947   |
| 5S rRNA (hsa,mmu) PCR primer set, UniRT                                  | Exiqon          | #203906   |
| <b>Foxp3 CNS2 Methylation Analysis</b>                                   |                 |   |
| EZ DNA Methylation-Direct Kit  | Zymo Research   | #D5021  |
| SensiFAST HRM Kit  | Bioline         | #5001484  |
| Primers used together with SensiFAST HRM Kit                             | Sigma           | fwd: TTG GGT TTT<br>GTT GTT ATA ATT<br>TGA ATT TGG<br>biotinylated rev: ACC<br>TAC CTA ATA CTC<br>ACC AAA CAT C |
| PyroMark Gold Q24 Reagents   | Qiagen          | #970802   |
| Specific sequencing primer used together with PyroMark Gold Q24 Reagents | Sigma           | AAT TTG AAT TTG<br>GTT AGA TTT TT   |
| TMB Substrate Reagent Set  | BD              | #555214   |
| <b>RNAseq</b>  |                 |   |
| SMARTer ultra low input RNA Kit for Sequencing-v4                        | Clontech/Takara | #634890   |
| Agilent High Sensitivity DNA Kit   | Agilent         | #5067-4626  |
| Illumina Nextera XT DNA library preparation kit                          | Illumina        | #FC-131-1096  |

|                                |  |   |
|--------------------------------|--|---|
| HiSeq® Rapid SBS Kit v2        | Illumina   | #FC-402-4022  |
| HiSeq® Rapid SR Cluster Kit v2 | Illumina   | #GD-402-4002  |
| Index Primers: Nextera N501    | self designed, AG<br>Prof. M.Pfaffl, TU<br>München | AATGATACGGCGAC<br>CACCGAGATCTACA<br>CTAGATCGCTCGTC<br>GGCAGCGTC |
| Index Primers: Nextera N502    | self designed, AG<br>Prof. M.Pfaffl, TU<br>München | AATGATACGGCGAC<br>CACCGAGATCTACA<br>CCTCTCTATTCGTC<br>GGCAGCGTC |
| Index Primers: Nextera N503    | self designed, AG<br>Prof. M.Pfaffl, TU<br>München | AATGATACGGCGAC<br>CACCGAGATCTACA<br>CTATCCTCTTCGTC<br>GGCAGCGTC |
| Index Primers: Nextera N504    | self designed, AG<br>Prof. M.Pfaffl, TU<br>München | AATGATACGGCGAC<br>CACCGAGATCTACA<br>CAGAGTAGATCGTC<br>GGCAGCGTC |
| Index Primers: Nextera N505    | self designed, AG<br>Prof. M.Pfaffl, TU<br>München | AATGATACGGCGAC<br>CACCGAGATCTACA<br>CGTAAGGAGTCGTC<br>GGCAGCGTC |
| Index Primers: Nextera N506    | self designed, AG<br>Prof. M.Pfaffl, TU<br>München | AATGATACGGCGAC<br>CACCGAGATCTACA<br>CACTGCATATCGTC<br>GGCAGCGTC |
| Index Primers: Nextera N507    | self designed, AG<br>Prof. M.Pfaffl, TU<br>München | AATGATACGGCGAC<br>CACCGAGATCTACA<br>CAAGGAGTATCGTC<br>GGCAGCGTC |
| Index Primers: Nextera N508    | self designed, AG<br>Prof. M.Pfaffl, TU<br>München | AATGATACGGCGAC<br>CACCGAGATCTACA<br>CCTAAGCCTTCGTC<br>GGCAGCGTC |
| Index Primers: Nextera N701    | self designed, AG<br>Prof. M.Pfaffl, TU<br>München | CAAGCAGAAGACG<br>GCATACGAGATTCG<br>CCTTAGTCTCGTGG<br>GCTCGG     |

|                             |  |  |
|-----------------------------|--|--|
| Index Primers: Nextera N702 | self designed, AG<br>Prof. M.Pfaffl, TU<br>München | CAAGCAGAAGACG<br>GCATACGAGATCTA<br>GTACGGTCTCGTGG<br>GCTCGG  |
| Index Primers: Nextera N703 | self designed, AG<br>Prof. M.Pfaffl, TU<br>München | CAAGCAGAAGACG<br>GCATACGAGATTTTC<br>TGCCTGTCTCGTGG<br>GCTCGG |
| Index Primers: Nextera N704 | self designed, AG<br>Prof. M.Pfaffl, TU<br>München | CAAGCAGAAGACG<br>GCATACGAGATGCT<br>CAGGAGTCTCGTG<br>GGCTCGG  |
| Index Primers: Nextera N705 | self designed, AG<br>Prof. M.Pfaffl, TU<br>München | CAAGCAGAAGACG<br>GCATACGAGATAGG<br>AGTCCGTCTCGTGG<br>GCTCGG  |
| Index Primers: Nextera N706 | self designed, AG<br>Prof. M.Pfaffl, TU<br>München | CAAGCAGAAGACG<br>GCATACGAGATCAT<br>GCCTAGTCTCGTGG<br>GCTCGG  |
| Index Primers: Nextera N707 | self designed, AG<br>Prof. M.Pfaffl, TU<br>München | CAAGCAGAAGACG<br>GCATACGAGATGTA<br>GAGAGGTCTCGTG<br>GGCTCGG  |
| Index Primers: Nextera N708 | self designed, AG<br>Prof. M.Pfaffl, TU<br>München | CAAGCAGAAGACG<br>GCATACGAGATCCT<br>CTCTGGTCTCGTGG<br>GCTCGG  |
| Index Primers: Nextera N709 | self designed, AG<br>Prof. M.Pfaffl, TU<br>München | CAAGCAGAAGACG<br>GCATACGAGATAGC<br>GTAGCGTCTCGTGG<br>GCTCGG  |
| Index Primers: Nextera N710 | self designed, AG<br>Prof. M.Pfaffl, TU<br>München | CAAGCAGAAGACG<br>GCATACGAGATCAG<br>CCTCGGTCTCGTGG<br>GCTCGG  |
| Index Primers: Nextera N711 | self designed, AG<br>Prof. M.Pfaffl, TU<br>München | CAAGCAGAAGACG<br>GCATACGAGATTGC<br>CTCTTGTCTCGTGG<br>GCTCGG  |

|                             |  |   |
|-----------------------------|--|---|
| Index Primers: Nextera N712 | self designed, AG Prof. M.Pfaffl, TU München | CAAGCAGAAGACG<br>GCATACGAGATTCC<br>TCTACGTCTCGTGG<br>GCTCGG |
|-----------------------------|--|---|

### LC-MS/MS (Proteomics)

Consumables compare: **chapter 2.17**

### Immunofluorescence

|  |                           |              |
|--|---------------------------|--------------|
| Roti-Histofix 4 %                                  | Carl Roth                 | #P087.5      |
| Phospho-S6 Ribosomal Protein (Ser235/236) antibody | Cell Signaling Technology | #2211        |
| Glucokinase (GCK) antibody                         | Abcam                     | #ab88056     |
| anti-rabbit Alexa Fluor 647 antibody               | Dianova                   | #711-605-152 |

### Instruments

|                                   |                          |      |
|-----------------------------------|--------------------------|------|
| FACS Aria III                     | BD                       | n.a. |
| Thermal Cycler, peqStar 2X        | Peqlab                   | n.a. |
| Real-Time PCR System, CFX96 Touch | Bio-Rad                  | n.a. |
| Glomax Multi Detection System.    | Promega                  | n.a. |
| Pyro-Sequencer PyroMark Q24       | Qiagen                   | n.a. |
| Illumina HiSeq 2500               | Illumina                 | n.a. |
| Agilent Bioanalyzer 2100          | Agilent                  | n.a. |
| Sonifier                          | Branson                  | n.a. |
| EASY-nLC™ 1200 System             | Thermo Fisher Scientific | n.a. |

|  |   |   |
|--|---|---|
| Q Exactive HF                              | Thermo Fisher Scientific  | n.a.  |
| <b>Software</b>                            |   |   |
| FACSDiva software (version 6.1.3)          | Beckton Dickinson   | n.a.  |
| FlowJo (version 10)                        | TreeStar, OR  | <a href="https://www.flowjo.com/solutions/flowjo/downloads/">https://www.flowjo.com/solutions/flowjo/downloads/</a>   |
| GraphPad Prism (version 7)                 | GraphPad  | <a href="https://www.graphpad.com/scientific-software/prism/">https://www.graphpad.com/scientific-software/prism/</a> |
| CFX Manager 3.1                            | Bio-Rad   | n.a.  |
| PyroMark Q24 2.0.6                         | Qiagen  | n.a.  |
| Gene5 Data Analysis                        | BioTek  | n.a.  |
| Expert 2100                                | Agilent   | n.a.  |
| HiSeq Control Software 2.2.70              | Illumina  | n.a.  |
| Real-Time Analysis (RTA) 1.18.66           | Illumina  | n.a.  |
| CASAVA BCL2FASTQ Conversion Software v2.20 | Illumina  | n.a.  |
| MaxQuant version 1.5.1.6                   | developed by the Computational Systems Biochemistry under Prof. J.Cox, Max Planck Gesellschaft, München | (Cox & Mann, 2009)  |
| Perseus version 1.5.6.2                    |   | (Tyanova et al., 2016)  |

## Danksagung

Meine Dissertation glich einer alpinen Wanderung mit einigen Höhen und Tiefen und einem grandiosen Ausblick am Ziel. Ich möchte mich herzlich bei allen bedanken die mich dabei fachlich, mental und finanziell unterstützt haben.

Zuerst möchte ich mich bei Prof. Dr. Carolin Daniel bedanken für die sehr gute Betreuung, Unterstützung und Förderung. Vielen Dank für deine Offenheit, Motivation und die Marie-Curie-Zitate.

Ich bedanke mich herzlich bei Prof. Dr. Matthias Tschöp für die Möglichkeit meine Doktorarbeit an seinem Institut durchzuführen. Danke für deine Unterstützung, Motivation und die hilfreichen Diskussionen.

Mein Dank gilt auch Prof. Dr. Klaus Kästner für das Interesse an meiner Doktorarbeit, die Bereitstellung von Materialien und für die kritischen Anmerkungen in den „Thesis Committee Meetings“.

Für die Unterstützung der RNA-Sequenzierung, sowie dem Interesse an meiner Doktorarbeit und den hilfreichen Diskussionen im Montagsseminar und den „Thesis Committee Meetings“ bedanke ich mich bei Prof. Dr. Michael Pfaffl.

Des Weiteren gilt mein Dank Prof. Dr. Anette-Gabriele Ziegler für die Möglichkeit meine Doktorarbeit an ihrem Institut durchzuführen.

Ich bedanke mich beim TUM-IAS für die Finanzierung meiner Doktorandenstelle und den Mitarbeitenden des TUM-IAS für angenehme Zusammenarbeit.

Danke an alle Mitarbeitenden des IDF1 und IDO für die hervorragende Zusammenarbeit. Besonders wertvoll waren die Anmerkungen und Ideen im IDO Internal Seminar.

Mein Dank gilt allen Kollaborationspartnern die Reagenzien oder Mäuse bereitgestellt haben und die mich bei meinen Experimenten unterstützt haben. Insbesondere bedanke ich mich bei Dr. Natalie Kraemer, Dr. Benno Weigmann, Ming Wu und Kristiyan Kanev.

Ein herzliches Dankeschön geht an die gesamte Arbeitsgruppe „Immune tolerance in Diabetes“ und alle gegenwärtigen und ehemaligen Mitarbeitenden für die angenehme und motivierende Arbeitsatmosphäre und die großartige Zusammenarbeit. Insbesondere möchte ich mich bei Isabelle Serr und Maike Becker bedanken. Ihr wart immer erreichbar, habt euch Zeit genommen für wertvolle Diskussionen und habt selbst zu später oder sehr früher Stunde mit angepackt.

Mein ganz besonderer Dank gilt meiner Familie für die wertvolle, bedingungslose Unterstützung auf meinem gesamten bisherigen Lebensweg. Insbesondere danke ich Johannes für seine Kraft und Energie vor allem auf der Zieletappe. Ohne dich hätte ich den Gipfel nicht erreicht!